School of Computing Science,
University of Newcastle upon Tyne

21st UK Performance Engineering Workshop

Nigel Thomas

Technical Report Series

CS-TR-916

June 2005

Published by the University of Newcastle upon Tyne,
School of Computing Science, Claremont Tower, Claremont Road,
Newcastle upon Tyne, NE1 7RU, UK.

21st UK Performance Engineering Workshop

University of Newcastle

14th/15th July 2005

Edited by
Nigel Thomas

ISSN 1368-1060

Contents

Applications 2

Addendum

Preface

Welcome to the 21st UK Performance Engineering Workshop, being held for the first time in Newcastle. UKPEW is designed to be a forum for researchers across the UK and beyond to meet and share experiences of their work in the field of performance. The meeting is intended to be approachable to researchers at any stage of their career and is an ideal place to make new contacts and to meet old friends. I very much hope that the 21st UKPEW will be as much of a success in this regard as the previous 20 events.

This year the programme consists of eighteen submitted papers across five loosely themed sessions spread over two days. The papers reflect the rise of security, MANETs and web services as important growing concerns for performance engineers, as well as the continued importance of more traditional topics, such as queueing theory.

As usual the majority of papers are from the UK, but there are also contributions from Germany, Hungary and Brazil. It is very pleasing to see so many people active in this area in the UK and so many familiar faces returning once more to UKPEW. The level of interest demonstrates a healthy community. I would like to take this opportunity to thank all the authors for preparing their papers professionally and for (almost) sticking to the deadlines. Your hard work made my job much easier.

In addition to the regular papers there are also two invited talks, given by Boudewijn Haverkort and Jeremy Bradley. We are delighted to welcome such esteemed researchers to present at UKPEW. Jeremy is an old friend of UKPEW, having been co-chair in Bristol in 1999 and Durham in 2000 and a delegate every year since. He is well known for his work on stochastic process algebra. And will talk about a collaborative environment for performance engineering. Boudewijn is new to the UKPEW forum but is very well known and respected throughout the community. He is currently Professor of Design and Analysis of Communication Systems at the University of Twente and has worked for many years in the area of performance and reliability modelling. Boudewijn will present work undertaken jointly with his PhD student Lucia Cloth on the use of model checking techniques for survivability evaluation.

In recent years Newcastle has become one of the pre-eminent cities in the UK, with a reputation for lively night life, modern art and architecture. It is a great place to live and work, and we hope that the UKPEW delegates will find it a great place to visit. If you have time then please make the effort to walk down to the Quayside and over the Millennium Bridge ("The Winking Eye") to The Sage Gateshead and the Baltic Arts Centre. These buildings have become symbols of the regeneration of this once industrial area of the city and are well worth the walk.

I hope you enjoy what Newcastle has to offer and more importantly I hope you enjoy the papers and presentations at UKPEW. If this is your first visit to either Newcastle or UKPEW, I trust that both will impress you enough to want to return.

Nigel Thomas

(Chair of UKPEW 2005)

Model Checking for Survivability!

Boudewijn Haverkort and Lucia Cloth

University of Twente, The Netherlands

Abstract

Business and social life have become increasingly dependent on large-scale communication and information systems. A partial or complete breakdown as a consequence of natural disasters or purposeful attacks might have severe impacts. Survivability refers to the ability of a system to recover from such disaster circumstances. Evaluating survivability should therefore be an important part of communication and information system design. In this paper we take a model checking approach toward assessing survivability. We use the logic CSL to phrase survivability in a precise manner. The system operation is modelled through a labelled CTMC. Model checking algorithms can then decide automatically whether the system is survivable. We illustrate our method by evaluating the survivability of the Google file system using stochastic Petri nets in combination with CSL model checking.

The Future is Collaborative Performance Engineering

Jeremy Bradley

Department of Computing, Imperial College London

Abstract

Performance engineering is a hard task involving not only a large portion of concurrency theory, but also incorporating stochastic, deterministic and probabilistic concepts of time and choice at the modelling end. More widely performance engineering incorporates the gathering of instrumentation of real systems, the simulation of models of such systems and the real challenge is to have the modelling and simulation results match the performance experiments on the target system. We are working on a performance engineering environment called Perform-db which has at its core the notion that performance engineers need to collaborate in order to maximise the reuse of performance models, analysis, simulations, experiments and structural results. We believe that only in making use of formal modelling results that others have derived or in spotting patterns in experimental data that was produced from other related systems can the overall goal of a performance engineering lifecycle be achieved.

Fault Detection Mechanisms for Autonomic Distributed Applications.

*E.Grishikashvili Pereira, **R. Pereira, **A. Taleb-Bendiab
** Department of Computing and IS Edge Hill Uni. College, St. Helen's Road, Ormskirk, L39 4QP, pereirae@edgehill.ac.uk*
**School of Computing and Mathematical Sciences Liverpool John Moores University, Byrom Street, Liverpool, L3 3AF, UK, R.Pereira@livjm.ac.uk

Abstract:
Autonomic computing includes a range of desirable properties, which are best achieved through middleware support. One of these properties is self-healing, the ability that systems may have to reconfigure themselves following the failure of some component. Recently, we have witnessed the development of models to provide middleware-based support for self-healing, service oriented distributed systems. The On-Demand Assembly and Delivery (OSAD) proposed previously by the authors consists of a number of components associated with fault-detection and fault-recovery. In this paper, we consider the performance impact of a number of fault-detection mechanisms, including pre-emptive detection and on-use detection.

Introduction:

There is a growing body of knowledge associated with techniques related to self-healing[1-3]. Although to a certain extent self-healing is not yet well defined in terms of scope and architectural models, it has received increased attention lately. A short definition of a self-healing system is a system that is capable of performing a reconfiguration step in order to recover from a permanent fault. The following requirements are likely to be relevant to most self-healing systems: adaptability, dynamicity, awareness, autonomy, robustness, distributability, mobility and traceability. In addition, it is also essential that self-healing systems have strong monitoring abilities.

Self-healing properties are particularly useful in dynamic systems, particularly distributed, service oriented systems, where new services may be added and removed from the network, leading to the need for applications to reconfigure themselves [4, 5]. Ideally, such reconfiguration steps would be carried out without user intervention. Distributed service oriented systems provide application developers with the ability to build applications using services provided by other systems across available in a network. Such arrangement requires some form of organisation, normally involving a look up service, which contains information about all services that are available in the network. Applications wishing to use a networked service would carry out a search on the look up service and select, based on some criteria, the service that best matches its requirements. A well-known system based on distributed services is JINI, which provides some support for distributed service-oriented systems [6].

The OSAD model

The On-demand Service Assembly and Delivery (OSAD) model [4] provides an abstract view of the relationship of the distributed components and services. The objective of the OSAD model is to organize the following issues in a uniform framework:

- On-demand service delivery and invocation regardless of the location of the service;

- The automatic assembly of the application in ad-hoc manner based on the user's requirements;
- The ability to self-heal at runtime in terms of replacing a failed component of an application.

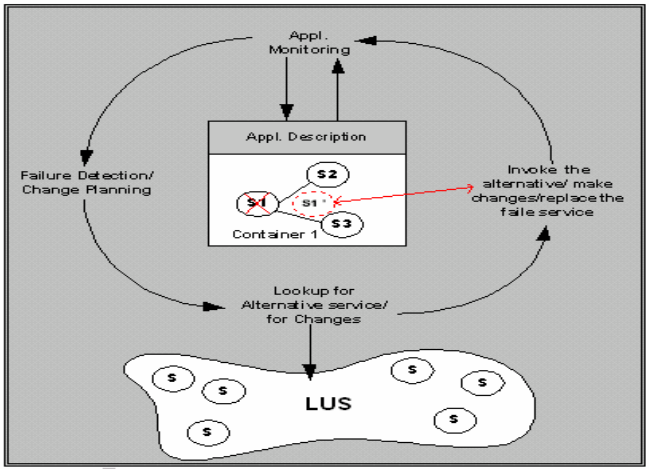

Figure 1: the lifecycle of self-healing behaviour in OSAD

One of the tasks of the model is to find distributed components offering specific functionality, that we call offering the service. After the component is found the next task is to make use of this functionality. Finding and assembling components is the role of the Assembly Service:

Assembly Service – this is the core service of the framework and it combines a number of functionalities of the model. Therefore the Assembly service is a combination of different sub-services and modules. It contains:

- *A Task Definition service*;
- *Registration and Discovery Service*;
- *Service Invocation Service*.

Control and monitoring are needed to identify failure, and alert the system to find an alternative replacement for the failed service as the control mechanism should be implemented with self-healing behaviour, in order to improve the newly formed application performance. The control and monitoring are performed by the System Manager. The system manager is responsible for recovering the application from failure. Following failure detection, it notifies the assembly service that a replacement service should be found and selected amongst possible alternatives

Fault Detection Mechanisms

Failure detection can be implemented in different ways, which can have considerable impact on the performance of the system. Two mechanisms that we put forward for consideration are: Pre-emptive detection and on-use detection. With pre-emptive detection, the service manager checks, on a regular basis, that each of the services associated with the application is alive. If a service fails to respond to the service manager, it is assumed that the service has failed and the recovery process is started and the service manager then notifies the assembly service. With the on-use detection, the service manager monitors locally the service requests and, if a request times-out, it

is assumed that the service has failed and the recovery process is started and the service manager then notifies the assembly service.

The performance considerations in this study relates to how these two mechanisms impact on service replacement waiting time and on network traffic. The notion of service replacement waiting time is important: It is the amount of time the application is prevented from using the service, because it is found to have failed and is being replaced. The main advantage of the pre-emptive detection is that, as the service manager periodically polls the services, they may be found to be faulty prior to the moment when the application would wish to use them, therefore they can be replaced with zero replacement waiting time. The figure below shows the replacement waiting time for the on-use replacement mechanism, against the total number of services in used by the application:

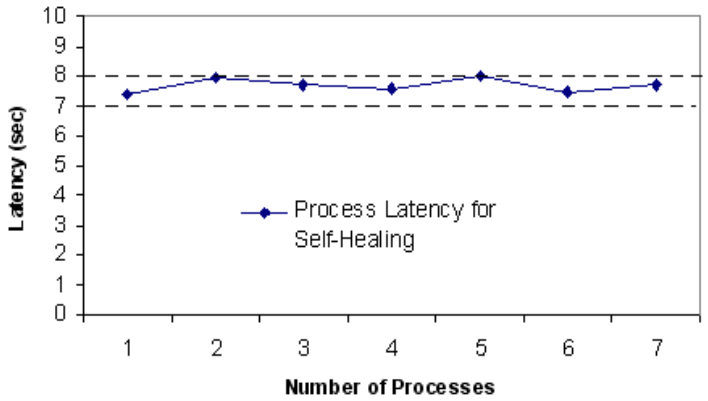

On the other hand, the pre-emptive mechanism, although reducing the replacement waiting time, generates more network traffic, which may lead to congestion if there are large numbers of applications and services being used by these applications.

Conclusion

This paper presents a performance discussion of the relative merits of two mechanisms for fault detection in our middleware for self-healing applications. The pre-emptive and on-use mechanisms are introduced and a discussion of their relative merits presented. It is argued that the pre-emptive mechanism reduces waiting time at the expense of higher network traffic. The full paper will present more results that could not be included here for lack of space.

References

[1] J. O. Kephart, D.M.C., *The Vision of Autonomic Computing*. 2003, IBM Tomas J. Watson Research Center.

[2] Koopman, P. *Elements of the Self-Healing System Problem Space*. In *ICSE WADS03*. 2003. Portland

[3] P. Oriezy, M.M.G., R. N. Taylor, G. Johnson, N. Medvidovic, A. Quilici, D. Rosenblum, and A. Wolf, *An Architecture-Based Approach to Self-Adaptive Software.* IEEE Intellingent Systems, 1999.

[4] E.Grishikashvili, N.B., D. Reilly, A. Taleb-Bendiab. *From Componen-Based to Service-Based Distributed Applications Development and Life-Time Management*. in *EuroMicro*. 2003. Antalya, Turkey

[5] G. Bieber, J.C., *Introduction to Service-Oriented Programming*, in *Motorola ISD*. 2002.

[6] Newmarch, J., *A Programmer's Guide to Jini Technology,* 2000, Apress: USA.

Performance Measurement of Web Services Security Software

Christiaan Lamprecht [*] Aad van Moorsel [†]

Abstract

Web Services are built on open standards to provide a generic way of communication between heterogeneous environments. Web Service security is an important factor for Web Services to gain increased acceptance. This paper presents how message level security is achieved in web services interactions and in particular explores whether VeriSign's Trusted Services Integration Kit (TSIK) is a viable option for realising this. Through measurement of TSIK as well as of an implementation using Java Cryptography Extensions (JCE), we conclude that TSIK provides an adequate level of security with minimal additional overheads. However, it would benefit from using SHA-256 in future releases and decreasing algorithm operation time when processing larger messages.

1 Introduction

Web Services have been met with growing interest from academia as well as industry due to its potential to provide a generic global service oriented network which is flexible enough to cater for individual service needs as well as providing increased interoperability between services. For businesses to fully embrace such a new technology they need to be confident that it is secure and can provide them with adequate security features for business interactions [Rat]. Focusing on security at message level, such business interactions typically require: message integrity to ensure messages are unaltered during transit; message confidentiality to ensure message content remain secret; non-repudiation to ensure that the sending party cannot deny sending the received message; and sender authentication to prove sender identity.

This paper will analyse the performance of Web Service security mechanisms. In particular we investigate if VeriSign's publicly available Trusted Services Integration Kit (TSIK) is a viable security tool with respect to the level of security it provides as well as its efficiency at doing so. We therefore first discuss in section 2 how message integrity, confidentiality, non-repudiation and sender authentication are typically achieved. Section 3 will focus on the level of security provided by TSIK for each of the above. Section 4 will look at asymmetric cryptography in more detail to provide a basis for section 5 which details a comparative evaluation of TSIK's performance with respect to using the standard Java Cryptography Extensions (JCE). The paper concludes with a summary in section 6.

* School of Computing Science, University of Newcastle upon Tyne, C.J.Lamprecht@ncl.ac.uk
† School of Computing Science, University of Newcastle upon Tyne, Aad.vanMoorsel@ncl.ac.uk

2 Message level security

We provide a very brief overview of the well-known techniques available to achieve message integrity, confidentiality, non-repudiation and sender authentication.

2.1 Symmetric cryptography

Symmetric cryptography tries to ensure message confidentiality by encrypting the message (the plaintext) using a secret key to produce an encrypted version of the message (the cipher text), which is then sent instead of the original message. Message integrity is implicitly provided, as altering the cipher text would result in an illegible decrypted message. 'Symmetric' refers to the fact that the same secret key is required to decrypt the message on the recipient's side. Typical symmetric encryption algorithms include DES, Triple DES, RC2, RC5, IDEA and AES. The main problem in this scheme is the key distribution problem; since the same secret key is used to decrypt the message, one must find a way to securely transport the key from sender to recipient.

2.2 Hashing

Hashing tries to ensure message integrity by producing a condensed version of the message, the message digest, which is unique to that message. The hashing algorithm is publicly known and so the recipient can perform the same hash on the received message, to produce another message digest, and compare it to the received digest to asses whether the original message has been altered. Typical hashing algorithms include MD2, MD4, MD5, SHA-1, SHA-256, SHA-384 and SHA-512. Hashing does not provide confidentiality, non-repudiation or authentication. On its own, hashing does not provide message integrity either as both the hash and the message could be replaced by a third party and so prevent the recipient from detecting the attack. Section 2.4 explains how hashing is utilized to ensure message integrity.

2.3 Asymmetric cryptography (public key cryptography)

Asymmetric cryptography provides the same message security guarantees as symmetric cryptography, but additionally provides the non-repudiation guarantee. 'Asymmetric' refers to the fact that different keys are used for encryption and decryption. One key is kept secret ('secret key') and the other is made public ('public key'), and are both unique. The recipient's public key should be used during the encryption process to ensure message confidentiality as only the recipient has the necessary secret key to decrypt the message. If, however, the message is encrypted using the sender's private key the sender cannot deny sending the message as his private key is unique and is only known to him. Typical asymmetric encryption algorithms include RSA and Elgamal. Asymmetric cryptography is extremely powerful, but this comes at a cost. Especially for longer messages and keys, it is much slower than its symmetric cryptography counterparts [Adams].

2.4 Experiment Scenario

The results in this paper assume the following typical scenario, in which the above techniques are combined to achieve a more effective security solution through signing, verifying, encryption and decryption. They are combined as follows:

The key, in symmetric cryptography, can be securely transported using public key cryptography by encrypting the symmetric key using the receiver's public key. The receiver, and only the receiver, can then first decrypt the symmetric key

using his private key and then decrypt the message using the decrypted symmetric key. Also note that only the key, which is relatively short, is encrypted using public key cryptography and so reduces encryption overhead.

The message digest, produced by the hash function, can be encrypted using an asymmetric cryptography algorithm to avoid and interception attack. Thus, if the message digest is encrypted using the sender's private key, only the message can be replaced during transit and not the message digest, since the interceptor does not have the sender's private key to encrypt the new message digest.

Generating a message digest and then encrypting the message digest using a private key is referred to as signing the message. Decrypting the message digest using the sender's public key, generating a new message digest of the received message and then comparing the digests is called verifying the message. The performance results of these two techniques, among others, are analysed in this paper.

Sender authentication is achieved when the sender's public key is signed by a mutually trusted third party. The receiver can then verify the public key as the third party's public key is trusted.

3 RSA [Ronald]

Understanding the security implications and performance results in sections 4 and 5 requires a deeper understanding of public key cryptography. In particular RSA, which was developed by Ron Rivest, Adi Shamir and Leonard Adleman in 1977 and is used by VeriSign's TSIK toolkit. We do not explain all the details of RSA, but instead focus on the particular use of RSA in our measurements setup.

3.1 The algorithm [Rivest][Hung]

- Choose 2 large primes *p* and *q* such that *pq = N*
- Select 2 integers *e* and *d* such that $ed = 1 \bmod \phi(N)$
  - Where $\phi(N) = (p-1)(q-1)$ is the Euler totient function of N

In general, N is called the Modulus, *e* the public exponent and *d* the private exponent. The public key is the pair (N, e) which is made public and the private key is the pair (N, d) which is kept secret.

RSA encryption and decryption explained in context of the experiment scenario (section 2.4):

Encryption:

The symmetric key M:

Encrypted key = $M^e \bmod n$

The message digest M:

Encrypted digest = $M^d \bmod n$

Decrypting:

The symmetric key C:

Decrypted key = $C^d \bmod n$

The message digest C:

Decrypted digest = $C^e \bmod n$

Where M is the key or digest converted to an integer according to [PKCS#1], C the encrypted key or digest and n the particular modulus, chosen to be either 512, 1024, 2048, 3072 or 4096.

In particular, it should be noted that encrypting the key and encrypting the message digest is not the same function as one uses the public- and the other the private exponent.

Therefore, encrypting the symmetric key and decrypting the message digest (in the verification process) is mathematically equivalent as they both use the public exponent. The same can be said for encrypting the message digest (in the signing process) and decrypting the symmetric key as they both use the private exponent.

RSA operation time greatly depends on the length of *e* and *d* [Free], such that longer exponents incur much larger time overheads. It would therefore be desirable to use smaller values for *e* and/or *d* if possible.

3.2 Smaller public exponent

We consider how the length of the public exponent affects security as both security mechanisms (section 5) exploit this to achieve faster symmetric key encryption and message verification. The smallest value for *e* is 3 [Dan]. This can however weaken RSA confidentiality assertions. In particular, if $M < \sqrt[e]{N}$ the plaintext can easily be recovered [Rivest]. Also, Hastad's broadcast attack can be mounted if *k* cipher texts, encrypted with the same public exponent, can be collected such that *k* >= *e*. [Dan]. The Chinese Remainder Theorem (CRT) can then be used to recover the plaintext message [RFC3110] [Dan].

A defense against such attacks would be to 'pad' the message using some random bits [Bellare]. Coppersmith imposed further restrictions on this in his "Short Pad Attack" which concludes that for *e* = 3 an attack can still be mounted, even though a random set of bits are used, if the pad length is less than $1/9^{th}$ of the message length [Dan].

PKCS#1 [RFC3447] [PKCS#1] does however propose the use of Optimal Asymmetric Encryption Padding (OAEP) [Bellare] for new applications and PKCS1-v1_5 for backward compatibility with existing applications.

Although *e* = 3 can provide adequate security, if necessary precautions are taken, the current recommendation is $e = 2^{16} + 1$ [Dan] which is still small, requiring only 17 multiplications, but big enough to solve the above problems at the cost of a slight increase in encryption time.

Short public exponents are not however a concern for signature schemes [RFC3110][Rivest].

3.3 Smaller private exponent

A shorter private exponent would result in faster key decryption and message signing. Typically the private exponent is the same length as the modulus regardless of the public exponent length. M. Wiener [Wiener] has however shown that if $d < \frac{1}{3}N^{0.24}$ the private exponent can be obtained from the public key (N, e). Since N is typically 1024 bits long, *d* must be at least 256 bits long. More recently, Boneh and Durfree have shown this to be closer to $d < N^{0.292}$ [Durfee] [Hung] and predicted the likely final result to be closer to $d < N^{0.5}$ [Dan][Durfee].

Other techniques used to decrease algorithm operation time include the use of the Chinese Remainder Theorem [Dan], know as RSA-CRT, which is said to be

approximately 4 times faster than using standard RSA algorithms [Hung]. Rebalanced RSA-CRT can also be used and tries to shift the cost towards the usage of the public exponent *e* [Shacham] [Wiener].

4 Security software analysis

Java keytool, Java's Key and Certificate Management Tool, is used to create the Java keystore, with appropriate key pairs, used by TSIK and JCE. The keytool generates key pairs where N is user specified (512, 1024 or 2048), *d* is the same length as *N* and *e* defaults to $2^{16} + 1$ (i.e. 17 bits long). As stated in section 3.2 and 3.3, these values are adequate and it is currently recommended that the user selects the modulus to be at least 1024 bits.

TSIK 1.10 provides additional functionality, above that of the Java Cryptography Extensions (JCE), to construct valid XML messages after encryption/decryption or signing/verifying. These messages conform to the W3C XML Signature and Encryption specifications [xmldsig] [xmlenc]. TSIK supports Triple DES (in Cipher Bite Chaining mode) for symmetric encryption, as defined by W3C [tdes]. Using a key length of at least 112 bits will currently provide sufficient security. Triple DES is however relatively slow compared to other more recent contenders such as AES [Junaid]. Conversely, it has stood the test of time and so is potentially a more reliable solution.

Only SHA-1 is provided for message digest generation (Digest length of 160 bits). SHA-1 has very recently been shown to be less secure than predicted and it is recommended that SHA-256 or above should be used [sha]. RSAES-PKCS1-v1_5 algorithm, specified by W3C [rsa15] and [RFC2437], is used as the RSA standard. As stated in section 3.2 above; if backward compatibility is not an issue OAEP should be used in preference to PKCS1-v1_5. However, PKCS1-v1_5 provides adequate security assuming the programmer is aware of certain issues. Also, [RFC2437] indicates that RSA-CRT is used.

JCE does not support the creation of valid XML messages but supports various symmetric key algorithms including AES, Triple DES and RC5. It also supports SHA-1, SHA-256, SHA-512 and MD5, amongst others, for message digest generation. It also specifies that the padding is applied according to [PKCS#1]. RSA-CRT is also used.

5 Performance analysis

The following section details a comparative evaluation of the performance of VeriSign's TSIK toolkit with respect to the standard Java Cryptography Extensions (JCE) in order to identify whether TSIK is a viable tool to secure web service transactions.

5.1 Environment

All experiments were run on a 3GHz Intel Pentium 4 with 1GB RAM, running Java(TM) 2 Runtime Environment, Standard Edition (build 1.4.2-b28) on top of Linux Fedora Core 2. We used Bouncycastle [bounce] as the Java RSA provider for both JCE and TSIK, and used Apache Axis 1.2 to generate the appropriate WSDL interface for the web service, which was hosted on Tomcat 5. Axis was used to both generate the appropriate SOAP messages, from the java code and TSIK XML documents, to be sent to the web service, also know as the server, and also generate

the SOAP messages to be sent back from the web service to the client. We took performance measurements on the client and server side where the TSIK and JCE implementations reside. Message transmission and conversion delays were not measured.

5.2 Experiments

We set up three experiments, as detailed below.

Experiment 1:

In experiment 1 we analyse the performance of Triple DES, as function of message size:

- Client side: Message plaintext encrypted using Triple DES with a keysize of 168. Symmetric key encrypted using an RSA public key (Modulus 1024)
- Server side: Encrypted symmetric key decrypted using RSA private key (bit length 1024) and cipher text then decrypted.

Experiment 2:

In experiment 2 we analyse the combined performance of SHA-1 and RSA algorithms, as a function of the message size:

- Client side: Message signed using SHA-1 and RSA private key (bit length 1024)
- Server side: Message verified using SHA-1 and RSA public key

Experiment 3:

In experiment 3 we analyse how the modulus size affects the performance of RSA during signature creation and verification:

- Client side: Message signed (as in experiment 2) using RSA key sizes 512, 1024 and 2048.
- Server side: Message verified.

5.3 Results

We executed above experiments for TSIK as well as JCE. We repeated the first two experiments for messages with a range of plaintext sizes, namely 2, 4, 8, 16, … , 512 and 1024 kB. Experiment 3 was done using a 2 kB plaintext size. The results are shown in the graphs below. It should be noted that all points on graphs 1 and 3 exhibit confidence intervals of 3 milliseconds and points on graphs 2 and 4 exhibit confidence intervals of 0.1 milliseconds. Both with probability 0.9 (Where 1.0 is certain).

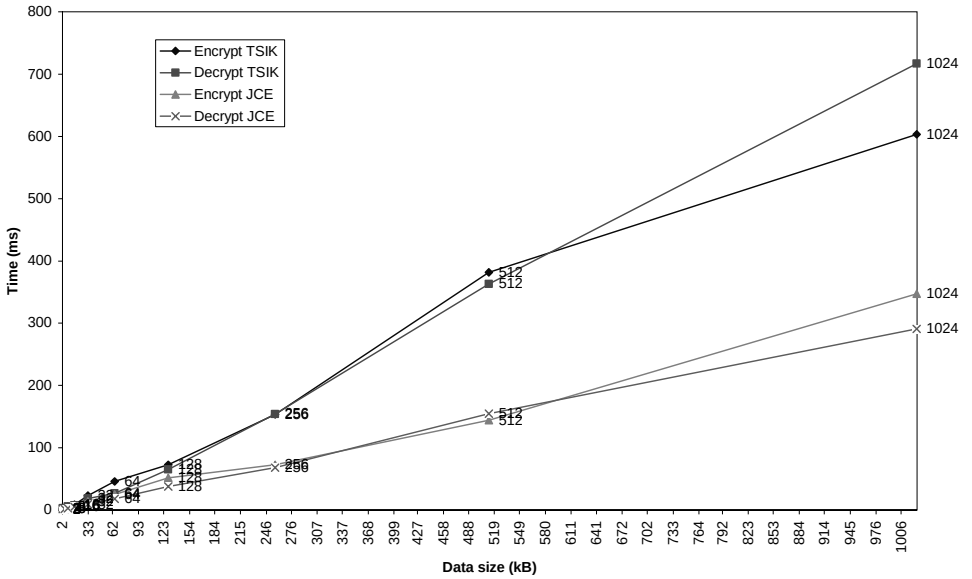

Figure 1: Triple DES encryption time

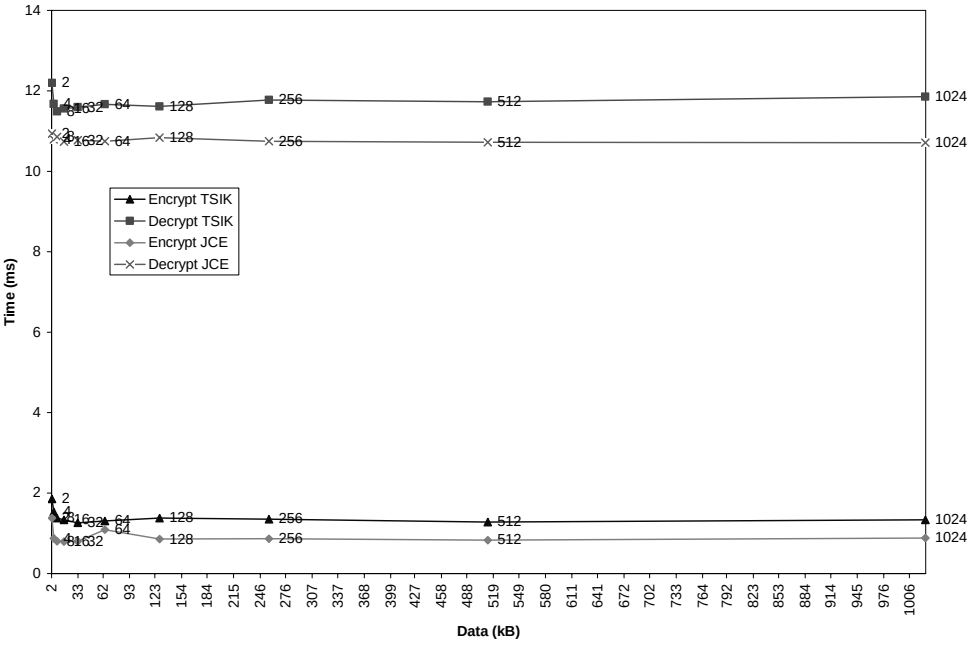

Figure 2: RSA-1024 encryption time of 168 bit Triple DES key

Experiment 1

Figure 1 shows that JCE performs noticeably better for large file sizes. It also shows that Triple DES encryption takes longer than decryption in both cases (TSIK and JCE). Note that the graph also indicates that for very large messages it is decryption that takes longer when using TSIK. We have no explanation for this, and suspect it has to do with the particulars of the implementation.

For RSA we see the opposite effect. Figure 2 indicates that RSA encryption takes less time than decryption. As we hinted at earlier in this paper, that is caused by the size of the keys used in encryption and decryption. For encryption, the public key is used, which has a small public exponent of 17 bits. When comparing TSIK with JCE, we see that the differences are minimal. Decryption varies by an average of about 1 millisecond between the implementations and encryption even less.

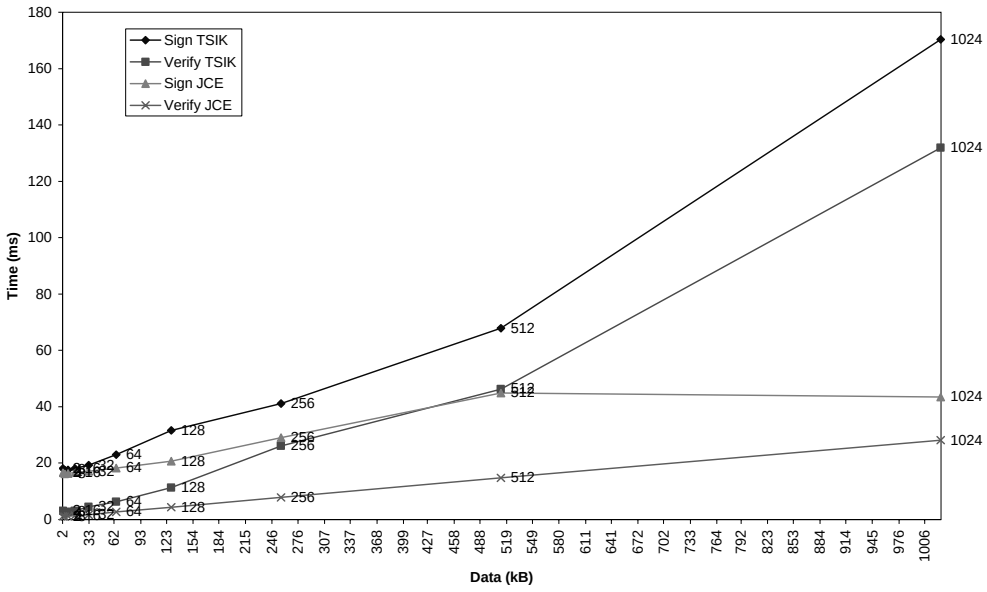

Figure 3: Message signing/verifying (using SHA-1 and RSA-1024)

Experiment 2

Figure 3 shows that signing takes more time in both cases. This is once again expected as the messages are signed using the large 1024 bit RSA private key. Encrypting the message digest should take constant time for each file size and so the graph pattern should be wholly due to SHA-1 hashing. Whereas signing and verification time increase steadily for JCE, TSIK performs markedly worse for large file sizes.

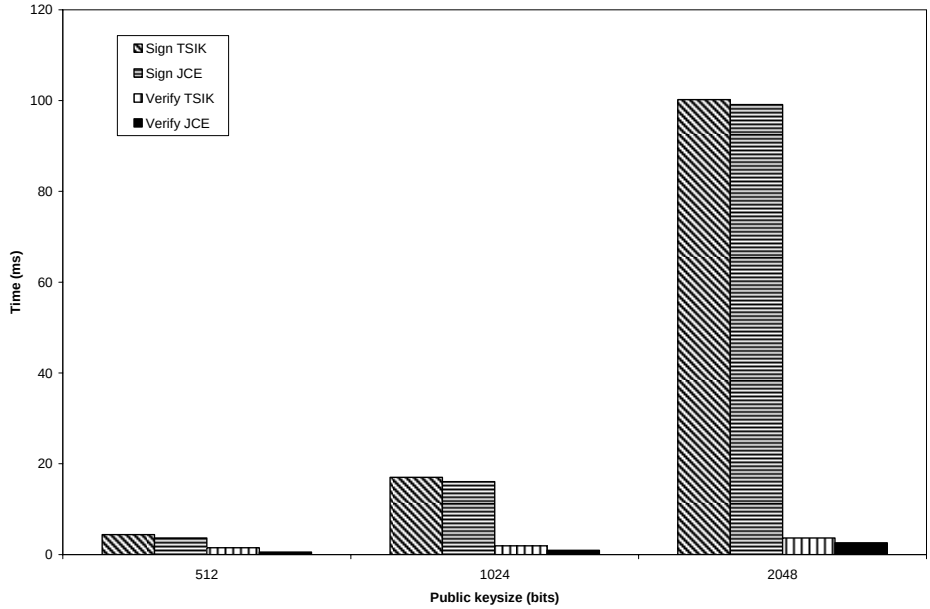

Figure 4: Message signing/verifying (2kB message size)

Experiment 3

The graph shows that doubling the RSA key size causes signing time to increase rapidly whilst having little effect on the verification time. This can partly be explained by the fact that doubling the key size effectively doubles the length of the private exponent (used in signing) whilst keeping the public exponent length constant.

6 Conclusion

TSIK is a toolkit to aid secure Web Service interactions. In this paper, we show through performance measurements that TSIK has comparable performance to Java's Cryptography Extensions (JCE). Its performance is similar to JCE, except that it slows down when processing messages with large plaintext sizes. It also provides adequate confidentiality, non-repudiation and sender authentication guarantees through the use of Triple DES and RSA, though should consider using SHA-256 for message verification in future releases as is suggested in recent literature [sha]. With respect to technical ability, TSIK appears to be a viable and competitive option in securing web based business interactions.

7 References

[Rat] Jason. Bloomberg, *Testing Web Services Today and Tomorrow*, Rational Edge, October 2002.

[Free] William Freeman and Ethan Miller, "An Experimental analysis of cryptographic overhead in performance-critical systems", *MASCOTS*, October 1999.

[Adams] Carlistle Adams and Steve Lloyed, *Understanding PKI second edition*, Addison-Wesley 2003 p14.

[Ronald] Ronald L. Rivest, Adi Shamir, and Leonard M. Adleman. "A method for obtaining digital signatures and public-key cryptosystems," *Communications of the ACM*, 21(2):120-126, 1978.

[Rivest] Ronald L. Rivest and Burt Kaliski, *RSA problem*, December 10, 2003.

[Hung] Hung-Min Sun and Mu-En Wu, *An approach towards Rebalanced RSA-CRT with short public exponent.*

[PKCS#1] RSA Laboratories, *PKCS#1 v2.1: RSA Cryptography Standard*, June 14, 2002.

[Dan] Dan Boneh, *Twenty Years of attacks on the RSA cryptosystem.*

[RFC3110] D. Eastlake, "RSA/SHA-1 SIGs and RSA KEYs in the Domain Name System (DNS)," *IETF Network Working Group*, RFC 3110, May 2001.

[Bellare] M. Bellare and P. Rogaway. "Optimal asymmetric encryption," In *EUROCRYPT* '94, Lecture Notes in Computer Science volume 950, pages 92-111. Springer-Verlag, 1994.

[RFC3447] J. Jonsson and B. Kaliski, "Public-Key Cryptography Standards (PKCS) #1: RSA Cryptography, Specifications Version 2.1," *IETF Network Working Group*, RFC 3447, February 2003.

[Wiener] M. Wiener. "Cryptanalysis of short RSA secret exponents," *IEEE Transactions on Information Theory*, 36:553-558, May 1990.

[Durfee] D. Boneh and G. Durfee. "Cryptanalysis of RSA with private key *d* less than $N^{0.292}$," *IEEE Transactions on Information Theory*, 46(4):1339-1349, July 2000.

[Shacham] D. Boneh and H. Shacham, "Fast Variants of RSA," *CryptoBytes*, 2002, Vol. 5, No. 1, Springer, 2002.

[xmldsig] http://www.w3.org/2000/09/xmldsig#

[xmlenc] W3C Recommendation, *XML Encryption Syntax and Processing*, http://www.w3.org/TR/xmlenc-core, 10 December 2002.

[tdes] http://www.w3.org/2001/04/xmlenc#tripledes-cbc

[Junaid] Junaid Aslam, Saad Rafique and S. Tauseef-ur-Rehman, "Analysis of Real-time Transport Protocol Security," *Information Technology Journal* 3 (3):311-314, 2004.

[sha] Arjen K. Lenstra, *Further progress in hashing cryptanalysis*, February 26, 2005.

[rsa15] http://www.w3.org/2001/04/xmlenc#rsa-1_5

[RFC2437] B. Kaliski and J. Staddon, "PKCS #1: RSA Cryptography Specifications Version 2.0," *IETF Network Working Group*, RFC 2437, October 1998.

[bounce] http://www.bouncycastle.org

The Impact of Network Bandwidth on Worm Propagation

Sam St. Clair-Ford, Mohamed Ould-Khaoua, Lewis Mackenzie

Department of Computer Science
University of Glasgow
Glasgow G12 8RZ
UK

***Abstract*- This paper evaluates the performance impact that real world ratios of different machine connection speeds has on worm propagation through a computer network. The impact is analysed on three different topologies, notably scale free, small world and random networks, to assess whether results are specific to a particular topology or taking bandwidth into account has an overall effect regardless of the topology in question.**

I. INTRODUCTION

The propagation speeds and the size of the infection base for viruses and worms to infect has increased dramatically over the years. From the Melissa virus in 1999 to the SQL Slammer worm in 2003 through to the MyDoom worm and its variants in 2004, machines connected to the Internet have been barraged with threats which could have an impact on a global scale. If an attacker could infect and gain control of a large number of machines then the damage they can do is immense, from ordering Distributed Denial of Service attacks on specific sites to harvesting confidential data and credit card information. Also they can sow misinformation from user's machines and have a major role in provoking warfare between nations and servicing terrorism across the world [1].

Research into simulating worm propagation and devising new ways of counteracting their spread has focused chiefly on the spread of warnings, [2-4] the detection and filtering of "malicious" traffic [3-6] and the inoculation of specific nodes to slow or stop the spread of infection [7-8]. However these studies have focused on the network at an abstract level to simplify network complexities. One of the main complexities that is missing is that of bandwidth capacity that each node is able to send and receive both worms and warnings. This paper will show that considering the bandwidth factor has a great impact on the outcome of any performance analysis.

The authors in [1] have introduced two theoretical worms, "Warhol" and "flash" worm, which could potentially infect every vulnerable machine in a few minutes or as a little as 30 seconds for flash worms. The limiting factor that restricts these worms is the bandwidth that an infected machine can send out copies of itself [9] and as such taking this parameter out of simulations will have an impact on being able to test new strategies against these potential worms.

CodeRed (crV2), the first worm to reach over 90% of vulnerable hosts in less than 14 hours [10] has been taken by much of the literature as being the benchmark to test new strategies against. However as the SQL Slammer or Sapphire worm showed in early 2003 that CodeRed is by no means the worst that could be unleashed on the internet. The SQL Slammer worm was the fastest spreading worm in history doubling in population size every 8.5 seconds, and showed the world what potential damage a

malicious worm could do.

One of the key differences between the two worms was that while Code Red was TCP based, in other words having to establish a connection with its destination, SQL Slammer was UDP based, needing no acknowledgement what so ever. On this principle it could invoke a fire and forget principle and could send out packets as fast as the particular channel could allow. In other words the SQL Slammer worm limiting factor was bandwidth based, restricted only by the connection speed of the infected host. Code Red on the other hand, was latency based, having to wait for a connection to be established before infecting the target host.

The SQL slammer worm therefore is a much closer approximation of what the worst case worms of [1] might look like and as a consequence this research looks into simulating such devastating worms that are only limited by bandwidth and seeing if previous models and solutions withstand such attacks.

II. BACKGROUND

In order to delay or prevent the spread of malicious viruses and worms there are three main areas that have been examined as possible strategies. Firstly the technique of intrusion detection where either machines or the network links themselves are monitored for potential threats. This is known as host based and network based intrusion detection for machine monitoring and network monitoring respectively. [3, 5, 6] have all highlighted the main drawback of these techniques, namely that of having a centralized detection system which handles all the monitoring for the network. Having this setup presents a single point of failure, that if exploited could turn the whole defence system against itself [11].

Another problem that intrusion detection techniques face is that of differentiating the malicious from regular traffic. These again fall into two main categories, anomaly and rule based detection. Rule based detection systems, as the name implies make decisions based on matching scenarios to a set of rules. Rules such as rejecting all packets from a particular source can be very effective if the rule set is well designed; however the system does have the weakness that it can't cope with attacks that it doesn't have a rule to deal with. Attacks that are novel and not expected will break such systems as the defences are not attuned to dealing with them.

To address this issue the alternative method of anomaly detection establishes a definition of what is normal traffic and anything outside this is deemed dangerous and in need of investigation. The natural problem that occurs of course is that of defining what is normal. Users may suddenly decide to use the network in a way that is different than normal or not expected and thus many false positives or false alarms may be raised. On the flip side, an attacker can work to the borderline of what is deemed normal slowing expanding this definition, if it is dynamically created, until creating an exploit is considered normal by the system.

An alternative to intrusion detection is that of broadcasting warning to machines to tell them to look out for a new attack, similar in principle to the media alerting the public to a particular threat. Following through with this analogy both situations are confronted with the same problem of how much to trust an information source. Furthermore there is the difficulty of warning potential targets faster than the worm can propagate [4].

The Indra project, [3] established in 2003 is a peer-to-peer based intrusion detection system that warns other peers when it detects dangerous traffic. Also following a similar peer-to-peer based system [2, 7] are designed to have peers encourage other nodes it considers to be friends to increase their defences in the case of an attack.

With regards to automated attacks such as viruses and worms the principle behind both these systems is the ability to find and compromise new hosts in order survive and propagate. Common methods to do this are email based propagation that rely on sending copies of a virus to email addresses found on a new victims machine, or exploit based propagation that rely on attacking a particular fault in a given application or operating system. Depending on the exploit further propagation can be made by either randomly scanning IP addresses until targets are found by chance or by having a pre-built list of vulnerable IP addresses which can be attacked [1]. In turn this list of vulnerable hosts can be generated by either doing the random scanning before the attack is launched, or by making use of the actual exploit. For example, if the exploit were in an application that is designed for network communication, such as a file sharing application or instant messenger then, assuming a significant portion of the users of this system use the same application to interact with each other, a network of vulnerable machines is already available to the attacking program.

As different infections can clearly use different methods of distribution, each of these methods can be regarded in terms of how their targets are connected. As with all networks, each one follows a particular topology, be it scale-free, random, lattice and so on, and as such, defences can be designed to exploit characteristics of these topologies. In their paper [8] Pastor-Satorras and Vispignani have explored immunization strategies for scale-free networks, focusing on immunizing specific highly connected nodes in order to quarantine an infection to a small section of the network.

Each of these defence techniques defines their relative results in terms of the fraction of nodes that were saved from infection and uses parameters such as propagation speed to define different kinds of infections. As well as this common theme of measurement they also have a common theme of expecting each node to behave in a similar manner, warning or infecting at the same speed. This research shows that if nodes have variable bandwidth then there is a large difference in the propagation rate of the worm.

III. System Model

This section describes real world scenarios and relates these scenarios to properties that the simulator will try to emulate and adjust. While it will relate to specific examples the simulator was designed to replicate properties of the scenario not just the particular scenario in question.

In order to examine the propagation of bandwidth limited worms the first consideration was to define what types of machines such worms will be targeted at. To emphasise this is a cross section of three different classes of machines were considered, from home systems running on dial up connections to broadband connections and finally high-speed university campus connections. The ratios for how these three classes of connection were divided up were taken from [13] by David Alderson where he describes that the distribution in connection speeds world wide is divided into these three main categories. These ratios are divided 50% 20% and 30% of internet users for the dial up, broad band and campus connections respectively.

Each of these nodes could be used for different purposes, from simple emailing to high bandwidth file sharing. In order to accommodate this, the bandwidth distribution was done two different ways; firstly connectivity based where high bandwidth capacities were allocated on a highest number of links first. To clarify, using the ratios described, the top 30% most connected nodes are allocated the campus speed connection, the next 20% are allocated the broadband connection and the remainder are left with dialup speeds. This method was selected to emulate a file-sharing network with high capacity nodes acting as hubs and taking up the slack of lower capacity nodes.

The second distribution method was that of random allocation, in order to replicate a network defined by email or instant messenger links. Logically connectivity should have no bearing on bandwidth load as a user's email ties can be accessed from different machines and therefore from potentially different connection speeds.

In examining different topologies, in order to justify confining a worm to follow a particular topology instead of just moving to any node it could successfully probe, this research assumes that the worm is designed with speed as a priority and as such will try to exploit any means necessary to reduce wasted scanning of large address spaces. In order to do this, the worm could use a number of strategies such as having a pre-built list of nodes that it can infect, or it could exploit a systems connection structure itself. Such exploits could be using email addresses stored on a machine, or peers that a file sharing program is currently connected to. This therefore confines the worm to following the topology that email contacts or file-sharing networks follow, giving this research its different topologies to examine.

The SQL Slammer worm propagates by using up all the available bandwidth. While the worm propagates from a particular machine all normal background traffic from that machine is prevented from reaching the network. Other machines which are not transmitting the worm still respond with the portion of their available bandwidth capacity not used by their background traffic

IV. Simulation Model

This section describes the design of the simulation model, the input parameters and metrics used in the performance analysis. Below are two tables that summarise the input and output parameters that have been used.

Table 1: Input Parameters

Name	Range/Value
Nodes	106
Iterations	5,000
Simulation Time	20,000
Topology	Scale-Free Small-World Random
Bandwidth	255,1,25,500
Bandwidth Distribution	Uniform, Connectivity based random

Table 2: Output Parameters

Name	Range/Value
Infected Nodes	0-106
Simulation Time	0-20,000

The number of nodes was set to 106 to replicate the network size set in [4] and also to allow for a faster run time of simulation. The value of 5,000 for number of iterations was set in order to assure the results were a fair average and that the output wouldn't be affected by a few anomalous simulations. The three that were chosen were selected to represent the three network topologies that infection strategies could spread across given their infection method. Scale-free to represent a topology of a file-sharing network[12] which could be exploited, small-world to represent the social network of email or messenger based exploits and random to represent a random scanning worm.

In order to get values for these speeds described in [13], a bandwidth tester provided by cnet.com[1] was used to probe different machines around the computer science department at the University of Glasgow. These probes where carried out at different times the day and different days of the week in order to gauge an approximation of a typical machine's connection speed. The average connection returned was 25Mbps and was taken to be the top speed that a single infected machine could transmit an infection.[2] For the broadband connection, different ADSL and cable suppliers were checked and an average of 1Mbps was taken as the broadband speed representation. The dial up was taken at 56Kbps as indicated by [13]

Taking these values with the university connection as the base unit, a broadband connection at a 25th of the speed was denoted logically as 25 times that value, and the dialup at 500 times that value. To get a uniform speed, these values combined with the ratios of the different speeds giving a value of 255.

In order to focus on whether these varying bandwidth rates had an effect everything else in terms of the virus propagation was fixed. The probability of a node infecting a neighbouring node was taken to be 1 however the time to transmit the infection was based on the bandwidth. The speed of the links is calculated as follows:

$$A_1 = C_1 / S_1 \quad (1)$$

$$A_2 = C_2 / S_2 \quad (2)$$

$$\text{If } A_1 < A_2 \text{ link} = \text{A}_1 \text{ else link} = A_2 \quad (3)$$

where C is the number of connections to a node and S is the nodes network connection capacity. With this setup the distribution of bandwidth is not optimally assigned, as the link is the smaller of the two connections and thus the larger connection has more bandwidth available to distribute to the other connections. While dealing with this complexity is outside the scope of this paper from the perspective of a spreading infection, unless a worm is aware of what connections its targets have, the logical option would be to distribute its available network capacity evenly in order to reduce wasted bandwidth given the limited information it has.

[1] This website: http://reviews.cnet.com/Bandwidth_meter/7004-7254_7-0.html was used to test the bandwidth

[2] The speed calculated was only the download speed and does not necessarily represent the upload capacity. This limitation has been acknowledged and will be addressed in future work

B. ASSUMPTIONS

- Probability of a targeted node being infected is 1
- No defensive strategies such as immunization or warnings allowed
- Random node and link failure or node recovery is removed from the simulator

The reason for a probability of 1 is that this simulator defines a worst case scenario where it is the bandwidth of a node that decides how soon a neighbouring node becomes infected. Relating this to a real world situation, the infected source node sends out copies to a limited set of known targets and as such sends copy after copy until the target node is infected. As this is the worst case scenario then the first copy of the worm always reaches its destination representing a probability of 1.

The reason for removing node failure and node recovery from the simulator is two fold. Firstly, as this is simulating a fast spreading worm, or a worm that travels faster than human intervention could occur, then a node cannot recover within the simulation time window; i.e. the length of time it takes for all nodes to become infected. With regards to node and link failure, a link or node failure from a spreading worm's perspective would be equivalent to an immunization defensive strategy and therefore would not constitute a worst case scenario.

IV. RESULTS OF THE SIMULATIONS

Figures 1, 2 and 3 show a similar pattern of propagation for both variable and identical capacity nodes, suggesting that the effect of variable bandwidth capacities is not tied to any particular topology, but is a common property that could have an effect on any propagation models that are looking at bandwidth limited worms.

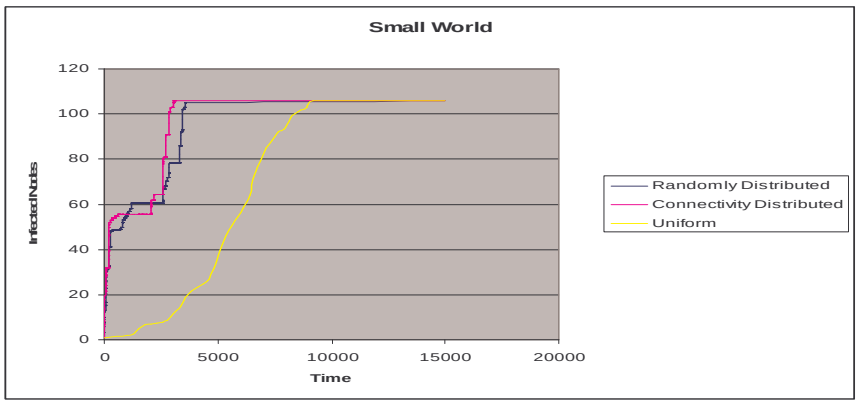

Figure 1: Small World topology to represent a worm propagating across a social network

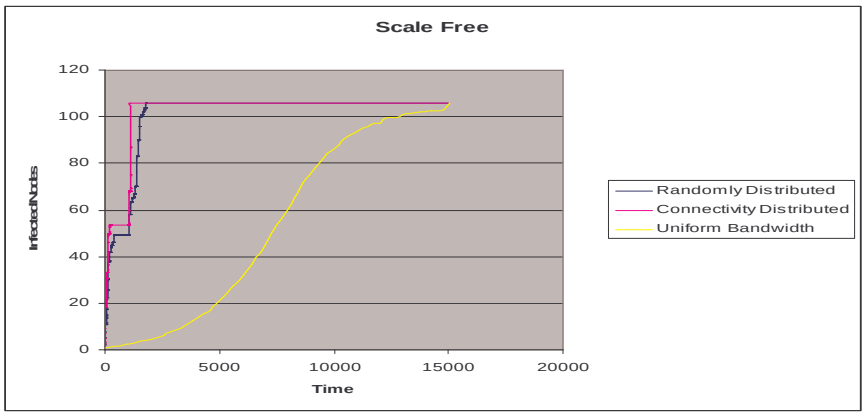

Figure 2: Scale Free topology to represent a worm propagating across peer to peer file sharing network

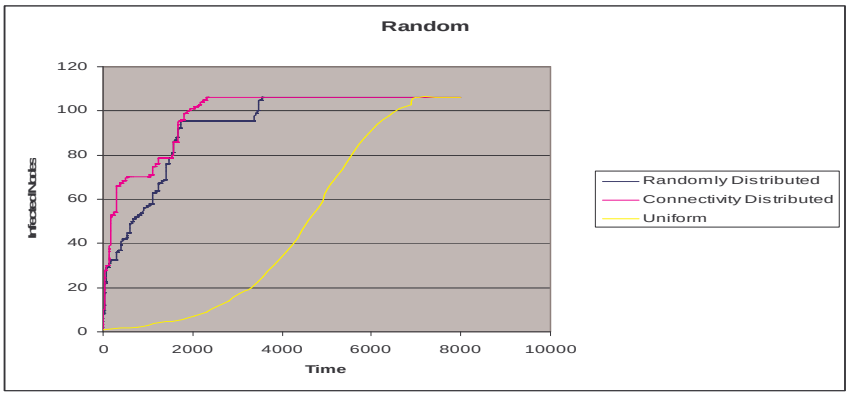

Figure 3: Random Topology to represent a worm propagating by following a random hit-list

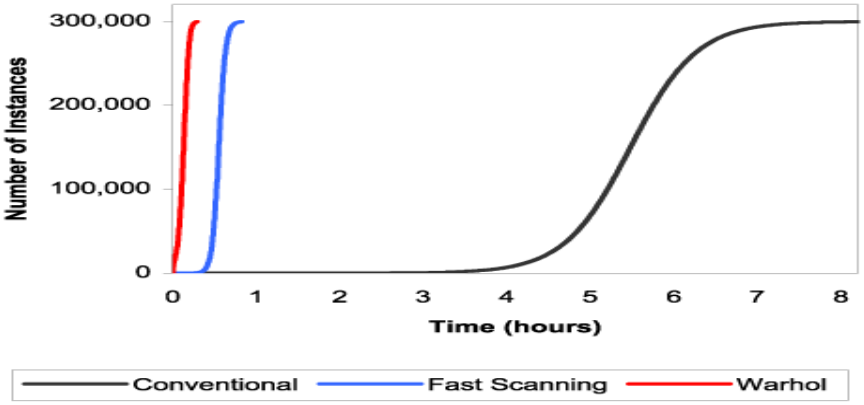

Figure 4: The potential infection speed for a Warhol worm. Figure taken from [1]

As can been seen on any of the figures, the propagation speed is much more severe for variable node bandwidth as there is the possibility of finding a few fast routes through the network due to the wide range of different possible connection speeds. While 50% of all the nodes are almost twice as slow for the variable bandwidth as they are for the uniform speed network there are a few high speed nodes that the simulators results show can more than make up for this weakness.

While the uniform bandwidth simulations follow that of a sigmoid function, trailing off as they near complete infection of the network, the variable bandwidth graph goes in almost two waves, with a slight pause in the middle before very virulent propagation once again. This pause is due to all the fast connections finishing infecting everyone they are aware of while the slower connections are still transmitting the worm to other hosts. Even with this delay the propagation speed is much faster, over 25 times faster (in Figure 2, the difference between variable bandwidth distribution and static bandwidth at time 1000) in some cases and is a good representation of the Warhol worm shown in Figure 4.

VI. CONCLUSIONS

Our above performance results have revealed that varying the bandwidth has a major effect on how a bandwidth limited worm propagates in a network of varying capacity nodes. Moreover, a random distribution of capacities produces similar results to allocating bandwidth based on connectivity suggesting that possible immunization strategies taking bandwidth into account might prove to be an effective countermeasure to such worms.

This research has considered the worst case scenario, that is no defence strategy has been implemented, and as such in order to enrich the simulator, other scenarios need to be examined. In particular, the immunization and warning strategies could have a significant effect if node selection includes taking node bandwidth into account. One of the assumptions used in this study is that nodes do not recover and so if this were relaxed then a long term analysis could be made into looking into if there is a particular threshold that could sustain a worms spread given a variable bandwidth scenario.

Another potential area is to examine is the limiting factors of the present simulation experiments, namely the bandwidth ratios, the values used in the simulator and efficient bandwidth distribution. With the numbers of broadband subscribers rising all the time, the ratios that were given would naturally change over time, and as a result changing the ratios to reflect possible future connection distributions could have an effect on how to develop better protection strategies.

REFERENCES

[1] Stuart Staniford, Vern Paxson and Nicholas Weaver. How to 0wn the Internet in Your Spare Time. Proceedings of the 11th USENIX Security Symposium, August 2002.

[2] Vasileios Vlachos, Stephanos Androutsellis-Theotokis, Diomidis Spinellis. Security applications of peer-to-peer networks. Computer Networks 45: 195-205 (2004).

[3] R Janakiraman, M Waldvogel, Q Zhang. Indra: A peer-to-peer approach to network intrusion detection and prevention. Proceedings of IEEE WETICE 2003.

[4] Li-Chiou Chen and Kathleen M. Carley. “The Impact of Countermeasure Propagation on the Prevalence of Computer Viruses”. IEEE Transactions on Systems, MAN, and Cybernetics-Part B: Cybernetics, Vol. 34, No. 2, April 2004.

[5] Srinivas Mukkamala and Andrew H. Sung. A Comparative Study of Techniques for Intrusion Detection. Proceedings of the 15th IEEE International Conference on Tools with Artificial Intelligence, 2003.
[6] Anita K. Jones and Robert S. Sielken. Computer System Intrusion Detection: A Survey, Technical report. Computer Science Department., University of Virginia, 2000.
[7] C.G. Senthilkurnar and Karl Levitt. Hierarchically Controlled Co-operative Response Strategies for Internet Scale Attacks. Computer Science Department, University of California , 2003.
[8] R. Pastor-Satorras and A. Vispignani. Epidemics and immunization in scale-free networks. ACM conference on Computer and Communications Security, Proceedings of the ACM workshop on Rapid Malcode, 2003.
[9] Tom Vogt. Simulating and optimising worm propagation algorithms. SecuriTeam.com review 23rd Oct 2003.
[10] David Moore and Colleen Shannon. The Spread of the Code Red Worm (CRv2) analysis. www.caida.org July 24, 2001.
[11] Thomas H. Ptacek. Insertion, Evasion, and Denial of Service: Eluding Network Intrusion Detection. Secure Networks Inc. 1998.
[12] Matei Ripeanu, Adriana Iamnitchi and Ian Foster. Mapping the Gnutella Network. IEEE Internet Computing, IEEE Educational Activities Department Piscataway, 2002.
[13] David L. Alderson. Technological and Economic Drivers and Constraints in the Internet's "Last Mile". Engineering and Applied Science, MS 107-81 California Institute of Technology March 2004.

Constructing Reliable and Efficient Overlays for P2P Live Media Streaming *

Stephen A. Jarvis, Guang Tan, Daniel P. Spooner and Graham R. Nudd
Department of Computer Science, University of Warwick,
Coventry, CV4 7AL, United Kingdom
{saj,gtan,dps,grn}@dcs.warwick.ac.uk

Abstract

For single-source, single-tree-based peer-to-peer live media streaming, it is generally believed that a short (and wide) data delivery tree provides the best comprehensive performance in terms of reliability and service delay. While a short tree directly benefits delay optimization, it is unclear whether such a structure maximizes reliability, which is sometimes more critical for a streaming Internet service. This paper compares several prevalent overlay construction algorithms in terms of (1) service reliability; (2) service delay and (3) protocol overhead. A new *Heap Algorithm* is proposed to enhance reliability by leveraging the peers' time properties while maintaining a short tree, which in turn helps to reduce service delay. This new algorithm dynamically moves peers between different layers of the tree according to a simple metric called *Service Capacity Contribution* (SCC), and gradually adjusts the overlay toward a short tree with peers ordered in time. Extensive simulations show that this new algorithm achieves better comprehensive performance than existing algorithms.

1 Introduction

There has been a good deal of research in recent years on the topic of live media streaming services over the Internet [3][4][12][16]. Due to the stringent requirements on network resources and increasing market demand, the traditional client-server framework faces significant challenges. For example, during busy periods, the server's bandwidth may easily be overwhelmed by a surge in the client population. A direct solution to this problem is upgrading the server system hardware or clustering a large number of single systems into a server farm. However, this approach will only scale so far. Dedicated content distribution networks (CDN) provide an alternative solution, however its prohibitive deployment costs make it uneconomical for many small- or medium-sized sites.

Given the fact that IP multicast has not been widely deployed and this situation is unlikely to improve in the near future, the peer-to-peer (P2P) paradigm offers an attractive solution. In this architecture, the clients or peers help to relay the received content to other clients and thus form a large content distribution network. This approach is

*This research is sponsored in part by grants from the NASA AMES Research Center (administrated by USARDSG, contract no. N68171-01-C-9012), the EPSRC (contract no. GR/R47424/01) and the EPSRC e-Science Core Programme (contract no. GR/S03058/01).

perfectly scalable in the sense that available bandwidth increases with the growth of the network. Even if the source server can support only a limited number of concurrent clients, the data can be distributed to a large network population in a self-scaling manner. In the context of live media streaming, the peer-to-peer transfer mode mostly serves to complement the client-server mode, since a number of clients will need to receive the content from the server first-hand.

An overlay of peers is often viewed as a tree rooted at the content provider. To provide satisfactory quality of service (QoS), the data delivery tree needs to address three problems: (1) to reduce the impact of peer dynamics – peers are free to join and leave at any time, and abrupt departure or failure of a node will result in service interruptions on all of its descendants in the tree. Losses due to such failures are more significant than regular packet losses in the physical network and may cause streaming breaks in the order of tens of seconds; (2) to minimize end-to-end service delay – transfers over the logical overlay generally involve longer delays than unicast in the physical network, and hence introduce a prolonged startup delay and increase network dynamics to the streams; (3) to maintain a reasonable overhead – peers may need to reconnect to other peers for the purpose of overlay adjusting, which usually requires coordination among multiple peers. In a distributed environment lacking time synchronization, such operations may require transient pauses in the streaming.

Given a set of peers with heterogenous out-degrees (limited by the actual bandwidth resource and under the condition that no network congestion occurs near the nodes), it is generally believed that a short (and wide) tree provides a good peer structure [12][19][16][7] for meeting these requirements. Intuitively, the shortness helps to reduce the probability of service breaks due to the departure, failure, or congestion at an ancestor node, and hence enhances tree reliability. A short tree also means a small average hop count from the root to the peers, and this helps to minimize the average network delay if the peers are appropriately mapped to the physical network.

For the tree to be reliable, Sripanidkulchai et al. proposes another approach [16] which leverages the peer's time property: if the peers' lifetimes follow a distribution with a long tail, then the older peers are less likely to leave before the younger ones. This characteristic has also been observed in a number of statistical studies [20][15].

This paper presents a new overlay construction algorithm, namely the *heap algorithm*, which leverages peers' properties in both bandwidth and time. It moves high-bandwidth and long-lived peers upward in the tree according to a metric called *service capability contribution* (SCC), which is defined as the product of a peer's outbound bandwidth (or simply called bandwidth) and its age in the overlay. This way the tree is gradually adjusted toward a layout which exhibits partial time order and partial bandwidth order, and consequently has the advantages of high reliability and a short tree. Besides the overlay-level operations, the heap algorithm uses a simple parent switching technique to re-map the parents to children so that the actual network delay can be minimized.

When designing the algorithm, the overlay adjusting cost (called the protocol overhead in this paper) is also an important consideration, since it has an immediate effect on the overlay optimization quality, and also reflects the overhead imposed on the end-users and is thus directly related to the QoS.

Simulations have been conducted to compare the performance of different algorithms. The results show the advantages of the heap algorithm over existing schemes in a variety of performance respects.

The rest of the paper is structured as follows. Section 2 introduces several existing methods; Section 3 gives a detailed description of the algorithm; Section 4 introduces

the simulation methodology; Section 5 presents the experimental results and Section 6 concludes the paper.

2 Existing algorithms

A peer tree has its root at the content provider, and organizes all M peers in layers $L_0, L_1, \cdots, L_N$, with L_0 consisting of the root, L_1 consisting of all peers directly connected with L_0, and so on. Generally, $L_i (i >= 1)$ receives data from L_{i-1} and forwards it to L_{i+1}. Each peer has an *out-degree* $d \geq 0$, which is defined as the number of children it can serve simultaneously. A peer in the tree is also called a *node*.

A central part of the tree management is the so-called *parent selection* strategy, which identifies a parent for a newly arriving peer. This strategy is crucial to shaping the tree. A selection of the more significant existing algorithms include the:

- **Random algorithm** that provides the the simplest approach [16] to parent selection. It randomly chooses a node with spare bandwidth capacity as the parent for a new peer. Clearly this algorithm is efficient and requires no global topological knowledge, but it results in a large tree depth and thus performs badly in almost all other performance respects.

- **High-bandwidth-first algorithm** [7] that places the peers from high to low layers in a non-increasing order of outbound bandwidths, that is, peers do not have more bandwidth capacity than any peer higher up in the tree. See Figure 1 (a) for an example. This algorithm allows later arriving peers to preempt the positions of existing peers with smaller bandwidths. This approach can achieve a minimum tree depth, but needs frequent disconnections and reconnections between peers to maintain such a globally ordered layout. For example, if node *a* in Figure 1 (a) leaves, then node *b* should be moved to node *a*'s position, which further forces all of node *b*'s children rejoin the tree. This recursive rejoin imposes very high overheads on the peers and is therefore impractical for real implementations. The overhead of disconnections and reconnections for maintenance purposes is termed the *protocol overhead*, which should be differentiated from service interruption since the connection tear-downs and re-establishments can be performed in a coordinated manner and therefore avoid unexpected breaks in the streaming.

- **Minimum depth algorithm** obtains a tradeoff between simplicity and high overheads [7][12][16]. It searches from the tree root downward to the leaf layer to identify a parent with spare bandwidth capacity for a new peer. A variant of this approach is also proposed [11] so as to reduce the reliance on an understanding of the global overlay topology; this algorithm combines the heuristics of the minimum depth algorithm with some randomness, i.e., it first selects a number of peers randomly from the overlay and then performs the minimum depth algorithm.

- **Longest-first algorithm** [16] is intended to minimize service interruptions incurred by the departure of peers. It selects the longest-lived peer as the new peer's parent; the intuition behind this is that when the peers' lifetime follows a heavy-tailed distribution, the older peers generally remain longer than younger peers. This approach has been verified by the experimentation found in [16], the algorithm does not however guarantee that an older peer can always be identified.

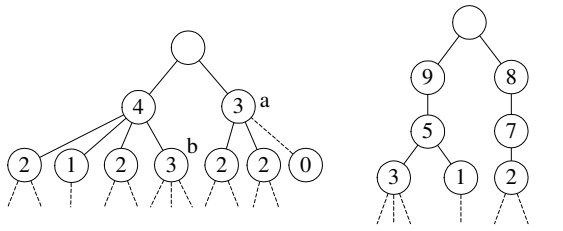

(a) Bandwidth-ordered tree (b) Time-ordered tree

Figure 1: Examples of the bandwidth-ordered and time-ordered trees. The numbers in (a) and (b) represent the peers' outbound bandwidths and ages, respectively.

Of these algorithms, the high-bandwidth-first algorithm and the random algorithm achieve optimal tree depth and protocol overhead, respectively. The longest-first algorithm can be easily extended to generate a more reliable tree by placing the peers in order of arrival time (or ages) order, just as in the bandwidth ordering performed by the high-bandwidth-first algorithm. Figure 1 (b) gives an example of this type of tree. Clearly, the time ordering may result in a tall tree because it arranges the peers regardless of the peers' bandwidth properties, which themselves determine the tree shape. Moreover, this approach requires position adjusting when peers rejoin the tree after failures occur, and thus incurs higher protocol overheads. Hereinafter, the extended longest-first algorithm is termed the *time-ordered algorithm*, and a tree constructed by such an algorithm is termed a *time-ordered tree*. Likewise, the high-bandwidth-first algorithm is termed the *bandwidth-ordered algorithm* which builds a *bandwidth-ordered tree*.

While the bandwidth-ordered tree achieves a short tree which helps minimize service delay, it is unclear how tree reliability can be maximized: on the one hand, the short tree reduces the average number of peers affected by a failed node, while on the other hand, the time-ordered tree, at the expense of a large depth, enhances the reliability of an arbitrary top-down tree path. The main driver of this research is the following: Is it possible to construct a peer tree that achieves time ordering to some degree, while attaining the characteristics of a short tree; that is, can reliability and service delay can be improved at the same time?

3 The Heap Algorithm

This section describes the proposed heap-based approach. Its performance implications are also discussed qualitatively.

3.1 Fundamental approach

The heap algorithm uses the same strategies for peer joining and leaving as the minimum-depth algorithm. The only difference lies in the sift-up procedure during the normal streaming process. The criteria guiding the sift-up procedure is a metric $SCC = B \times T$, where B is the outbound bandwidth of a peer and T is its age. As such, SCC can be alternatively interpreted as the volume of media data one peer has helped to (or can) forward, and thus can be regarded as its "service capacity contribution" to the peer community. The basis of the algorithm is to move peers with large SCC's higher in the tree so that better service quality (less service interruptions and possibly smaller service delay) can be offered to these peers. This has an interesting result: since either

a large bandwidth or a long service time helps to increase SCC, a peer can be encouraged to contribute more bandwidth resource or longer service time as a trade for service quality. From the user perspective, this forms an incentive mechanism that encourages cooperation among peers and helps increase overall system resources. Note that the use of a dynamic metric combining both bandwidth and time properties differentiates this mechanism from other incentive schemes [4][10], which themselves usually consider only a static metric such as bandwidth.

3.2 The sift-up operation

The root is pre-assigned an infinite SCC, and always remains at the top of the tree. When a peer enters the network, its SCC is 0, and it will be placed using the same join operation as in the minimum-depth algorithm. In most cases, the high layers are occupied and the new peer becomes a leaf node. As time continues, the SCC increases at a rate proportional to its bandwidth. If its bandwidth is larger than its parent, then there must exist some time in the future when its SCC exceeds its parent. At that time the algorithm will exchange the roles of these two nodes. Figure 2 gives an example of this operation.

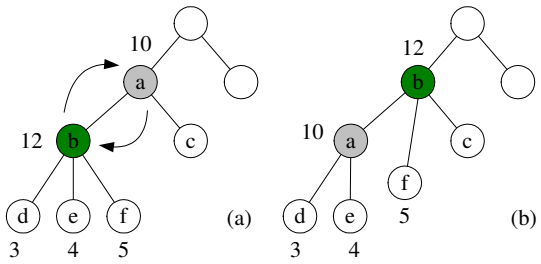

Figure 2: Illustration of the sift-up operation. (a) Before sift-up; (b) After sift-up. The numbers beside the nodes represent the SCCs.

In Figure 2 (a), node a's SCC is 10 and has an out-degree of 2; node b has an SCC of 12 and an out-degree of 3. Node b is therefore moved up to become the parent and node a is moved down to become the child. Now that node a can support only two of the three nodes d, e, f, one child must be assigned a new parent. The algorithm chooses f, the node with the largest SCC and reconnects to node b, which now has a spare out-degree. Node f is promoted because it has contributed the largest "service capacity" among all its siblings.

The sift-up is performed periodically over all peers. At set time intervals, the algorithm scans from the leaf layer to the first layer and updates the SCCs of all peers. At the same time, it checks if a node has a smaller SCC than one of its children. If so, it picks the child with the largest SCC and compares its own bandwidth with that child. If the child's bandwidth is larger, the sift-up will be performed between these two nodes. The bandwidth comparing avoids unnecessary sift-up since if the child has a smaller bandwidth, the SCC will eventually be exceeded by the parent, and it will ultimately be placed below the parent. The sift-up operation is illustrated in Algorithm 1.

With the sift-up operations, the tree nodes will be placed in the tree from the high to low layers in decreasing order of SCCs. This ordering process is analogous to the sift-up operation in the conventional Heap Sort algorithm, and thus we name this new approach the "heap algorithm".

Algorithm 1 Sift-up

```
1: for i = N to i = 1 do
2:   for all P(j) in L(i) do
3:     Scc(j) ← B(i) × A(i) {update SCC}
4:     c ← the first child of P(j)
       {find the child with maximum SCC}
5:     for all P(k) that is P(j)'s child do
6:       if Scc(k) > Scc(c) then
7:         c ← k
8:       end if
9:     end for
       {sift-up the child peer c}
10:    if Scc(c) > Scc(j) and B(c) > B(j) then
11:      for r = 1 to r = D(j) do
12:        s ← child of P(c) with minimum SCC
13:        P(s).parent ← P(j)
14:        remove P(s) from P(c)'s children list
15:      end for
16:      grandp ← P(j).parent
17:      P(grandp).child ← P(c)
18:      P(c).parent ← P(grandp)
19:      P(c).child ← P(j)
20:      P(j).parent ← P(c)
21:    end if
22:  end for
23: end for
```

The algorithm moves peers up the tree in a gradual manner. This accounts for the fact that many peers may leave within a short time after their arrival [20][17], resulting in a large number of service interruptions if they are placed high in the tree upon arrival. In contrast, placing a new peer at the leaf layer first and then adjusting its position according to its behavior can reduce this risk. The longer a peer stays in the network, the safer it is to be moved up the tree.

The sift-up procedure requires a per-node operation which involves an updating of the SCC, and potentially a peer exchange. The peer exchange requires $\overline{d}$ time, where $\overline{d}$ is the average out-degree of the peers. So each pass of the sift-up operation requires $O(M)$ time.

3.3 Topology-aware delay optimization

A short overlay path does not necessarily means a short network delay due to the mismatching between the logical overlay network and the physical underlying network [9]. The heap algorithm addresses this problem in two ways. First, when a peer initially joins the network, the algorithm provides a number of candidate parents, of which the nearest will be chosen. Second, for peers that are already in the network, the algorithm uses a parent switching technique to dynamically re-connect the peers so that the average network delay between the peers remains optimal.

Parent switching is performed between any two consecutive layers, (e.g., L_k and L_{k+1}). An example is given in Figure 3: due to changes in the underlying network,

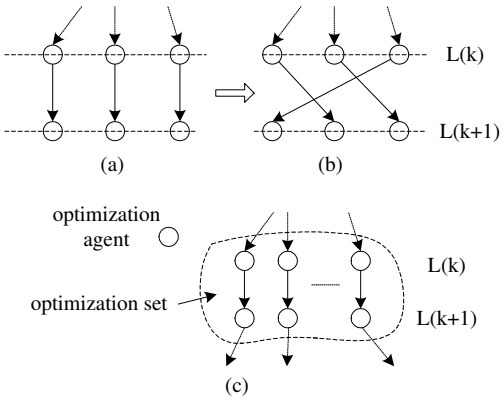

Figure 3: Topology-aware delay optimization.

the optimized mapping between the three pairs of peers in (a) is transformed to the mapping in (b) to minimize the average delay. It can be seen that this combinatorial optimization problem is NP-hard and when the number of peers in each layer is large (e.g. 2000), it can only be resolved using some approximate algorithms.

The heap algorithm assigns to each peer upon arrival an *optimization agent*, which is selected from the peers that have existed for a relatively long time and are thought to be stable. During the streaming service, peers exchange neighbors information between each other and periodically measure the network distances (in terms of delay) between themselves and other peers, including their immediate neighbors, and the neighbors' neighbors, and so on. These data are reported to their optimization agent, which periodically computes for a good solution for the peer mapping problem using a genetic algorithm. The agent does not necessarily compute for all its associated peers, instead it randomly selects a subset of peers, which form an *optimization group*. A limited population size in the genetic algorithm allows a good solution to be obtained quickly, and thus is more suitable for a dynamic environment. When a solution is obtained, the agent coordinates the peers to adjust their connections. If an agent leaves, its associated peers simply request from the server for a new agent. Figure 3 (c) illustrates the optimization agent and grouping.

The approach of switching trees has also been studied in [8][2][9]. While these studies make use of fully distributed optimization schemes, the heap algorithm uses a hybrid approach: a subset of peers are optimized by a single agent, and there are multiple such agents in the network. This mechanism has the advantage of being simple to implement. For example, Banerjee et al. define five deterministic local transformations and one probabilistic transformation, which make the protocol much more complicated. The switch-tree in [8] also defines multiple transformations. These distributed algorithms generally have a slower convergence speed than a centralized scheme, which means they may require more reconnections between peers than the proposed hybrid approach.

3.4 Discussion

Accurate bandwidth estimates are critical for the heap algorithm and they should not entirely rely on the users' settings. In the heap algorithm, the user-advertised band-

width is only taken as an upper bound; actual bandwidth estimates are derived from the active end-to-end measurements as described in [5]. When a peer joins, its outbound bandwidth is set to zero, and an active measurement is launched between itself and another peer in the leaf layer. The measured bandwidth is then used in the calculation of SCC. To keep the estimate up to date, the bandwidth is measured periodically for peers whose bandwidths have not been fully utilized. The techniques of choosing the end host to transfer testing data, smoothing estimation and estimate discretization all follow the methods introduced in [5].

A peer tree resulting from the sift-up operation integrates the characteristics of both the bandwidth-ordered and time-ordered tree, since the peers are adjusted with a metric that mixes bandwidth and time properties, and those peers at the higher layers either possess high-bandwidths or long lifetimes, or both. As a hybrid of the two types of baseline tree, the new tree is expected to inherit their merits in both tree depth and tree reliability.

4 Simulation methodology

An event-driven simulator has been developed to study the performance of the different algorithms. The following five algorithms are implemented:

- Minimum-depth algorithm: This algorithm follows that in [16][12][7], but with a minor modification – when a layer that can support a new peer is found, the new peer chooses the nearest peer in terms of network delay (from up to 200 peers) in that layer as its parent. Since in practise a tree hierarchy may have thousands of peers in a layer, imposing a limit to the number of candidates would be more practical for implementation;

- Longest-first algorithm: This follows the scheme presented in [16].When a new peer chooses its parent from the highest possible layer, it always chooses the oldest peer (from up to 200 peers) in that layer.

- *Relaxed bandwidth-ordered algorithm* and *Relaxed time-ordered algorithm*: These are two variants of the bandwidth-ordered and time-ordered algorithms as introduced in Section 3. The (strict) bandwidth-ordered and time-ordered trees are found to have a extremely high protocol cost, which makes them unacceptable in practise and only of theoretical value. Therefore, a modification is made to make the compared scenarios more realistic – when a peer joins/rejoins the tree, it always searches from the high to low layers to see if there is a smaller-bandwidth or younger peer, and if so, the identified peer is replaced with the new one. The evicted peer, and possibly together with some of its children in the case of time ordering, are forced to rejoin the tree. This results in bandwidth/time ordering locally within each layer and among parents and children, but not in a strict hierarchical structure; that is, a peer may have a smaller bandwidth/age than another non-child peer in the next layer. Since they still follow the basic ideas of bandwidth/time ordering, they are used for performance comparisons.

- Heap algorithm: This is implemented as introduced in Section 3, but with the parent switching disabled. It should be noted that such a technique can be applied to any of the other algorithms previously documented. Disabling this component helps to reveal the performance of the proposed algorithm in its “naive” form, and also avoids any bias in comparison with other algorithms.

The GT-ITM transit-stub model [21] is used to generate an underlying network topology consisting of 15600 nodes. Link delays between two transit nodes, transit nodes and stub nodes, and two stub nodes are chosen uniformly between $[15, 25]$ ms, $[5, 9]$ ms and $[2, 4]$ ms, respectively. Of all the 15360 stub nodes, a fraction of them are randomly selected to participate in the peer tree. The server's location is fixed at a randomly chosen stub node.

In all simulations, the root node's bandwidth is set to 100; the peers' outbound bandwidths follow a Bounded Pareto distribution[1] with shape, lower bound and upper bound parameters set to 1.2, 0.5 and 100 respectively (denoted by BP(1.2, 0.5, 100)), with which 55.5% of the peers have out-degrees less than 1 and are therefore termed "free-riders"; the peers' lifetimes follow a lognormal distribution with the μ (location parameter) and σ (shape parameter) set to 6.0 and 2.0 respectively (denoted by LN(6.0, 2.0)), which are chosen according to the findings in [20].

The simulation considers different network scales in terms of the average number of peers M in a steady state. According to *Little's Law*, the peer arrival rate λ is determined from M divided by the mean value of LN(6.0, 2.0). For the heap algorithm, the sift-up operation is performed every time 200 new peers join by default. Other selections of parameters are also tested and the results are found to be consistent.

5 Performance evaluation

This section presents and discusses the performance results with respect to service reliability, service delay, protocol overhead and the impact of sift-up frequency on tree depths.

5.1 Service reliability

Service reliability is measured by the average number of service interruptions experienced by a single peer during its lifetime in the steady state of a tree. The experiments consider the extreme case in which every peer departs abruptly without notification to others, and hence results in a service interruption on each of its descendants. This metric reflects the stability of a tree in the most uncooperative and dynamic environment.

Figure 4 compares the performance of the five algorithms under different network sizes.

As expected, the minimum-depth algorithm performs the worst in most cases, because it is designed completely blind of reliability. The longest-first algorithm has very limited improvement over the minimum-depth algorithm, as it operates in a very conservative way when ordering the peers' times.

It is surprising to see that the relaxed time-ordered algorithm performs worse than the heap algorithm. There are two reasons for this: first, the heap algorithm also achieves a partial time order in the process of sift-ups (the older peers are gradually moved upward in the tree), and consequently benefits from this in terms of reliability; the second reason is that the heap algorithm builds a much shorter tree than the relaxed time-ordered algorithm, which means that a failed node generally introduces fewer service interruptions to its descendants.

[1] Previous studies [15][16][14] have shown that the bandwidths of peers exhibit characteristics of heavy-tailed distributions, a typical example of which is the Pareto distribution. Considering the practical limits of possible bandwidth values, a bounded Pareto distribution is used to model the peers' bandwidths.

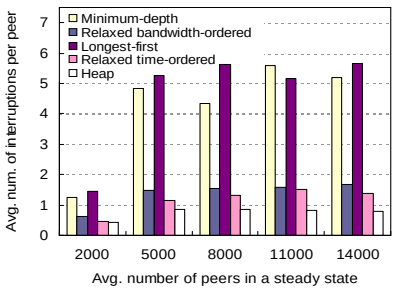

Figure 4: Comparison of reliability.

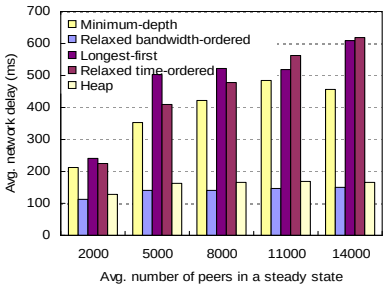

Figure 5: Comparison of service delays.

Therefore, with the advantages of both bandwidth-ordering and time-ordering, the heap algorithm appears to be a scheme that produces the most reliable tree among all the algorithms examined.

5.2 Service delay

The metric *average service delay* measures the actual physical network delay from the root to the peers. Figure 5 plots the results obtained under different network sizes. All the values are averages over a certain number of samples in a steady network state. It can be seen that the heap algorithm significantly outperforms all other algorithms with the exception of the relaxed bandwidth-ordered algorithm. This shows how bandwidth-ordering benefits the tree depth, even though it is only implicitly and partially realized.

Compared with the relaxed bandwidth-ordered tree, the heap algorithm has a small increase of 10-15%. This is because the heap algorithm optimizes the layout in a more confined space (only along the child-parent paths regardless of the bandwidth order between siblings), and hence yields a more sub-optimal bandwidth layout.

5.3 Protocol overhead

Both bandwidth ordering and time ordering require re-establishment of connections between certain peers to optimize the layout of the tree, thus introducing a protocol overhead. This overhead is measured in the average number of re-connections imposed on a single peer during its lifetime. Figure 6 compares the protocol overhead of the five algorithms. Note that the minimum-depth algorithm and the longest-first algorithm do not impose any protocol overheads at all; they are plotted in the figure with small values for convenience of observation.

The results show that the relaxed time-ordered algorithm yields the highest overhead, and the heap algorithm is better the relaxed bandwidth-ordered algorithm. Besides which, the relaxed bandwidth-ordered algorithm and the heap algorithm both require less than one reconnection for a single peer during its lifetime. This should be at an acceptable level for a practical system.

5.4 Impact of sift-up frequency

Intuitively, the more frequently the sift-up operations are performed, the more chance there is for the tree to be optimized, and consequently the higher overhead on the tree manager. To show how the sift-up frequency impacts on the service delay, Figure 7

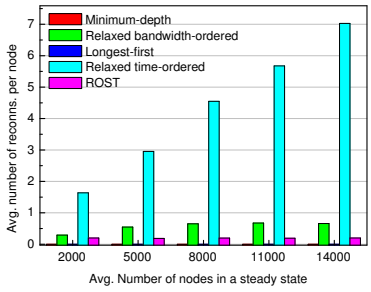

Figure 6: Comparison of protocol overheads.

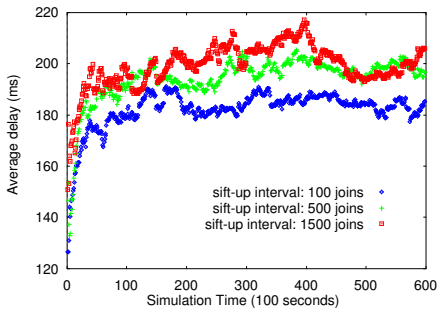

Figure 7: Average service delays changing over time under different sift-up frequencies.

plots the average network delays changing over a time interval of 16.7 hours with different sift-up frequencies. The network is fixed at 10,000 peers. The sift-up interval is measured by the number of newly joining peers. It can be seen that a higher sift-up frequency achieves smaller average delays. The protocol overhead corresponding to three intervals, 100 joins, 500 joins and 1500 joins, are 0.069, 0.17 and 1.338, respectively. This reveals the trade-off between the overlay performance and the required protocol overhead.

6 Conclusions

This paper presents an analysis for the performance of overlays constructed by several algorithms for P2P live media streaming. Three performance criteria are considered: (1) service delay; (2) service reliability and (3) protocol overhead. Two principles of peer placement, bandwidth ordering and time ordering, are discussed and their impact on different aspects of the overlay's performance are analyzed.

Based on this, a new algorithm called the *heap algorithm* is devised with the objective of taking advantage of both bandwidth ordering and time ordering. It adjusts peers in the tree during the normal streaming process according to a metric that combines both bandwidth and time properties of a peer, and employs a technique to optimize the mapping of overlay connections to physical network connections so as to minimize the actual network delay. Simulations show that the heap algorithm achieves superior comprehensive performance in comparison with existing algorithms.

References

[1] S. Banerjee, B. Bhattacharjee, C. Kommareddy. Scalable Application Layer Multicast. *Proc. of ACM SIGCOMM 2002*, August 2002

[2] S. Banerjee, C. Kommareddy, K. Kar, S. Bhattacharjee, and S. Khuller. Construction of an efficient overlay multicast infrastructure for real-time applications. *Proc. of IEEE INFOCOM, 2003*.

[3] Y. Chawathe. Scattercast: An Architecture for Internet Broadcast Distribution as an Infrastructure Service. *Ph.D. Thesis, University of California, Berkeley*, Dec. 2000.

[4] Y. Chu, A. Ganjam, T. S. E. Ng, S. G. Rao, K. Sripanidkulchai, J. Zhan and H. Zhang. Early Experience with an Internet Broadcast System Based on Overlay Multicast. *Proc. of USENIX 2004 Annual Technical Conference*.

[5] Y. Chu, S. G. Rao, S. Seshan, and H. Zhang. Enabling conferencing applications on the Internet using an overlay multicast architecture. *Proc. of ACM SIGCOMM 2001*.

[6] Y. Chu, S. Rao, and H. Zhang. A Case for End System Multicast. *Proc. of ACM SIGMETRICS*, June 2000.

[7] M. Guo, M. Ammar. Scalable live video streaming to cooperative clients using time shifting and video patching. *Proc. of IEEE INFOCOM 2004*.

[8] D. Helder and S. Jamin. End-host Multicast Communication Using Switch-tree Protocols. In *Proc. of Internation Conference on Global and Peer-to-Peer Computing on Large Scale Distributed Systems, 2002*.

[9] Y. Liu, Z. Zhuang, Li Xiao. A Distributed Approach to Solving Overlay Mismatching Problem. In *Proc. of 24th International Conference on Distributed Computing Systems (ICDCS'04)*

[10] Wei Tsang Ooi. Dagster: contributor-aware end-host multicast for media streaming in heterogeneous environment. *Proc. of Multimedia Computing and Networking (MMCN)*, 2005.

[11] Venkata N. Padmanabhan, Helen J. Wang, Philip A. Chou. Resilient Peer-to-Peer Streaming. *11th IEEE International Conference on Network Protocols (ICNP)*, 2003.

[12] V. N. Padmanabhan, H. J. Wang, P. A. Chou, and K. Sripanidkulchai. Distributing Streaming Media Content Using Cooperative Networking. *ACM NOSSDAV*, May 2002.

[13] D. Pendarakis, S. Shi, D. Verma, and M. Waldvogel. ALMI: An Application Level Multicast Infrastructure. In Proc. of *3rd Usenix Symposium on Internet Technologies and Systems (USITS)*, March 2001.

[14] S. Saroiu, P. Gummadi and S. Gribble A Measurement Study of Peer-to-Peer File Sharing Systems. *Proc. of Multimedia Computing and Networking (MMCN)*, 2002.

[15] S. Sen and J. Wang. Analyzing peer-to-peer traffic across large networks. *IEEE/ACM Trans. on Networking.* Vol. 12, No. 2, April 2004.

[16] K. Sripanidkulchai, A. Ganjam, B. Maggs and H. Zhang. The feasibility of supporting large-scale live streaming applications with dynamic application end-points. *Proc. of ACM SIGCOMM*, 2004, Portland, Oregon, USA.

[17] K. Sripanidkulchai, B. Maggs and H. Zhang An analysis of live streaming workloads on the Internet. *Proc. of the 4th ACM SIGCOMM IMC*, Oct., 2004. Italy.

[18] G. Tan, S. A. Jarvis, D. P. Spooner and G. R. Nudd. On Efficient and Robust Overlay Construction for Large-scale P2P Live Media Streaming. *TR-2005-02*, Dept. of Computer Science, University of Warwick, UK.

[19] D. A. Tran, K. A. Hua, and T. T. Do. A peer-to-peer architecture for media streaming. *IEEE Journal on Selected Areas in Communications (JSAC), Special Issue on Recent Advances in Service Overlay Networks*. 22, Jan. 2004.

[20] E. Veloso, V. Almeida, W. Meira, A. Bestavros, and S. Jin. A Hierarchical Characterization of A Live Streaming Media Workload. *IEEE/ACM Trans. on Networking*, 12(5), 2004.

[21] E. W. Zegura, K. Calvert and S. Bhattacharjee. How to Model an Internetwork. *Proc. of IEEE INFOCOM '96*, San Francisco, CA.

A Practical Guide to Measuring the Hurst Parameter

Richard G. Clegg

June 28, 2005

Abstract

This paper describes, in detail, techniques for measuring the Hurst parameter. Measurements are given on artificial data both in a raw form and corrupted in various ways to check the robustness of the tools in question. Measurements are also given on real data, both new data sets and well-studied data sets. All data and tools used are freely available for download along with simple "recipes" which any researcher can follow to replicate these measurements.

1 Introduction and Background

Long-Range Dependence (LRD) is a statistical phenomenon which has received much attention in the field of telecommunications in the last ten years. A time-series is described as possessing LRD if it has correlations which persist over all time scales. A good guide to LRD is given by [3] and a summary in the context of telecommunications is given by [4, chapter one] (from which some of the material in this paper is taken). In the early nineties, LRD was measured in time-series derived from internet traffic [8]. The importance of this is that LRD can impact heavily on queuing. LRD is characterised by the parameter H, the Hurst parameter, (named for a hydrologist who pioneered the field in the fifties [7]) where $H \in (1/2, 1)$ indicates the presence of LRD. There are a number of different statistics which can be used to estimate the Hurst parameter and several papers have been written comparing these estimators both in theory and practice [16, 15, 1]. The aim of this paper is not to make a rigorous comparison of the estimators but, instead, to present a simple and readable guide to what a researcher can expect from attempting to assess whether LRD is absent or present in a data set. All the tools used are available online using free software. Software can be downloaded from:
`http://www.richardclegg.org/lrdsources/software/`

1.1 A Brief Introduction to Long-Range Dependence

Let $\{X_t : t \in \mathbb{N}\}$ be a time-series which is weakly stationary (that is it has a finite mean and the covariance depends only on the separation or "lag" between two points in the series). Let $\rho(k)$ be the auto-correlation function (ACF) of X_t.

Definition 1. The ACF, $\rho(k)$ for a weakly-stationary time series, $\{X_t : t \in \mathbb{N}\}$ is given by

$$\rho(k) = \frac{\mathrm{E}\left[(X_t - \mu)(X_{t+k} - \mu)\right]}{\sigma^2},$$

where $\mathrm{E}[X_t]$ is the expectation of X_t, μ is the mean and σ^2 is the variance.

There are a number of different definitions of LRD in use in the literature. A commonly used definition is given below.

Definition 2. The time-series X_t is said to be *long-range dependent* if $\sum_{k=-\infty}^{\infty} \rho(k)$ diverges.

Often the specific functional form

$$\rho(k) \sim C_\rho k^{-\alpha}, \tag{1}$$

is assumed where $C_\rho > 0$ and $\alpha \in (0, 1)$. Note that the symbol $\sim$ is used here and throughout this paper to mean *asymptotically equal to* or $f(x) \sim g(x) \Rightarrow f(x)/g(x) = 1$ as $x \to \infty$ or, where indicated, as $x \to 0$. The parameter α is related to the Hurst parameter via the equation $\alpha = 2 - 2H$.

If (1) holds then a similar definition can be shown to hold in the frequency domain.

Definition 3. The *spectral density* $f(\lambda)$ of a function with ACF $\rho(k)$ and variance σ^2 can be defined as

$$f(\lambda) = \frac{\sigma^2}{2\pi} \sum_{k=-\infty}^{\infty} \rho(k) e^{ik\lambda},$$

where λ is the frequency, σ^2 is the variance and $i = \sqrt{-1}$.

Note that this definition of spectral density comes from the Wiener-Kninchine theorem [17].

Definition 4. The weakly-stationary time-series X_t is said to be *long-range dependent* if its spectral density obeys

$$f(\lambda) \sim C_f |\lambda|^{-\beta},$$

as $\lambda \to 0$, for some $C_f > 0$ and some real $\beta \in (0, 1)$.

The parameter β is related to the Hurst parameter by $H = (1 + \beta)/2$.

LRD relates to a number of other areas of statistics, notably the presence of statistical self-similarity. Self-similarity can be characterised by a self-similarity parameter H and the increment process of a self-similar process with stationary increments and $H \in (1/2, 1)$ is itself an LRD process with Hurst parameter H. Indeed analysis of telecommunications traffic is often described in terms of self-similarity and not long-range dependence.

In summary, LRD can be thought of in two ways. In the time domain it manifests as a high degree of correlation between distantly separated data points. In the frequency domain it manifests as a significant level of power at frequencies near zero. LRD is, in many ways, a difficult statistical property to work with. In the time-domain it is measured only at high lags (strictly at infinite lags) of

the ACF — those very lags where only a few samples are available and where the measurement errors are largest. In the frequency domain it is measured at frequencies near zero, again where it is hardest to make measurements. Time series with LRD converge slowly to their mean. While the Hurst parameter is perfectly well-defined mathematically, it will be shown that it is, in fact, a very difficult property to measure in real life.

1.2 Long-Range Dependence in Telecommunications

In their classic paper, Leland et al [8] measure traffic past a point on an Ethernet Local Area Network. They conclude that "In the case of Ethernet LAN traffic, self-similarity is manifested in the absence of a natural length of a 'burst'; at every time scale ranging from a few milliseconds to minutes and hours, bursts consist of bursty sub-periods separated by less burst sub-periods. We also show that the degree of self-similarity (defined via the Hurst parameter) typically depends on the utilisation level of the Ethernet and can be used to measure 'burstiness' of LAN traffic." Since then, a number of authors have replicated these experiments on a variety of measurments of internet traffic and the majority found evidence of LRD or related multi-fractal behaviour. Summaries are given in [14, 18]. The reason for the interest in the area is that LRD can, in some circumstances, negatively impact network performance. The exact details of the scale and nature of the effect are uncertain and depend on the particular LRD process being considered.

2 Measuring the Hurst Parameter

While the Hurst parameter is perfectly well-defined mathematically, measuring it is problematic. The data must be measured at high lags/low frequencies where fewer readings are available. Early estimators were biased and converged only slowly as the amount of data available increased. All estimators are vulnerable to trends in the data, periodicity in the data and other sources of corruption. Many estimators assume specific functional forms for the underlying model and perform poorly if this is misspecified. The techniques in this paper are chosen for a variety of reasons. The R/S parameter, aggregated variance and periodogram are well-known techniques which have been used for some time in measurements of the Hurst parameter. The local Whittle and wavelet techniques are newer techniques which generally fare well in comparative studies. All the techniques chosen have freely available code which can be used with free software to estimate the Hurst parameter.

The problems with real-life data are worse than those faced when measuring artificial data. Real life data is likely to have periodicity (due to, for example, daily usage patterns), trends and perhaps quantisation effects if readings are taken to a given precision. The naive researcher taking a data set and running it through an off-the-shelf method for estimating the Hurst parameter is likely to end up with a misleading answer or possibly several different misleading answers.

2.1 Data sets to be studied

A large number of methods are used for generating data exhibiting LRD. A review of some of the better known methods are given in [2]. In this paper trial data sets with LRD and a known Hurst parameter are generated using fractional auto-regressive integrated moving average (FARIMA) modelling and fractional Gaussian noise (FGN).

A FARIMA model is a well-known time series modelling technique. It is a modification of the standard time series ARIMA (p, d, q) model. An ARIMA model is defined by

$$(1 - \sum_{j=1}^{p} \phi_j \mathbf{B}^j)(1 - \mathbf{B})^d X_i = (1 - \sum_{j=1}^{q} \theta_j \mathbf{B}^j)\varepsilon_i,$$

where p is the order of the AR part of the model, the ϕ_i are the AR parameters, p is the order of the MA part of the model, the θ_j are the MA parameters, $d \in \mathbb{Z}$ is the order of differencing, the ε_i are i.i.d. noise (usually normally distributed with zero mean) and $\mathbf{B}$ is the backshift operator defined by $\mathbf{B}(X_t) = X_{t-1}$. If, instead of being an integer, the model is changed so that $d \in (0, 1/2)$ then the model is a FARIMA model. If the ϕ_i and θ_i are chosen so that the model is stationary and $d \in (0, 1/2)$ then the model will be LRD with $H = d + 1/2$. FARIMA processes were proposed by [6] and a description in the context of LRD can be found in [3, pages 59–66].

Fractional Brownian Motion is a process $B_H(t)$ for $t \geq 0$ obeying,

- $B_H(0) = 0$ almost surely,
- $B_H(t)$ is a continuous function of t,
- The distribution of $B(t)$ obeys

$$\mathbb{P}\left[B_H(t+k) - B_H(t) \leq x\right] = (2\pi)^{-\frac{1}{2}} k^{-H} \int_{-\infty}^{x} \exp\left(\frac{-u^2}{2k^{2H}}\right) du,$$

where $H \in (1/2, 1)$ is the Hurst parameter. The process $B_H(t)$ is known as fractional Brownian motion (FBM) and its increments are known as fractional Gaussian noise (FGN). FBM is a self-similar process with self-similarity parameter H and FGN exhibits long-range dependence with Hurst parameter H. When $H = 1/2$ in the above, then the process is the well known Weiner process (Brownian motion) and the increments are independent (Gaussian noise). A number of authors have described computationally efficient methods for generating FGN and FBM. The one used in this paper is due to [11].

Data generated from these models will be tested using the various measurement techniques and then the same data set will be corrupted in several ways to see how this disrupts measurements:

- Addition of zero mean AR(1) model with a high degree of short-range correlation ($X_t = 0.9X_{t-1} + \varepsilon_t$). This simulates a process with high degree of short-range correlation which might be mistaken for a long-range correlation.

- Addition of periodic function (sine wave) — ten complete cycles of a sin wave are added to the signal. This simulates a seasonal effect in the data, for example, a daily usage pattern.
- Addition of linear trend. This simulates growth in the data, for example the data might be a sample of network traffic at a time of day when the network is growing busier as time continues.

The noise signals are normalised so the standard deviation of the corrupting signal is identical to the standard deviation of the original LRD signal to which it is being added. Note that, strictly speaking, while the addition of an AR(1) model does not change the LRD in the model, techincally the addition of a trend or of periodic noise makes the time-series non-stationary and hence the time-series produces are, strictly speaking, not really LRD.

In addition, some real-life traffic traces are studied to provide insight into how well different measurements agree across data sets with and without various transforms being applied to clean the data. The data sets used are listed below.

- The famous (and much-studied) Bellcore data [9] which was collected in 1989 and has been used for a large number of studies since. Note that, unfortunately, the exact traces used in [8] are not available for download. This data is available online at:
  `http://ita.ee.lbl.gov/html/contrib/BC.html`
- A data set collected at the University of York in 2001 which consists of a tcpdump trace of 67 minutes of incoming and outgoing data from the external link to the university from the rest of the internet.

Various techniques are tried to filter real-life traces in addition to making measurements purely on the raw data. These methods have been selected from the literature as commonly used by researchers in the field. Often in such cases, a high pass filter would be used to remove periodicity and trends, however, since LRD measurements are most important at low-frequency that is an obviously inappropriate technique. The techniques used to pre-process data before estimating H are listed below.

- Transform to log of original data (only appropriate if data is positive).
- Removal of mean and linear trend (that is, subtract the best fit line $Y = at + b$ for constant a and b).
- Removal of high order best-fit polynomial of degree ten (the degree ten was chosen after higher degrees showed evidence of overfitting).

2.2 Measurement techniques

The measurement techniques used in this paper can only be described briefly but references to fuller descriptions with mathematical details are given. The techniques used here are chosen for various reasons. The R/S statistic, aggregated variance and periodogram are well-known techniques with a considerable history of use in estimating long-range dependence. The wavelet analysis technique and local Whittle estimator are newer techniques which perform well in comparative studies and have strong theoretical backing.

The R/S statistic is a well-known technique for estimating the Hurst parameter. It is discussed in [10] and also [3, pages 83–87]. Let $R(n)$ be the range of the data aggregated (by simple summation) over blocks of length n and $S^2(n)$ be the sample variance of the data aggregated at the same scale. For FGN or FARIMA series the ratio $R/S(n)$ follows

$$\mathrm{E}\left[R/S(n)\right] \sim C_H n^H,$$

where C_H is a positive, finite constant independent of n. Hence a log-log plot of $R/S(n)$ versus n should have a constant slope as n becomes large. A problem with this technique which is common to many Hurst parameter estimators is knowing which values of n to consider. For small n short term correlations dominate and the readings are not valid. For large n then there are few samples and the value of $R/S(n)$ will not be accurate. Similar problems occur for most of the estimators described here.

The aggregated variance technique is described in [3, page 92]. It considers $\mathrm{var}\left(X^{(m)}\right)$ where $X_t^{(m)}$ is a time series derrived from X_t by aggregating it over blocks of size m. The sample variance $\mathrm{var}\left(X^{(m)}\right)$ should be asymptotically proportional to m^{2H-2} for large N/m and m.

The periodogram, described by [5] is defined by

$$I(\lambda) = \frac{1}{2\pi N}\left|\sum_{j=1}^{N} X_j e^{ij\lambda}\right|^2,$$

where λ is the frequency. For a series with finite variance, $I(\lambda)$ is an estimate of the spectral density of the series. From Definition 4 then, a log-log plot of $I(\lambda)$ should have a slope of $1-2H$ close to the origin.

Whittle's estimator is a Maxmimum Likelihood Estimator which assumes a functional form for $I(\lambda)$ and seeks to minimise parameters based upon this assumption. A slight issue with the Whittle estimator is that the user must specify the functional form expected, typically either FGN or FARIMA (with the order specified). If the user misspecifies the underlying model then errors may occur. Local Whittle is a semi-parametric version of this which only assumes a functional form for the spectral density at frequencies near zero [13].

Wavelet analysis has been used with success both to measure the Hurst parameter and also to simulate data [12]. Wavelets can be thought of as akin to Fourier series but using waveforms other than sine waves. The estimator used here fits a straight line to a frequency spectrum derived using wavelets. A 95% confidence interval is given, however, this should be interpreted only as a confidence interval on the fitted line and, as will be seen, not as a confidence inteval on the fitted Hurst parameter.

3 Results

Results here are in two sections. Firstly, results are given for simulated data. In these cases the expected "correct" answer is known and therefore it can be seen how well the estimators have performed. The data is then corrupted by the addition of noise with the same standard deviation as the original data sets. Three types of noise are considered as described previously.

In the second section results are given for real data. The York data is analysed as a time series of bytes per unit time for two different time units. The Bellcore data is analysed both in terms of interarrival times and in terms of bytes per unit time. Note that, strictly speaking, the interarrival times do not consititute a proper "time-series" since the time units between readings are not constant.

3.1 Results on Simulated Data

For each of the simulation methods chosen, traces have been generated. Each trace is 100,000 points of data. Hurst parameters of 0.7 and 0.9 have been chosen to represent a low and a high level of long-range dependence in data. The errors on the wavelet estimator are a 95% confidence interval on the fitted regression line (not, as might be thought, the Hurst parameter measured).

Table 1 shows results for various FGN models. Three runs each are done with a Hurst parameter of 0.7 and then 0.9. Firstly it should be noted that, in all case, for H=0.7 all estimators are relatively close when no noise is applied. The R/S method performs worst, as it consistently underestimates the Hurst parameter. The addition of AR(1) noise confuses all the methods with the Local Whittle performing particularly poorly. The correct answer is well outside the confidence intervals of the Wavelet estimate after this addition. Addition of a sine wave or a trend causes trouble for the aggregated variance method but the frequency domain methods (wavelets and local Whittle) do not seem greatly affected.

When considering runs with Hurst parameter H=0.9, the R/S method gets a considerable underestimate even with no corrupting noise. Note also that the R/S and aggregated variance method actually produce quite different estimates for the three runs. Most methods seem to perform badly with the AR(1) noise corruption. Again the frequency domain methods seem to be able to cope with the sine wave and with the addition of a trend.

Table 2 shows a variety of results for FARIMA models. The first three runs are for a FARIMA $(0, d, 0)$ model (that is one with no AR or MA components) and with a Hurst parameter $H = 0.7$. In this case, all methods peform adequately with no noise (although the R/S plot perhaps underestimates the answer). Addition of AR(1) noise causes problems for the R/S plot, wavelet and local Whittle methods and to a lesser extent the periodogram. The addition of a sin wave and a trend causes problems for the aggregated variance.

For a FARIMA $(1, d, 1)$ model with $H = 0.7$ and with the AR parameter $\phi_1 = 0.5$ and the MA parameter $\theta_1 = 0.5$ (implying a moderate degree of short range correlation) all estimators provide a reasonable result for the uncorrupted series. As before, the wavelet and local Whittle method seem relatively robust to the addition of a trend. The AR(1) noise again causes problems for most of the methods.

For a FARIMA $(0, d, 0)$ model with $H = 0.9$ the R/S method under predicts the Hurst parameter but all others perform well in the absence of noise. The AR(1) noise causes problems for the local Whittle and wavelet methods and the sine wave and trend cause problems for the aggregated variance.

For a FARIMA $(1, d, 1)$ model with $H = 0.9$ and with the AR parameter $\phi_1 = 0.5$ and the MA parameter $\theta_1 = 0.5$ (implying, as before, a moderate degree of short range correlation) all estimators do relatively well initially. The

Added Noise	R/S Plot	Aggreg. Variance	Period. ogram	Wavelet Estimate	Local Whittle
100,000 points FGN — H= 0.7 — run one.					
None	0.66	0.668	0.686	0.707 ± 0.013	0.72
AR(1)	0.767	0.657	0.794	0.888 ± 0.034	0.904
Sin	0.667	0.969	0.692	0.707 ± 0.013	0.787
Trend	0.66	0.968	0.777	0.707 ± 0.013	0.766
100,000 points FGN — H= 0.7 — run two.					
None	0.641	0.692	0.7	0.694 ± 0.007	0.721
AR(1)	0.775	0.671	0.795	0.882 ± 0.036	0.902
Sin	0.66	0.97	0.705	0.694 ± 0.007	0.788
Trend	0.641	0.968	0.769	0.694 ± 0.007	0.765
100,000 points FGN — H= 0.7 — run three.					
None	0.636	0.69	0.704	0.708 ± 0.009	0.723
AR(1)	0.734	0.654	0.79	0.876 ± 0.038	0.905
Sin	0.64	0.969	0.709	0.708 ± 0.009	0.787
Trend	0.636	0.971	0.783	0.708 ± 0.009	0.77
100,000 points FGN — H= 0.9 — run one.					
None	0.782	0.864	0.905	0.901 ± 0.009	0.934
AR(1)	0.805	0.784	0.88	0.969 ± 0.042	1.066
Sin	0.772	0.961	0.907	0.901 ± 0.009	0.945
Trend	0.782	0.958	0.928	0.901 ± 0.009	0.939
100,000 points FGN — H= 0.9 — run two.					
None	0.862	0.837	0.891	0.902 ± 0.003	0.933
AR(1)	0.856	0.76	0.877	0.969 ± 0.038	1.062
Sin	0.858	0.955	0.894	0.902 ± 0.003	0.943
Trend	0.862	0.954	0.921	0.902 ± 0.003	0.938
100,000 points FGN — H= 0.9 — run two.					
None	0.793	0.884	0.907	0.904 ± 0.007	0.93
AR(1)	0.818	0.802	0.871	0.972 ± 0.041	1.066
Sin	0.8	0.967	0.91	0.904 ± 0.007	0.943
Trend	0.794	0.959	0.924	0.904 ± 0.007	0.936

Table 1: Results for Fractional Gaussian Noise models plus various forms of noise.

Added Noise	R/S Plot	Aggreg. Variance	Period. ogram	Wavelet Estimate	Local Whittle
100,000 points FARIMA (0,d,0) — H = 0.7 — run one.					
None	0.663	0.692	0.699	0.696 ± 0.004	0.681
AR(1)	0.823	0.673	0.792	0.896 ± 0.033	0.876
Sin	0.665	0.972	0.704	0.696 ± 0.004	0.765
Trend	0.662	0.973	0.786	0.696 ± 0.004	0.746
100,000 points FARIMA (0,d,0) — H= 0.7 — run two.					
None	0.706	0.701	0.71	0.702 ± 0.007	0.679
AR(1)	0.837	0.673	0.791	0.891 ± 0.034	0.873
Sin	0.714	0.972	0.714	0.702 ± 0.007	0.764
Trend	0.706	0.972	0.782	0.702 ± 0.007	0.742
100,000 points FARIMA (0,d,0) — H= 0.7 — run three.					
None	0.718	0.684	0.696	0.687 ± 0.005	0.679
AR(1)	0.827	0.667	0.776	0.868 ± 0.044	0.872
Sin	0.723	0.973	0.701	0.687 ± 0.005	0.765
Trend	0.718	0.972	0.778	0.687 ± 0.005	0.743
100,000 points FARIMA (1,d,1) — H= 0.7, $\phi_1 = 0.5, \theta_1 = 0.5$.					
None	0.684	0.693	0.706	0.697 ± 0.006	0.68
AR(1)	0.818	0.656	0.774	0.88 ± 0.041	0.878
Sin	0.689	0.973	0.71	0.697 ± 0.006	0.766
Trend	0.684	0.972	0.786	0.697 ± 0.006	0.743
100,000 points FARIMA (0,d,0) — H = 0.9.					
None	0.757	0.882	0.91	0.886 ± 0.004	0.861
AR(1)	0.804	0.789	0.873	0.969 ± 0.036	1.011
Sin	0.764	0.967	0.913	0.886 ± 0.004	0.883
Trend	0.757	0.974	0.933	0.886 ± 0.004	0.875
100,000 points FARIMA (1,d,1) — H= 0.9, $\phi_1 = 0.5, \theta_1 = 0.5$.					
None	0.856	0.854	0.881	0.887 ± 0.006	0.858
AR(1)	0.888	0.773	0.874	0.959 ± 0.04	1.001
Sin	0.86	0.963	0.885	0.887 ± 0.006	0.879
Trend	0.856	0.968	0.92	0.887 ± 0.006	0.872
100,000 points FARIMA (2,d,1) — H= 0.7, $\phi_1 = 0.5, \phi_2 = 0.2, \theta_1 = 0.1$.					
None	0.807	0.74	0.817	0.966 ± 0.048	1.05
AR(1)	0.814	0.691	0.822	1.007 ± 0.059	1.136
Sin	0.8	0.94	0.821	0.966 ± 0.048	1.052
Trend	0.807	0.939	0.856	0.966 ± 0.048	1.051

Table 2: Results for various FARIMA models corrupted by several forms of noise.

Filter Type	R/S Plot	Aggreg. Variance	Period. ogram	Wavelet Estimate	Local Whittle
York trace (bytes/second) — 4047 points					
None	0.749	0.88	1.186	0.912 ± 0.052	0.981
Log	0.758	0.894	1.105	0.921 ± 0.039	0.932
Trend	0.749	0.873	1.212	0.912 ± 0.052	0.981
Poly	0.756	0.723	0.732	0.895 ± 0.04	0.972
York trace (bytes/tenth) — 40467 points					
None	0.826	0.924	0.928	0.909 ± 0.012	0.881
Trend	0.826	0.923	0.932	0.909 ± 0.012	0.881
Poly	0.827	0.892	0.863	0.909 ± 0.012	0.878

Table 3: Analysis of bytes/unit time data collected at the University of York.

corruption produces the same problems with the same estimators — that is to say, wavelets and local Whittle do not cope with the AR(1) noise and Aggregated variance reacts badly to the sine wave and local trend.

For a FARIMA $(2, d, 1)$ model with $H = 0.9$ and with the AR parameters $\phi_1 = 0.5$, $\phi_2 = 0.2$ and the MA parameter $\theta_1 = 0.1$ indicating quite strong short-range correlations, none of the estimators perform particularly well. The aggregated variance estimate is initially close and remains so in the presence of AR(1) noise but presented with these results, a researcher would certainly not know the Hurst parameter of the underlying model from looking at the results given by the estimators. All five are producing different results in most cases (there is some aggreement between the R/S plot and periodogram but it would be hard to put this down to anything more than coincidence and, in any case, they are agreeing on an incorrect value for the Hurst parameter). It is interesting that, even in this relatively simple case where the theoretical correct result is known, five well-known estimators of the Hurst parameter all fail to get the correct answer.

3.2 Results on Real Data

In analysing the real data it is hard to know where to begin. Since the genuine answer (if, indeed, it can be really said that there is a genuine answer) is not known it cannot be said that one result is more "right" than another. The suggested methods for preprocessing data (taking logs, removing a linear trend and removing a best fit polynomial — in this case of order ten) have all been found in the literature on measuring the Hurst parameter.

Table 3 shows analysis of data collected at the University of York. The same data set is analysed firstly as a series of bytes/second and then as bytes/tenth of a second. While theoretically the results should be the same, in practice this is not the case. Obviously there are only one tenth as many points in the data set when seconds are used rather than tenths of seconds. Firstly, looking at the data aggregated over a time period of one second, there is no good agreement between estimators. The periodogram estimate is hopelessly out of the correct range. The other estimators, while in the range $(1/2, 1)$ show no particular agreement. Of the suggested filtering techniques, little changes between them

Filter Type	R/S Plot	Aggreg. Variance	Period. ogram	Wavelet Estimate	Local Whittle
Bellcore data BC-Aug89 (interarrival times) — first 360,000 points.					
None	0.73	0.742	0.762	0.73 ± 0.018	0.661
Log	0.722	0.806	0.797	0.77 ± 0.02	0.652
Trend	0.73	0.74	0.762	0.73 ± 0.018	0.661
Poly	0.73	0.733	0.751	0.73 ± 0.018	0.66
Bellcore data BC-Aug89 (interarrival times) — second 360,000 points.					
None	0.709	0.703	0.742	0.746 ± 0.025	0.655
Log	0.721	0.795	0.779	0.778 ± 0.011	0.673
Trend	0.709	0.703	0.742	0.746 ± 0.025	0.655
Poly	0.709	0.691	0.732	0.746 ± 0.025	0.654
Bellcore data BC-Aug89 (bytes/10ms) — first 1000 secs.					
None	0.707	0.8	0.817	0.786 ± 0.017	0.822
Trend	0.707	0.797	0.815	0.786 ± 0.017	0.822
Poly	0.707	0.789	0.787	0.786 ± 0.017	0.822
Bellcore data BC-Aug89 (bytes/10ms) — second 1000 secs.					
None	0.62	0.802	0.808	0.762 ± 0.012	0.825
Trend	0.62	0.802	0.808	0.762 ± 0.012	0.825
Poly	0.618	0.786	0.777	0.762 ± 0.012	0.824

Table 4: Analysis of bytes/unit time and interarrival times for the Bellcore data with various methods to attempt to remove non-stationary components.

except that removal of a polynomial greatly reduces the estimate found by the periodogram and slightly reduces the estimate found by aggregated variance. No conclusion can realistically be drawn about the data from these results.

Considering the data aggregated into tenths of a second time units the picture is somewhat clearer. Taking a log of data was impossible at this time scale due to presence of zeros. The estimators, with the exception of the R/S plot are all relatively near $H = 0.9$. While it seems somewhat arbitrary to ignore the results of the R/S plot it should be remembered that this technique performed poorly with high Hurst parameter measurements on theoretical data and underestimated badly in those cases. No great difference is observed from any of the suggested filtering techniques except, perhaps, a slight reduction in the aggregated variance and periodogram results from removal of a polynomial. A tentative conclusion from this data would be that $0.85 < H < 0.95$ and that the R/S plot is inaccurate for this trace.

In the case of the Bellcore measurements, the data has been split into two sections and analysed seperately for interarrival times and for bytes per unit time. Considering first the interarrival times, all estimators seem to have a result which is not too distant from $H = 0.7$ in both cases. The various filtering techniques tried do little to change this. It is hard to come to a really robust conclusion since the estimators are as high as 0.806 (aggregated variance after taking logs) and as low as 0.652 (local Whittle after taking logs).

When the bytes per unit time are considered, the log technique cannot be used due to zeros in the data. The most comfortable conclusion abou this data might be that the Hurst parameter is somewhere around $H = 0.8$ with the R/S

plot underestimating again. As before, it is hard to reach a strong conclusion on the exact Hurst parameter. Certainly it would be foolish to take the confidence intervals on the wavelet estimator at face value. The various filters tried seem to make little difference except perhaps a slight reduction in the answer given by some estimators after the polynomial is removed. A tentative conclusion might be that $0.75 < H < 0.85$ for this data with the R/S plot being in error.

4 Conclusion

This paper has looked at measuring the Hurst parameter, firstly in the case of artificial data contaminated by various types of noise and secondly in the case of real data with various filters to try to improve the performance of the estimators used.

The most striking conclusion of this paper is that measuring the Hurst parameter, even in artificial data, is very hit and miss. In the artificial data with no corrupting noise, some estimators performed very poorly indeed. Confidence intervals given should certainly not be taken at face value (indeed should be considered as next to worthless).

Corrupting noise can affect the measurements badly and different estimators are affected in by different types of noise. In particular, frequency domain estimators (as might be expected) are robust to the addition of sinusoidal noise or a trend. All estimators had problems in some circumstances with the addition of a heavy degree of short-range dependence even though this, in theory, does not change the long-range dependence of the time series.

When considering real data, researchers are advised to use extreme caution. A researcher relying on the results of any single estimator for the Hurst parameter is likely to be drawing false conclusions, no matter how sound the theoretical backing for the estimator in question. While simple filtering techniques are suggested in the literature for improving the performance of Hurst parameter estimation, they had little or no effect on the data analysed in this paper.

All the data and tools used in this paper are available for download from the web and can be found at:
`http://www.richardclegg.org/lrdsources/software/`

References

[1] J.-M. Bardet, G. Lang, G. Oppenheim, A. Phillipe, S. Stoev, and M. S. Taqqu. Semi-parametric estimation of the long-range dependence parameter: A survey. In P. Doukhan, G. Oppenheim, and M. S. Taqqu, editors, *Theory and Applications of Long-Range Dependence*, pages 557–577. Birkhäuser, 2003.

[2] J.-M. Bardet, G. Lang, G. Oppenheim, A. Phillipe, and M. S. Taqqu. Generators of long-range dependent processes: A survey. In P. Doukhan, G. Oppenheim, and M. S. Taqqu, editors, *Theory and Applications of Long-Range Dependence*, pages 579–623. Birkhäuser, 2003.

[3] J. Beran. *Statistics For Long-Memory Processes*. Chapman and Hall, 1994.

[4] R. G. Clegg. *Statistics of Dynamic Networks*. PhD thesis, Dept. of Math., Uni. of York., York., 2004. Available online at: `www.richardclegg.org/pubs/thesis.pdf`.

[5] J. Geweke and S. Porter-Hudak. The estimation and application of long memory time series models. *J. Time Ser. Anal.*, 4:221–238, 1983.

[6] C. W. J. Granger and R. Joyeux. An introduction to long-range time series models and fractional differencing. *J. Time Ser. Anal.*, 1:15 – 30, 1980.

[7] H. E. Hurst. Long-term storage capacity of reservoirs. *Transactions of the American Society of Civil Engineers*, pages 770–808, 1951.

[8] W. E. Leland, M. S. Taqqu, W. Willinger, and D. V. Wilson. On the self-similar nature of Ethernet traffic. In D. P. Sidhu, editor, *Proc. ACM SIGCOMM*, pages 183–193, San Francisco, California, 1993.

[9] W. E. Leland and D. V. Wilson. High time-resolution measurement and analysis of lan traffic: Implications for lan interconnection. *Proc. IEEE INFOCOM*, pages 1360–1366, April 1991.

[10] B. B. Mandelbrot and J. R. Wallis. Computer experiments with fractional gaussian noises. *Water Resources Research*, 5:228–267, 1969.

[11] V. Paxson. Fast, approximate synthesis of fractional gaussian noise for generating self-similar network traffic. *Computer Comm. Rev.*, 27:5–18, 1997.

[12] R. H. Riedi. Multifractal processes. In P. Doukhan, G. Oppenheim, and M. S. Taqqu, editors, *Theory And Applications Of Long-Range Dependence*, pages 625–716. Birkhäuser, 2003.

[13] P. M. Robinson. Gaussian semiparametric estimation of long-range dependence. *The Annals of Statistics*, 23:1630–1661, 1995.

[14] Z. Sahinoglu and S. Tekinay. On multimedia networks: Self similar traffic and network performance. *IEEE Communications Magazine*, pages 48–52, January 1999.

[15] M. S. Taqqu and V. Teverovsky. Robustness of Whittle type estimators for time series with long-range dependence. *Stochastic Models*, 13:723–757, 1997.

[16] M.S. Taqqu, V. Teverovsky, and W. Willinger. Estimators for long-range dependence: an empirical study. *Fractals*, 3(4):785–788, 1995.

[17] N. Weiner. Generalized harmonic analysis. *Acta. Math.*, 55:178–258, 1930.

[18] W. Willinger, V. Paxson, R. H. Riedi, and M. S. Taqqu. Long-range dependence and data network traffic. In P. Doukhan, G. Oppenheim, and M. S. Taqqu, editors, *Theory And Applications Of Long-Range Dependence*, pages 373–407. Birkhäuser, 2003.

An Alternative Algorithm to Multiply a Vector by a Kronecker Represented Descriptor

Paulo Fernandes* Ricardo Presotto† Afonso Sales‡
Thais Webber§

Abstract

The key operation to obtain stationary and transient solutions of models described by Kronecker structured formalisms using iterative methods is the Vector-Descriptor product. This operation is usually performed with the Shuffle algorithm, which was proposed to Stochastic Automata Networks, but it is also currently used by Stochastic Petri Nets and Performance Evaluation Process Algebra solvers. This paper presents an alternative algorithm to perform the Vector-Descriptor product, called Slice algorithm. The numerical advantages of this new algorithm over the previous one is shown to SAN models, in which the computational costs are compared. Finally, we discuss some possible optimizations of the Slice algorithm and implementation issues regarding parallel versions of both algorithms.

1 Introduction

All formalisms used to model complex systems are based on a structured description. This is particularly the case of Markovian performance and reliability evaluation models. A myriad of formalisms is available in the research community, *e.g.*, Stochastic Activity Networks [13], Queueing Networks [9], Stochastic Petri Nets (SPN) [1], Performance Evaluation Process Algebra (PEPA) [11], and Stochastic Automata Networks (SAN) [12]. Among such formalisms we are specially interested in those which use Tensor (or Kronecker) Algebra to represent the infinitesimal generator of the underlying Markov chain [7, 8]. Such tensor formula representation is referred in the literature as *descriptor*.

The key operation to perform iterative solutions, both stationary and transient, of models described as a descriptor is the multiplication by a probability vector [14]. Such operation is performed using the *Shuffle* algorithm [8] which has a quite efficient way to handle tensor structures and takes advantage of several techniques developed to SAN [4], to PEPA [10], and to SPN [6].

The main purpose of this paper is to propose an alternative algorithm to perform the vector-descriptor product, which we call *Slice*. The main advantage of the Slice algorithm is the possible reduction of computational cost (number of multiplications)

*PUCRS, paulof@inf.pucrs.br (corresponding author). P. Fernandes is partially funded by CNPq/Brazil.
†PUCRS, rpresotto@inf.pucrs.br
‡PUCRS, asales@inf.pucrs.br
§PUCRS, twebber@inf.pucrs.br, T. Webber is funded by CAPES/Brazil.

for very sparse tensor components. Such reduction is achieved keeping the compact tensor format of the descriptor. In some way, the Slice algorithm can be considered as a trade-off between the sparse matrix approach used for straightforward Markov chains, and the fully tensor approach used by the Shuffle algorithm.

Nevertheless, this paper does not exploit the Slice algorithm possibilities to its limits, since very few considerations are made concerning possible optimizations. In particular, we do not analyse the possible benefits of automata reordering according to functional dependencies, which was deeply studied for the Shuffle algorithm. Also a possible hybrid approach using Shuffle and Slice algorithms are not discussed in detail. Actually, we focus our contribution in the presentation of an original way to handle the vector-descriptor product and we present encouraging measures to develop further studies based on this new approach.

This paper is organized with a brief introduction to the descriptor structure (Section 2). Section 3 presents the basic operation of the vector-descriptor product followed by sections describing the Shuffle algorithm principle (Section 3.1) and the proposed Slice algorithm (Section 3.2). In Section 4, we show some comparative measures of both *Shuffle* and *Slice* algorithms applied to two distinct structured models. Finally the conclusion points out some future works necessary to raise the Slice algorithm to a similar level of optimization as the level already obtained by the Shuffle algorithm.

2 Tensor Represented Descriptor

Regardless of the structured formalism adopted, *e.g.*, SAN, SPN, PEPA, the basic principle consists in the representation of a whole system by a collection of subsystems with an independent behavior (*local behavior*) and occasional interdependencies (*synchronized behavior*). According to the formalism, the primitives to describe local and synchronized behaviors may change their denomination, the reader interested in the formalisms definitions can found information in [12, 4] for SAN, in [1, 6] for SPN, and [11, 10] for PEPA.

For the purpose of this paper it is only important to consider that, unlike the non-structured approaches, *e.g.*, straightforward Markov chains, a structured model is not described by a single sparse matrix, but instead, by a *descriptor*. For a structured model with N subsystems and E synchronizing primitives, the descriptor (Q) is an algebraic formula containing $N + 2NE$ matrices:

$$Q = \bigoplus_{i=1}^{N}{}_g \, Q_l^{(i)} + \sum_{j=1}^{E} \left(\bigotimes_{i=1}^{N}{}_g \, Q_{e_j^+}^{(i)} + \bigotimes_{i=1}^{N}{}_g \, Q_{e_j^-}^{(i)} \right) \tag{1}$$

where:

- $Q_l^{(i)}$ represents N matrices describing each local behaviors of the i^{th} subsystem;
- $Q_{e_j^+}^{(i)}$ represents NE matrices describing the occurrence of synchronizing primitive e in the i^{th} subsystem;
- and $Q_{e_j^-}^{(i)}$ represents NE analogous matrices describing the diagonal adjustment of synchronizing primitive e in the i^{th} subsystem.

Table 1 details descriptor Q, which is composed of two separated parts: a tensor sum corresponding to the local events; a sum of tensor products corresponding to the synchronizing events [8]. The tensor sum operation of the local part can be decomposed into the ordinary sum of N normal factors, *i.e.*, a sum of tensor products where all matrices but one are identity matrices[1]. Therefore, in this first part, only the non-identity matrices ($Q_l^{(i)}$) need to be stored.

$\sum$	N		$Q_l^{(1)} \underset{g}{\otimes} I_{n_2} \underset{g}{\otimes} \cdots \underset{g}{\otimes} I_{n_{N-1}} \underset{g}{\otimes} I_{n_N}$ $I_{n_1} \underset{g}{\otimes} Q_l^{(2)} \underset{g}{\otimes} \cdots \underset{g}{\otimes} I_{n_{N-1}} \underset{g}{\otimes} I_{n_N}$ $\vdots$ $I_{n_1} \underset{g}{\otimes} I_{n_2} \underset{g}{\otimes} \cdots \underset{g}{\otimes} Q_l^{(N-1)} \underset{g}{\otimes} I_{n_N}$ $I_{n_1} \underset{g}{\otimes} I_{n_2} \underset{g}{\otimes} \cdots \underset{g}{\otimes} I_{n_{N-1}} \underset{g}{\otimes} Q_l^{(N)}$
	$2E$	e^+	$Q_{e_1^+}^{(1)} \underset{g}{\otimes} Q_{e_1^+}^{(2)} \underset{g}{\otimes} \cdots \underset{g}{\otimes} Q_{e_1^+}^{(N-1)} \underset{g}{\otimes} Q_{e_1^+}^{(N)}$ $\vdots$ $Q_{e_E^+}^{(1)} \underset{g}{\otimes} Q_{e_E^+}^{(2)} \underset{g}{\otimes} \cdots \underset{g}{\otimes} Q_{e_E^+}^{(N-1)} \underset{g}{\otimes} Q_{e_E^+}^{(N)}$
		e^-	$Q_{e_1^-}^{(1)} \underset{g}{\otimes} Q_{e_1^-}^{(2)} \underset{g}{\otimes} \cdots \underset{g}{\otimes} Q_{e_1^-}^{(N-1)} \underset{g}{\otimes} Q_{e_1^-}^{(N)}$ $\vdots$ $Q_{e_E^-}^{(1)} \underset{g}{\otimes} Q_{e_E^-}^{(2)} \underset{g}{\otimes} \cdots \underset{g}{\otimes} Q_{e_E^-}^{(N-1)} \underset{g}{\otimes} Q_{e_E^-}^{(N)}$

Table 1: SAN descriptor

3 Vector-Descriptor Product

The vector-descriptor product operation corresponds to the product of a vector v, as big as the product state space ($\prod_{i=1}^{N} n_i$), by descriptor Q. Since the descriptor is the ordinary sum of $N + 2E$ tensor products, the basic operation of the vector-descriptor product is the multiplication of vector v by a tensor product of N matrices:

$$\sum_{j=1}^{N+2E} \left(v \times \left[\bigotimes_{i=1}^{N}{}_g \, Q_j^{(i)} \right] \right) \tag{2}$$

where $Q_j^{(i)}$ corresponds to I_{n_i}, $Q_l^{(i)}$, $Q_{e^+}^{(i)}$, or $Q_{e^-}^{(i)}$ according to the tensor product term where it appears.

For simplicity in this section, we describe the Shuffle and Slice algorithms for the basic operation *vector* $\times$ *tensor product term* omitting index j from equation 2, *i.e.*:

$$v \times \left[\bigotimes_{i=1}^{N}{}_g \, Q^{(i)} \right] \tag{3}$$

[1] I_{n_i} is an identity matrix of order n_i.

3.1 Shuffle Algorithm

The Shuffle algorithm is described in this section without any considerations about optimizations for the evaluation of functional elements. A thorough study about matrices reordering and generalized tensor algebra properties with this objective can be found in [8]. All those optimizations aim to reduce the overhead of evaluate functional elements, but they do not change the number of multiplications needed by the Shuffle algorithm. Therefore, we ignore the functional elements in the context of this paper, and the basic operation (equation 3) is simplified to consider classical ($\otimes$) and not generalized ($\underset{g}{\otimes}$) tensor products.

The basic principle of the Shuffle algorithm concerns the application of the decomposition of a tensor product in the ordinary product of normal factors property:

$$\begin{aligned} Q^{(1)} \otimes \ldots \otimes Q^{(N)} \quad = \quad & (Q^{(1)} \otimes I_{n_2} \otimes \ldots \otimes I_{n_{N-1}} \otimes I_{n_N}) \quad \times \\ & (I_{n_1} \otimes Q^{(2)} \otimes \ldots \otimes I_{n_{N-1}} \otimes I_{n_N}) \quad \times \\ & \vdots \\ & (I_{n_1} \otimes I_{n_2} \otimes \ldots \otimes Q^{(N-1)} \otimes I_{n_N}) \quad \times \\ & (I_{n_1} \otimes I_{n_2} \otimes \ldots \otimes I_{n_{N-1}} \otimes Q^{(N)}) \end{aligned} \tag{4}$$

Rewritten the basic operation (equation 3) according to this property:

$$v \times \left[\prod_{i=1}^{N} I_{nleft_i} \otimes Q^{(i)} \otimes I_{nright_i} \right] \tag{5}$$

where $nleft_i$ corresponds to the product of the order of all matrices before the i^{th} matrix of the tensor product term, *i.e.*, $\prod_{k=1}^{i-1} n_k$ (particular case: $nleft_1 = 1$) and $nright_i$ corresponds to the product of the order of all matrices after the i^{th} matrix of the tensor product term, *i.e.*, $\prod_{k=i+1}^{N} n_k$ (particular case: $nright_N = 1$).

Hence, the Shuffle algorithm consists in multiplying successively a vector by each normal factor. More precisely, vector v is multiplied by the first normal factor, then the resulting vector is multiplied by the next normal factor and so on until the last factor. In fact, the multiplication of a vector v by the i^{th} normal factor corresponds to ***shuffle*** the elements of v in order to assemble $nleft_i \times nright_i$ vectors of size n_i and multiply them by matrix $Q^{(i)}$. Therefore, assuming that matrix $Q^{(i)}$ is stored as a sparse matrix, the number of multiplications needed to multiply a vector by the i^{th} normal factor is:

$$nleft_i \times nright_i \times nz_i \tag{6}$$

where nz_i corresponds to the number of nonzero elements of the i^{th} matrix of the tensor product term ($Q^{(i)}$). Considering the number of multiplications to all normal factors of a tensor product term, we obtain [8]:

$$\prod_{i=1}^{N} n_i \times \sum_{i=1}^{N} \frac{nz_i}{n_i} \tag{7}$$

3.2 Slice Algorithm

Slice is an alternative algorithm to perform the vector-descriptor product not based only on the decomposition of a tensor product in the ordinary product of normal factors

property (equation 4), but also applies a very basic property, the *Additive Decomposition* [8]. This property simply states that a tensor product term can be described by a sum of unitary matrices[2]:

$$Q^{(1)} \otimes \ldots \otimes Q^{(N)} = \sum_{i_1=1}^{n_1} \ldots \sum_{i_N=1}^{n_N} \sum_{j_1=1}^{n_1} \ldots \sum_{j_N=1}^{n_N} \left(\hat{q}^{(1)}_{(i_1,j_1)} \otimes \ldots \otimes \hat{q}^{(N)}_{(i_N,j_N)} \right) \quad (8)$$

where $\hat{q}^{(k)}_{(i,j)}$ is an unitary matrix of order n_k in which the element in row i and column j is equal to element (i,j) of the matrix $Q^{(k)}$.

Obviously, the application of such property over a tensor product with fully dense matrices results in a catastrophic number of $\prod_{i=1}^{N}(n_i)^2$ unitary matrix terms, but the number of terms is considerably reduced for sparse matrices. In fact, there is one unitary matrix to each possible combination of one nonzero element from each matrix. We may define $\theta(1 \ldots N)$ as the set of all possible combinations of nonzero elements of the matrices from $Q^{(1)}$ to $Q^{(N)}$. Therefore, the cardinality of $\theta(1 \ldots N)$, and consequently the number of unitary matrices to decompose a tensor product term, is given by $\prod_{i=1}^{N} nz_i$.

Generically evaluating the unitary matrices from equation 8, the sole nonzero element appears in the tensor coordinates (i_1, j_1) for the outermost block, coordinates (i_2, j_2) for the next inner block, and so on until the coordinates (i_N, j_N) for the innermost block. By the own definition of the tensor product, the value of an element is $\prod_{k=1}^{N} q^{(k)}_{(i_k,j_k)}$, where $q^{(k)}_{(i_k,j_k)}$ is the element in row i and column j of matrix $Q^{(k)}$. For such unitary matrices, we use the following notation:

$$\hat{Q}^{(1\ldots N)}_{i_1,\ldots,i_N,j_1,\ldots,j_N} = \hat{q}^{(1)}_{(i_1,j_1)} \otimes \ldots \otimes \hat{q}^{(N)}_{(i_N,j_N)} \quad (9)$$

The pure application of the Additive Decomposition property corresponds to generate a single equivalent sparse matrix to the tensor product term. For many cases, it may result in a too large number of elements. It is precisely to cope with this problem that the Shuffle algorithm was proposed. However, the manipulation of considerably sparse tensor product terms like this is somewhat awkward, since a decomposition in N normal factors may be a too large effort to multiply very few resulting elements.

The basic principle of the Slice algorithm is to handle the tensor product term in two distinct parts. The Additive Decomposition property is applied to all first $N-1$ matrices, generating $\prod_{i=1}^{N-1} nz_i$ very sparse terms which are multiplied (tensor product) by the last matrix, *i.e.*:

$$Q^{(1)} \otimes \ldots \otimes Q^{(N)} = \sum_{\substack{\forall i_1,\ldots,i_{N-1},j_1,\ldots,j_{N-1} \\ \in \theta(1\ldots N-1)}} \hat{Q}^{(1\ldots N-1)}_{i_1,\ldots,i_{N-1},j_1,\ldots,j_{N-1}} \otimes Q^{(N)} \quad (10)$$

Therefore, the Slice algorithm consists in dealing with $N-1$ matrices as a very sparse structure, and dealing with the last matrix as the Shuffle approach did. The multiplication of a vector v by the tensor product term (equation 3) using the Slice algorithm can be rewritten as:

$$v \times \left[\sum_{\substack{\forall i_1,\ldots,i_{N-1},j_1,\ldots,j_{N-1} \\ \in \theta(1\ldots N-1)}} \hat{Q}^{(1\ldots N-1)}_{i_1,\ldots,i_{N-1},j_1,\ldots,j_{N-1}} \otimes Q^{(N)} \right] \quad (11)$$

[2] A unitary matrix is a matrix in which there is only one nonzero element.

Applying the distributive property, equation 11 can be rewritten as:

$$\sum_{\substack{\forall i_1,\ldots,i_{N-1},j_1,\ldots,j_{N-1} \\ \in\theta(1\ldots N-1)}} v \times \left(\hat{Q}^{(1\ldots N-1)}_{i_1,\ldots,i_{N-1},j_1,\ldots,j_{N-1}} \otimes Q^{(N)}\right) \tag{12}$$

We call each term of the previous equation as *Additive Unitary Normal Factor*, since it is composed of an unitary matrix times a standard normal factor. The decomposition in normal factors applied to each additive unitary normal factor of equation 12 results in:

$$v \times \left[\left(\hat{Q}^{(1\ldots N-1)}_{i_1,\ldots,i_{N-1},j_1,\ldots,j_{N-1}} \otimes I_{n_N}\right) \times \left(I_{nleft_N} \otimes Q^{(N)}\right)\right] \tag{13}$$

It is important to notice that the first multiplication takes only n_N elements of vector v and it corresponds to the product of this *sliced* vector (called v_s) by the single scalar which is the nonzero element of matrix $\hat{Q}^{(1\ldots N-1)}_{i_1,\ldots,i_{N-1},j_1,\ldots,j_{N-1}}$. The resulting vector, called v'_s, must then be multiplied only once by matrix $Q^{(N)}$, since all other positions of the intermediate vector (except those in v'_s) are zero.

The application of the Slice algorithm must generate the nonzero element (c) of matrix $\hat{Q}^{(1\ldots N-1)}_{i_1,\ldots,i_{N-1},j_1,\ldots,j_{N-1}}$. Hence, it must pick a *slice* of vector v (called v_s) according to the row position of element c, and multiply all elements of v_s by c. In fact, this multiplication by a scalar corresponds to the first multiplication by a normal factor of equation 13. The resulting vector, called v'_s, must be multiplied by the matrix $Q^{(N)}$ (second multiplication in equation 13), accumulating the result (r_s) in the positions of the resulting vector r corresponding to the column position of element c.

The Slice algorithm (Algorithm 1) can be summarize for all Additive Unitary Normal Factors in the operation:

$$r = v \times \left[\left(\hat{Q}^{(1\ldots N-1)}_{i_1,\ldots,i_{N-1},j_1,\ldots,j_{N-1}} \otimes I_{n_N}\right) \times \left(I_{nleft_N} \otimes Q^{(N)}\right)\right]$$

Algorithm 1 Slice Algorithm

1: **for all** $i_1,\ldots,i_{N-1},j_1,\ldots,j_{N-1} \in \theta(1\ldots N-1)$ **do**
2: $c \leftarrow \prod_{k=1}^{N-1} q^{(k)}_{(i_k,j_k)}$
3: slice v_s from v according to $i_1,\ldots,i_{N-1}$
4: $v'_s \leftarrow c \times v_s$
5: $r_s \leftarrow v'_s \times Q^{(N)}$
6: add r_s to r according to $j_1,\ldots,j_{N-1}$
7: **end for**

The computational cost (number of needed multiplications) of the slice algorithm considers: the number of unitary matrices ($\prod_{i=1}^{N-1} nz_i$); the cost to generate the nonzero element of each unitary matrix ($N-2$); the cost to multiply it by each element of sliced vector v_s (n_N); and the cost to multiply v_s by the last matrix $Q^{(N)}$ (nz_N), *i.e.*:

$$\prod_{i=1}^{N-1} nz_i \times \left[(N-2) + n_N + nz_N\right] \tag{14}$$

4 Numerical Analysis

In order to analyze the performance of both Shuffle and Slice algorithms, two different sets of models were considered. The first set of models describes a two-classes mixed finite capacity queueing network model (Figure 1).

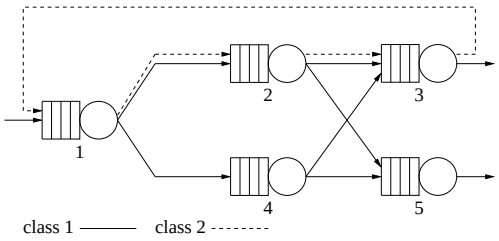

Figure 1: Mixed Queueing Network model

For this model, customers of the first class will act as an open system visiting all queues, and the customers of the second class will act as a closed system visiting only the first three queues. In this model, all queues have only one server available and the customers of class 1 have priority over the customers of class 2. Such model was modeled using the SPN formalism and it was split in 8 subnets ($N = 8$) with 9 synchronized transitions ($E = 9$).

The second set of models describes a parallel implementation of a master/slave algorithm developed by SAN formalism. This model was introduced in [2] and, considering an implementation with S slave nodes, it has $S + 2$ automata ($N = S + 2$) and $3 + 2 \times S$ synchronizing events ($E = 3 + 2 \times S$).

The numerical results for this section were obtained on a 2.8 GHz Pentium IV Xeon under Linux operating system with 2 GBytes of memory. The actual PEPS 2003 implementation [4] was used to obtain the Shuffle algorithm results and a prototype implementation was used to obtain the Slice algorithm results.

4.1 Shuffle and Slice Comparison

The first set of experiments is conducted for the two examples using both algorithms (columns *Shuffle* and *Slice*). For each option we compute the number of multiplications performed (computational cost - *c.c.*), and the time to execute a complete multiplication in seconds (*time*). For the Mixed Queue Network model (*Mixed QN*), we consider all queues with the same capacity (K) assuming the values $K = 3..7$. For the Parallel Implementation model (*Parallel*) described in [2], we assign the number of slaves (S) with the values $S = 3..7$. For all models, we also measured the memory needs to store the descriptor in KBytes, which is indicated in column *mem*[3] (see Table 2).

The number of multiplications needed for the Slice algorithm (equation 14) is less significant than the number needed in the Shuffle algorithm (equation 7). Even though the time spent in the Slice algorithm is still better than Shuffle one, the gains are slightly less significant than the computational cost gain. This happens probably due to a more optimized treatment of the function evaluations in the Shuffle algorithm.

[3]Obviously, the memory needs for the Shuffle and Slice approach are equal, since the choice of algorithm does not interfere with the descriptor structure.

Mixed QN						
	Shuffle			*Slice*		
	c.c.	*time*	*mem.*	*c.c.*	*time*	*mem.*
$K = 3$	9.14×10^6	0.16	4	2.59×10^6	0.05	4
$K = 4$	5.53×10^7	0.87	5	1.58×10^7	0.28	5
$K = 5$	2.40×10^8	3.77	6	6.86×10^7	1.19	6
$K = 6$	8.30×10^8	12.86	6	2.36×10^8	4.06	6
$K = 7$	2.43×10^9	47.31	7	6.85×10^8	14.82	7
Parallel						
	Shuffle			*Slice*		
	c.c.	*time*	*mem.*	*c.c.*	*time*	*mem.*
$S = 3$	2.43×10^5	< 0.01	9	6.59×10^4	< 0.01	9
$S = 4$	1.10×10^6	0.02	12	2.61×10^5	< 0.01	12
$S = 5$	4.67×10^6	0.09	15	9.97×10^5	0.02	15
$S = 6$	1.88×10^7	0.33	18	3.71×10^6	0.07	18
$S = 7$	7.31×10^7	1.14	21	1.35×10^7	0.23	21

Table 2: Shuffle and Slice algorithms comparison

4.2 Slice Algorithm Optimizations

The second set of experiments is conducted over the Mixed Queue Network example assuming all queues, but the last one, with the same capacity ($K = 4$). The capacity of the last queue (K_5) is tested with values 3, 4, 5, 6, and 7. Figure 2 shows a table with the numeric results obtained for these experiments and a plot of the time spent in both approaches.

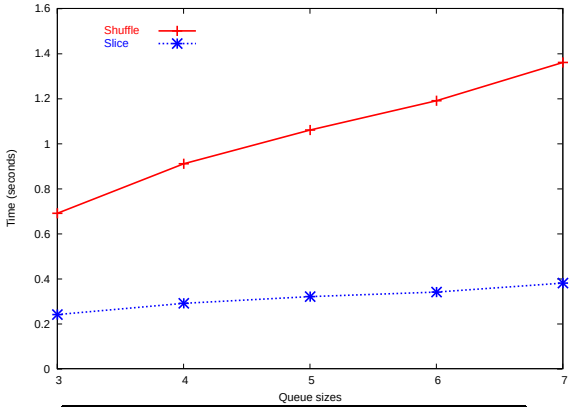

K_5	*Shuffle*		*Slice*	
	c.c.	*time*	*c.c.*	*time*
3	4.42×10^7	0.69	1.38×10^7	0.24
4	5.53×10^7	0.91	1.58×10^7	0.29
5	6.65×10^7	1.06	1.79×10^7	0.32
6	7.76×10^7	1.19	1.99×10^7	0.34
7	8.88×10^7	1.36	2.20×10^7	0.38

Figure 2: Experiments on Slice Optimization for Mixed Queue Network model

Observing equations 7 and 14, it is possible to notice that, unlike the cost of the Shuffle algorithm, the cost of the Slice algorithm is less dependent on the order of the last matrix. This can be verified by the results in Figure 2, since both Slice and Shuffle curves have clearly different behaviors.

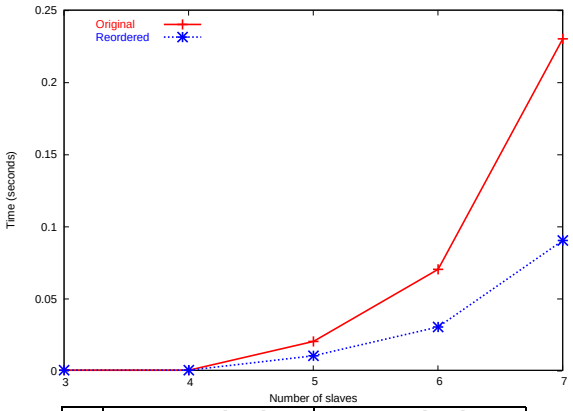

	Non Ordered		*Reordered*	
S	*c.c.*	*time*	*c.c.*	*time*
3	6.59×10^4	< 0.01	3.67×10^4	< 0.01
4	2.61×10^5	< 0.01	1.37×10^5	< 0.01
5	9.97×10^5	0.02	4.92×10^5	0.01
6	3.71×10^6	0.07	1.73×10^6	0.03
7	1.35×10^7	0.23	5.95×10^6	0.09

Figure 3: Experiments on Slice Optimization for Parallel Implementation model

The last set of experiments (Figure 3) shows the effect of automata reordering for the Parallel Implementation model. This model has one very large automaton (40 states) and all other automata with only 3 states. For these experiments, only the results of the Slice algorithm are indicated. The left hand side columns (*Non Ordered*) indicate the results obtained for the example with the larger automaton appearing at the beginning. The right hand side columns (*Reordered*) indicate the results obtained putting the largest automaton as the last one. The results show clearly the improvements in the number of multiplications as well as in the time spent. Such encouraging result suggests that many other optimizations could still be found to the Slice algorithm.

It is important to notice that an analysis of the functional evaluations for the Slice algorithm may reveal further optimizations, but as said in the introduction such analysis is out of the scope of this paper.

5 Conclusion

This paper proposes a different way to perform vector-descriptor product. The new Slice algorithm has shown a better overall performance than the traditional Shuffle algorithm for all examples tested. In fact, the Shuffle algorithm would only be more efficient for quite particular cases in which the descriptor matrices would be nearly full. Even though we could imagine such tensor products (with only nearly full matrices), we were not able to generate a real model with such characteristics. It seems that real case models have naturally sparse matrices. The local part of a descriptor is naturally very sparse due to the tensor sum structure. The synchronizing primitives are mostly

used to describe exceptional behaviors, therefore it lets the synchronizing part of the descriptor also quite sparse.

As a matter of fact, the Slice algorithm seems to offer a good trade-off between the unique sparse matrix approach used for straightforward Markov chains and the pure tensor approach of the Shuffle algorithm. It is much more memory efficient than the unique sparse matrix approach, and it would only be slower than the Shuffle algorithm in hypothetical models with nearly full matrices. However, even for those hypothetical models, the Slice approach may be used for some terms of the descriptor. Such hybrid approach could analyze which algorithm should be used to each one of the tensor product terms of the descriptor.

Besides the immediate future works to develop further experiments with the Slice algorithm already mentioned in the previous section, we may also foresee studies concerning parallel implementations. The prototyped parallel implementation of the Shuffle algorithm [3] has already shown consistent gains to solve particularly slow SAN models. Nevertheless, the Shuffle algorithm parallelization suffers an important limitation that consists in the passing of a whole tensor product term to each parallel node. This is a problem since all nodes must compute multiplications of the whole vector v by a tensor product term that usually has nonzero elements in many positions.

The Slice algorithm can offer a more effective parallelization since its Additive Unitary Normal Factors only affect few positions of vector v. A parallel node could receive only similar terms and, therefore, not handle the whole vector v. This can be specially interesting for parallel machines with nodes with few memory resources.

Concentrating back in the sequential implementation, our first results with the Slice algorithm prototype were very encouraging, but we expect to have many improvements to do before integrate this new algorithm in a new version of the PEPS software tool [4]. As we said before, this paper is just a first step for this new approach and much numerical studies have to be done. However, the current version of the Slice algorithm already shows better results than Shuffle.

References

[1] M. Ajmone-Marsan, G. Conte, and G. Balbo. A Class of Generalized Stochastic Petri Nets for the Performance Evaluation of Multiprocessor Systems. *ACM Transactions on Computer Systems*, 2(2):93–122, 1984.

[2] L. Baldo, L. Brenner, L. G. Fernandes, P. Fernandes, and A. Sales. Performance Models for Master/Slave Parallel Programs. *Electronic Notes In Theoretical Computer Science*, 128(4):101–121, April 2005.

[3] L. Baldo, L. G. Fernandes, P. Roisenberg, P. Velho, and T. Webber. Parallel PEPS Tool Performance Analysis using Stochastic Automata Networks. In M. Donelutto, D. Laforenza, and M. Vanneschi, editors, *Euro-Par 2004 International Conference on Parallel Processing*, volume 3149 of *Lecture Notes in Computer Science*, pages 214–219, Pisa, Italy, August/September 2004. Springer-Verlag Heidelberg.

[4] A. Benoit, L. Brenner, P. Fernandes, B. Plateau, and W. J. Stewart. The PEPS Software Tool. In *Computer Performance Evaluation / TOOLS 2003*, volume 2794 of *LNCS*, pages 98–115, Urbana, IL, USA, 2003. Springer-Verlag Heidelberg.

[5] L. Brenner, P. Fernandes, and A. Sales. The Need for and the Advantages of Generalized Tensor Algebra for Kronecker Structured Representations. *International Journal of Simulation: Systems, Science & Technology*, 6(3-4):52–60, February 2005.

[6] G. Ciardo, R. L. Jones, A. S. Miner, and R. Siminiceanu. SMART: Stochastic Model Analyzer for Reliability and Timing. In *Tools of Aachen 2001 International Multiconference on Measurement, Modelling and Evaluation of Computer-Communication Systems*, pages 29–34, Aachen, Germany, September 2001.

[7] M. Davio. Kronecker Products and Shuffle Algebra. *IEEE Transactions on Computers*, C-30(2):116–125, 1981.

[8] P. Fernandes, B. Plateau, and W. J. Stewart. Efficient descriptor - Vector multiplication in Stochastic Automata Networks. *Journal of the ACM*, 45(3):381–414, 1998.

[9] E. Gelenbe. G-Networks: Multiple Classes of Positive Customers, Signals, and Product Form Results. In *Performance*, volume 2459 of *Lecture Notes in Computer Science*, pages 1–16. Springer-Verlag Heidelberg, 2002.

[10] S. Gilmore and J. Hillston. The PEPA Workbench: A Tool to Support a Process Algebra-based Approach to Performance Modelling. In *Computer Performance Evaluation*, pages 353–368, 1994.

[11] S. Gilmore, J. Hillston, L. Kloul, and M. Ribaudo. PEPA nets: a structured performance modelling formalism. *Performance Evaluation*, 54(2):79–104, 2003.

[12] B. Plateau and K. Atif. Stochastic Automata Networks for modelling parallel systems. *IEEE Transactions on Software Engineering*, 17(10):1093–1108, 1991.

[13] W. H. Sanders and J. F. Meyer. Stochastic Activity Networks: Formal Definitions and Concepts. In *Lectures on Formal Methods and Performance Analysis : First EEF/Euro Summer School on Trends in Computer Science*, volume 2090 of *Lecture Notes in Computer Science*, pages 315–343, Berg En Dal, The Netherlands, July 2001. Springer-Verlag Heidelberg.

[14] W. J. Stewart. *Introduction to the numerical solution of Markov chains*. Princeton University Press, 1994.

A moment-based estimation method for extreme probabilities

Árpád Tari*, Miklós Telek† and Peter Buchholz‡

Abstract

The performance analysis of highly reliable and fault tolerant systems requires the investigation of events with extremely low or high probabilities. This paper presents a simplified numerical method to bound the extreme probabilities based on the moments of the distribution. This simplified method eliminates some numerically sensitive steps of the general moments based bounding procedure.

Numerical examples indicate the applicability of the proposed approach.

Keywords: reduced moment problem, moments based distribution bounding, tail distribution

1 Introduction

Performance analysis of real-life systems usually requires the evaluation of the distribution of some random variables. The direct analysis of these distributions is often infeasible due to the high computational complexity. A possible way to overcome this difficulty is to simplify the model or to calculate only an estimate of the measure of interest. Both types of simplification result in inaccuracies in calculation, but this is the price of the solvability.

In this paper we investigate the second option, the estimation of the measure of interest based on a set of its moments. There are several classes of performance analysis problems for which the analysis of the moments of a random variable is far less complex than the analysis of the distribution. For example, for the class of Markov reward models the moments of the reward measures can be computed by the effective methods presented in [12, 15], while the direct analysis of the distribution of these measures based on [8, 3, 4] is far more complex and practically infeasible for models with more than 10^4 states [7]. In these cases moments based estimation of the distribution is the only feasible solution method for large models. There are two ways of moments based estimation: to fit a certain class of distribution functions to the set of moments (e.g. [16] presents a method for fitting with matrix exponential distribution); and to calculate maximal and minimal values for the distribution among all possible distributions having the prescribed set of moments. The first approach results

*Universität Dortmund, Germany, email: arpad@sch.bme.hu
†Budapest University of Technology and Economics, Hungary, email: telek@hit.bme.hu
‡Universität Dortmund, Germany, email: peter.buchholz@cs.uni-dortmund.de

in an unknown error if the performance measure does not belong to the considered class of distributions. To bound the error of moments based distribution approximation we apply the second approach.

Determining a distribution function based on its moments is called the *reduced moment problem* (where reduced refers to the finite number of moments). This is a well-known problem for more than 100 years and has an extensive literature. A good overview is given in [13].

We denote the i^{th} moment of a distribution function $\sigma(x)$ supported on the interval $[a, b]$ by

$$\mu_i = \int_a^b x^i \, \mathrm{d}\sigma(x), \qquad i = 0, 1, 2, \ldots, m \ . \tag{1}$$

The problem of determining a distribution whose support interval is the real axis (hence $a = -\infty$, $b = \infty$) based on its moments is called the *Hamburger* moment problem after the German mathematician who first solved this problem in 1920 [6]. We also refer to this as the *infinite case* and we discuss this problem in this paper. Other moment problems are the *Stieltjes* (when $a = 0$ and $b = \infty$) and *Hausdorff* (if $a = 0$, $b = 1$) moment problems.

The performance analysis of highly reliable or safety critical fault-tolerant systems requires the analysis very unlikely events, i.e., the distribution of a random variable at very low (close to 0) or very high (near to 1) probabilities.

In the paper we focus on the analysis of these kinds of extreme values and provide a simplified moments based estimation analysis algorithm with respect to the one that calculates lower and upper bounds for the distribution function based on a set of moments in the general case [11]. The modified algorithm is numerically stable, simple and fast.

The paper is organized as follows: Section 2 introduces the moments based estimation method. The numerical procedures involved in the solution are summarized in Section 3 and some useful expressions are deduced in Section 4. An example is analyzed in Section 5. Section 6 concludes the paper.

2 Discrete reference distribution

The method discussed here is based on the idea introduced in [10, 11]. We briefly present it here as it is the basis of our investigation.

The considered task can be formalized as follows. Find the smallest and largest values, that any distribution function $\sigma(x)$ with $\mu_0, \mu_1, \ldots, \mu_m$ moments may have at a given point C, i.e:

$$L = \min \left\{ \sigma(C) : \ \mu_i = \int_{-\infty}^{\infty} x^i \mathrm{d}\sigma(x), i = 0, \ldots, m \right\}, \tag{2}$$

$$U = \max \left\{ \sigma(C) : \ \mu_i = \int_{-\infty}^{\infty} x^i \mathrm{d}\sigma(x), i = 0, \ldots, m \right\} \ . \tag{3}$$

This means that we estimate the distribution in a single point. Estimation in an interval is only possible with a series of applications in points of the interval, but this can be done effectively repeating only parts of the algorithm.

The L and U values result from a discrete distribution that have the maximal probability mass at point C and is characterized by the $\mu_0, \mu_1, \ldots, \mu_m$ moments.

Before calculating L and U, we need to check whether the series of moments $\mu_0, \mu_1, \ldots, \mu_m$ can belong to a valid distribution function. This can be verified through the following inequalities:

$$|\boldsymbol{M}_k| \geq 0, \qquad k = 0, 1, \ldots, \left\lfloor \frac{m}{2} \right\rfloor, \tag{4}$$

where

$$\boldsymbol{M}_k = \begin{pmatrix} \mu_0 & \mu_1 & \ldots & \mu_k \\ \mu_1 & \mu_2 & \ldots & \mu_{k+1} \\ \vdots & \vdots & \ddots & \vdots \\ \mu_k & \mu_{k+1} & \ldots & \mu_{2k} \end{pmatrix} . \tag{5}$$

The maximum number of moments that satisfy (4) is denoted by $2n+1$, i.e. the considered moments are $\mu_0, \mu_1, \ldots, \mu_{2n}$, and the matrix of largest order satisfying (4) is denoted by $\boldsymbol{M} := \boldsymbol{M}_n$.

Let the roots of

$$P(x) = \begin{vmatrix} \mu_0 & \mu_1 & \ldots & \mu_n \\ \vdots & \vdots & \ddots & \vdots \\ \mu_{n-1} & \mu_n & \ldots & \mu_{2n-1} \\ 1 & x & \ldots & x^n \end{vmatrix} \tag{6}$$

be denoted by $u_1 < u_2 < \ldots < u_n$ in increasing order. These roots are also real and simple [14].

If $C = u_i$ for some i then the discrete distribution consists only of n points (including C) and we have to take $\boldsymbol{M} := \boldsymbol{M}_{n-1}$ [13, p. 42], so this must be checked before the calculations.

Odd number of input is needed to form the matrices $\boldsymbol{M}_k$. As a consequence if even number of moments is given, the last one (μ_{2n+1}) does not carry further information about the distribution, so this can be ignored.

The maximal probability mass that can be concentrated at C is denoted by p and calculated by [1]:

$$p = \frac{1}{\boldsymbol{c}^T \, \boldsymbol{M}^{-1} \, \boldsymbol{c}}, \tag{7}$$

where

$$\boldsymbol{c}^T = \left(1, C, C^2, \ldots, C^n\right)^T \quad . \tag{8}$$

Furthermore, the difference between any two distribution functions with moments $\mu_0, \mu_1, \ldots, \mu_{2n}$ is not larger than p [1]. Note that the formula for p contains the inverse of $\boldsymbol{M}$, a symmetric and positive definite (due to (4)) matrix. The computation of the inverse of symmetric positive definite matrices is numerically more stable than the inversion of general matrices.

The other points of the discrete distribution are the roots of the following polynomial:

$$\chi(x) = \boldsymbol{c}^T \, \boldsymbol{M}^{-1} \, \boldsymbol{x}, \tag{9}$$

where $\boldsymbol{x} = \left(1, x, x^2, \ldots, x^n\right)^T$.

This is an order n polynomial and based on the theory of orthogonal polynomials [14] its roots are all real and distinct. We denote them by $x_1 < x_2 < \ldots < x_n$ in increasing order. The corresponding probability masses are

$$p_i = \frac{1}{\boldsymbol{x_i}^T \, \boldsymbol{M}^{-1} \, \boldsymbol{x_i}}, \qquad i = 1, 2, \ldots, n, \tag{10}$$

where $\boldsymbol{x_i} = \left(1, x_i, x_i^2, \ldots, x_i^n\right)^T$.

The lower limit of the distribution is obtained as the sum of the weights of the points smaller than C. The upper limit is the sum of the lower limit and the maximum mass at C:

$$L = \sum_{i:\, x_i < C} p_i, \qquad U = L + p \ . \tag{11}$$

This discrete distribution is extreme in that sense, that no other distribution function with moments μ_i has either a lower or higher value at C than L and U, respectively.

The algorithm can be simplified using the following interesting property of the points x_i. These points depend on C, but their locations can be characterized by a series independent of C. The $x_1, x_2, \ldots, x_n, C$ and the $u_1, u_2, \ldots, u_n$ roots (see (6)) are mutually separated as

$$x_1 < u_1 < x_2 < u_2 < \ldots < u_{j-1} < C < u_j < x_j < u_{j+1} < \ldots < u_n < x_n \ . \tag{12}$$

The number of points x_i which are smaller (greater) than C equals the number of points u_i that are smaller (greater) than C. As a consequence the roots $u_1, u_2, \ldots, u_n$ define the number of terms considered in (11). Therefore it is sufficient to calculate only the roots x_i smaller than C (or alternatively the roots x_i greater than C). If $C < u_1$ or $C > u_n$ we do not need to calculate the points of the discrete distribution, because in these cases the lower and upper limits are determined by p as follows:

$$L = 0, \qquad U = p, \qquad \text{if } C < u_1, \tag{13}$$

$$L = 1 - p, \qquad U = 1, \qquad \text{if } C > u_n \ . \tag{14}$$

We use these simple relations to bound the probability of extreme events and this type of estimation is called the *simplified* case. The numerical procedure is summarized in Figure 1.

3 Computational complexity

Some tasks in the proposed algorithm may involve numerical difficulties in the general case (e.g. evaluating determinants, inverting matrices, finding roots of polynomials), however the matrices and the polynomial considered here have special properties that make it possible to use numerically more stable methods to calculate them.

To calculate the determinants of symmetric matrices we use the *LU decomposition* [9, p. 43 – 50]. Testing with known distributions the maximum dimension of the matrix whose determinant could be computed correctly is 15×15, bigger matrices resulted negative determinants showing numerical instabilities in the method. Therefore the limit of the applicability is 29 moments using standard floating point arithmetic, but the maximum number of moments that satisfy (4) largely depends on the original distribution: our experiences show that in general the number of usable moments is around 20, but in some cases it is below 15.

We use *Cholesky decomposition* with backsubstitution to invert the positive definite matrix $\boldsymbol{M}$ [9, p. 96–98]. This method is known to be extremely stable

Input: $\mu_0, \mu_1, \ldots, \mu_m$; a set of C values where we need to bound the distribution.

1. Test if the moments satisfy the

$$|\boldsymbol{M}_k| \geq 0 \qquad k = 0, 1, \ldots, \lfloor m/2 \rfloor \tag{15}$$

inequalities, where

$$\boldsymbol{M}_k = \begin{pmatrix} \mu_0 & \mu_1 & \ldots & \mu_k \\ \mu_1 & \mu_2 & \ldots & \mu_{k+1} \\ \vdots & \vdots & \ddots & \vdots \\ \mu_k & \mu_{k+1} & \ldots & \mu_{2k} \end{pmatrix} \quad . \tag{16}$$

We denote the number of applicable moments (for which the (15) inequalities hold) by $2n+1$ ($\mu_0, \ldots, \mu_{2n}$).

2. Find the roots of the polynomial $P(x)$:

$$P(x) = \begin{vmatrix} \mu_0 & \mu_1 & \ldots & \mu_n \\ \vdots & \vdots & \ddots & \vdots \\ \mu_{k-1} & \mu_k & \ldots & \mu_{2n-1} \\ 1 & x & \ldots & x^k \end{vmatrix} \quad . \tag{17}$$

The roots are called $u_1 < u_2 < \ldots < u_n$.

3. Do for each $C < u_1$ or $C > u_n$ point of interest

   (a) Calculate the largest possible p:

$$p = \frac{1}{\boldsymbol{c}^T \, \boldsymbol{M}^{-1} \, \boldsymbol{c}}, \tag{18}$$

where

$$\boldsymbol{c}^T = \left(1, C, C^2, \ldots, C^n\right)^T \quad . \tag{19}$$

   (b) If $C < u_1$, then $L = 0,\ U = p$.
   If $C > u_n$, then $L = 1 - p,\ U = 1$.

Figure 1: Steps of the algorithm

numerically and approximately two times faster than the alternative methods for solving linear equations. It fails only if the matrix is not positive definite.

It is hard to find the roots of a polynomial if we do not know anything about the location of the roots. But all the roots of $P(x)$ are real, and in this case *Laguerre's method* [9, p. 371 – 374] works well as it is theoretically guaranteed that this algorithm converges to a root from any starting point.

Figure 1 shows that at different values of C only p has to be recalculated, hence the overall algorithm is neither CPU, nor memory intensive. Table 1 shows the required operations in order to estimate a distribution in N points using m moments $(\mu_0, \mu_1, \ldots, \mu_{m-1})$ out of whom $2n+1$ $(\mu_0, \mu_1, \ldots, \mu_{2n})$ defines a valid moment sequence.

Task	Nr. of executions
calculation of determinants	$\lfloor m/2 \rfloor + 1$
finding n roots of $P(x)$	1
inversion of an $(n+1) \times (n+1)$ matrix	1
vector-matrix multiplications of size $(n+1) \times (n+1)$	$2N$
scalar product of vectors of size $(n+1)$	$2N$
reciprocal	$2N$

Table 1: Computational cost of the simplified estimation

4 Closed-form expressions

The applicability of the simplified estimation depends on the smallest and the largest root of $P(x)$. If the degree of the polynomial $P(x)$ is less than 5, then closed form expressions can be deduced for u_i, though for degrees 3 and 4 these expressions are much too complicated and would fill several pages.

However if the degree of $P(x)$ is equal to 2 (hence we have 5 moments as input: $\mu_0, \mu_1, \mu_2, \mu_3$ and μ_4) the formulas for u_1, u_2 and even for p are quite simple. Discrete construction is needed only in the interval $[u_1, u_2]$.

$$u_{1,2} = \frac{\mu_1\mu_2 - \mu_0\mu_3 \pm \sqrt{-3\mu_1^2\mu_2^2 + 4\mu_0\mu_2^3 + 4\mu_1^3\mu_3 - 6\mu_0\mu_1\mu_2\mu_3 + \mu_0^2\mu_3^2}}{2\mu_1^2 - 2\mu_0\mu_2}, \tag{20}$$

$$\begin{aligned}\frac{1}{p} =& \frac{C^4(\mu_1^2 - \mu_0\mu_2) + C^3(-2\mu_1\mu_2 + 2\mu_0\mu_3) + C^2(3\mu_2^2 - 2\mu_1\mu_3 - \mu_0\mu_4) +}{\mu_2^3 + \mu_0\mu_3^2 + \mu_1^2\mu_4 - \mu_2(2\mu_1\mu_3 + \mu_0\mu_4)} \\ & \frac{+C(-2\mu_2\mu_3 + 2\mu_1\mu_4) + (\mu_3^2 - \mu_2\mu_4)}{\mu_2^3 + \mu_0\mu_3^2 + \mu_1^2\mu_4 - \mu_2(2\mu_1\mu_3 + \mu_0\mu_4)} \ .\end{aligned} \tag{21}$$

Having 3 input moments ($\mu_0 = 1, \mu_1$ and μ_2) the discrete reference distribution contains only 1 point: C . The only root of $P(x)$ and the maximal concentrated mass at C are the following:

$$u_1 = \mu_1, \qquad p = \frac{\mu_2 - \mu_1^2}{C^2 - 2C\mu_1 + \mu_2} \ . \tag{22}$$

The lower and upper bounding functions can be expressed by simple formulas along the whole real axis.

$$L = \begin{cases} 0 & \text{if } C < \mu_1 \ , \\ \dfrac{(C-\mu_1)^2}{C^2 - 2C\mu_1 + \mu_2} & \text{if } C \geq \mu_1 \ , \end{cases} \tag{23}$$

$$U = \begin{cases} \dfrac{\mu_2 - \mu_1^2}{C^2 - 2C\mu_1 + \mu_2} & \text{if } C < \mu_1 \ , \\ 1 & \text{if } C \geq \mu_1 \ . \end{cases} \tag{24}$$

It is easy to see that L and U are continuous functions of C .

These formulas are simple but they make only rough estimations possible. The next section shows how the increasing number of moments affects accuracy.

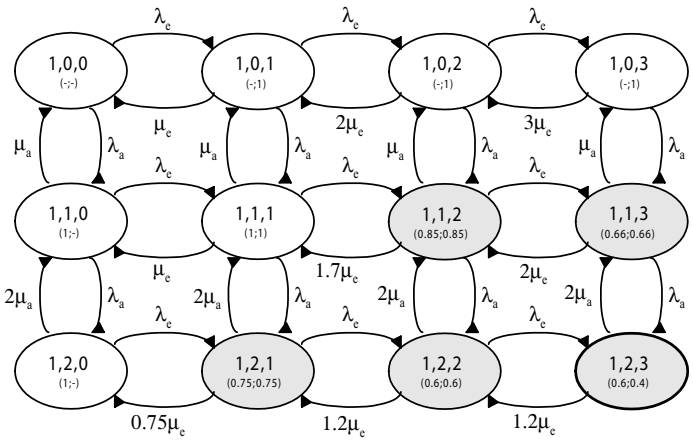

Figure 2: State space of the sample model

5 Example of application

This section demonstrates the properties of the proposed approach through an example, pointing out its strengths and weaknesses.

[5] introduced a strategy to share a telecommunication link between different traffic classes to satisfy certain pre-defined Quality of Service (QoS) constraints. Three traffic classes are defined:

- **rigid**: require constant bandwidth (b_r) allocation;
- **adaptive**: characterized by peak (b_a) and minimum bandwidth (b_a^{min}) requirements, the actual bandwidth usage depends on the link utilization (for example a video stream with adaptive compression level, where quality degradation is allowed to a certain degree, but high delay variance in not);
- **elastic**: similar to the adaptive class regarding their bandwidth requirements (b_e and b_e^{min}), but they stay in the system until a given amount of data has been transmitted (for example an ftp-session, where transfer rate changes are allowed, but data loss is not).

A Markov reward model (MRM) is used to describe system behavior. The states of the system are represented by a triple (n_r, n_a, n_e) which are the number of active flows in the system belonging to the rigid, adaptive and elastic flows, respectively. The arrival rates are $\lambda_r, \lambda_a, \lambda_e$, and the departure rates are μ_r, μ_a, μ_e. μ_e is called the *maximal* departure rate of an elastic flow experienced when maximal bandwidth is available, the *actual* departure rate is proportional to the available bandwidth, which is a function of n_r, n_a and n_e. The transition rates of the MRM are calculated from these rates, and the reward rates associated with each state are the actual bandwidth of the elastic class.

Figure 2 shows a portion of the state space in case of $n_r = 1$. The states where the elastic flows do not get the maximal bandwidth are printed in grey. The numbers below the state identifiers indicate the actual bandwidth of the adaptive and elastic flows as a fraction of their peak bandwidth.

The performance measure of our interest is the distribution of the amount of time, $T(\xi)$, required to transmit ξ amount of data by an elastic traffic flow.

We would like to ensure that the transmission completes before time t with a very high probability:

$$\Pr\left(T(\xi) < t\right) > \varepsilon, \tag{25}$$

where ε is a prescribed constant close to 1 $(0.99, \ldots, 0.99999)$. The amount of data is given and we are interested in the minimum value of t which means that the transfer of ξ amout of data will be finished during the interval $[0, t_{\min})$ with probability e.g. 0.9999 but this is not true for any $t < t_{\min}$.

This investigation requires evaluation of the MRM. We compare two different analysis approaches:

1. the moment-based method in [15] with estimation based on the moments;
2. direct analysis of the distribution of the completion time: methods of Nabli and Sericola [8], De Souza e Silva and Gail [2], Donatiello and Grassi [4].

The algorithms were implemented by their original paper. We use a dual AMD Opteron 248 (2.2 GHz) system with 6 GB of RAM running Linux for computations.

5.1 Correctness

To verify the procedures we evaluate a sample system with 105 states and calculate the whole distribution of the amount of transmitted data. The three direct methods result in the same values and the moments-based method gives real bounds as it is depicted in Figure 3. The more moments are given the tighter the bounds are. It is also observable that convergence slows down with the increasing number of moments. The bounds are the widest around the mean of the distribution. We are able to do the estimations with maximum 17 moments, because using more moments results in negative determinant while testing the necessary condition of existence (4). This is due to numerical instabilities in the procedure that calculates the determinant of a matrix.

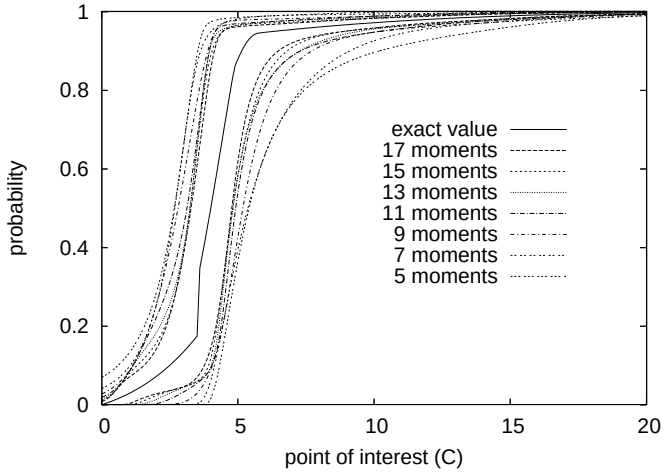

Figure 3: Distribution of the transmission time of ξ amount of elastic data

Moments	Valid from	0.9999	0.99999	0.999999
5	13.668	48.542	78.919	122.966
7	19.760	33.093	43.244	55.756
9	23.188	29.364	34.462	44.324
11	25.071	28.268	31.472	34.967
13	26.285	27.902	30.121	32.451
15	27.129	27.818	29.486	31.144
17	27.698	27.815	29.169	30.405
Exact		26.590	28.373	29.145

Table 2: Moments based bounding of the tail distribution

5.2 Numerical results

We evaluate and estimate $t_{\min}$, i.e. the minimum of t that satisfies (25). Three values of ε are considered: 0.9999, 0.99999 and 0.999999, ξ is set to 100. Fig. 4 shows the exact distribution and the bounds we get using different number of moments in case of $\varepsilon = 0.9999$. Thick black line represents this value. All the three direct analysis methods result the same values, the corresponding curve is labeled "exact" and $t_{\min}$ is the point where it reaches 0.9999 . When estimating a distribution based on its moments we get a lower and an upper bounding function. In these special cases that we investigate the upper bounding function is always equal to 1 and that's why it is omitted in the figure. The lower estimation is always smaller than the real value in any point of interest C, hence all the lower bounding functions corresponding to different number of moments are below the exact distribution function. As a consequence these functions intersect the line 0.9999 at greater values of t than $t_{\min}$.

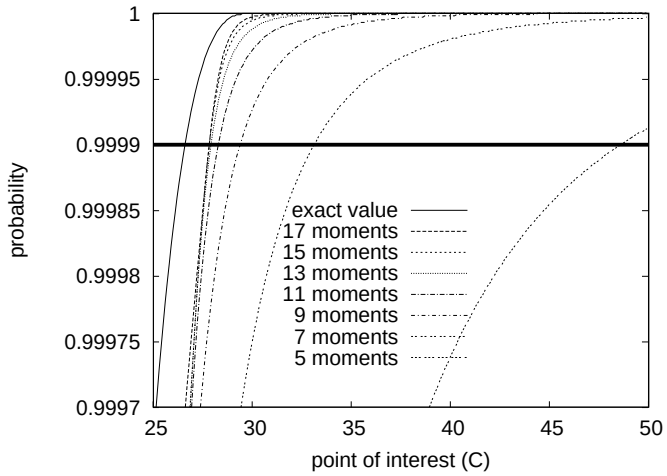

Figure 4: Lower estimation reaches to 0.9999

Table 2 presents the experiences. The 3^{rd}, 4^{th} and 5^{th} columns contain the results at different values of accuracy ε . The last row contains the "Exact" values which result from the direct distribution analysis. The other rows show

the points where the moment-based estimation reaches the predefined level of accuracy. The "Valid from" column indicates u_n, i.e. from which the presented simple bounding method is applicable (see (13)) and no reference discrete distribution is needed.

The table clearly shows that more moments contain more information about the tail distribution, and the estimated value of $t_{\min}$ is closer to the real one in these cases. However convergence slows down as the number of used moments increases.

5.3 Size of the state space

We evaluated a series of runs to determine the maximum number of states which the different types of solvers are still capable to calculate. We considered a method unusable if it resulted in clearly invalid values (e.g., negative possibilities) or the running time was more than 20× of the previous configuration.

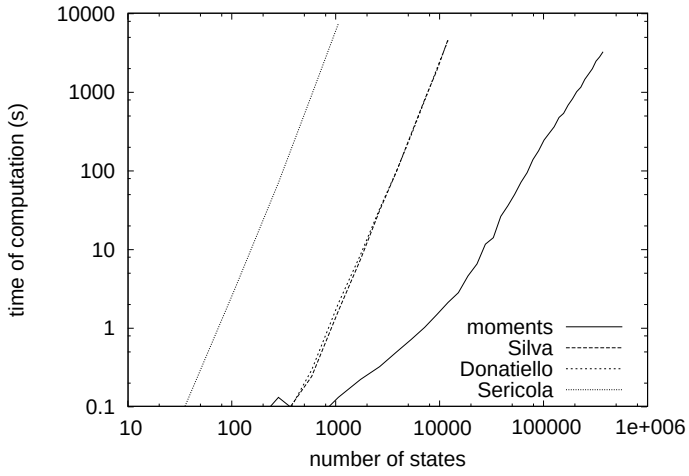

Figure 5: Evaluation time vs. state space size in logarithmic scale

Using the moments based method we could calculate the model with 370,000 states, while direct methods calculated the model with maximum 12,000 states. On the other hand the moments based approach yields less information about the distribution. The evaluation time of the estimation from the moments is 0.01s, its contribution to the overall calculation time in all considered cases is negligible.

6 Conclusion

In this paper we focus on a special use of our previously developed moments based distribution bounding method. For the computation of the distribution of extreme events the moment based analysis simplifies, because the maximal probability mass at the point of interest defines the bounds of the distribution.

We present an example where the simple bounding method is efficient and accurate compared to the results of other methods that calculate directly the

values of the distribution function.

We plan to increase the accuracy of our algorithm by using extended precision arithmetic and to improve our method using additional information about the distribution functions such as finite support intervals.

References

[1] N. I. Akhiezer. *The classical moment problem and some related questions in analysis*. Hafner publishing company, New York, 1965. (translation of Н. И. Ахиезер: Классическая Проблема Моментов и Некоторые Вопросы Анализа, published by Государственное Издательство Физико-Математической Литературы, Moscow, 1961).

[2] E. de Souza e Silva and H.R. Gail. Calculating cumulative operational time distributions of repairable computer systems. *IEEE Transactions on Computers*, C-35:322–332, 1986.

[3] E. de Souza e Silva and R. Gail. An algorithm to calculate transient distributions of cummulative rate and impulse based reward. *Commun. in Statist. – Stochastic Models*, 14(3):509–536, 1998.

[4] L. Donatiello and V. Grassi. On evaluating the cumulative performance distribution of fault-tolerant computer systems. *IEEE Transactions on Computers*, 1991.

[5] G. Fodor, S. Rácz, and M. Telek. On providing blocking probability- and throughput guarantees in a multi-service environment. *International Journal of Communication Systems*, 15:4:257–285, May 2002.

[6] H. Hamburger. Über eine Erweiterung des Stieltjes'schen Momentproblems. *Mathematische Annalen*, 81:235–319, 1920.

[7] G. Horváth, S. Rácz, Á. Tari, and M. Telek. Evaluation of reward analysis methods with MRMSolve 2.0. In *1st International Conference on Quantitative Evaluation of Systems (QEST) 2004*, pages 165–174, Twente, The Netherlands, Sept 2004. IEEE CS Press.

[8] H. Nabli and B. Sericola. Performability analysis: a new algorithm. *IEEE Transactions on Computers*, 45:491–494, 1996.

[9] W. H. Press, B. P. Flannery, S. A. Teukolsky, and W. T. Vetterling. *Numerical Recipes in C: The Art of Scientific Computing*. Cambridge University Press, 1993. http://lib-www.lanl.gov/numerical/bookcpdf.html.

[10] S. Rácz. *Numerical analysis of communication systems through Markov reward models*. PhD thesis, Technical University of Budapest, 2000.

[11] S. Rácz, Á. Tari, and M. Telek. A moments based distribution bounding method. 2005. to appear in Computers and mathematics with applications.

[12] S. Rácz and M. Telek. Performability analysis of Markov reward models with rate and impulse reward. In M. Silva B. Plateau, W. Stewart, editor, *Int. Conf. on Numerical solution of Markov chains*, pages 169–187, Zaragoza, Spain, 1999.

[13] J. A. Shohat and D. J. Tamarkin. *The problem of moments*. Americal Mathematical Society, Providence, Rhode Island, 1946. Mathematical surveys.

[14] G. Szegö. *Orthogonal polynomials*. American Mathematical Society, Providence, Rhode Island, 1939.

[15] M. Telek and S. Rácz. Numerical analysis of large Markovian reward models. *Performance Evaluation*, 36&37:95–114, Aug 1999.

[16] A. van de Liefvoort. The moment problem for continuous distributions. Technical report, University of Missouri, WP-CM-1990-02, Kansas City, 1990.

A New End-to-End Traffic-Aware Routing for MANETs

R.S. Al-Qassas, M. Ould-Khaoua and L.M. Mackenzie

Department of Computing Science
University of Glasgow
Glasgow G12 8RZ
UK
Email: {raad, mohamed, lewis}@dcs.gla.ac.uk

Abstract. In MANETs, resources, such as power and channel bandwidth are often at premium, and therefore it is important to optimise their use as much as possible. Consequently, a traffic aware technique to distribute the load is very desirable in order to make good utilisation of nodes' resources. Therefore a number of end-to-end traffic aware techniques have recently been proposed for reactive routing protocols to deal with this challenging issue. In this paper we contribute to this research effort by proposing a new load aware technique that can overcome the limitations of the existing methods. Results from an extensive comparative evaluation show that the new technique has superior performance over similar existing end-to-end techniques in terms of the achieved packet delivery ratio and delay.

Keywords: Ad hoc networks, routing protocol, traffic, load balancing, latency, throughput, ns-2 simulation.

1. Introduction

Mobile Ad hoc Network (MANET) is a collection of wireless mobile nodes that form a temporary network without the need of any infrastructure or centralized administration. In such an environment, it may be necessary for one mobile node to enlist the aid of others in forwarding a packet to its destination due to the limited propagation range of each mobile node's wireless transmissions [1]. The communication in MANETs is peer-to-peer as the mobile nodes communicate directly with one another. In MANET resources like power and bandwidth are at premium and it is important to minimise the use of these resources.

The routing protocol in MANETs is responsible for establishing and maintaining paths between nodes in the network. The topology of a MANET may change

frequently as nodes may move or power themselves off to save energy. In addition, new nodes can join the network [2]. Consequently, connectivity information is often required to be collected periodically in order to get a consistent view of the network, which in turn increases the bandwidth consumption resulting from collecting this information. MANETs have limited bandwidth, and therefore need an efficient routing protocol that can establish and maintain routes for both stable and dynamic topologies with minimum bandwidth consumption.

A major challenge in MANETs is the design of a routing protocol that can accommodate their dynamic nature and frequent topology changes; the topology can change unpredictably, so the routing protocol should be able to adapt automatically. However, the issue that has to be dealt with when designing a protocol is not only the frequent changes in the network, but also the natural limitations that these networks suffer from such as limited bandwidth and power. To deal with such issues a number of routing protocols have been proposed [3, 4, 5, 6, 7, 8, 9, 10, 11, 12, 13].

There has been a lot work on developing reactive routing algorithms for ad hoc networks [3, 10, 12]. Most of these algorithms consider finding the shortest path from source to destination in building a route. However, this can lead to some nodes being overloaded more than others in the network. Therefore, a traffic aware technique to distribute the load is highly desirable in order to make good utilisation of nodes' scarce resources. In addition it can be useful to prevent the creation of congested areas in the network, which can lead at the end into an improvement on the network performance. Furthermore, such technique is a good way to achieve fairness in using node's limited resources.

A number of studies [15, 16, 17, 18] have recently proposed traffic aware techniques for distributing the load in reactive routing. These techniques can be classified into two main categories: *end-to-end* and *on-the-spot*; based on the way they establish and maintain routes between any source and destination. The first category is based on using end-to-end information collected along the path from source to destination. In this category intermediate nodes participate in building the route by adding some information about their status. However the decision for selecting the path is taken at one of the ends, either the source or the destination. In the second category, information is not required to be passed to one of the ends to make a path selection decision; it is most likely that intermediate node will do this job. Therefore the decision of selecting a path is made on-the-spot and taken by intermediate nodes.

This research focuses on the end-to-end techniques. In particular, its objective is to develop a new reactive routing load aware technique that can overcome the limitations of the existing ones. A major limitation of existing techniques, such as those proposed in [15, 16], arise from the lack of information about the real traffic load experienced by routes, which indeed affect the performance of the routing protocol and its efforts in distributing the load over nodes. A special characteristics of the new metric over existing ones is that it takes more accurate information about traffic transiting a network node; this is computed by using the lengths of packets passed over nodes and the one waiting the at nodes' interface queue. The rationale behind using packets sizes in the calculations rather than just using the number of

packets as in [15] is that packets can vary in size so it is better to use packets sizes as it can cover all the variations, and give a better indication of message contention. As a result, the new technique can potentially make a better judgment than the existing methods of [15, 16] in selecting routes, which improves the overall performance of the network, and distribute the load more fairly over the nodes in the network.

The remainder of this paper is organised as follows. Section 2 reviews two existing end-to-end techniques, namely *degree of nodal activity* and *traffic density*. Section 3 describes the proposed traffic aware technique. Section 4 conducts a comparative analysis of our proposed technique and the existing degree of nodal activity and traffic density techniques. Finally, section 5 concludes this study.

2. End-to-end traffic aware techniques

This section describes the end-to-end traffic aware techniques: *degree of nodal activity* suggested in the routing protocol "Load-Balanced Ad hoc Routing" (LBAR) [16] and *traffic density* suggested in "Load Aware Routing in Ad hoc" (LARA) [15].

2.1 Degree of nodal activity

The degree of nodal activity was defined in LBAR as a technique or metric for selecting the route with least traffic load. LBAR is a reactive routing protocol that focuses on how to find a path, which would reflect the least traffic load based on a cost function. The cost function is calculated using two components: *nodal activity* and *traffic interference*. Nodal activity of a node is defined as the number of active paths passing through that node. An active path is an established path from a source to a destination. Traffic interference is defined as the sum of nodal activity for the node's immediate neighbours. The cost of a route is defined as the sum of nodes' nodal activity plus the activity of their neighbouring nodes. The path with minimum cost is considered as the path with minimum traffic and is selected to be the path between source and destination.

Route discovery:
In LBAR route discovery process is initiated whenever a source node needs to establish a path with another node. The source node broadcasts a setup messages to its neighbours. The setup message carries the cost seen from the source to the current node. A node that receives a setup message will forward it to its neighbours after updating the cost based on its nodal activity value and traffic interference value. In order to prevent looping when setup messages are routed, the setup message contains a list of all node IDs used in establishing the path from source node to the current intermediate node. The destination node collects arriving setup messages within a route-select waiting period, which is a predefined timer for selecting the best-cost path. After the waiting period expires the destinations sends an ACK message to the source node along the selected path. When the source node receives an ACK message,

it recognises that a path has been established to the destination and then starts transmission.

Route maintenance:
Route maintenance is triggered whenever a node on the active path moves out of the communication range, the case on which an alternate path must be found. If the source node moves away from the active path, the source has to reinitiate the route discovery procedure to establish a new route to the destination. When either the destination node or some intermediate node moves outside the active path, path maintenance will be initiated to correct the broken path. Once the next hop becomes unreachable, the node upstream of the broken hop propagates an error message to the destination node. The destination then picks up an alternative path and then sends an ACK message to the initiator of the error message. If the destination has no alternative path, it propagates an error message to the source, which will initiate a new route discovery if needed.

2.2 Traffic Density

The *traffic density* was proposed in LARA as a metric for selecting the route with the minimum traffic load. LARA uses *traffic density* to represent the degree of contention at the medium access control layer. This metric is used to select the route with the minimum traffic load when the route is setup. LARA protocol requires that each node maintain a record of the latest *traffic queue* estimations at each of its neighbours in a table called the neighbourhood table. *Traffic queue* is defined as the average value of the interface queue length measured over a period of time. *Traffic density* of a node is defined as the sum of *traffic queue* of that node plus the *traffic queues* of all its neighbours.

Route discovery:
In LARA route discovery process is initiated whenever node needs to establish a path with another node. In the route request process, the source broadcasts a route request packet that contains a sequence number, a source id and a destination id. A node that receives the request, broadcasts the request further, after appending its own traffic density to the packet. This process continues until the request packet reaches the destination. After receiving the first request, the destination waits for a fixed time-interval for more route request packets to arrive. When the timer expires, the destination node selects the best route from among the candidate routes and sends a route reply to the source. When the source node receives the route reply, it can start data transmission. If it does not receive any route reply within a route discovery period, it can restart the route discovery procedure afresh.

Route maintenance:
Route maintenance is triggered whenever a node on the active path moves out of the communication range, the case on which an alternate path must be found. If a link

failure occurs during a data transmission session, the source is informed of the failure via a *route error* packet. On receiving a route error packet, the source initiates a new route request and queues all subsequent packets for that destination until a new route is found.

3. The Proposed Load-density Metric

The existing end-to-end traffic aware techniques use a metric or cost function to select the route with a minimum load, such techniques are represented by *nodal activity* [16] and *traffic density* [15]. The nodal activity metric cost function calculation is based on monitoring the number of active paths passed over nodes. On the other hand, the traffic density metric is measured using number of packets at interface queue. However in order to make a good judgment about a given path's load, it is not enough just to capture the number of active paths or number of packets at the interface queue over a period of time. Number of active paths can be useful when the used traffic flows are equal in characteristics. Number of packets at the interface queue is useful to capture the contention at the MAC layer if all packets are equal in size. However, this is not sufficient to represent the load. Therefore, what is needed is a metric that can deal with most of the cases that could appear in the network. Whether flows are with equal characteristics or not, or whether packets are equal in size or not, it should not affect the efficiency of the traffic aware technique. Our goal here is to devise a new end-to-end metric that selects the less congested route with the least traffic history regardless of the shape of the traffic passed over it.

Our proposed metric, named *load-density*, is calculated using two main components; the load history information represented by the total traffic passed over nodes, and the contention information represented by and the number of packets waiting at the nodes' interface queue in order to take the possible contention in the network into consideration in the metric calculations. The load-density is embedded under a reactive routing algorithm like other existing metrics the degree of *nodal activity* and *traffic density*. The sections below describe this algorithm. As an alternative solution to represent the contention, we can use the sum of packets' length occupying the queue as it can cover the variance in packets sizes instead of using the number of packets at interface queue.

Route discovery:

The route discovery process starts whenever a node wants to communicate with another node for which it does not have a known route. The source node broadcasts a request packet to its neighbours. Every node receives the request packet will forward it to its neighbours after updating the cost information carried in the request packet, by adding the values of its load-history and contention information (see sec. 3.1) to the those carried in the packet. The cost information carried in the request packet, which includes the load history and the contention information, represents the cost seen from the source to the current node. The process of forwarding the request packet continues until the packet is received by the destination node. The destination

collects the arriving request packets within a route selection period; activated upon receiving the first request packet, for selecting the best-cost route. Once the selection period is expired the destination selects the route with the best cost and sends a reply packet to the source node. The route selection process is illustrated in more details in Fig. 1.When the source node receives the reply packet, the path is then established and communication can be started.

```
// For selecting the route three parameters are used:
// traffic load, contention information and path length in hops.
Collect all route requests packets sent from source S and received within the selection-period
// The selection-period is started when the first request packet is received.
// Each request packet corresponds to a route from source to destination
Find the set of routes R that has contention value ≤ max-contention-threshold
    From the set R find the route r with minimum traffic-load
        Compare the routes' traffic-load with r's traffic-load If the difference < acceptable-load-difference
            then select the route with the lowest number of hops and send reply to the source
            else select r as route and send reply to the source
If all routes available have contention values > max-contention-threshold
    then select the route with minimum traffic-load and send reply to the source
```

Fig. 1: Route selection algorithm in the new load aware metrics.

Route maintenance

The route maintenance is triggered when there is a change in the topology that affects the validity of an active route. If the source node, an intermediate node or the destination node on an active route moves out of the communication range, an alternative route must be found. Once a node detects that the next hop is unreachable, it propagates an error message to the destination node. Upon receiving the error message, the destination node picks up an alternative route and then sends a reply message to the initiator of the error message. If the destination has no alternative path, it sends an error message to the source to start a route discovery process.

3.1 Route cost computation

The cost function has two main components: the data traffic load (in bytes) forwarded by nodes and number of packets at the interface queue. Every node keeps information about the amount of traffic passed over it during a predetermined period of time in the addition to the interface queue history represented by the averaged number of packets occupying the queue over a period of time. Route cost is calculated by gathering traffic load and contention information for the nodes along the route. The contention information for a node represents the number of packets at the interface queue plus the number of packets at the interface queue for its neighbours.

Nodes exchange contention information using hello packets. Each node broadcasts a *hello* packets every *hello interval,* to its neighbours, containing its identity and contention information. The hello packet is broadcasted only for one hop i.e. only to the immediate neighbours. Neighbours who receive this packet update their neighbourhood information.

4. Performance Evaluation

The performance comparison of the *load-density* metric against *traffic density* and *nodal activity* is carried out through extensive simulations implemented using the well-known network simulator *ns*-2 [14]. The simulation model we have used in the evaluation is illustrated in the sequel.

4.1. Simulation Model

The simulation model consists of the following main components: simulation area, simulation time, number of nodes, mobility model, maximum node speed, number of traffic flows, and traffic rate. Simulation model is represented by two scenario files, which are topology scenario and traffic scenario. The topology scenario corresponds to how nodes are distributed over the simulation area and there movement during the simulation time. The traffic scenario files contain the type of data, number of flows, traffic rate, and flow start time and end time. In all scenarios nodes are equipped with the wireless standard IEEE 802.11 with transmission range of 250m and a bandwidth of 2 Mbps.

In order to maximise the opportunity of forming multiple paths between data flow sources and their destinations we have chosen to make them stationary and the rest of the nodes in the network are mobile. The reason for this is that sources could become within the range of each other or very close due to mobility. Therefore keeping them stationary can boost our study of the traffic aware techniques.

We have implemented the traffic aware techniques *load density*, *traffic density* and *nodal activity* under AODV-like routing algorithm that is the AOMDV [19]. AOMDV is a multi-path algorithm that supports loop-free multiple paths. The ns-2 source code for this algorithm was available, and therefore it was easier to modify this source code to simulate the *load density*, *traffic density* and *degree of nodal activity* metrics rather than writing it from scratch.

4.2 Simulation Results

The evaluation is based on the simulation of 100 wireless nodes forming a MANET over a flat space of size (1200m × 1000m) for a period of 900 seconds. Flows with Constant Bit Rate (CBR) data have been used. The traffic rate varied between 2, 4 and 8 packets per second representing low, medium and high traffic loads, respectively. The numbers of CBR flows used are 3 and 5 flows with packet size of 512 bytes.

Nodes move according to the random waypoint model [3] with a maximum speed of 10m/s. In random waypoint model each node remains stationary for a pause time period. The pause time has been varied from 0 to 900 seconds. When the pause time expires, the node selects a random destination in the simulation space and moves towards it. When the node reaches its destination, it pauses again for the same pause time. This behaviour is repeated throughout the simulation time. Simulation parameters are illustrated in Table 1.

Number of nodes	100
MAC layer	IEEE 802.11
Transmission range	250m
Simulation area	1200m x 1000m
Simulation time	900s
Mobility model	Random waypoint model
Maximum speed	10m/s
Pause times	0, 150, 450, 900
Traffic type	CBR
Packet size	512 bytes
Packet rate	2, 4, 8
Number of flows	3, 5

Table 1: The system parameters used in the simulation experiments

The performance of the three techniques is measured by: *packet delivery ratio* and *end-to-end delay*. The packet delivery ratio is the number of packets received at their final destinations over the total number of packets injected into the network. This measure provides an indication on the efficiency of a given routing protocol as it shows the amount of data packets that the protocol is able to deliver to destinations. End-to-end delay is the average time interval between the generation of a packet in a source node and the successful delivery of the packet at the destination node. It counts all possible delays that can occur in the source and all intermediate nodes.

Figures 2-7 depicts the delivery ratio for the three traffic aware techniques: load density, traffic density and nodal activity. Fig. 2 demonstrates the behaviour of the three techniques under 3 light traffic flows with a rate of 2 packets per second. The load density shows better delivery ratio compared to traffic density and nodal activity especially at pause time 0. Fig. 3 shows how the three techniques behave under medium traffic rate of 4 packets per second. The traffic density has higher delivery than nodal activity especially at low pause times. However, the load density outperforms the other techniques in all the simulated scenarios. Fig. 4 shows the performance of the three techniques under 3 high traffic flows with rate of 8 packets per second. Although the delivery ratio decreases compared to that in Fig. 3, our technique still outperforms the other techniques. In Fig. 5, the three methods exhibit comparable performance behaviour. However load density shows better performance than the other two techniques for all pause times. Figs. 6 and 7 illustrate how increasing the traffic rate would affect on the performance of the three methods. While the two methods; nodal activity and traffic density, have comparable performance under medium and high traffic rates, the load density method outperforms the other techniques in the simulated scenarios.

Figures 8-13 present the end-to-end delay for the three techniques. Fig. 8 shows delays when the traffic is light; 3 flows with a rate of 2 packets per second. The figure reveals lower delay for both the traffic density and load density techniques in most of the mobility conditions especially at pause time of 0 where high mobility conditions exist. The same behaviour is noticed under moderate traffic where 3 flows are used with a packet rate of 4 packets per second as it is shown in Fig. 9, except at 0 pause time where the load density is the one with better performance. In Fig. 10, although the three techniques show similar delays under high traffic rate of 8 packets per second, load density shows better performance than the other techniques.

Figures 11-13 shows the latency results under light, moderate as well as high traffic for 5 traffic flows with rates of 2, 4 and 8 packets per second, respectively. Fig. 11 shows that the load density technique with better performance than traffic density and nodal activity techniques under high mobility conditions, at 0 and 150 pause times. However the techniques have similar performance under low or no mobility conditions. Fig. 12 shows an increase in the end-to-end delay compared to that in Fig. 11. However load density has a lower packet delay, while the other techniques show close performance in most considered cases. Fig. 13, which depicts the behaviour of the techniques under high traffic, shows a great increase in the delay compared to that in figures 11 and 12. Although the techniques have similar performance, it is worth pointing out that the load density technique manages to achieve higher delivery ratios under the same operating conditions.

5. Conclusions

This study has suggested a new traffic aware technique, referred here to as load density that can overcome the limitations of the existing methods in reactive routing protocols. It has also conducted a performance evaluation of the new method against the two existing similar methods, notably, degree of nodal activity and traffic density under various working environments. Simulation results have revealed that in most circumstances the load density method exhibits superior performance in terms of both packet delivery ratios and end-to-end-delays. As a next step of this research, we plan to carry out further investigation on the performance of the techniques considering other working conditions by changing the node mobility pattern, traffic patterns, network size, and topological area.

References

[1] D.B. Johnson, Routing in Ad hoc Networks of Mobile Hosts, *Proc. Workshop on Mobile Computing Systems and Applications*, IEEE Computer Society, Santa Cruz, CA, December 1994 pp. 158-163.

[2] W. Chen, N. Jain and S. Singh, ANMP: Ad hoc Network Management Protocol, *IEEE Journal on Selected Areas in Communications*, Vol. 17, No. 8, August 1999, pp. 1506-1531.

[3] D.B. Johnson and D.A. Maltz, Dynamic Source Routing in Ad Hoc Wireless Networks, *In Mobile Computing*, edited by T. Imielinski and H. Korth, Chapter 5, Kluwer Publishing Company, 1996, pp. 153-181.
[4] Z. Haas and M. Pearlman, The Performance of Query Control Schemes For the Zone Routing Protocol, *IEEE/ACM Transactions on Networking (TON)*, Vol. 9, Issue 4, August 2001, pp. 427-438.
[5] C.E. Perkins and P. Bhagwat, Highly Dynamic Destination-Sequenced Distance Vector Routing (DSDV) for Mobile Computers, *Proc. ACM SIGCOMM'94*, London, September 1994, pp. 234-244.
[6] C.-C. Chiang, Routing in Clustered Multihop, Mobile Wireless Networks with Fading Channel, *Proc. of IEEE SICON'97*, April 1997, pp. 197-211.
[7] S. Murthy and J.J. Garcia-Luna-Aceves, An Efficient Routing Protocol for Wireless Networks, *ACM Mobile Networks and Application, Special Issue on Routing in Mobile Communication Networks*, Vol. 1, No. 2, October 1996, pp. 183-197.
[8] T. Clausen and P. Jacquet, Optimized Link State Routing Protocol, *IETF MANET*, Internet Draft, Jul. 2003.
[9] R. Ogier, F. Templin and M. Lewis, Topology Dissemination Based on Reverse-Path Forwarding (TBRPF), *IETF MANET*, Internet Draft, Oct. 2003.
[10] Y. Ko, N.H. Vaidya, Location-Aided Routing (LAR) in mobile ad hoc networks, Wireless Networks, Vol. 6, No. 4, 2000, pp. 307-321.
[11] C.-K. Toh, Associativity Based Routing For Ad Hoc Mobile Networks, *Wireless Personal Communications Journal, Special Issue on Mobile Networking and Computing Systems*, Vol. 4, No. 2, March 1997, pp.103-139.
[12] C.E. Perkins and E.M. Royer, Ad-hoc On-demand Distance Vector Routing, *Proc. 2nd IEEE Workshop on Mobile Computing Systems and Applications*, New Orleans, LA, Feb. 1999, pp. 90-100.
[13] V.D. Park and M.S. Corson, A Highly Adaptive Distributed Routing Algorithm for Mobile Wireless Networks, *Proc. of IEEE INFOCOM '97,* Kobe, Japan, April 1997, pp. 1405-1413.
[14] The Network Simulator ns-2, *http://www.isi.edu/nsnam/ns*.
[15] V. Saigal, A.K. Nayak, S.K. Pradhan and R. Mall, Load balanced routing in mobile ad hoc networks, *Computer Communications*, Vol. 27, Issue 3, Feb. 2004, pp. 295-305.
[16] H. Hassanein and A. Zhou, Load-aware destination-controlled routing for MANETs , *Computer Communications*, Vol. 26, Issue 14, Sep. 2003, pp. 1551-1559.
[17] S.B. Lee, Jiyoung Cho, and A.T. Campbell, A Hotspot Mitigation Protocol for Ad hoc Networks, *Ad hoc Networks Journal*, Vol. 1, No. 1, March 2003.
[18] M.R. Pearlman, Z.J. Haas, P. Sholander, and S.S. Tabrizi, On the impact of alternate path routing for load balancing in mobile ad hoc networks, *Proc. ACM MobiHoc*, 2000, pp. 3-10.
[19] M. K. Marina and S. R. Das, On-demand Multipath Distance Vector Routing in Ad Hoc Networks, *Proc. International Conference for Network Protocols* (*ICNP*), Nov. 2001, pp. 14-23.

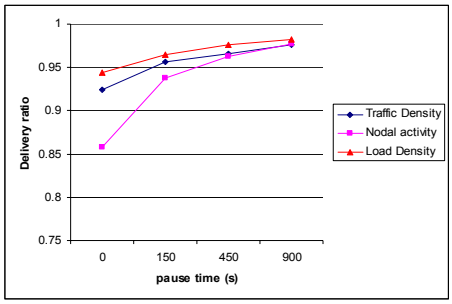

Fig. 2: Packet delivery ratio for 3 flows of traffic with a rate of 2 packets/s.

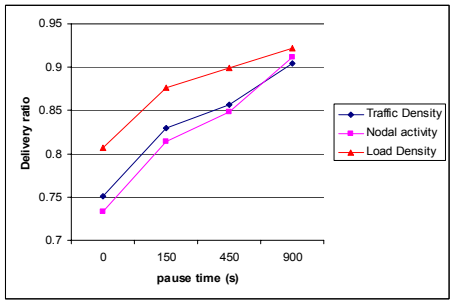

Fig. 6: Packet delivery ratio for 5 flows of traffic with a rate of 4 packets/s.

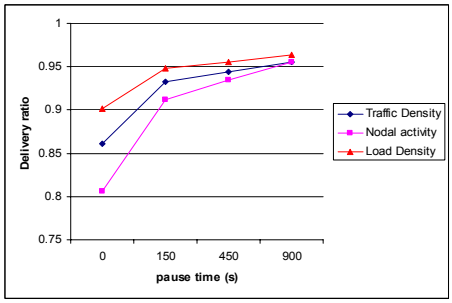

Fig. 3: Packet delivery ratio for 3 flows of traffic with a rate of 4 packets/s.

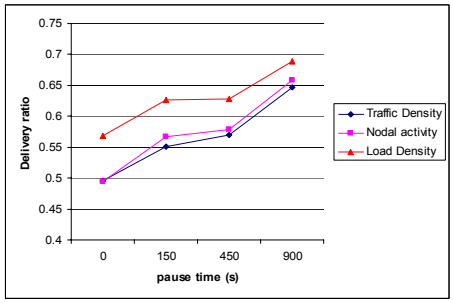

Fig. 7: Packet delivery ratio for 5 flows of traffic with a rate of 8 packets/s.

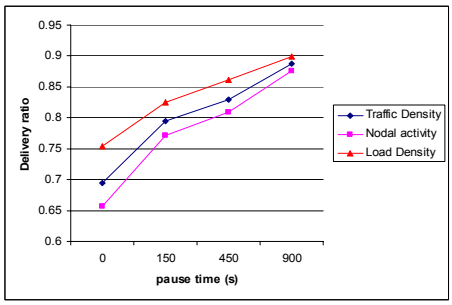

Fig. 4: Packet delivery ratio for 3 flows of traffic with a rate of 8 packets/s.

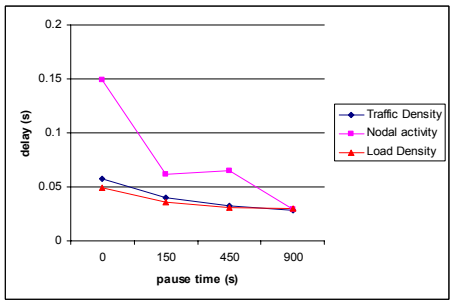

Fig. 8: Packet delay for 3 flows of traffic with a rate of 2 packets/s.

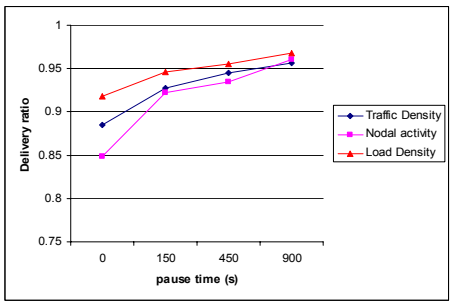

Fig. 5: Packet delivery ratio for 5 flows of traffic with a rate of 2 packets/s.

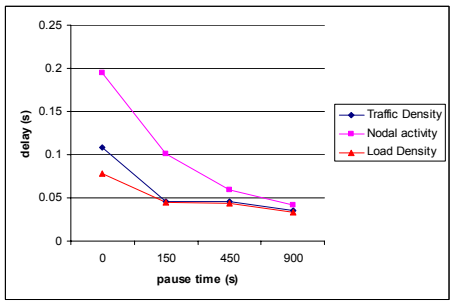

Fig. 9: Packet delay for 3 flows of traffic with a rate of 4 packets/s.

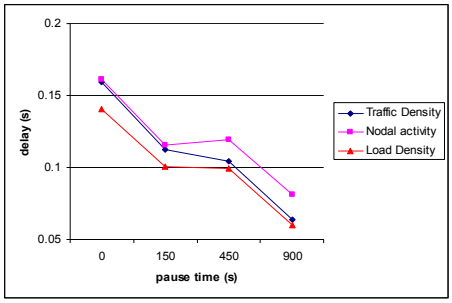

Fig. 10: Packet delay for 3 flows of traffic with a rate of 8 packets/s.

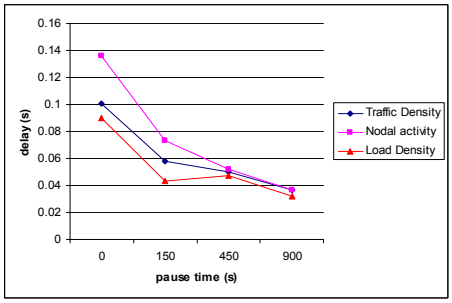

Fig. 11: Packet delay for 5 flows of traffic with a rate of 2 packets/s.

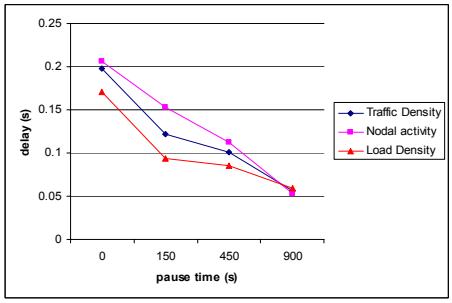

Fig. 12: Packet delay for 5 flows of traffic with a rate of 4 packets/s.

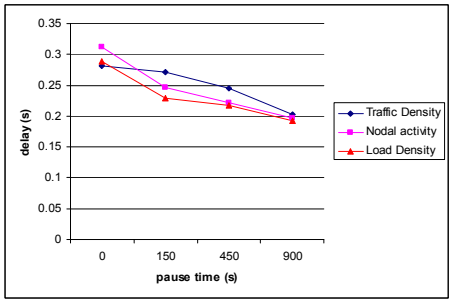

Fig. 13: Packet delay for 5 flows of traffic with a rate of 8 packets/s.

Effective Admission and Congestion Control for Interconnection Networks in Cluster Computing Systems

Shihang Yan, Geyong Min, and Irfan Awan

Department of Computing, School of Informatics,
University of Bradford, Bradford, BD7 1DP, U.K.
{shyan, g.min, i.u.Awan}@brad.ac.uk

Abstract. Admission and congestion control mechanisms are integral parts of network design for providing Quality of Service (QoS) of real-world applications. The InfiniBand defines a System Area Networks (SANs) environment where multiple processor nodes and I/O devices are interconnected using a switched point-to-point fabric. InfiniBand is quickly becoming the interconnection of choice for cluster computing systems. This paper proposes an improved link-by-link based admission control mechanism and an effective source response function, named as Power Increase and Power Decrease (PIPD), for traffic congestion control. These proposed schemes adopt rate control to reduce congestion of multiple-class traffic in InfiniBand networks. Simulation experiments have demonstrated that the admission control algorithm and the new source response function are quite effective for the InfiniBand networks.

Keywords. InfiniBand, Congestion Control, Admission Control, ECN, PIPD.

1 Introduction

InfiniBand is quickly becoming the interconnection of choice for many high-performance computing systems, e.g., cluster systems, because of its compelling price/performance and standard-based technology [6]. InfiniBand Architecture (IBA) has been proposed as a new industry standard for high-speed I/O inter-processor communication. It is designed around a switch-based interconnection technology with high-speed point-to-point links [10] (see Fig. 1). The point-to-point interconnection means that every link in the IBA networks has exactly one device connected at each end of the link, thus providing better performance than traditional bus-shared architectures. InfiniBand switches were designed not only to enable large-scale server clusters but also to provide the ability to tie those clusters into Grid computing environments [3]. Because the InfiniBand-based interconnection provides the high bandwidth, low latency required by the Grid computing systems consisting of cluster applications, databases, shared network and storage resources. An IBA network is divided into subnets interconnected by routers, each subnet comprising one or more switches, processing nodes and I/O devices [2].

InfiniBand Architecture (IBA) has three mechanisms to support QoS: Service Level (SL), Virtual Lanes (VL), and Virtual Lane Arbitration (VLA) [1]. The switch in the InfiniBand networks consists of a crossbar where link and VL have dedicated access to the crossbar. Each link supports one or more VLs, each of which has its own buffer resources including an input buffer and an output buffer. Admission control algorithms help to meet the specific SL of the InfiniBand networks. However, admission control alone may not be effective enough to guarantee the QoS when the network operates under heavy traffic load. The overload can degrade the overall network performance seriously. Therefore, a congestion control mechanism should be used to monitor the network loads and intervene traffic actions when the loads reache a certain threshold indicating possible network congestion [19]. So both admission control and congestion control mechanisms are collectively required to guarantee various QoS constraints.

System Area Networks (SANs) provide high throughput and low latency for efficient I/O and cluster communication. The adoption of SANs has increased quickly in recent years and should accelerate with the emergence of industry standards such as InfiniBand [16]. InfiniBand can experience congestion spreading [4], where one bottleneck link causes traffic to be blocked throughout the network. The characteristics of IBA make the congestion control mechanism specifically challenging. Firstly, unlike traditional networks, InfiniBand switch cannot drop packets to deal with traffic congestion. Secondly, InfiniBand switches are single-

chip devices [10] with small packet buffers. So there are only a few packets in transit at any time. Thirdly, the latencies of switch and end-device processing are very low. For end-to-end congestion control in traditional networks, flow sources use packet dropping [11] or changes in network latencies [5, 13] as a signal of congestion. In this paper, we use the Explicit Congestion Notification (ECN) to detect congestion and notify the flow endpoint. ECN has been widely used in ATM networks [9] and Internet with TCP protocols [8, 14]. We adopt the ECN mechanism for InifniBand networks because the configuration of the switches with the input buffer is the same as that with output buffer in ATM networks. A source adjusts its packet injection rate after receiving congestion information. We propose a new source response function to improve the performance of the InfiniBand.

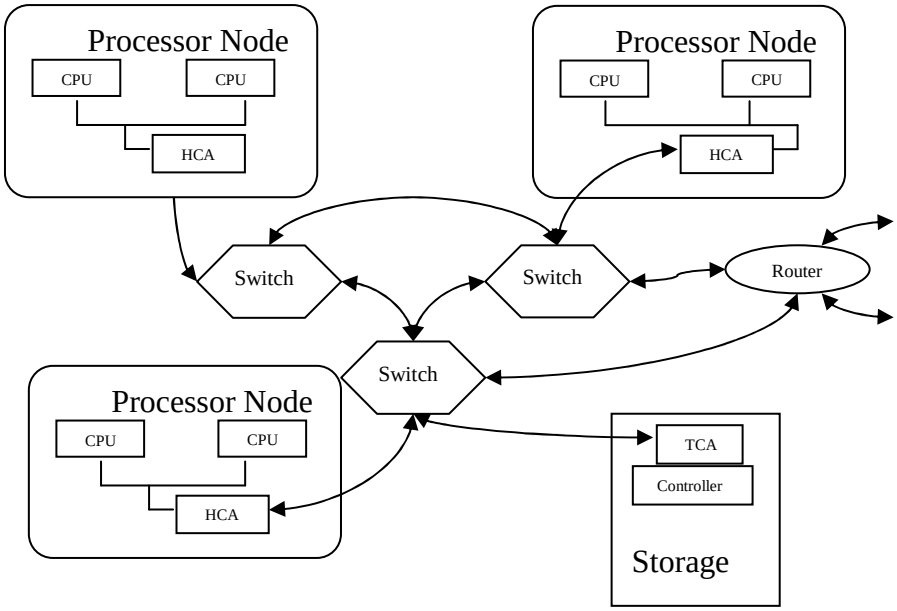

Fig. 1 IBA subnet: each subnet includes a set of switches and point-to-point links.

The major contributions of this paper are twofold: 1) to extend the traditional admission control mechanism so that it is suitable to the InfiniBand architecture by considering different connections with various SLs in the networks subject to multiple-class traffic, 2) to propose a new effective source response function that can support the higher bandwidth utilization and ensure the fairness.

The rest of this paper is organized as follows: Section 2 presents an improved link-by-link based admission control mechanism. Section 3 describes the congestion control mechanism and source response function methodology. A new source response function will then be proposed. Section 4 uses simulation experiments to evaluate the effectiveness of our improved admission control mechanism and the new response function in an InfiniBand network subject to multiple-class traffic with different priorities. Finally Section 5 concludes this study and indicates future work.

2 Admission Control

This section will present the link-by-link based admission control mechanism with the proposed extension so that it is suitable to the InfiniBand architecture. In the link-by-link approach a bandwidth broker records the load on each link and consults the availability of the bandwidth before accepting or rejecting a new connection requirement. We adopt the approach described in [12] which ensures the sum of requested resources does not exceed link capacity. Let bw be the total link bandwidth, s the sum of bandwidth already admitted to existing connections, and p the bandwidth requested by the new potential connection. This algorithm accepts the new connection only the condition $p + s < bw$ is satisfied. In the

InfiniBand architecture, connections with different SLs have the different bandwidth requirements. Let s_{sl_i} be the sum of the bandwidth that has been admitted to connections with the SL sl_i. The connection is accepted only when $p + s_{sl_i} < bw_{sl_i}$ is satisfied, where bw_{sl_i} is the effective bandwidth available to SL sl_i. The InfiniBand architecture defines a maximum of 16 SLs.

3 Congestion Control

This section will describe the congestion control mechanism for InfiniBand using an Explicit Congestion Notification (ECN) packet marking scheme and a source response function.

3.1 Packet marking

An alternative to implicit notification is ECN, in which switches detect incipient congestion and notify flow endpoints, for example, by marking packets when the occupancy of a switch buffer exceeds a desired operating point [15]. There is a single bit ECN field in the header of an identified packet that indicates the occurrence of congestion to the destination. The destination returns an acknowledgment packet (ACK) that includes the ECN value and the source will use this information to control the packet injection rate. We will extend the packet marking mechanism [16] that needs two counters for each output link. The first counter cnt_1 records the current number of packets in the switch waiting for that output link. The second counter cnt_2 records the number of subsequent packets that need to be marked when transmitted on that output ink. Whenever a buffer becomes full, the value of counter cnt_1 is copied to counter cnt_2. This packet marking mechanism and descriptions of additional schemes are discussed in more detail in [17].

3.2 Source response function

The flow rate is adjusted in response to the feedback of network congestion. Because the feedback is received through the ACK packet, the flow injection rate will be adjusted whenever an ACK packet is received. If the receipt is an unmarked ACK, the source response must increase the flow rate. Similarly, if the receipt is a marked ACK, the source response must decrease the flow rate.

In order to design $f_{inc}(r)$ and $f_{dec}(r)$, we use the condition defined in [16] as follows:

Condtion1. Avoiding Congested State

The flows experience the same (or higher) degree of congestion after recovery.

$$f_{inc}(f_{dec}(r)) \le r \tag{1}$$

Condition2. Fairness

If the recover time $T_{rec}(r)$ for lower rate flows does not exceed that of higher flows, the fairness is guaranteed.

$$T_{rec}(r_1) \le T_{rec}(r_2) \text{ for } r_1 \le r_2 \tag{2}$$

Condtion3. Efficiency

In order to ensure the source response function efficient, the flows should recover rate quickly to maximize bandwidth utilization.

$$T_{rec}(r_1) = \frac{1}{R_{\min}} \quad \text{for} \quad f_{dec}^{-1}(R_{\min}) \le r \le R_{\max} \tag{3}$$

Some conclusions based on the conditions can be found in [16].

$$F_{inc}(t) = f_{dec}(F_{inc}(t + T_{rec})) \tag{4}$$

After an adjustment to rate r, the next ACK is received in a time interval $1/r$, thus we get

$$f_{inc}(r) = \min(F_{inc}^{r}(1/r), R_{\max}) \tag{5}$$

In summary, to obtain an increase function $f_{inc}(r)$ we need to find a function $F_{inc}(t)$ that satisfies with Equation (4). In the next section, we will show how to obtain $f_{inc}(r)$ for a specific response function.

3.3 Power Increase Power Decrease (PIPD) function

Based on the unique characteristics, the source response function of the InfiniBand networks should be different from the current functions, such as the Additive Increase Multiplicative (AIMD) [7]. It is known that with the traditional increase function, such as the AIMD, the rate increase is the linear. Therefore, the injection rate can not reach a high speed quickly. The most bandwidth of the InfiniBand networks is under-utilized for a long time. So we consider using the power increase for the new function.

To design the increase function, we need to define a decrease function firstly, which uses the power function.

$$f_{dec}^{pipd}(r) = \max(r^{1/m}, R_{\min}) \text{ where } m > 1 \text{ is constant.} \tag{6}$$

In order to avoid congested state from Equation (1), $F_{inc}(t)$ must satisfy the following equation:

$$F_{inc}(t + T_{rec}) = F_{inc}(t)^{m} \tag{7}$$

This equation shows that after each interval time T_{rec} the function is powered by m. From this equation, we can get an obvious solution that an exponential function is based on the T_{rec}. For $T_{rec} = 1 \times T_{rec}, 2 \times T_{rec}, 3 \times T_{rec} \ldots$ and with $F_{inc}(0) = R_{\min}$ we get

$$F_{inc}(t) = R_{\min}^{\,m^{t/T_{rec}}} \tag{8}$$

For any rate r, there exists a t' for which $r = F_{inc}(t') = R_{\min}^{\,m^{t'/T_{rec}}}$.

Therefore,

$$F_{inc}^{r}(r) = F_{inc}(t + t') = R_{\min}^{\,m^{t'/T_{rec} + t/T_{rec}}} = r^{t/T_{rec}} \tag{9}$$

In order to obtain the increase function $f_{inc}(t)$ form Equation (4),

$$\begin{aligned} f_{inc}^{pipd}(r) &= \min(F_{inc}^{r}(1/r), R_{\max}) \\ &= \min(r^{R_{\min}^{1/r * T_{rec}}}, R_{\max}) \\ &= \min(r^{m^{R_{\min}/r}}, R_{\max}) \end{aligned} \tag{10}$$

Noticing the increase function $f_{inc}(r)$ of PIPD, we can find that the change of the injection rate is based on the value of $R_{\min}/r$. Therefore, the PIPD mechanism can classify the different traffic priorities by giving them different value of $R_{\min}$. The increase function of PIPD make the injection increasing by power, unlike the linear increase function it can reach very high transmission rate in a short time.

Next we analyze how the PIPD function regulates the transmission rate in the InfiniBand networks. At the beginning, injection rate r is set to $R_{\min}$ and the value of $R_{\min}/r$ is equal to

1. The injection rate will increase very quickly because it is powered by m in fact. This can improve the utilization of the bandwidth. Then the injection rate is bigger than $R_{\min}$ and the value of $R_{\min}/r$ is less than 1, so the injection rate does not increase as fast as at the beginning. This will try to avoid congestion condition in the networks. From our analysis, the increase function of PIPD will not only control the rate well to suit the InfiniBand networks but also can improve the utilization of the bandwidth.

The decrease function also suits the InfiniBand networks environment. Because of small buffer size and the low network latency, the multiplicative decrease function cannot deal with the congestion in the InfiniBand networks. The power function decrease reduces the injection rate quickly enough to make the traffic flows relieve the congestion condition.

4 Simulation Scenarios and Performance Results

We have developed a discrete-event simulator to conduct a series of experimental study on the scenario illustrated in Fig. 2. Following [16], the network includes five endpoints and two switches A and B connected by a single physical link. The traffic flow generated at endpoint B_1 and destined to endpoint B_c; we call it local flow as it is connected to the same switch of the receiver. The traffic flow generated at endpoint A_1 and destined to endpoint B_c; we call it remote flow because its packets need to be forwarded by switch A to switch B, through an inter switch link. A victim flow generated at endpoint A_v and destined to endpoint B_v through the inter-switch link between the two switches. Victim flow is destined to a non-congested endpoint B_v and suffers from congestion spreading [16]. Table 1 lists the parameters used in our simulation.

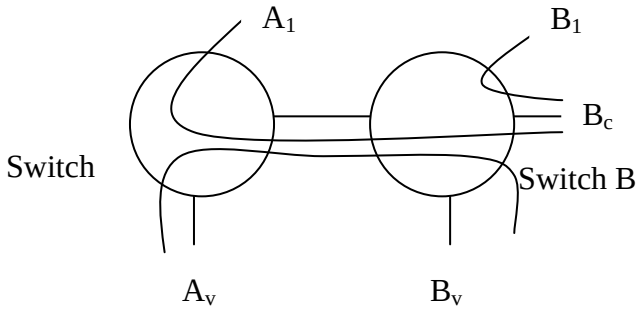

Fig. 2 Simulation scenario

Table 1. Simulation Parameters

Parameters	Value
Link bandwidth	1GB/sec (InfiniBand 4X link)
Packet header	20 bytes (InfiniBand Local Header)
Data packet size	20 + 2048 = 2068 bytes
Packet transmission time	2.068 μs
Buffer size	8 packets

Our experiments test the performance of the improved link-by-link based admission control mechanism and the new source response function PIPD. We assume there are two classes of traffic flows injected into each link with different SLs priorities and there is one remote flow and one local flow in the network. In the admission control stage, we set the bandwidth required by the high priority SL connection is two times of that required by the low priority SL connection. In the congestion stage, we set $R_{\min-high} = R_{\max}/128$ for the high priority flow r_2 and $R_{\min-low} = R_{\max}/256$ for the low priority flow r_1 with $m = 4$.

Figs. 3&4 reveal how the flow injection rates oscillate in the two switches with our admission control mechanism and the PIPD function. From these figures we can notice the injection rate of the high priority SL connection is almost twice of that of the low priority SL connection. Comparing these two figures, it can be found that the utilization of the root link is better than the utilization of the inter-switch link. Because of the congestion spreading, switch A will be blocked if switch B is under the congestion condition. We can also find that the flow with the high priority gets the higher transmission rate than the flow with the lower priority. Figs. 3&4 reveal the high priority flow r_2 easily achieves the very high injection rate. Table 2 shows the average injection rate of each flow based on the proposed PIPD function. The simulation results show an improved performance mechanism with PIPD function which justifies our analysis that it suits to the InfiniBand networks well.

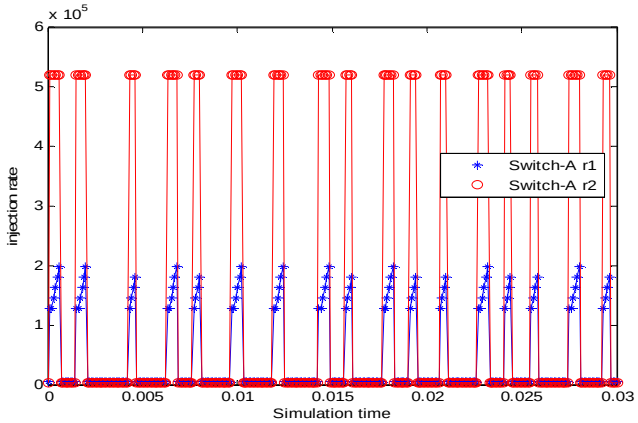

Fig. 3 Result of Switch-A with PIPD

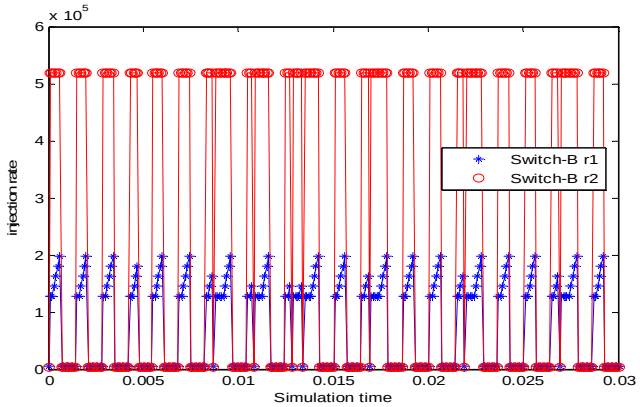

Fig. 4 Result of Switch-B with PIPD

Table 2. Average Injection Rate in PIPD

	Average Injection Rate
Switch-A-r1	47234.08637836817
Switch-A-r2	149789.83324444026
Switch-B-r1	76440.10564262095
Switch-B-r2	259756.99827139667

5 Conclusions and Future Work

This paper has proposed an improved admission control mechanism and a new congestion control function for multiple-class traffic in the InfiniBand networks. The traditional admission control algorithm has been extended so that it is suitable to the InfiniBand

networks. Base on the characteristics of InfiniBand networks, such as no packet dropping, small buffer size and low latencies, the development of the proposed congestion scheme comprises two parts: a simple ECN packet marking mechanism and a new source response mechanism that combines rate control. The experimental study has demonstrated that the proposed schema can maintain the performance of the InfiniBand networks at a good level. The future work will focus on extending simulation scenarios in order to explore the congestion control mechanisms with richer traffic patterns and larger network topologies.

References

[1] F. J. Alfaro, J. L. Sanchez, and J. Duato, "QoS in InfiniBand Subnetworks", IEEE Transactions on Parallel and Distributed Systems, vol. 15, no. 9, pp. 810-823, 2004.

[2] J. Burt, "InfiniBand Switches Enable Clusters, Grid Options", http://www.eweek.com/article2/0,1759,1562054,00.asp, 2004.

[3] A. Bermudez, R. Casado, F. J. Quiles, T. M. Pinkston, and J. Duato, "Modeling InfiniBand with OPNET," Spanish CICYT under Grant TIC2000-1151-C07-02, 2002

[4] W. J. Boden, "Virtual-channel flow control," IEEE Transactions on Parallel and Distributed Systems, vol. 3, no. 2, pp. 194-205, 1992.

[5] L. S. Brakmo and L. L. Peterson, "TCP Vegas: End to end congestion avoidance on a global internet," IEEE Journal on Selected Areas in Communications vol. 13, no. 8, pp. 1465-1480, 1995.

[6] O. Celebioglu, R. Rajagopalan, R. Ali, "Exploring InfiniBand as an HPC Cluster Interconnect", High- Performance Computing, Dell Power Solution, 2004.

[7] D. Chiu and R. Jain, "Analysis of the increase and decrease algorithms for congestion avoidance in computer networks," Computer Networks and ISDN Systems, vol. 17, no. 1, pp. 1-14, 1989.

[8] S. Floyd, "TCP and explicit congestion notification," Computer Communication Review, vol. 24, no. 5, pp. 8-23, 1994.

[9] N. Golmie, Y. Saintillan, and D. Su, "ABR switch mechanisms: design issues and performance evaluation," Computer Networks and ISDN Systems, vol. 30, no. 1, pp. 1749-1761, 1998.

[10] InfiniBand Trade Assoc, InfiniBand Architecture Specification Volume 1, Release 1.2 Http://www.infinibandta.org, 2004.

[11] V. Jacobson, "Congestion avoidance and control," Proc. ACM-SIGOCOMM, Lawrence Berkeley Laboratory, ACM press, pp. 314-329, 1988.

[12] S. Jamin and S. J. Shenker and P. B. Danzig, "Comparison of Measurement-Based Admission Control Algorithms or Controlled-Load Service," Proc. IEEE-INFOCOM, pp. 973-980, 1997.

[13] C. Parsa and J. J. Garcia-Luna_Aceves, "Improving TCP congestion control over internets with heterogeneous transmission media," Proc. IEEE-ICN. IEEE Computer Society, pp. 213-221, 1999

[14] K. K. Ramakrishnan, S. Floyd, and D. Black, "The addition of Explicit Congestion Notification (ECN) to IP," IETF, Tech. Rep. RCF 3168, 2001.

[15] K. K. Ramakrishnan and R. Jain, "A binary feedback scheme for congestion avoidance in computer networks," ACM Transactions on Computer System, vol.8, no.2, pp. 158-181, 1990.

[16] J. R. Santos, Y. Turner, G. Janakiraman, "End-to-End Congestion Control for InfiniBand," Proc. IEEE INFOCOM, San Francisco, CA, 2003.

[17] J. R. Santos, Y. Turner, and G. J. Janakiramam, "Evaluation of congestion detection mechanisms for InfiniBand switches," Proc. IEEE GLOBECOM – High-speed networks Symposium, 2002

[18] Y. Turner, J. R. Santos, and G. Janakiraman, "An Approach For Congestion Control In InfiniBand" Internet Systems and Storage Laboratory, HP Laboratories Palo Alto, HPL-2001-227 (R.1), 2002.

[19] K. H. Yum, E. J. Kim, C. R. Das, M. Yousif, and J. Duato, "Integrated Admission and Congestion Control for QoS Support in Clusters," Proc. IEEE International Conference on Cluster Computing, pp.325-332, Chicago, IL, 2002.

Analysis of Active Queue Management under Two Classes of Traffic

Lan Wang, Geyong Min, Irfan Awan

Department of Computing, School of Informatics,
University of Bradford, Bradford, BD7 1DP, UK
{lwang9,G.Min,I.U.Awan}@Bradford.ac.uk

Abstract - Active Queue Management (AQM) is an effective mechanism to support end-to-end traffic congestion control in network routers. Dropping packets before the queue reaches its maximum capacity is the main idea behind AQM. This paper develops an analytical model for a finite capacity queueing system with AQM mechanisms subject to two classes of traffic. The joint and marginal performance measures including the mean queue length, response time, system throughput, probability of packet losses and mean waiting time have been derived. The validity of the analytical results has been demonstrated through simulation experiences. The analytical model has been used to evaluate the performance of the queueing system with the AQM scheme subject to two classes of traffic.

1. Introduction

In very large networks with heavy traffic, sources compete for bandwidth and buffer space while being unaware of the current state of the system resources. This situation can easily lead to congestion even when the demand for resources does not exceed those available [9]. Consequently, system performance degrades seriously due to the increase of packet loss. In this context, congestion control mechanisms play important roles in effective network resource management.

End-to-end congestion control mechanisms are not sufficient to prevent congestion collapse in the Internet. Basically, there is a limit to how much control can be accomplished from the edges of the network. Therefore, intelligent congestion control mechanisms for FIFO-based or per-flow queue management [11] and scheduling mechanisms are required in the routers to complement the endpoint congestion avoidance mechanisms. Scheduling mechanisms determines the sequence of packets to be sent, while queue management algorithms control the queue length by dropping packets when necessary.

Buffer is an important resource in a router or switch. The larger buffer can absorb larger burst arrivals of packets but can tend to increase queueing delays as well. The traditional approach to buffering is to set a maximum limit on the amount of data that can be buffered. The buffer accepts each arriving packet until the queue space is exhausted and drops all subsequent arriving packets until some space becomes available in the queue. This mechanism is referred to as Tail Drop (TD) that is still the most popular mechanism in IP routers today owing to its robustness and simple implementation. However, “Lock-Out” and “Full Queues” [3] due to dropping packets only when the congestion has occurred are the main drawbacks of TD. The other two alternative queue disciplines, “Random drop on full” and “Drop front on full”, which is applied when the queue becomes full, can solve the “Lock-Out” problem but not “Full Queues” problem [3].

To overcome these problems and to provide low end-to-end delay along with high throughput, a widespread deployment of Active Queue Management (AQM) in routers has been recommended in the IETF publications [3]. To avoid the buffer maintaining a full status for a long time, AQM mechanism starts dropping packets before the queue is full in order to notify incipient stages of congestion. By keeping the average queue length small, AQM decreases the average delay, thus resulting in increased link utilisation by avoiding global synchronisation. Two important points in an AQM mechanism are when and how to drop packets. The former is mainly based on either the averaging queue length or the actual queue length. The latter is based on the threshold and dropping function. Both have a significant impact on the average delay, throughput and probability of packet loss. However, it is difficult to set values for the parameters of an AQM mechanism. For example, as the most popular AQM mechanism, Random Early Detection (RED) was initially described and analyzed in [4] with the anticipation to overcome the disadvantages of TD. There are five parameters in RED that can individually or cooperatively affect its performance. How to

set parameters for RED was discussed by Sally in 1993 [7] and 1997 [5] separately in detail. But it is hard to choose a set of these parameter values to balance the trade-off between various performance measures with different scenarios. As a result, most studies on RED are using the values introduced by Sally in 1997 [5]. In order to reflect the real variation of the queue, the instantaneous queue length is used to compare with the set thresholds and a linear function is adopted to drop packets.

Analysing the effects of an AQM mechanism on the aggregate traffic becomes more and more important. A simple simulation scenario where only four FTP sources were considered has shown that RED performs better than TD in [7]. But against to Sally and Van's original motivation, the more scenarios are considered, the more disadvantages of RED appear. Based on the analysis of extensive experiments of aggregate traffic containing various categories of flows with different proportions, Martin *et al* [10] concluded that the harm of RED due to using the average queue size appears, especially when the average value is far away from the instantaneous queue size. The interaction between the averaging queue length and the sharp edge in the dropping function results in some pathology such as increasing the drop probability of the UDP flows and the number of consecutive losses. On the other hand, Mikket et al [4] studied the effect of RED on the performance of Web traffic using HTTP response time, a user-centric measure of performance, and found RED can not provide a fast response time for end-user as well. In [6], a modification to RED, named as Gentle-RED (GRED), was suggested to use a smoothly dropping function even when avg>=max_{th} but not the sharp edge in the dropping function as before. In [10], an extension of GRED, named GRED-I, was suggested to use an instantaneous queue length instead of the averaging queue length, one threshold and the dropping probability varies smoothly from 0 to 1 between the threshold and the queue size. The surprised result in [2, 6, 10] reveals that GRED-I performs better than both RED and GRED in terms of the aggregate throughput, UDP loss probability, queueing delay and number of consecutive losses. Compared to RED, GRED appears less advantageous than GRED-I because, for RED, the averaging strategy causes more negative effects than the cooperation of the average queue length and the sharp edge in the dropping function.

All existing studies [2, 4, 6, 7, 10] on the performance of AQM are based on software simulation. It is known that simulation is time-consuming and analytical model becomes a cost-effective alternative to simulation for evaluating system performance under different design spaces. With the aim to develop such a tool for investigating the performance of AQM and justifying the choice of different parameters, this study develops a new analytical queueing model for AQM mechanisms with two classes of traffic.

The rest of this paper is organized as follows. Section 2 describes a queueing system model with AQM mechanisms for two classes of traffic. The joint and marginal performance measures are presented in Section 3. The performance results are validated and analysed in Section 4. Finally, Section 5 concludes the study.

2. The Analytical Model

We consider two classes of traffic in a single-server queueing system using FIFO discipline. The arrival of each class k $(k=1,2)$ follows a Poisson process with an average arrival rate λ_k. The service time of both classes is exponentially distributed with mean $1/\mu$. The system capacity is L. As shown in Figure 1, the packets of class k will be dropped randomly based on a linear dropping function when the customer number in the system exceeds the threshold th_k. The maximum dropping probabilities of both classes, $d_{\max 1}$ and $d_{\max 2}$, are 1.

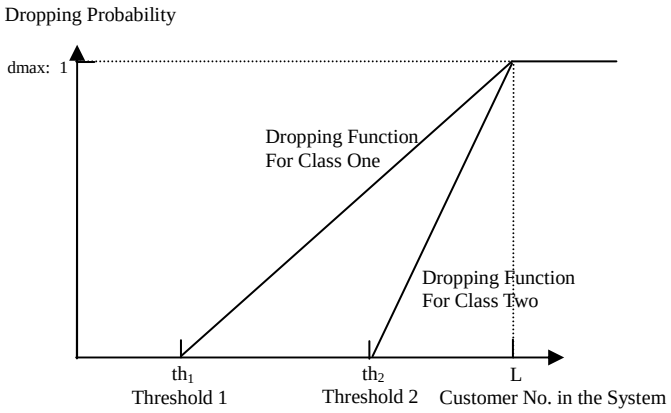

Figure 1: Dropping Functions for Two Classes

The dropping process can be seen as a decrease of the arriving rate with the probability d_i^k, where i represents the customer number in the system. A state transition rate diagram of the M/M/1/L queueing system with the AQM mechanism is shown in Figure 2.

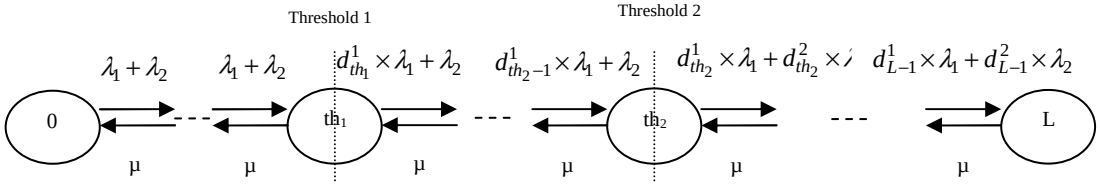

Figure 2: A state transition rate diagram

The d_i^k for each class k is given as follows.

$$d_i^1=\begin{cases}1 & 0\le i<th_1\\ 1-(\frac{i-th_1+1}{L-th_1+1})*d_{\max 1} & th_1\le i\le L\end{cases} \tag{1}$$

$$d_i^2=\begin{cases}1 & 0\le i<th_2\\ 1-(\frac{i-th_2+1}{L-th_2+1})*d_{\max 2} & th_2\le i\le L\end{cases} \tag{2}$$

Let p_i, $0 \le i \le L$ represent the probability of each state in the state transition diagram. According to the transition equilibrium between in-coming and out-coming streams of each state and Probability Theory, the following equations can be found.

$$\left.\begin{aligned}&(d_0^1\lambda_1+d_0^2\lambda_2)p_0=\mu p_1\\ &(d_i^1\lambda_1+d_i^2\lambda_2+\mu)p_i=(d_{i-1}^1\lambda_1+d_{i-1}^2\lambda_2)p_{i-1}+\mu p_{i+1} \qquad 1\le i<L\\ &\mu p_L=(d_{L-1}^1\lambda_1+d_{L-1}^2\lambda_2)p_{L-1}\end{aligned}\right\} \tag{3}$$

Solving these equations, the probability can be expressed as:

$$\left.\begin{aligned}&p_0=\frac{1}{1+\sum_{i=1}^{L}(\prod_{k=0}^{i-1}\frac{d_k^1\lambda_1+d_k^2\lambda_2}{\mu})}\\ &p_i=(\prod_{k=0}^{i-1}\frac{d_k^1\lambda_1+d_k^2\lambda_2}{\mu})\times p_0 \qquad 1\le i\le L\end{aligned}\right\} \tag{4}$$

3. Performance Analysis

In what follows, we will derive the joint system performance metrics including the mean queue length ($\overline{L}$), mean response time ($\overline{R}$), system throughput (T), probability of packet losses ($\overline{P}$) and the mean waiting time ($\overline{W_q}$) and relevant marginal performance metrics for each class of traffic.

3.1 The joint performance measures

The joint mean queue length and throughput can be calculated using the same way as for the traditional M/M/1/L queueing system. Then the mean response time and the mean waiting time in the queue can be solved by Little's Law. The packet loss probability consists of the probability of packet loss after the queue is full and that of packet dropped before the queue is full.

$$\overline{L} = \sum_{i=0}^{L} (p_i \times i) \tag{5}$$

$$T = (1 - p_0) \times \mu = \sum_{i=0}^{L-1} p_i \times (d_i^1 \times \lambda_1 + d_i^2 \times \lambda_2) \tag{6}$$

$$\overline{R} = \frac{\overline{L}}{T} \tag{7}$$

$$\overline{W_q} = \frac{\overline{L_q}}{T} \tag{8}$$

$$\overline{P} = \sum_{i=0}^{L} p_i \times \frac{(1 - d_i^1) \times \lambda_1 + (1 - d_i^2) \times \lambda_2}{\lambda_1 + \lambda_2} \tag{9}$$

3.2 The marginal performance measures

For a system in the steady-state, the average arrival rate equals to its throughput. So the throughput of each class can be expressed as Eq. (10). In Eq. (11), the ratio of the instant arrival rate of class k ($k = 1,2$) to the total arrival rate $\lambda_1 + \lambda_2$ is the instant probability of loss packets from class k. Because both classes of traffic are served identically, the average response time and the delay of each class can be derived using Eqs. (12) and (13) [8]. The delay of a packet from class k can be decomposed into two parts: the mean residual life due to the other packets found in service and the waiting time due to customers found in the queue upon its arrival. In an M/M/1/L queueing system, the mean residual life equals to the mean service time. The average response time consists of the delay and mean service time for the packet.

$$T^k = \sum_{i=0}^{L-1} p_i \times d_i^k \times \lambda_k \tag{10}$$

$$\overline{P^k} = \sum_{i=0}^{L} p_i \times \frac{(1 - d_i^k) \times \lambda_k}{\lambda_1 + \lambda_2} \tag{11}$$

$$\overline{R^k} = \frac{\sum_{i=0}^{L-1} \left(\frac{d_i^k \lambda_k}{d_i^1 \lambda_1 + d_i^2 \lambda_2} \times p_{i+1} \times \frac{i+1}{\mu} \right)}{\sum_{i=0}^{L-1} \left(\frac{d_i^k \lambda_k}{d_i^1 \lambda_1 + d_i^2 \lambda_2} \times p_{i+1} \right)} \tag{12}$$

$$\overline{W_q^k} = \frac{\sum_{i=0}^{L-1} \left(\frac{d_i^k \lambda_k}{d_i^1 \lambda_1 + d_i^2 \lambda_2} \times p_{i+1} \times \frac{i}{\mu} \right)}{\sum_{i=0}^{L-1} \left(\frac{d_i^k \lambda_k}{d_i^1 \lambda_1 + d_i^2 \lambda_2} \times p_{i+1} \right)} \tag{13}$$

In order to calculate the probability distribution of the marginal queue length for each class, the probability that packets of each class stay in any position in the system should be calculated firstly. There are L positions in the system with the number being $1 \ldots L$ from server to the tail of the

queue. If a packet from class k is allocated in the position i $(1 \le i \le L)$ when it arrives in the system, it will experience all the positions j before i, $j \le i$. In other words, the probability that there is a packet from class k in the state j should be the summation of all the probabilities that the packet arrives in the system and is allocated at position i, $1 \le j \le i \le L$. From the transition diagram above, the later probability can be calculated intuitively as $p_i \times \frac{d_i^k \times \lambda_k}{d_i^1 \times \lambda_1 + d_i^2 \times \lambda_2}$ $1 \le j \le i \le L$. So the probability that a packet from class k is in position i, noted as m_i^k, can be derived as:

$$m_i^k = \frac{\sum_{j=i-1}^{L-1} (p_j \times \frac{d_j^k \times \lambda_k}{d_j^1 \times \lambda_1 + d_j^2 \times \lambda_2})}{\sum_{j=i-1}^{L-1} p_j} \qquad 1 \le i \le L \quad k = 1,2 \qquad (14)$$

If the number of packets from class k is q, $0 \le q \le L$, then the number of aggregate packets in the system should be not smaller than q. When the length of the system is l $l \ge q$, there are C_l^q composition of two classes to make the length of class k be q. Furthermore, the probability of each composition is different and can be calculated using m_i^k. So the marginal probability distribution of queue length for each class k, p_q^k can be derived as follows:

$$p_q^1 = \begin{cases} p_0 + \sum_{l=1}^{L} \left\{ p_l \times \left[\sum_{i=0}^{C_l^q - 1} \left(\prod_{j=0}^{l-1} m_{j+1}^{\mathbf{A_l^q}[i,j]} \right) \right] \right\} & \mathrm{q} = 0 \\ \sum_{l=q}^{L} \left\{ p_l \times \left[\sum_{i=0}^{C_l^q - 1} \left(\prod_{j=0}^{l-1} m_{j+1}^{\mathbf{A_l^q}[i,j]} \right) \right] \right\} & 1 \le q \le L \end{cases} \qquad (15)$$

$$p_q^2 = \begin{cases} p_0 + \sum_{l=1}^{L} \left\{ p_l \times \left[\sum_{i=0}^{C_l^q - 1} \left(\prod_{j=0}^{l-1} m_{j+1}^{\mathbf{B_l^q}[i,j]} \right) \right] \right\} & q = 0 \\ \sum_{l=q}^{L} \left\{ p_l \times \left[\sum_{i=0}^{C_l^q - 1} \left(\prod_{j=0}^{l-1} m_{j+1}^{\mathbf{B_l^q}[i,j]} \right) \right] \right\} & 1 \le q \le L \end{cases} \qquad (16)$$

To represent p_q^k, two matrices $\mathbf{A_i^j}$ and $\mathbf{B_i^j}$ are used to describe the possible compositions and defined as:

$$\mathbf{A_i^j} = \begin{cases} (2\ 2\ \cdots\ 2)_{C_i^j \times i} & i = 1,2,\ldots;\ j = 0 \\ (1\ 1\ \cdots\ 1)_{C_i^j \times i} & i = 1,2,\ldots;\ j = i \\ \begin{pmatrix} \boldsymbol{\alpha}_{(i-1)\times 1} & \mathbf{A_{(i-1)}^{(j-1)}} \\ \boldsymbol{\beta}_{(i-1)\times 1} & \mathbf{A_{(i-1)}^{j}} \end{pmatrix}_{C_i^j \times i} & i = 2,\ldots L;\ j = 1,2,\ldots i-1 \end{cases} \qquad (17)$$

$$\mathbf{B_i^j} = \begin{cases} (1\ 1\ \cdots\ 1)_{C_i^j \times i} & i = 1,2,\ldots;\ j = 0 \\ (2\ 2\ \cdots\ 2)_{C_i^j \times i} & i = 1,2,\ldots;\ j = i \\ \begin{pmatrix} \boldsymbol{\beta}_{(i-1)\times 1} & \mathbf{B_{(i-1)}^{(j-1)}} \\ \boldsymbol{\alpha}_{(i-1)\times 1} & \mathbf{B_{(i-1)}^{j}} \end{pmatrix}_{C_i^j \times i} & i = 2,\ldots L;\ j = 1,2,\ldots i-1 \end{cases} \qquad (18)$$

Both matrices are of size $C_i^j \times i$. Each row of $\mathbf{A_i^j}$ is a possible composition of class one and class two when the aggregate queue length is i and the queue length for class 1 is j. $\mathbf{B_i^j}$ can be defined for class two similarly. Another two basic matrices $\boldsymbol{\alpha}_{i\times 1}$ and $\boldsymbol{\beta}_{i\times 1}$ are defined as:

$$\boldsymbol{\alpha}_{i\times 1} = \begin{pmatrix} 1 \\ 1 \\ \vdots \\ 1 \end{pmatrix}_{i\times 1} \quad i = 1,2,\cdots \qquad (19) \qquad \boldsymbol{\beta}_{i\times 1} = \begin{pmatrix} 2 \\ 2 \\ \vdots \\ 2 \end{pmatrix}_{i\times 1} \quad i = 1,2,\cdots \qquad (20)$$

The relationship between $\mathbf{A_i^j}$ and $\mathbf{B_i^j}$ is shown as follow:

$$\boldsymbol{\gamma}_{C_i^j \times i} = \begin{pmatrix} 3\cdots 3 \\ \vdots\ddots\vdots \\ 3\cdots 3 \end{pmatrix} \qquad (21) \qquad \mathbf{B_i^j} = \boldsymbol{\gamma}_{C_i^j \times i} - \mathbf{A_i^j} \qquad (22)$$

So the mean queue length can be calculated using the method similar as (5) and can be simplified as: $\overline{L^k} = \sum_{i=1}^{L}(p_i \times \sum_{j=0}^{i} m_j^k)$ (23)

4. Validation of the Model

A discrete-event simulator has been developed to validate the above analytical model. The effects of varying both thresholds on the marginal and joint performance have been analyzed in this section.

Within the first scenario, threshold th_1 is fixed and threshold th_2 increases. The marginal mean queue length, throughput, probability of loss packets and delay have been shown in Figures 3-6 respectively. We can find from these figures that the variation of th_2 affects all performance measures significantly. In particular, as the value of th_2 rises, the packet number of class two in the system increases. As a consequence, its mean queue length, throughput, and delay tend to increase. At the same time, the packet loss probability of class two tends to decrease. However, for class one, the throughput tends to decrease and the mean queue length, packet loss probability and delay tend to increase.

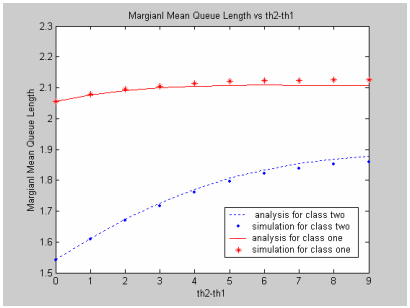

Figure 3: The marginal Mean Queue length with threshold 1 = 6, threshold 2 = 6~15

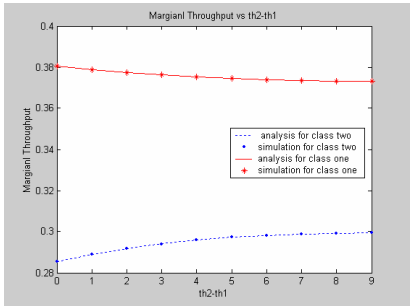

Figure 4: The marginal Throughput with threshold 1 = 6, threshold 2 = 6~15

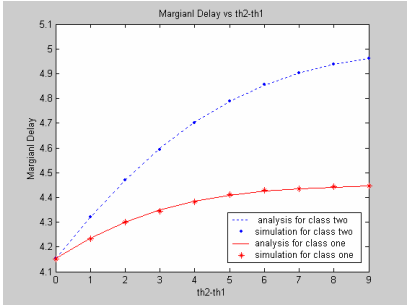

Figure 5: The marginal Delay with threshold 1 = 6, threshold 2 = 6~15

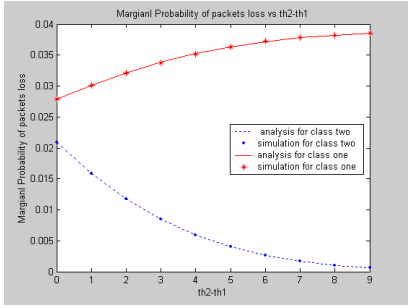

Figure 6: The marginal Probability of Packets Loss with threshold 1 = 6, threshold 2 = 6~15

We will then investigate the aggregate performance measures of the system. It is clear that the increase of th_2 enables more packets to enter in the system. The relative aggregate performance measures have been shown in Figures 7-10. It can be seen that the aggregate mean queue length, throughput and delay increase as the value of th_2 increase. But the probability of packets loss reduces.

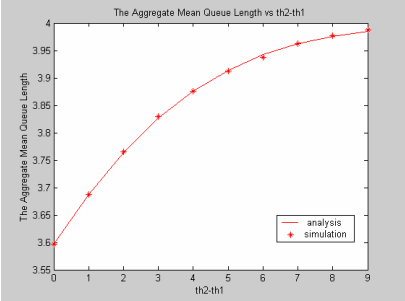

Figure 7: The aggregate Mean Queue length with threshold 1 = 6, threshold 2 = 6~15

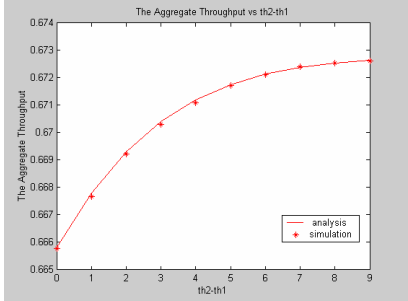

Figure 8: The aggregate Throughput with threshold 1 = 6, threshold 2 = 6~15

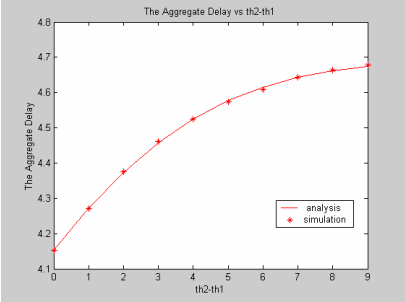

Figure 9: The aggregate Delay with threshold 1 = 6, threshold 2 = 6~15

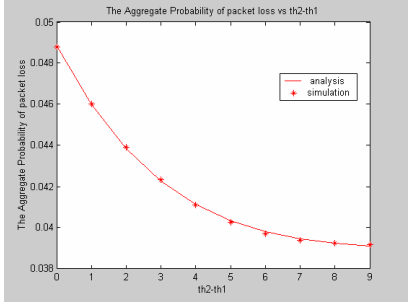

Figure 10: The aggregate Probability of Packets Loss with threshold 1 = 6, threshold 2 = 6~15

In order to evaluate the effects of the first threshold, threshold th_2 is fixed and threshold th_1 decreases within the second scenario. The marginal mean queue length, throughput, probability of loss packets and delay have been shown in Figures 11-14 respectively. The significant changes of all the performance measures can be found from these figures as threshold th_1 increases. For example, only the packet loss probability of class one tends to increase and the mean queue length, throughput, and delay of class two tend to decrease with the reduction of th_1. However, for class two, the throughput tends to increase and the mean queue length, packet loss probability and delay tend to decrease.

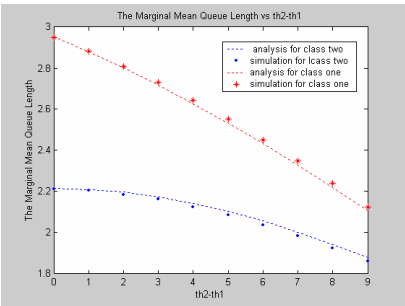

Figure 11: The aggregate Mean Queue length with threshold 1 = 6~15, threshold 2 = 15

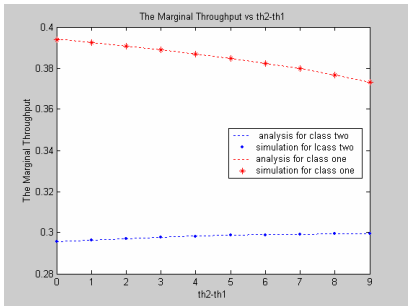

Figure 12: The aggregate Throughput with threshold 1 = 6~15, threshold 2 = 15

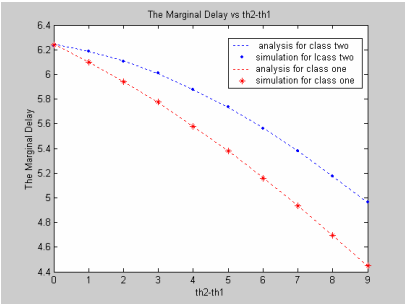

Figure 13: The aggregate Delay with threshold 1 = 6~15, threshold 2 = 15

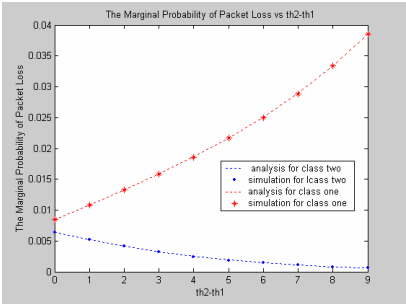

Figure 14: The aggregate Probability of Packets Loss with threshold 1 = 6~15, threshold 2 = 15

The relevant aggregate performance measures have been shown in Figures 15-18. With the decrease of the first threshold, less packets will be allowed to enter into the system. So it can be seen that the aggregate mean queue length, throughput and delay decrease when the distance between two thresholds becomes larger. But the probability of packets loss increases.

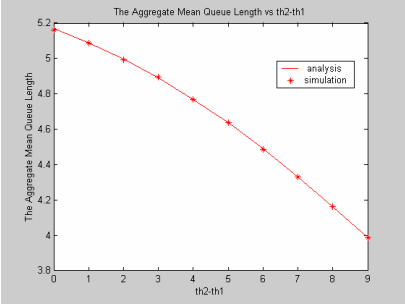

Figure 15: The aggregate Mean Queue length with threshold 1 = 6~15, threshold 2 = 15

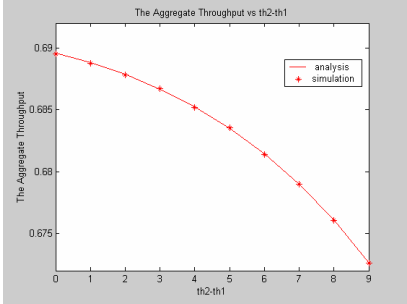

Figure 16: The aggregate Throughput with threshold 1 = 6~15, threshold 2 = 15

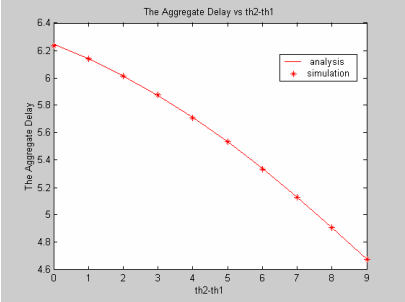

Figure 17: The aggregate Delay with threshold 1 = 6~15, threshold 2 = 15

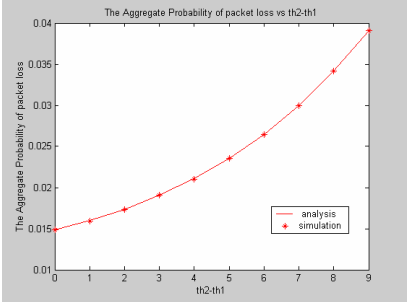

Figure 18: The aggregate Probability of Packets Loss with threshold 1 = 6~15, threshold 2 = 15

5. Conclusions

In this paper an analytical model of M/M/1/L queueing systems with AQM mechanisms under two classes of traffic has been developed. The model is able to calculate the joint and marginal mean queue length, throughput, probability of loss packets and delay. The comparison of analytical results and those obtained from simulation has demonstrated the accuracy of the model. Although our analysis is based on the well-known GRED-I method for AQM, the derivation of the model is general and can be easily extended for other AQM methods. Performance analysis using the derived model has shown that all performance measures change significantly as the threshold value increases. For instance, the packet loss probability of class two tends to decrease and the mean queue length, throughput, and delay of class two tend to increase as the distance between two thresholds enlarges. However, the throughput for class one tends to decrease and its mean queue length, packet loss probability tend to increase.

References

[1] T. Bonald, M. May, J.C. Bolot, Analytic evaluation of RED performance, *Proc.IEEE INFOCOM*, pp. 1415-1424, 2000.

[2] C. Brandauer, G. Iannaccone, C. Diot, T. Ziegler, Comparison of tail drop and Active Queue Management performance for bulk-date and Web-like Internet traffic, *Proc. ISCC*, pp. 122-129, 2001.

[3] B.Braden et al., Recommendations on queue management and congestion avoidance in the Internet, *IETF RFC2039*, 1998.

[4] M. Christiansen, K. Jeffay, D. Ott, F. Donelson Smith, Tuning RED for Web traffic, *IEEE/ACM Trans. Network*, vol 9, no. 3, pp. 249-264, 2001.

[5] S. Floyd, RED: discussions of setting parameters, http://www.icir.org/floyd/REDparameters.txt, 1997.

[6] S. Floyd, K. Fall, Promoting the Use of End-to-End Congestion Control in the Internet, *IEEE/ACM Trans. Network*, vol.7, no. 4, pp.485-472, 1999.

[7] S. Floyd, V. Jacobson, Random Early Detection gateways for congestion avoidance, *IEEE/ACM Trans. Network*, vol 1, no. 4, pp. 397-413, 1993.

[8] L.Kleinrock, *Queueing Systems: Compute Applications*, vol. 1, John Wiley & Sons, New York, 1975.

[9] D.E McDYSAN, *QoS & Traffic Management in IP & ATM Networks*, McGraw Hill, 1999.

[10] M. May, C. Diot, B. Lyles, J. Bolot, Influence of Active Queue Management parameters on aggregate Traffic Performance, INRIA.RR3995, 2000.

[11] S.W. Ryu, C. Rump, C.M. Qiao, Advances in Internet congestion Control, *IEEE Communications survey*, volume 5, no.1, 2003.

Performance Analysis of the LWQ QoS Model in MANETs

S. H. A. Wahab, M. Ould-Khaoua and S. Papanastasiou

Department of Computing Science
University of Glasgow
Glasgow G12 8RZ
U.K.
Email: {shaliza, mohamed, stelios}@dcs.gla.ac.uk

Abstract. Quality of Service (QoS) is essential in Mobile Ad Hoc Networks (MANETs) in order to satisfy communication constraints, e.g. delay, as set in real-time applications. Traffic from such applications is normally treated as high-priority in contrast to non delay sensitive applications such as FTP or e-mail, which are largely delay tolerant and have their flows treated as low-priority in the network. This paper analyses the performance behaviour of a recently proposed QoS model, notably LWQ, with respect to the number of high priority flows under a variety of mobility conditions. Our simulation results reveal that the number of high priority flows and different mobility states have a critical impact on the mean end-to-end delay and throughput of high priority traffic achieved by the LWQ QoS model.

Keywords: Mobile ad hoc networks, QoS, Delay, Throughput, High priority flows, Simulation.

1 Introduction

MANETs [1] are formed by wireless devices that communicate with each other using multi-hop wireless links without necessarily using pre-existing network infrastructure. Two nodes communicate directly if they are in transmission range of each other or otherwise achieve connectivity through a multi-hop route via intermediate nodes. Hence, it becomes possible to establish spontaneous communication between network-enabled electronic devices. MANETs can also be formed by making use of other technologies such as optical networks, but wireless communications is the natural choice for spontaneous networking [2].

Advances in wireless communications and the growth of real-time applications such as streaming audio and games, have drawn a lot of attention to wireless networks that support quality of service (QoS). Due to limited availability of transmission bandwidth in MANETs, QoS techniques need to optimise the scarce resource by prioritising the real-time flows over best-effort flows in order to comply with the QoS requirement such as delay bounds and real-time throughput. Unlike best-effort applications, real-time applications require these QoS guarantees if they are to operate to a sufficient degree. Examples of applications are conversational voice, streaming, interactive and background/best-effort. The main distinguishing factor between these four classes lies with sensitivity to delay [3, 23]. In this research we have divided the real-time flows into two categories: delay-sensitive real-time flows and non delay-sensitive real-time flows. Delay-sensitive real-time flows are commonly considered as high priority and

non delay-sensitive real-time flows are considered low priority. As MANETs have been proposed for disaster relief environments, it is important to prioritise high priority flows so that an important flow will not be blocked due to existing low priority flows.

Based on the above requirement, the goal of our research is to analyse an existing QoS model that deals with prioritisation. The reason we have chosen to analyse this model is because unlike existing models proposed in the literature [4, 5, 15], the LWQ model has a built-in mechanism that ensures tight QoS guarantees to high priority flows. We have performed extensive simulation experiments to investigate the performance behaviour of this model taking into account a number of important system parameters, including the number of high priority flows, node speed, pause time, and network size.

The rest of the paper is organised as follows. In the next section, we briefly review several approaches and their extension for service differentiation. Section 3 provides a detailed description of the LWQ QoS model that we have analyzed. Section 4 evaluates the performance of LWQ in scenario of several competing high-priority flows. Finally, Section 5 concludes the findings and offers a plan for future work.

2 Existing QoS Approaches

MANETs exhibit unique characteristics such as limited bandwidth availability and special mobility considerations. In order to guarantee QoS and given the limited bandwidth requirement it is necessary to prioritise certain flows over others; those high priority flows are then treated preferentially so as to meet given delay or throughput requirements. There exist several applications that need such type of treatment such as Voice over IP (VoIP). When the delay or the loss rate of such flows exceeds certain levels they become unusable.

The existing approaches to QoS in MANETs satisfy some subset of these requirements [4, 5]. Some QoS solutions are built directly into existing routing [6, 7, 8, 9] or link layer protocols [10, 11, 12], making them completely dependant on the adoption of those protocols. Furthermore, several QoS approaches dealing with flow priority differentiation have been proposed in literature [13, 14,15]. The granularity of such differentiation is usually two-levels coarse, i.e. there are two types of flow: high and low priority. However, these priority differentiations have also been built into routing and link layer protocols. The SWAN model [16, 17], for instance, provides guarantees that are soft for high priority flows which implies that they may be downgraded to best-effort flows [18] in the presence of congestion.

One of the recently QoS model that attempts to provide tight guarantees to high priority flows is Light-weight QoS model (LWQ) [19, 20]. The following section describes the operation of the LWQ model and the limitations of its mechanism which has been the main motivation for our present study.

3 The operation of the LWQ model

Light-weight QoS (LWQ) is a modified version of wired DiffServ QoS model [21] that takes into considerations the unique characteristics of multi-hop wireless environment. This model attempts to provide improved QoS to flows of *highest priority class* through a monitoring and correction mechanism which differentiates it with regard to other existing QoS models. As such, the packet rate of high priority flows is monitored

and triggers corrective action like SWAN [16] by stopping the transmission of low priority flows of one hop neighbour once the packet rate is below a certain threshold. When the monitoring mechanism signals the presence of interference, the H-Node (i.e. a node that carries high priority flow) broadcasts a control packet (which is named *Squelch* packet) with a time to live (TTL) of 1. This technique aims at improving network utilisation by probabilistically selecting the nodes that must take corrective action by adding a fixed value to the *Squelch* packet, called the p-value, which lies between 0 and 1. The direct interfering nodes, upon receiving the *Squelch* packet, compute a random number between 0 and 1. If the random number is greater than the p-value, the nodes take corrective action; otherwise, the *Squelch* packet is discarded. Thus, if the p-value is set to 0.5, then only about 50% of the nodes will take corrective action. A p-value of 0 corresponds to the basic corrective mechanism where all nodes take corrective action. The working model of LWQ is presented in Fig. 1.

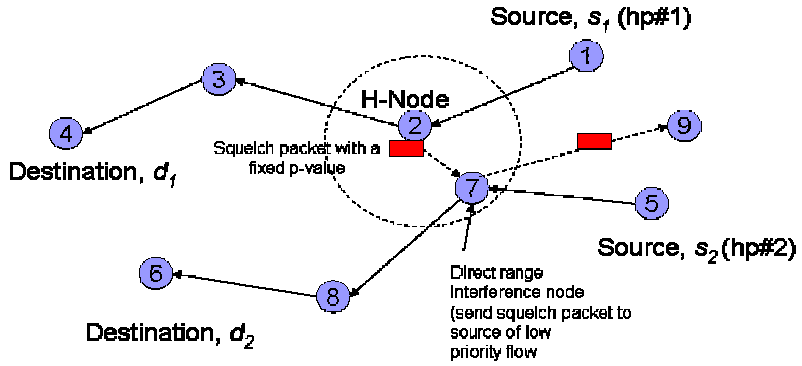

Fig. 1. The operation of the LWQ model

Despite having some guarantees to high priority packets, this architecture causes a reduction in the total throughput because of the corrective action taken by one-hop neighbours to stop transmission of other lower priority flows in attempt to maintain the rate of high priority flows. As a result, this scheme leads to under-utilisation of network resources. Nevertheless, this behaviour does not affect this model much since its objective is to provide tight guarantees to high-priority flow even at some cost in total throughput.

Arora and Greenwald [19] have used only one high priority flow in their reported simulations since its objective is to provide QoS to the highest priority flow. However, the authors have not considered the possibility of several competing high priority flows existing in the network.

4 Performance Evaluation

Considering the limitations of previous work [19, 20], we have analyzed the LWQ QoS model in the presence of a number of high priority flows in order to evaluate network performance in the presence of several competing such flows.

It is important to highlight here our assumed definition of high and low priority flow to

clarify our contribution in the context of previous work. We define high priority flows as 1) flows by delay-sensitive applications which require certain delay bound in order to operate properly and 2) flows that have high packet generation interval. As for low priority flows they are 1) non delay-sensitive application which do not require certain delay bound and 2) flows that have lower packet generation interval than the high priority flows. In order to perform a thorough analysis of this QoS model, we have considered the network topology and accompanying simulated traffic as indicated below:

Network topology: describes the way the interconnection topology of nodes with different mobility affects the performance of the LWQ QoS model.

Traffic: describes to the traffic load of high/low priority flows with different packet sending rate, packet length, and p-value of Squelch packet and in the way they affect the QoS requirement of high priority flows.

We have used the network simulator ns-2 (v 2.26) [22] to run our experiments due to its extensive support for MANETs and ability to support QoS module such as DiffServ [21]. We have generated scenarios in a manner consistent with the recent LWQ architecture in [19] in which 50 nodes are considered, distributed over a 1500 x 300 m area and moving using Random Waypoint Model. Routing is handled by the AODV routing protocol which is mature routing solution in MANETs and a proposed RFC by the IETF. The channel bandwidth is 11 Mbps and the traffic sources are chosen to be constant bit rate (CBR) with background traffic of 3 to 5 low priority flows. Each simulation run lasts for 400 seconds in order to allow the network to experience some congestion.

The offered load could be varied by changing the CBR packet size, the number of CBR flows or the CBR packet rate. In this experiment, we have fixed the CBR packet size and CBR packet rate but we have increased the number of high priority flows. When we increase the number of high priority flows, we decrease the number of low priority in order to maintain the same total number of running flows in the network. We set the rate of high priority flow to 32 80-byte packets per second so that it corresponds to audio streams of 20 Kbps and higher packet generation rate. The rate of low priority flow is 20 800-byte packets per second which in turn corresponds to multimedia on-demand retrieval application of 128 Kbps. The number of high priority flows is increased from 1 to 3 in our simulations. The number of low priority flows is decreased from 5 to 3 when we increase the number high priority flows in order to maintain the same amount of total high and low priority flows in the simulation.

Several pairs of source and destinations of all flows are manually selected. Due to the similarities of the simulation results with different source-destination pairs, we only present the results from one representative simulation. The selected source-destination pair of three high priority flows are (1, 4), (5, 6) and (16,15) whereas the source-destination pair of low priority flows are (9, 10), (22, 45) and (7, 8). These pairs are selected to create multi-hop paths across the network. The simulation parameters and the traffic parameter of high priority flows and low priority flows are summarised in Table 1 and Table 2 respectively.

Table 1. The parameter for the LWQ model used in the simulations.

Simulation Parameter	Value
Number of nodes	50
Simulation area	1500 x 300
Maximum node speed	5, 10, 15, 20, 25 m/s
Pause time	10s
Simulation time	400s
Routing protocol	AODV
MAC protocol	IEEE 802.11

Table 2. The parameter of the generated traffic used in the simulations.

Traffic	Value
Offered load	1 - 3 high priority flows, 3 - 5 low priority flows
Number of maximum high priority flows per node	2
Number of high priority flows	1, 2, 3
Source – destination pairs (*s* ,*t*) of high priority flows	(1, 4), (5, 6) and (16, 15)
Start time for high priority flows	0, 1.0, 2.0 seconds respectively
Packet length and packet interval	80 byte, 32 packets/second
Rate of high priority packet	20 kbps
Number of best-effort flows	5, 4, 3
Source – destination pairs (*s, t*) of low priority flows	(9, 10), (22, 45) and (7, 8)
Start time for low priority flows	0.5, 1.5, 2.5 seconds respectively
Packet length, packet interval	800 byte, 20 packets/sec
Rate of low priority packet	128 kbps

We have evaluated the QoS model by comparing two performance metrics, namely:

Mean end-to-end delay: is the time experienced by a packet between its initiation at the source and its reception at the destination. This is measured by the total packet delay of the flow per number of packets of the flow received at the destination. We have analysed the mean delay of high-priority packets since only high-priority flows is delay sensitive.

High priority throughput: is the number of high priority packets received per unit time, expressed in percentage of number of packets received less than certain bounded delay. Any high priority packet received whose delay is greater than 100 ms will not be included in this high priority throughput calculation as in a real world implementation the application would have no use for it (it would be too late to be meaningful). Delay-sensitive applications, such as voice typically require an end-to-end delay of 400 ms for acceptable quality. However in order to evaluate this model for high priority voice applications, delay less than 100 ms is required; such a delay ensure lips synchronization [23] in video applications.

5 Results and Discussions

This section presents the results for the mean end-to-end delay and high priority throughput considering different mobility conditions.

Fig. 2 shows the impact of competing flows and mobility on mean end-to-end delay of each high priority flows as the number of high priority flows increases and at different mobility levels. Flow ID 1 to Flow ID 3 are high priority flows whereas Flow ID 4 to Flow ID 6 are low priority flows, The results show that the mean end-to-end delay is still maintained at less than 100 ms for two high priority flows (as indicated by bars beneath the dotted line of 0.1 s). However this delay requirement is violated when there are 3 high priority flows as the mean end-to-end delay of high priority flows increases drastically. This is a strong indication that the networks can only handle limited amount of high priority flows.

As for low priority flows (Flow ID 4 to Flow ID 6), they also experience an increase in the mean end-to-end delay when there are 3 high priority flows. However this increase of the low priority flow delay is not significant enough to affect the application utilizing them since they are by definition resilient to delay changes.

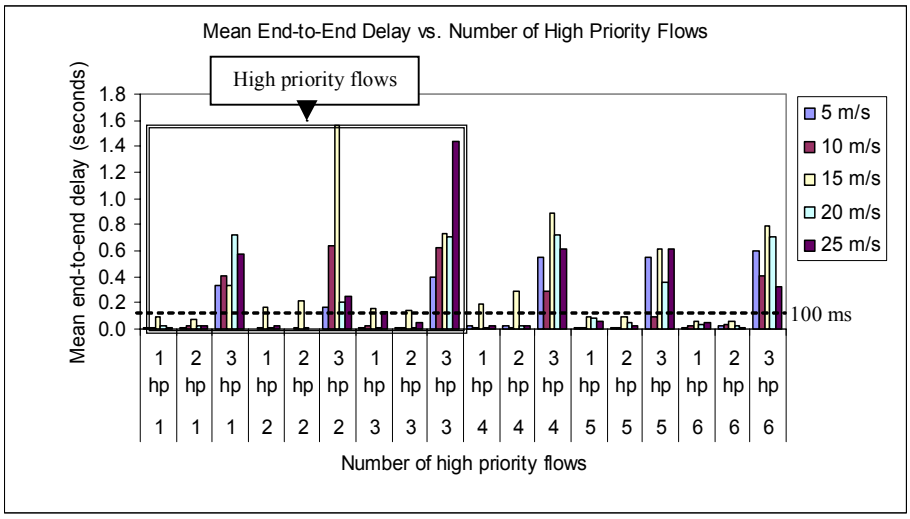

Fig. 2. Mean end-to-end delay of high priority flows with increasing number of high priority flows (grouped by Flow ID) at different mobility

Fig. 3 shows the impact to delay of increasing the number of high priority flows under given mobility conditions. The throughput of high priority flows is calculated as the percentage of packets received within 100 milliseconds. The result shows that the throughput of high priority flows is maintained above 94% when there are up to two high priority flows. However this model starts to experience a throughput requirement violation when there are 3 high priority flows. In such a case, the throughput of the high priority flows decrease drastically. Similarly as with the results presented in Fig. 2, it is shown here that the network can only handle limited amount of high priority flows in order to maintain QoS guarantee.

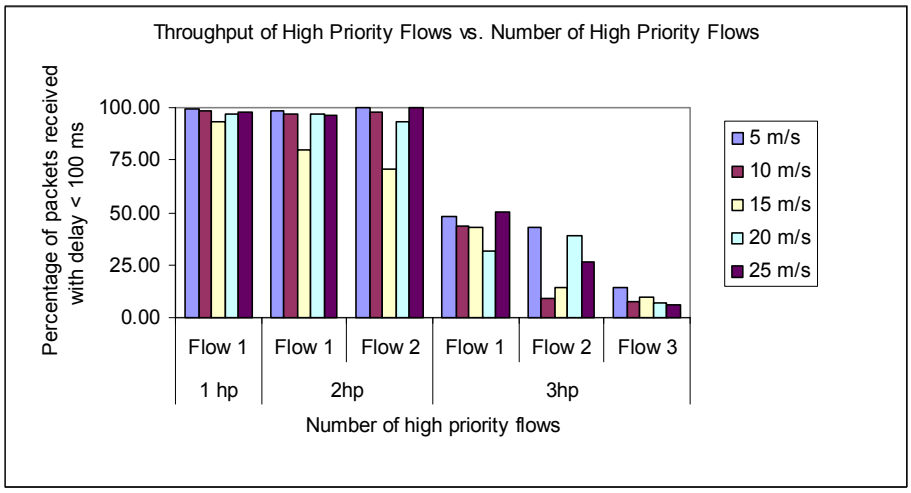

Fig. 3. Throughput of each high priority flows with increasing number of high priority flows (grouped by the number of high priority flows) with different mobility

6 Conclusions

This paper has discussed the effects of increasing the number of high-priory flows on the mean end-to-end delay in MANETs. Further the effect of increasing the number of high priority flows on the achieved throughput has been demonstrated and discussed. It is shown that by increasing the amount of high priority flow, the mean end-to-end delay will increase. Similarly, our results have shown that the same increment in the amount of high priority flows causes the throughput of high priority flows to decrease from 50% up to 80%. Because of the properties of the shared wireless medium, inherently, the flows compete for transmission time and bandwidth particularly with the same priority flows.

In the future, we plan to investigate the effects of suppressing low priority flow where probabilistic p-value is dynamically set. Our above simulations have revealed that the level of inter-flow interference among the flows could affect the choice of the p-value; high levels of interference imply that as limited amount of high priority flows is sustainable. Such conditions in turn imply a trade-off; limiting the amount of existing high priority traffic in order to ensure the surviving flows meets their QoS requirements.

References

[1] IETF MANET Working Group, Mobile Ad Hoc Networks (MANET) Charter. http://www.ietf.org/html.charters/manet-charter.html

[2] D. Remondo and I. G. Niemegeers, Ad hoc networking in future wireless communications, *Computer Communications*, 26(1), 36–40, 2003.

[3] Nortel Networks white paper, Benefits of quality of service (QoS) in 3G wireless internet, http://www.nortelnetworks.com, 2001.

[4] G. -S. Ahn, A. T. Campbell, A. Veres, and L. -H. Sun. Supporting service differentiation for real-time and best-effort traffic in stateless wireless ad hoc networks (SWAN), *IEEE Transactions on Mobile Computing*, 1(3): 192–207, 2002.

[5] S. -B. Lee, G. -S. Ahn, X. Zhang, and A. T. Campbell. INSIGNIA: An IP-based quality of service framework for mobile ad hoc networks, *Journal of Parallel & Distributed Computing*, 60(4): 374–406, 2000.

[6] Q. Xue and A. Ganz, Ad hoc QoS on-demand routing (AQOR) in mobile ad hoc networks, *Journal of Parallel and Distributed Computing*, 63(2): 154–165, February 2003.

[7] P. Sinha, R. Sivakumar and V. Bharghavan, CEDAR: A core extraction distributed ad hoc routing algorithm, *IEEE Journal on Selected Areas in Communications,* 17(8): 1454–1466, 1999.

[8] S. Chen and K. Nahrstedt, Distributed quality-of-service routing in ad hoc networks, *IEEE Journal on Selected Areas in Communications*, 17(8): 1488–1504, 1999.

[9] J. N. Al-Karaki, A. E. Kamal, Quality of service routing in mobile ad hoc networks: current and future trends, Mobile Computing Handbook, I. Mahgoub and M. Ilyas (eds.), *CRC Publishers*, 467–482, 2004.

[10] IEEE 802.11 WG, Draft Supplement to STANDARD FOR Telecommunications and Information Exchange Between Systems - LAN/MAN Specific Requirements - Part 11: Wireless Medium Access Control (MAC) and physical layer (PHY) specifications: Medium Access Control (MAC) Enhancements for Quality of Service (QoS), *IEEE 802.11e/D2.0*, Nov. 2001.

[11] P. Karn, MACA: A new channel access method for packet radio, in *Proc. of ARRL/CRRL Amateur Radio 9th Computer Networking Conference*, September 1990, 134–140.

[12] S. Kumar, V. S. Raghavan and J. Deng. Medium access control protocols for ad hoc wireless networks: a survey, *Ad Hoc Networks*, to appear, 2004.

[13] Y. Yang and R. Kravets. Throughput guarantees for multi-priority traffic in ad hoc networks, in *IEEE International Conference on Mobile Ad Hoc Network and Sensor Systems*, 2004, 379–388.

[14] X. Yang and N. Vaidya. Priority scheduling in wireless ad hoc networks, *Proc. of the 3rd ACM International Symposium on Mobile Ad Hoc Networking & Computing (MobiHoc '02)*, 2002, 71–79.

[15] G. -S. Ahn, Andrew T. Campbell, A. Veres, and L. -H. Sun. Supporting service differentiation for real-time and best-effort traffic in stateless wireless ad hoc networks (Swan), *IEEE Transactions on Mobile Computing*, 1(3): 192–207, 2002.

[16] G. -S. Ahn, A. T. Campbell, A. Veres and L. -H. Sun, SWAN: Service differentiation in stateless wireless ad hoc networks, *Proc. 21st Annual Joint Conf. IEEE Computer Communication Societies(INFOCOM'2002)*, June 2002. 457–466.

[17] A. Veres, A. T. Campbell, M. Barry, and L. -H. Sun, Supporting service differentiation in wireless packet networks using distributed control, *IEEE Journal of Selected Areas in Communications,* Special Issue on Mobility and Resource Management in Next-Generation Wireless Systems, 19(10): 2081–2093, October 2001.

[18] Y. L. Morgan and T. Kunz, Enhancing swan QoS model by adopting destination-based regulation (ESWAN), *Proc. Modeling and Optimization in Mobile, Ad Hoc and Wireless Networks (WiOpt'04)*, Mar. 2004. 112-121.

[19] H. Arora and L. Greenwald. Toward the use of local monitoring and network-wide correction to achieve QoS guarantees in mobile ad hoc networks**,** *First Annual IEEE Communications Society Conference on Sensor and Ad Hoc Communications and Networks, (IEEE SECON 2004)*, Oct. 4–7. 2004, 128–138.

[20] H. Arora, Towards achieving QoS guarantees in mobile ad hoc networks, *Masters Thesis*, Drexel University, Department of Computer Science, Philadelphia, PA, November 2003.

[21] S. Blake, D. Black, M. Carlson, E. Davies, Z. Wang, W. Weiss, An architecture for differentiated services, *IETF RFC2475*, December 1998.

[22] The Network Simulator (NS-2). University of California, Berkeley. http://www.isi.edu/nsnam/ns/

[23] N. Baghaei and R. Hunt, Review of quality of service performance in wireless LANs and 3G multimedia application services, *Computer Communications,* 27: 1684–1692, 2004.

Web Services Dependability and Performance Monitoring

Yuhui Chen[1], Peter Li[2] and Alexander Romanovsky[1]

[1]School of Computing Science, University of Newcastle upon Tyne, NE1 7RU, UK

Yuhui.Chen@newcastle.ac.uk

Alexander.Romanovsky@newcastle.ac.uk

[2]School of Chemistry, University of Manchester, M60 1QD, UK

Peter.Li@manchester.ac.uk

Abstract. The dependability of Web Services is becoming increasingly important for many application domains, such as e-Science, virtual organizations and service-oriented computing. The understanding of how a Web Service behaves in practice will help the developers to improve their service and provide clients with the information to determine the best ways of employing the Web Service. To fulfill such needs, we have developed a tool that monitors the dependability and performance of Web Services. The paper reports some initial results of the experiments in which the tool has been used.

1. Introduction

Dependability can be a major issue when using computational resources, for example, during the enactment of a scientific workflow [1]. The reliability of service resources can be erratic and this can lead to the failure of the workflow during its enactment [2]. The possibility of failure can be reduced by selecting those services which are the most reliable based on data representing their behavioural characteristics. We have developed a Java-based application which monitors the dependability of Web Services. Users can set policies to constrain the tests, for instance, test interval, test period and time out period. The tool collects this information from the Web Services and displays real time statistics. It was used to investigate the reliability of two BLAST Web Services from the bioinformatics domain. The performance characteristics of the BLAST services were found to differ according to response time and completion status. It is hoped that this tool will enable users and client applications to select those services which are the most reliable for their needs.

2. Overview of the Java tool

The tool measures the dependability of Web Services by acting as a client to the Web Service under investigation**.** The tool monitors a given Web Service by tracking the following reliability characteristics:

- ***Availability:*** The tool periodically makes dummy calls to the Web Service to check whether it is running.
- ***Functionality:*** The tool makes calls to the Web Service and checks the returned results to ensure the Web Service is functioning properly.
- ***Performance:*** The tool monitors the round-trip time of a call to the Web Services producing and displaying real time statistics on service performance.
- ***Faults and exceptions:*** The tool logs faults and exceptions during the test period of the Web Service for further analysis.

The tool can also test the dependability of a Web Service at geographically separated locations on different Internet backbones through the deployment of the tool at different physical locations. The tool and all information about it can be found at http://www.students.ncl.ac.uk/yuhui.chen/

3. Comparison of BLAST Web Services

An experiment measuring the performance of two BLAST Web Services was undertaken to test the monitoring tool. BLAST is an algorithm which is commonly used in the bioinformatics domain to search for sequences that are similar to a given query sequence [3]. However, the dependability of BLAST services can differ from one to another. For a computationally-intensive *in silico* analytical experiment, it is important that the most reliable services are used so that the chances of the experiment failing are reduced. To this end, the most reliable BLAST service can be judged based on performance characteristics which have been measured by a tool such as that described in this paper.

Performance metrics from two BLAST services were measured: a BLAST Web Service[1] deployed by the European Bioinformatics Institute (EBI), Cambridge, UK and the BLAST service[2] hosted by the DNA Database of Japan (DDBJ). Each BLAST Web Service was invoked from three servers, two located in Newcastle upon Tyne, UK and the other in China at 30 minute intervals for a period of 72 hours.

The response times of the EBI BLAST service varied dramatically during the 72 hour test period (Fig. 1A). The average response time of the service was ~900s. The response time curves of from domestic broadband and University campus network in Newcastle are similar, although the latter was slightly faster. The response time from

[1] http://www.ebi.ac.uk/collab/mygrid/service4/soap/services/alignment::blastn_ncbi?wsdl
[2] http://xml.nig.ac.jp/wsdl/Blast.wsdl

China is every unstable. One failure has been captured by the three roots synchronously during the test period which suggests a failure of the BLAST Web Service of unknown origin. A failure was also detected when a call was made from China suggesting a possible networking failure between China and EBI service.

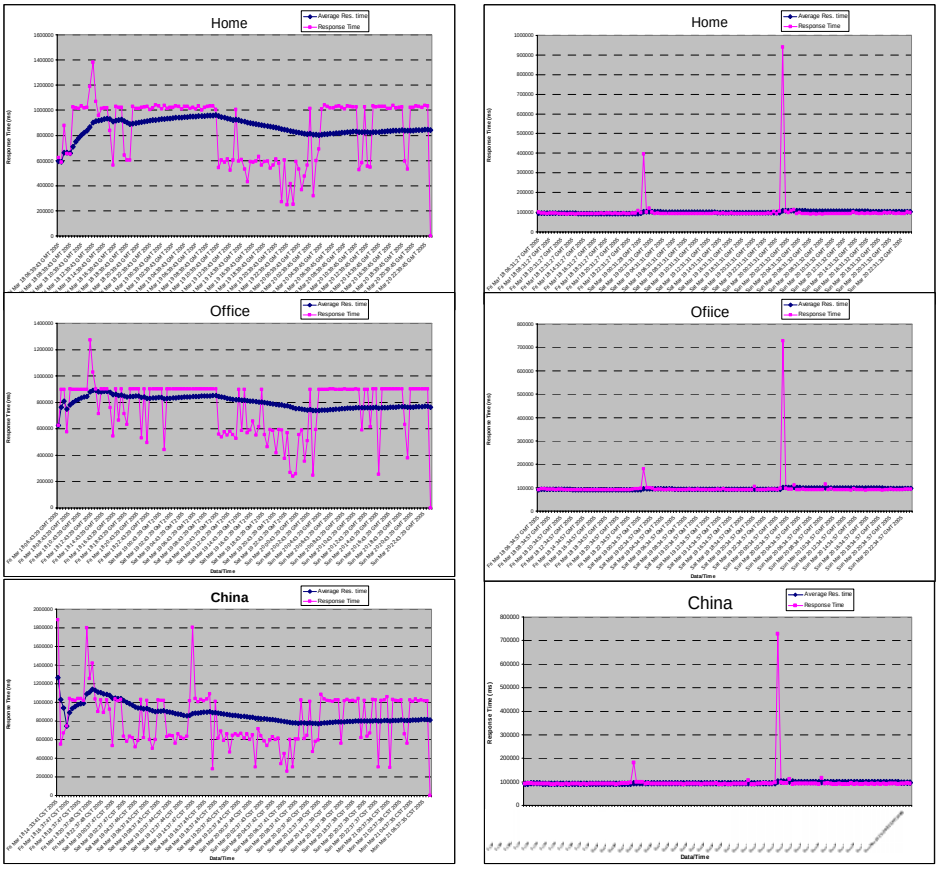

(A) (B)

Fig 1. Performance metrics from BLAST at (A) EBI and (B) DDBJ.

The results of experiment with the DDBJ BLAST service are shown in Figure 1B. The average response times of the DDBJ BLAST service from Newcastle using the domestic broadband and campus networks were similar at ~100 seconds. The response time from China was slightly longer, averaging at ~130 seconds. The response times from all these three locations were very stable which is in contrast to that of the EBI BLAST service. The reliability of the DDBJ BLAST was quite good since only one slow response was captured at 1:04am on Saturday March 19 (GTM standard time) by all three roots synchronously during the 72 hours test which indi-

cates an unknown Web service state. A timeout exception was also captured at 1:34am on Sunday March 20 (GTM standard time) by all three roots synchronously indicating an unknown failure of the DDBJ BLAST Web Service.

4. Discussion and future work

The dependability of Web Services can vary according to a number of independent internal and external factors. There are a number of solutions providing methods for monitoring the use of Web Services. For example, the Bionanny Project [4] is developing a tool that can intercept requests incoming from clients, passing the requests to the designated Web Service and measuring how many times the service is invoked and how many different requests it receives. In effect, it acts as a proxy component to the existing Web Services. However in order to develop dependable Web Services, it is important to understand how the Web Services behave as clients. Our tool provides measurements to fulfil this need. Since failures of Web Services can vary from internal faults to external errors, it is significant to understand where the faults are actually deployed. The tool logs all exceptions for further investigation; however it is difficult to understand some exceptions, especially those about timeout problems. It is planned to improve the tool to have the ability to monitor and analyze the outgoing and incoming SOAP messages to help discover the origin of service problems that have been recorded.

Acknowledgements

We are grateful to Aad van Moorsel for several useful comments and suggestions.

References

[1] Oinn T, Addis M, Ferris J, Marvin D, Greenwood M, Carver T, Senger M, Glover K, Wipat A and Li P. Taverna: a tool for the composition and enactment of bioinformatics workflows. Bioinformatics 20: 3045-3054. 2004.

[2] Stevens R, Tipney HJ, Wroe C, Oinn T, Senger M, Lord P, Goble CA, Brass A and Tassabehji M. Exploring Williams-Beuren Syndrome Using myGrid. Bioinformatics 20: i303-i310. 2004.

[3] Altschul SF, Gish W, Miller W, Myers EW, Lipman DJ. Basic local alignment search tool. J Mol Biol. 215: 403-410. 1990.

[4] Senger M, Niemi M, Bionanny-A Web Service monitoring other Web Services. 2005. http://bionanny.sourceforge.net/

Predictive Run-time Adaptation for Service Level Agreements on the Grid

James Padgett, Karim Djemame and Peter Dew [*]

Abstract. Performance prediction of execution run-times is a key component when delivering timely application services in decision support systems. The provision of Service Level Agreements (SLA) and components to manage tasks such as resource negotiation, monitoring and policing are needed to help meet this requirement. This paper presents an SLA management architecture for use in Grid environments focusing on a policing strategy for Grid services. This includes a method for generating execution run-time predictions for tracking application progress. Experiments to test the prediction model are presented and show the prediction trace compared with a reference schedule.

Introduction

Grid computing [4] offers scientists and engineering communities access to high performance computational resources and applications. Within these virtual organisations users and resources often belong to multiple administrative domains. By definition, these resources are heterogeneous with varying quality and reliability. The ability to uphold commitments and assurances on top of the allocated resources is an application requirement, sometimes referred to as Quality of Service. A key goal of Grid computing is to deliver management on top of the allocated resources including availability of resources (compute resources, storage etc), security and network performance (latency, throughput) [7]. Commitments and assurances are implemented using Service Level Agreements (SLA), which determine a contract between a user and service provider, stating the expectations and obligations that exist between the two.

To support Grid systems based on timely service response a SLA management system incorporating resource reservation and run-time adaptation is desirable. In such systems there is a need for some form of resource monitoring and run-time adaptation on top of resource selection and reservation. An additional requirement is the provision of a historical record of the execution plan for auditing.

SLA management systems found in the literature [12, 21, 27] focus on a limited subset of management functions such as negotiation and reservation, or reservation and monitoring; few extend support for run-time adaptation. The approach presented here deals with these issues, but extends support for run-time adaptation including a system of warnings and notifications.

The paper presents a SLA management architecture for automated SLA negotiation, monitoring and policing mechanisms. The SLA Manager negotiates a SLA for the rights to execute a Grid application service using an external resource broker. Once an agreement exists, management of the SLA involves monitoring, which is achieved using performance measurement data obtained from a set of Grid monitoring tools. Policing is performed using violation data obtained through

[*] School of Computing, University of Leeds, *{jamesp, karim, dew}@comp.leeds.ac.uk*

automated monitoring of the SLA against real-time performance measurement data. Run-time adaptation is supported thanks to SLA policing mechanisms to enforce changes to the execution to meet SLA guarantees.

The aims of this paper are: firstly, to present a Grid SLA management architecture. Secondly, taking an SLA for a compute service as a motivation, discuss how a prediction model and rule based controller combine to provide predictive run-time adaptation for an application service. With this in mind, experiments are designed to test the performance of the prediction model and the rule based adaptation mechanism when the application service is executing on a large distributed Grid infrastructure, the White Rose Grid (WRG), which consists of high performance computing resources at Leeds, Sheffield and York Universities [29]. An infrastructure such as the WRG exhibits heterogeneous resources and spans multiple administrative domains.

SLA Architecture

The SLA Manager provides SLA and resource management support to virtual organisations such as the Distributed Aircraft Maintenance Environment (DAME) Diagnostic Portal [2]. In this example the SLA Manager is supporting a Grid based decision support system where timely and reliable service provision is a requirement. The user gains access to application services with the option of attaching time / performance constraints. The architecture is illustrated in Figure 1 and highlights component responsibilities.

Instantiation and Modification

The SLA Factory provides a template for SLA specification based on user identification of relevant time or performance constraints. Additionally, the factory records provenance data within the SLA Instance during the policing phase. This provides a record of warnings and violations important for auditing after the agreement has terminated. Warnings are recorded when significant events are detected which may affect the SLA in the future but no actual violation has occurred. Violations are recorded when actual breaches in time or performance constraints have occured.

Negotiation and Reservation

In order to fulfil a time or performance constraint the SLA Manager is able to negotiate for resources using a Resource Broker which has responsibility for placing reservations with a resource provider. The architecture allows for a community of brokers providing reservations for resources of different types, e.g. compute, storage and even bandwidth. The example used in this research is a SNAP-based resource broker [10], which provides reservations for compute resources. During the negotiation phase the user specifies a Task Service Level Agreement (TSLA), representing an agreement specification for a desired level of performance or time constraint for the Grid application service. Negotiation follows a *request() / agree()* protocol similar to that specified within the SNAP framework [6]. The SLA Manager enters into an agreement with the Resource Broker which provides a reservation guarantee, a Resource Service Level Agreement (RSLA), with the resource provider. Together the TSLA and RSLA form a Binding Service Level Agreement (BSLA) which binds the task to the potential resource capabilities promised in the RSLA.

Monitoring

To demonstrate the concept of automated monitoring of a Grid infrastructure - the Globus Monitoring and Discovery System (MDS) is used. The SLA engine matches SLO's to relevant Grid monitoring tools so that validation can be made against performance measurement data.

Alternatively, any Grid Monitoring Service [5] which provides resource and service information using local Grid Monitoring Tools [3] such as Net Logger [9] and the Network Weather Service [28] can be used. The use of a Grid Monitoring Tool (GMT) compliant with the Grid Monitoring Architecture (GMA) [25] would allow a publish / subscribe mechanism to query resource information. Tools such as these enable the SLA Engine to automatically monitor the time and/or performance contraints based on dynamic resource and process information.

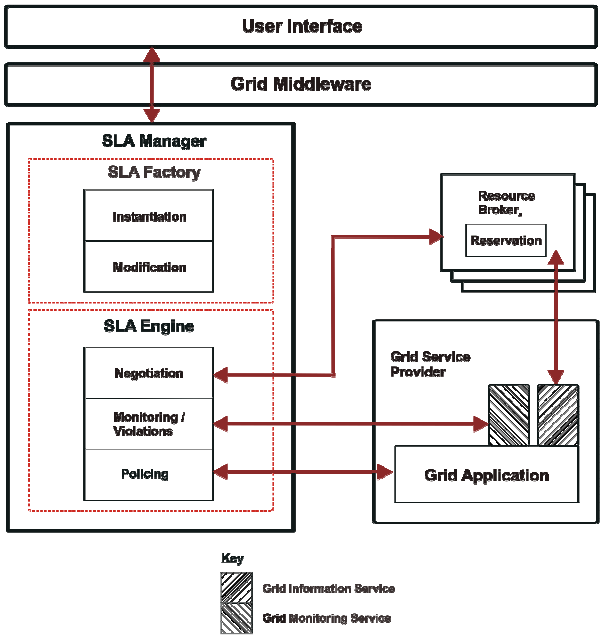

Fig. 1. SLA Management Architecture

Violations

A Grid infrastructure integrates heterogeneous resources with varying quality and availability which places importance on the ability to dynamically monitor the state of these resources and deploy reliable violation capture mechanisms. A record of warnings and violations is important for auditing once the agreement is in place. Warnings are recorded when significant events are detected which may affect the SLA in the future but no actual violation has occurred. Violations are recorded when it is beyond doubt that breaches in time or performance constraints have occurred.

Policing

The SLA Engine implements a predictive rule based decision maker. Rule based control strategy offers effective control where the control action does not have a continuous domain and where the controlling entity. In this case the SLA manager

does not have authoritative control over all applications submitted to the Grid infrastructure. In the first case the ability to effect the CPU processing potential is implemented either by migration onto a faster machine or one offering a load average which is less than that of the current resource. The adaptive process involves a prediction model, a rule based decision maker and a grid monitoring service. The decision maker takes input from two sources, the constraints stated in the SLA and the predicted remaining execution time generated by the predictive model.

Adaptation has the potential to significantly improve the performance and timely behaviour of an application bound with SLAs. Such an application can change its behaviour depending on available resources, optimising itself to its environment.

Prediction Model

The prediction model assumes the user has a reasonable approximation of the application execution time prior to submission. With this assumption the model provides a run-time assessment of the remaining execution time based on the CPU load immediately prior to and during application run-time. Assessments are made as to whether the application will complete within a specified time through comparison with the scheduled remaining execution time, which is agreed upon in the SLA during negotiation. Even when no approximation can be made, monitoring techniques can determine with some accuracy that the execution will take significantly longer than anticipated. In this situation the SLO cannot be expressed as a time constraint and another metric should be chosen. A good choice is a request to maintain a specified percentage of mean CPU usage for the application during run-time.

The fractional CPU usage F_i is measured over n samples at time T_i. $T_{100\%}$ is the time the task would take to execute if 100% CPU usage was maintained throughout application run-time. $F_{estimate}$ is the mean CPU usage over n samples.

$$T_{remaining} = \frac{T_{100\%} - \sum_{i=1}^{n-1} \Delta T_i F_i}{F_{estimate}} \quad \textbf{(1)}$$

$$F_{estimate} = \overline{F}_n = \frac{1}{n} \sum_{i=1}^{n} F_i \quad \textbf{(2)}$$

$T_{remaining}$ **(1)** is the predicted remaining execution time if $F_{estimate}$ **(2)** is maintained for the remainder of the execution. If F_i drops for a large proportion of this period the prediction will be invalid, subsequently, a new prediction is needed.

Experiments and Performance Results

Experiments are designed to test the policing phase of an application execution which operates in collaboration with the monitoring phase but after instantiation and negotiation is complete. Negotiation and monitoring have been the subject of previous study in [20] and [19]. When an SLA bound application is executing and a competing

appilication is submitted, the resource may no longer be able to meet its RSLA and subseqently the time or performance constraint in the TSLA may be violated.

Experiments are conducted on a large distributed Grid infrastructure; the WRG [29]. Once a SLA has been specified, the objective is to test the ability of the prediction model to generate reliable performance predictions for the remaining application execution time. The scenario uses a Grid application service used within the DAME project [2].

The prediction model assumes that the user knows *a priori* how long the application will take at 100% CPU usage. With this in mind the application service is executed at 100% CPU usage to determine a reference execution time. Once this is known the application service is executed from start to finish. During the course of the execution the predicted remaining execution time is generated periodically using the prediction model and is compared with the reference remaining execution time. This experiment is used to determine the accuracy of the RTP formula **(1)**.

Prior to the experiment the application was run and took 1800 secs to complete with a mean CPU usage of 98%, resulting in a value of 1764 secs for $T_{100\%}$. As a result T_{sla} was set at a reasonable 2100 secs.

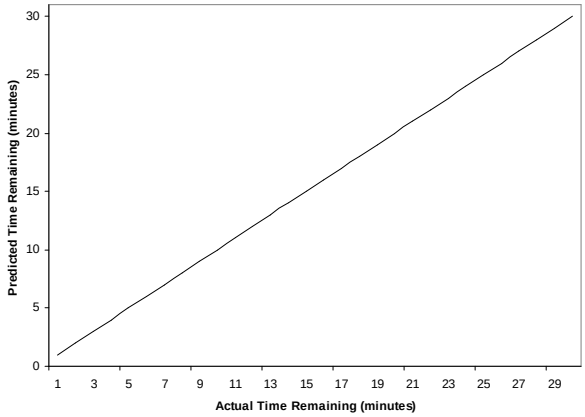

Fig. 2. Predicted time remaining vs. actual time remaining

The results in Figure 2 show the prediction model provides a good match with the reference remaining execution time suggesting that the model is accurate and can be used for the remaining experiments.

Following this, additional applications are submitted to the same resource to disrupt the SLA bound application. This creates a violation in the time constraint T_{sla} and initiates control actions as defined in the rule base. This is compared to the case where no adaptive technique is used. It is used to determine the effectiveness of the rule-based decision maker in ensuring timely application completion.

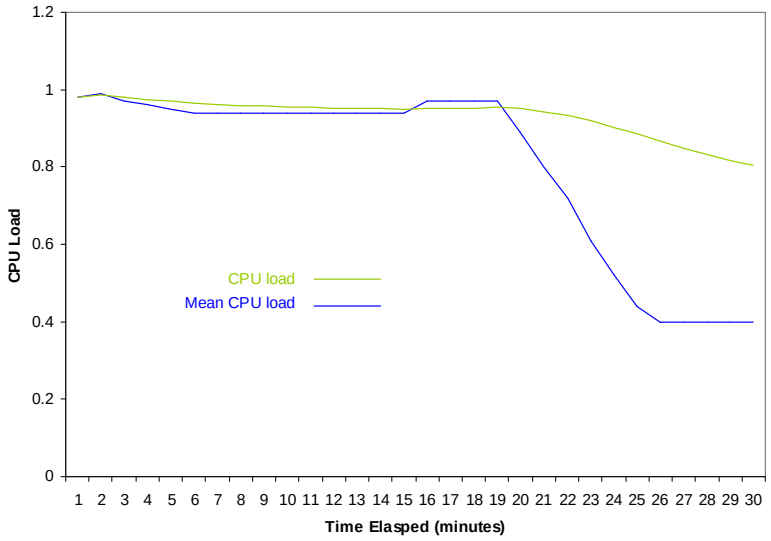

Fig. 3. CPU Load vs. Time – Disturbance added late in execution schedule

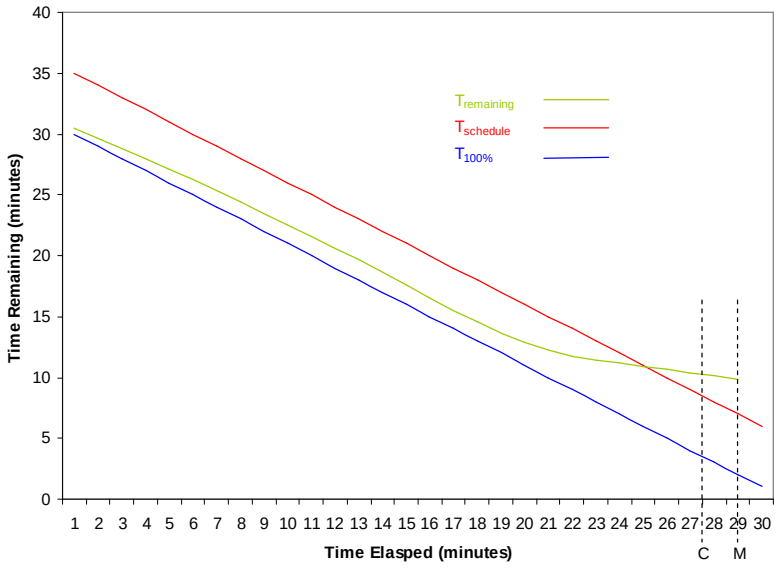

Fig. 4. Time remaining vs. Time elapsed – Disturbance added late in execution schedule

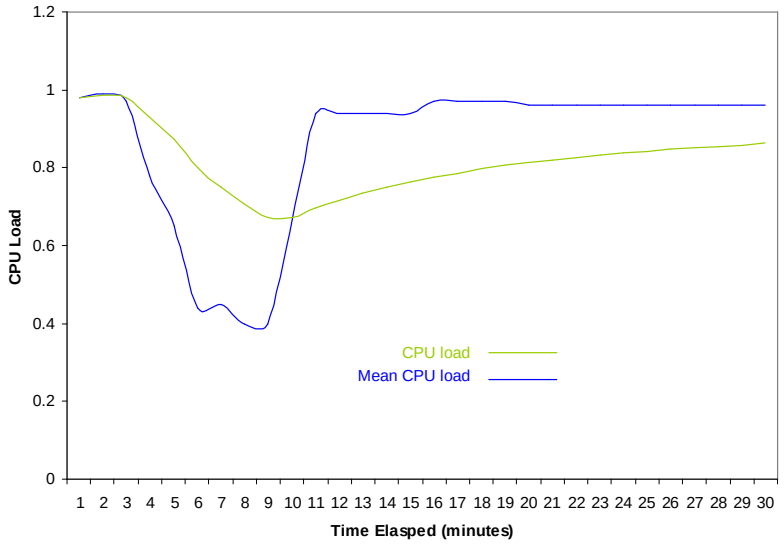

Fig. 5. CPU Load vs. Time – Disturbance added early in execution schedule

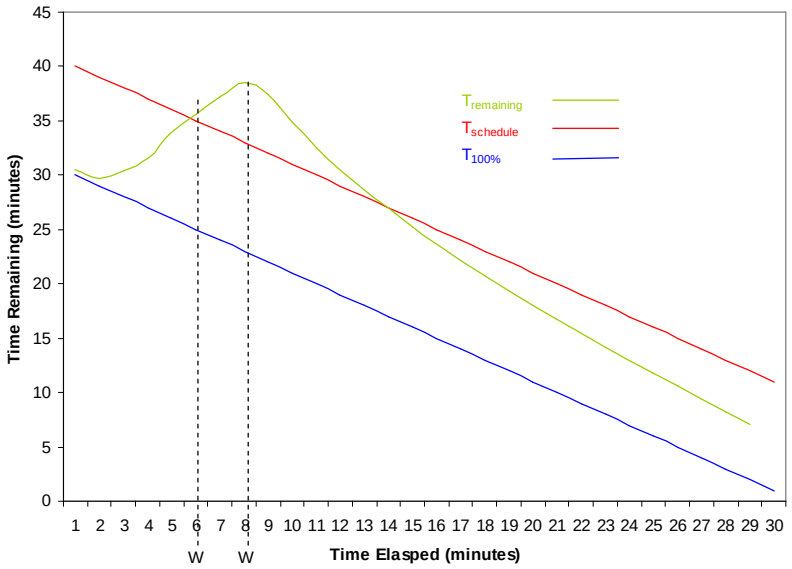

Fig. 6. Time remaining vs. Time elapsed – Disturbance added early in execution schedule

The effect of submitting an additional application late in the execution can be seen in Figure 3. After approximately 20 minutes the CPU load decreases producing a knock on effect in the mean CPU load. This is reflected in Figure 4, which shows the rate of change of $T_{remaining}$ decreasing. At approximately 25 minutes $T_{remaining}$ exceeds

$T_{schedule}$ and the decision maker sends a checkpoint and migration signal (marked C and M on Figure 4). Consequently, it can be speculated that the predictive adaptation results in a shorter application execution time compared to the case when no adaptation is used.

The effect of submitting an additional application early in the execution can be seen in Figure 5. After approximately 3 minutes the CPU load decreases, however, the effect on the mean CPU is greater at this stage in the execution. This is reflected in Figure 6 which shows a rapid increase in $T_{remaining}$. After approximately 6 minutes $T_{remaining}$ exceeds $T_{schedule}$ and the decision maker sends a warning signal (marked W on Figure 6). As a result a warning message is added to the SLA Instance. Further into the execution $T_{remaining}$ drops below $T_{schedule}$ and the the application completes within the time specified within the SLA.

Related Work

There have been a number of attempts at defining SLA's and a management architecture for both Web and Grid services. Architectures from Sahai et al [21], Leff et al [12] and Verma et al [27] concentrate on service level agreements within commercial Grids. The service level agreement language used is that presented by Ludwig et al [14]. The Global Grid Forum have defined WS-Agreement [1]; an agreement-based Grid service management specification designed to support Grid service management. Two other important works are automated SLA monitoring for Web services [11] and analysis of service level agreements for Web services [22]. Contract negotiation within distributed systems have been the subject of research where business-to-business (B2B) service guarantees are needed [8]. The mapping of natural language contracts into models suitable for contract automation [16] exist but has not been applied to a Grid environment, neither has it been applied as a SLA. An approach for formally modelling e-Contracts [15] exists at a higher level than the research by Ludwig et al [14]. Automated negotiation and authorisation systems for the Grid already exist [13] but involve no monitoring or run-time adaptation.

In [24] methods are discussed for predicting execution run-time for parallel applications using historical information. Execution times of similar applications run in the past, are used to estimate the execution time. Application of this method to executions run on a Grid using a local batch queuing system are considered in [23]. This work considers the prediction of execution start times for pending jobs in order to decrease the average job wait time. Although their results indicate that the approach is succesful at reducing the average wait time it does not provide information as to the anticipated execution time of the user's job.

An approach to migration of Grid applications using performance prediction is presented in [26]. Migration decisions are based on resource load, potential performance benefits and the time reached in the application. This technique is limited to MPI based programs but makes use of user specified execution times and tolerance thresholds.

A performance prediction based tool, known as PACE (Performance Analysis and Characterisation Environment) [17] has been developed at the University of Warwick. It uses a combination of source code analysis and hardware modelling to provide an application performance prediction. In [18], the use of PACE in the context of Grid resource scheduling is discussed. The hardware models used in this research are static, which provides the advantage of reusability but does not account for dynamic changes to resource performance.

Conclusions and Future Work

Performance prediction of execution run-times is a key component when delivering timely application services in decision support systems. The provision of a system of SLA's and components to manage tasks such as negotiation, monitoring and policing are needed to help meet these requirements. Making simplifying assumptions regarding the task requirements, this work considers a SLA Management architecture focussing on a method of execution run-time prediction.

Experiments were conducted in a Grid environment, the White Rose Grid [29]. Submitting an additional application on the candidate resource decreases the capability of the resource to satisfy the RSLA and starves the SLA bound application of processing power. The estimates produced by the prediction model show an increase in the remaining execution time. The rule based controller generates a series of warning messages which are recorded by the SLA Factory in the SLA. A violation is recorded resulting in a request to checkpoint and migrate the application service. Where no adaptive technique is used the application execution continues to violate its SLA and fails to deliver on its time constraint.

Future work will centre on a learning based technique to provide an initial prediction for $T_{100\%}$. It will use historical information based on execution run-times from previous runs of the same application service. Users will submit input parameters describing items such as dataset size and run-time flags in order to generate an initial prediction. Additional work comparing application and user level checkpointing will provide a deeper integration of SLA Manager and SLA bound application service.

Acknowledgements

The work reported in this paper was partly supported by the DAME project under UK Engineering and Physical Sciences Research Council Grant GR/R67668/01. We are also grateful for the support of the DAME partners, including the help of staff at Rolls-Royce, Data Systems & Solutions, Cybula, and the Universities of York, Sheffield and Oxford.

References

[1] Andrieux, A., K. Czajkowski, A. Dan, K. Keahey, H. Ludwig, J. Pruyne, J. Rofrano, S. Tuecke, and M. Xu, *Web Services Agreement Specification (WS-Agreement)*. 2004, Global Grid Forum.

[2] Austin, J., T. Jackson, M. Fletcher, M. Jessop, P. Cowley, and P. Lobner, *Predictive Maintenance: Distributed Aircraft Engine Diagnostics*, in *The Grid 2: Blueprint for a new computing infrastructure*, I. Foster and C. Kesselman, Editors. 2004, Morgan Kaufmann: Elsevier Science: Amsterdam; Oxford.

[3] Balaton, Z., P. Kacsuk, N. Podhorszki, and F. Vajda, *Comparison of Representative Grid Monitoring Tools*. 2000, Laboratory of Parallel and Distributed Systems, Hungarian Academy of Sciences, Budapest, Hungary.

[4] Berman, F., *Grid computing: making the global infrastructure a reality*. 2003, Chichester: Wiley.

[5] Czajkowski, K., S. Fitzgerald, I. Foster, and C. Kesselman. *Grid Information Services for Distributed Resource Sharing.* in *High performance distributed computing*. 2001. San Francisco, CA: IEEE Computer Society Press.

[6] Czajkowski, K., I. Foster, C. Kesselman, V. Sander, and S. Tuecke. *SNAP: A Protocol for Negotiating Service Level Agreements and Coordinating Resource Management in Distributed Systems.* in *Job scheduling strategies for parallel processing*. 2002. Edinburgh: Berlin.

[7] Foster, I., *The Anatomy of the Grid: Enabling Scalable Virtual Organizations.* Lecture Notes in Computer Science, 2001(2150): p. 1-4.

[8] Goodchild, A., C. Herring, and Z. Milodevic, *Business contracts for B2B*. 2000, Distributed Systems Technology Center (DSTC), Austrailia: Queensland, Austrailia.

[9] Gunter, D., B. Tierney, B. Crowley, M. Holding, and J. Lee. *NetLogger: A Toolkit for Distributed System Performance Analysis*. in *Modeling, analysis and simulation of computer and telecommunication systems.* 2000. San Francisco, CA: IEEE Computer Society.

[10] Haji, M., I. Gourlay, K. Djemame, and P. Dew, *A SNAP-based Community Resource Broker using a Three-Phase Commit Protocol: a Performance Study.* Computer Journal, 2005. **48**(3): p. 333-346.

[11] Jin, L., V. Machiraju, and A. Sahai, *Analysis on Service Level Agreement of Web Services*. 2002, HP Laboratories: Palo-Alto, CA.

[12] Leff, A., J.T. Rayfield, and D.M. Dias, *Service-Level Agreements and Commercial Grids.* Ieee Internet Computing, 2003. **7**(4): p. 44-50.

[13] Lock, R. *Automated contract negotiations for the grid*. in *Postgraduate Research Conference in Electronics, Photonics, Communications & Networks, and Computing Science*. 2004. University of Hertfordshire, UK: EPSRC.

[14] Ludwig, H., A. Keller, A. Dan, R. King, and R. Franck, *A Service Level Agreement Language for Dynamic Electronic Services.* Electronic Commerce Research, 2003. **3**(1/2): p. 43-59.

[15] Marjanovic, O. and Z. Milosevic. *Towards Formal Modeling of e-Contracts*. in *Enterprise distributed object computing*. 2001. Seattle, WA: IEEE Computer Society.

[16] Milosevic, Z. and R.G. Dromey. *On Expressing and Monitoring Behaviour in Contracts*. in *Enterprise distributed object computing*. 2002. Lausanne, Switzerland: IEEE Computer Society.

[17] Nudd, G.R., C. Junwei, D.J. Kerbyson, and E. Papaefstathiou. *Performance modeling of parallel and distributed computing using PACE*. in *19th IEEE International performance, computing and communications conference*. 2000. Phoenix, USA: IEEE Computer Society.

[18] Nudd, G.R., H.N.L.C. Keung, J.R.D. Dyson, and S.A. Jarvis. *Self-adaptive and self-optimising resource monitoring for dynamic grid environments*. in *15th International workshop on database and expert systems applications*. 2004. Zaragoza, Spain: Institut Für Anwendungsorientierte Wissensverarbeitung.

[19] Padgett, J., K. Djemame, and P. Dew, *Grid-based SLA Management*. Lecture Notes in Computer Science, 2005(3483): p. 1282-1291.

[20] Padgett, J., M. Haji, and K. Djemame, *SLA Management in a Service Oriented Architecture.* Lecture Notes in Computer Science, 2005(3470): p. 1076-1085.

[21] Sahai, A., A. Graupner, V. Machiraju, and A. van Moorsel. *Specifying and Monitoring Guarentees in Commercial Grids through SLA.* in *3rd IEEE/ACM International Symposium on Cluster Computing and the Grid.* 2003. Tokyo: IEEE Computer Society.

[22] Sahai, A., V. Machiraju, M. Sayal, L. Jin, and F. Casati, *Automated SLA Monitoring for Web Services*. 2002, HP Laboratories: Palo-Alto, CA.

[23] Smith, W., *Improving Resource Selection and Scheduling using Predictions*, in *Grid Resource Management: State of the Art and Future Trends*, J. Nabrzyski, J.M. Schopf, and J. Weglarz, Editors. 2003, Kluwer Academic Publishers.

[24] Smith, W., I. Foster, and V. Taylor, *Predicting Application Run Times Using Historical Information.* Lecture Notes in Computer Science, 1998(1459): p. 122-142.

[25] Tierney, B., R. Aydt, D. Gunter, W. Smith, M. Swany, V. Taylor, and R. Wolski, *A Grid Monitoring Architecture*. 2002, Global Grid Forum.

[26] Vadhiyar, S. and J. Dongarra. *A Performance Oriented Migration Framework for The Grid*. in *Cluster computing and the grid; CCGrid 2003*. 2003. Tokyo: IEEE Computer Society.

[27] Verma, D., M. Beigi, and R. Jennings, *Policy Based SLA Management in Enterprise Networks*, in *Policies for Distributed Systems and Networks*, M. Sloman, J. Lobo, and E.C. Lupu, Editors. 2001, Springer-Verlag. p. 137-152.

[28] Wolski, R., N.T. Spring, and J. Hayes, *The network weather service: a distributed resource performance forecasting service for metacomputing.* Future Generations Computer Systems, 1999. **15**(5-6): p. 757-768.

[29] WRG, *The White Rose Grid*, White Rose Consortium: http://www.wrgrid.org.uk/.

Performance Aspects in Web Service-based Integration Solutions

Andreas Schmietendorf [*+], Reiner R. Dumke [+], Stanimir Stojanov [#]

Abstract

In this contribution, we present the idea of an independent measurement service. We look at the developed concept and an initial prototype implementation. The measurement service can be used to assess the quality of Web services that are available on the Internet, with the aspects of performance and availability being specifically addressed. This can be used as a basis for certifying Web services and effectively supporting the selection process during the implementation of Web service-based integration solutions. Moreover, it is intended to make the measurement service itself available as a Web service in future, thus also enabling a dynamic selection of service offerings to be supported, taking qualitative aspects into account.

1 Introduction

Web services are attractive for industrial software development, and play an important role in the field of EAI solutions and the current challenge of establishing service-oriented architectures. However, they will only be suitable for commercial applications if non-functional as well as functional requirements are met. In order to achieve this goal, appropriate specifications and technologies will have to be developed which take account of the general quality of service. The references ([5], and [9]) cite the following aspects in relation to the general quality of service: accuracy, availability, accessibility, capacity, exception handling, integrity, interoperability, performance, reliability, regulatory, robustness, scalability, and security.

Web service technology is currently being used primarily within application development as a replacement for tried-and-tested middleware technology such as CORBA. This is advantageous particularly with regard to the independence of technology that can be achieved, meaning that a combination of SUN's J2EE technology and Microsoft's .net technology can be used for application development, for example. Web services are network-based applications that use the WSDL protocol (Web Service Description Language) to describe the functions they offer on the Internet, XML documents (eXtensible Markup Language) to exchange information, and the SOAP protocol (Simple Object Access Protocol) for calling remote methods and transferring data. The data and function calls that are packaged into XML documents are typically transferred using the http protocol, which means communication can also take place across firewalls. It is this property in particular

[*] T-Systems International GmbH, Wittestraße 30H, 13509 Berlin, Germany, *andreas.schmietendorf@t-systems.com*

[+] University of Magdeburg, Universitätsplatz 5, 39106 Magdeburg, Germany, *schmiete|dumke@ivs.cs.uni-magdeburg.de*

[#] Paisii-Hilendarski-University of Plovdiv, 4000 Plovdiv, 236 Bulgaria blv, Bulgaria, *csstani@pu.acad.bg*

that opens up the possibility of developing genuine B2B (Business to Business) applications. UDDI directory services (Universal Description, Discovery, and Integration) are used to localize the Web services that are provided on the Internet. Central UDDI directories are operated by IBM and Microsoft, for example. Even though the number of Web services available on the Internet is continuously increasing, they are used primarily in a semi-professional context. Moreover, Web services that make their functionality available via a defined interface are not really suitable for integrators who are dealing with many unknown factors. Such Web services can be directly compared to components, which is why the following statement by Ivar Jacobsen is directly applicable:

> ”If the components come with a bad reputation, no one will use them. Therefore, components must be of an extraordinary quality. They need to be well tested, efficient, and well documented. ... The component should invite reuse.” (Ivar Jacobson in [18])

It is particularly the non-functional properties that often remain concealed from the user. In this article, we want to present the idea of an independently functioning measurement service that is able to record the qualitative properties of Web services and make these available to potentially interested parties. We will be looking in particular at the aspects of performance, availability, and accessibility.

2 Current situation and existing studies

The current specifications (e.g. SOAP, WSDL, and UDDI) in Web service technology only support the description of qualitative aspects to a very limited extent. Correspondingly, most Web service offerings provide no indication of qualitative behavior. In this context, [13] and [17] quite rightly stress that using this type of Web service is associated with a wide variety of risks. Typical risks involve a lack of information regarding the availability, performance, and security or trustworthiness of the Web service offerings. We shall now briefly examine studies that are devoted to this subject and that comprehensively characterize the current situation:

- [1] discusses the static and dynamic properties that should be specified in a Web service description.
- [7] suggests using a specific framework for the use of quality-assured components. These components possess the ability to communicate to other components the qualitative properties of functions on offer, and carry out appropriate negotiations.
- [2] proposes a metaview of Web systems and their components, through the use of what is called a Web tomography. Performance properties are assessed on the basis of properties determined by Web tomographies.
- [10] proposes an automated and distributed SLA monitoring engine. This engine allows measurements at multiple sites and considers SLAs on Web service-based infrastructures.
- As described by [4], the WSLA framework forms part of the IBM Web Service Toolkit. This framework, which is currently available as a prototype, contains not only an XML schema definition for describing SLAs, but also a run-time environment for SLA management.

- The paper by [15] examines various ways of assuring the quality of Web services, and proposes a general quality model for the Web service access layer. A very comprehensive model is proposed for this purpose. However, it has to be adapted in order to carry out specific tasks, and therefore remains very generalized.
- Existing studies that look at the internal details of Web service technology can be found in [12], for example. This article relates to a specific performance test of the Apache Axis Web service environment. It compares the performance behavior of different access mechanisms (RPC vs. DOC-orientated method of work) on a Web service, with the DOC-oriented method of work being identified as clearly the better of the two.

In summary, the following subjects can be identified in the currently available studies with regard to quality issues and, more specifically, performance issues:

- The use of mathematical models to predict selected aspects of performance
- The management of Web service-based infrastructures
- Proposals for enhancing current Web service specifications
- Case studies/measurements of specific technologies and products
- The specification of performance characteristics via the use of ontologies.

Up to now, research has primarily focused on the question of specifying quality requirements and quality offerings. It has therefore clarified "what" needs to be taken into account with regard to the quality aspects of Web service-based integration solutions. However, it has not clarified "how" these quality characteristics can be determined.

3 The aims and design of a measurement service

3.1 Objectives

An appropriate measurement service should permit the qualitative properties of Web services provided on the Internet to be analyzed over a definable period of time, and should support any certification that may be required. The following points illustrate the objectives and anticipated advantages of implementing an independent measurement service:

- The provision of additional information regarding the qualitative behavior of Web service offerings, which can be used as selection criteria either statically or dynamically (i.e. when the application is running).
- A measurement service should enable the qualitative behavior of a selected Web service to be explicitly tested before it is actually integrated into the application, by
    - carrying out realistic testing using a load driver
    - creating force.asting models based on existing measurements.
- The results can be used as the basis for agreeing SLAs (Service Level Agreements), or alternatively, the measurement service can be used to verify the quality achieved and support an existing Service Level Agreement.

- Results as input quantities for the settlement process
- Basis for fail-over configurations.

- The measurement service can provide the basis for automating empirical investigations into available Web services.
- The measurement service should allow different communication mechanisms to be used to support the process of obtaining measurement results. We currently envisage the following approaches in order to achieve this:
  - Request model – measurements are carried out over the network, and in this context, we could also refer to this as polling
  - Event model – measurements are carried out using special measuring agents at the Web service end.

3.2 Measurement aspects of a Web service

The first thing to be clarified is the type of measurements that are of interest in the context of the Web services available on the Internet. Since the user does not have access to the source code, and the Web service will not be executed on the user's own hardware and software infrastructure, the interface description should include details of both functional and non-functional properties. Measurements of functional properties could, for instance, include metrics relating to the service interface and could therefore record granularity, but we are not examining this aspect any further in the present article. (See also [11].) In the context of non-functional properties, it is mostly the availability, performance, conformity to standards, and potential security aspects that are of interest.

- The *availability* relates to a Web service that is ready for operation, and whose functions can be called via the network. The availability is usually stated as a percentage, with availability rates also being frequently mentioned.

  Availability P and Time to Repair (TTR) of a specific Web service endpoint:

  $P_{availability} = C(X)/N$

  C(X) - Number of successful function calls

  N - Number of function calls

  $TTR = t_{restart}(X) - t_{failed}(X)$

  t_{failed} – Time at which service X failed

  $t_{restart}$ – Time at which the service was available again.

  An additional factor relating to availability involves the compatibility and stability of the interface description or the syntax and semantics of the functions provided.

  - Downwards compatibility – applications can use older versions of a Web service without modifications.
  - Upwards compatibility – applications can use new versions of a Web service without modifications.

The stability of the Web service interface can be measured by using peripheral variables (e.g. LoC) or by creating checksums.

- The *performance* of a Web service from a black box point of view can be recorded along the lines of [3] by using the throughput and response times. In addition, the network and processing times of any intermediaries should be considered. Internal metrics should be deliberately disregarded here.

  The response time (latency) of specific Web service operations:

  $t_{latency} = t_{o/p}(X) - t_{i/p}(X)$

  $t_{i/p}(X)$ – Time at which service X was called

  $t_{o/p}(X)$ – Time at which the reply to the call was available

  The throughput of specific Web service operations:

  $t_{throughput}$ = Number of service calls in time interval T

- The *conformity to standards* relates to the observance of recommendations and standards adopted within the Web service community (e.g. SOAP, UDDI, WSDL etc.). Only when these are observed can the technology-independent interoperability of Web services be truly guaranteed.

- *Security aspects* play an important role, particularly in the context of communication via the Internet, which is open to all. These aspects relate to authentication, the encryption of messages transmitted, and the access control or logging of operations that are carried out.

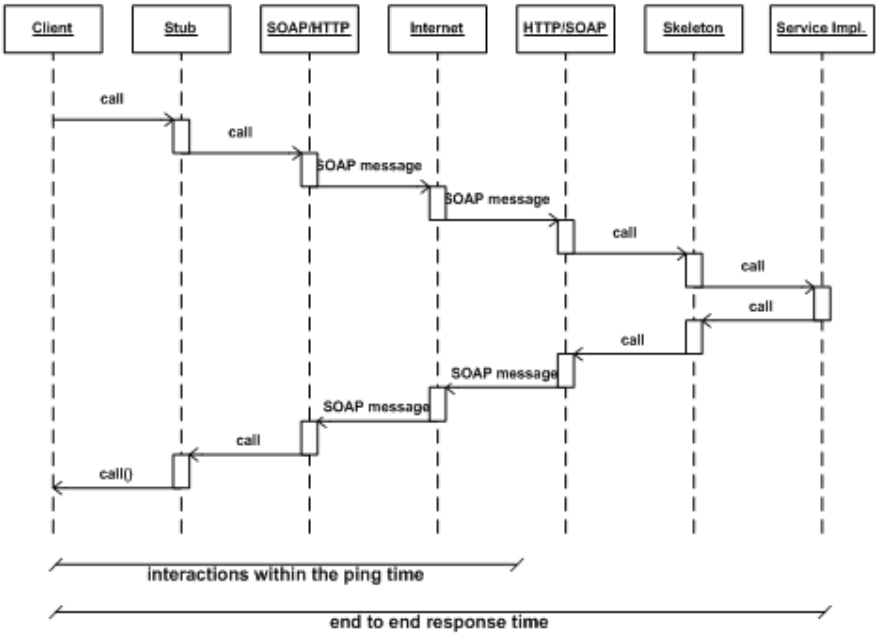

Figure 1: Interaction chain of a Web service call

Measuring response times on the client (*request model*) necessarily involves the entire interaction chain. This includes calling and setting up the SOAP message (generating

an XML file), transmitting the message over a suitable network (usually http in the case of Web services), and parsing the SOAP message at the Web service end. It also includes the actual execution time for the functions at the Web service end, and the generation, transmission, and relevant processing of the reply message. In order to eliminate the network runtimes in the request model, it is advisable to use a simple "ping" directly before the actual measurement, and subtract the ping time from the result of the actual measurement. Measuring response times at the Web service end (*event model*) requires a suitable measuring agent within the Web service runtime environment. The advantage of this type of model is that it eliminates the influence of the network. Comprehensive descriptions of factors influencing the performance of Web services can be found in [16], [6], and [14].

3.3 Designing a measurement service

The measurement service design described below primarily enables conclusions to be drawn regarding the performance, availability, and stability of a measured Web service. Based on the measurements carried out, potential interested parties can draw conclusions regarding the qualitative properties that can be expected from a Web service.

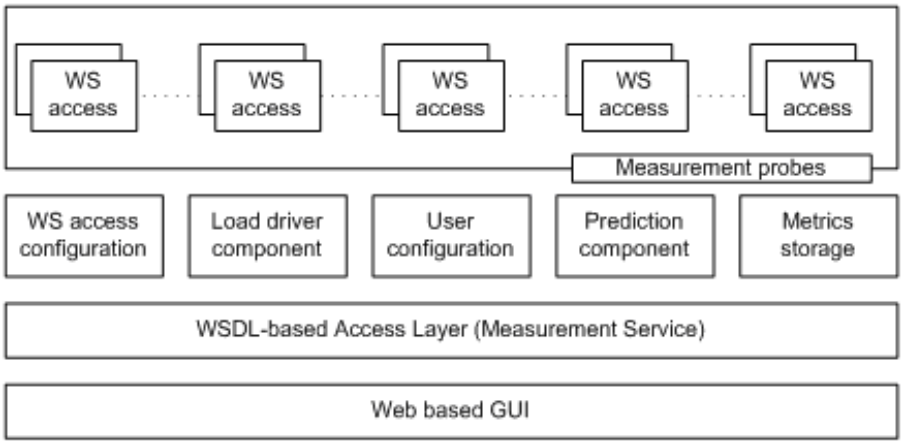

Figure 2: The architecture of the measurement service

The Web service access components carry out the actual measurement (i.e. they call the relevant methods) of a Web service. It is possible for several instances to be active simultaneously. The stability of the Web service interface is also determined at regular intervals, with an appropriate checksum of the WSDL description being calculated for this purpose. The measurement service functions can be accessed both via a graphical user interface (Web-based GUI) and a WSDL interface. This enables the measurement service to offer its own services as a Web service on the Internet, or incorporate its functions into complex, higher-level tasks. The other components that are available are described briefly below.

Configuration of the Web Service access – Configures the basic method of accessing the Web service that needs measuring.

- Selecting the methods to be measured
- Using the relevant parameters
- Determining simple measurement intervals

- Dealing with error conditions.

Load driver component – Enables an appropriate load mix to be configured, so that several Web service functions can be executed virtually simultaneously.

- Defining the behavior of method calls in relation to each other
- Defining target response times
- Substituting data to be transmitted.

User configuration & access – Assigns roles and access rights for measurement service users. Read access and also the right to measure new Web services can be assigned.

- Assigning read access to all visitors of the measurement service
- Assigning read and write access to administered users.

Prediction component – Provides a calculation procedure for predicting the performance of a Web service under a given load profile.

- Configuring the anticipated load profile
- Using a solution method based on the operational analysis.

Metrics storage & export component – Stores measurements and converts them to an appropriate format for transmission (e.g. XML).

- Storing measurements in a local database
- Preparing measurements for further processing.

There are many factors that influence the performance of Web services (particularly the associated network runtimes). As mentioned above, our current plan for isolating network runtimes involves transmitting a simple PING to the server on which the Web service runs directly before the actual measurement, and subtracting this PING time t_{ping} from the overall runtime t_{RTT} ("round trip time" of a SOAP-RPC) when measuring the Web service functions. Although measurement errors cannot be entirely eliminated in this way, we feel they can be significantly reduced. So the actual response time t_a (excluding network time) for a Web service is made up as follows: $t_a = t_{RTT} - t_{ping}$

4 A prototype measurement service

An initial prototype measurement service is currently being implemented at the software measurement laboratory of the Otto von Guericke University in Magdeburg, in collaboration with T-Systems International (Berlin Development Center). The current version allows you to measure any Web service that is available on the Internet.

Figure 3: Measurement service user interface (main window)

4.1 Configuring a Web site prior to measurement

Figure 3 shows the graphical interface of the measurement service, with several Web services that are in the process of being measured. The average call time of selected Web service operations and the "ping time" can be clearly seen. There are also various additional graphical analyses available, which display the performance profile of an appropriate time interval, for example.

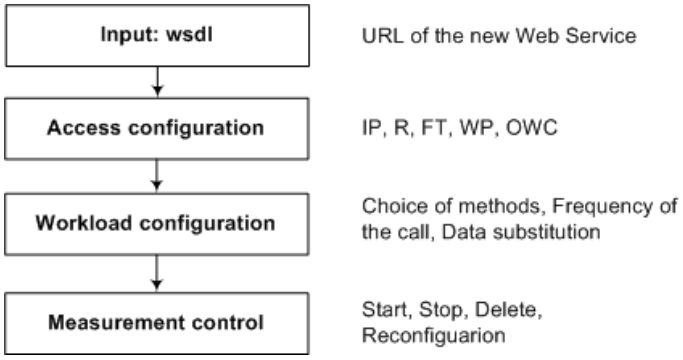

Figure 4: Administrative sequence for measurements

To prevent the measurement service from being misused, new Web services requiring measurement can only be included by users who have administration rights. In order to register a Web service for measurement on the measurement service, the URL of its WSDL document must be specified on the main page, and confirmed with "accept". The WSDL document is then downloaded and used to dynamically generate the relevant files for accessing the Web service. If no error occurs during this process, the user is given a dialog containing the basic configuration options for the actual measurement process (see Figure 4). This is where you select the methods you want to measure (the current version can only measure a single method), specify the data substitution, state how system failures are to be interpreted, and define the following parameters.

R - Batch length (number of repeat invocations)

In order to reduce measurement errors, it makes sense to execute the method call several times. Parameter R can be used to specify the number of successive repetitions of an operation call within a series. The result of a measurement is calculated as the average of the individual measurements within a series.

IP - Invocation period of a SOAP operation

This parameter is used to configure the call interval for the selected methods of the Web service. The time period between each series of measurements is specified in minutes.

FT - Failure tolerance

Permitted number of successive failed measurement series. A series is considered to have failed if at least one measurement (ping or operation call) in this series has failed. This parameter is useful because some Web services are occasionally temporarily unavailable.

WP - Period of checking for stability of WSDL description

Interval for checking the WSDL document for stability (potential changes), in minutes. The check involves the WSDL file being repeatedly read over the Internet, a checksum being calculated based on the Adler32 algorithm, and this checksum being compared with the previous checksum.

OWC - Be optimistic if the WSDL description changes

If the WSDL document has been changed, the parameters selected during the previous configuration or reconfiguration (i.e. service, port, and SOAP operation) may no longer be valid. The program can react to this either optimistically or pessimistically. In the former case, it will attempt to call the operation again in the next series as if nothing had happened; in the latter case, the measurement process is suspended and a reconfiguration of the Web service unit is requested.

Measurement parameters for Web services that are already being measured can only be configured if the measurements are stopped. The overview of measured Web services displays the following measurement parameters: "R=..., IP=..., WP=..., FT=..., OWC=...".

4.2 Internal states of the measurement service

Various items of status information are used to display how the measurement service is getting on with the registered Web services. These different states are necessary in order to react to changes to the Web service, and to permit the self-monitoring of the measurement service.

- *Not configured* – A Web service requiring measurement has either not been configured at all, or the configuration has been aborted or has failed.
- *Ready to start* – A Web service has been configured, but the measurement process has either not commenced, or has been suspended. The measurement will be automatically restarted following successful reconfiguration provided the "auto_start" parameter in the configuration file is set to "true".

- *Waiting for data* – The Web service measurement has commenced, but no measurement results are available yet.
- *O.K.* – The measurement has commenced, and results are available. In this case, the average ping and call times will also be shown in the table.
- *Temporarily not available* – An error has occurred during the measuring of a Web service, but the count of successive errors is smaller than the value of the "fault tolerance" parameter for the respective unit. The measurement process is not suspended.
- *Failure Stopped* – The number of errors encountered during the measurement of a Web service has exceeded the defined limit. This Web service is then classed as "unavailable" and its measurement is aborted.
- *Reconfiguration needed* – The procedure has ascertained that the WSDL document for the relevant Web service has been changed. The Web service measurements have been set to react pessimistically, i.e. a reconfiguration is required. The measurement process is suspended.
- *Zombie* –The Web service (WSDL and configured URL) is no longer available.

4.3 Reporting functions provided

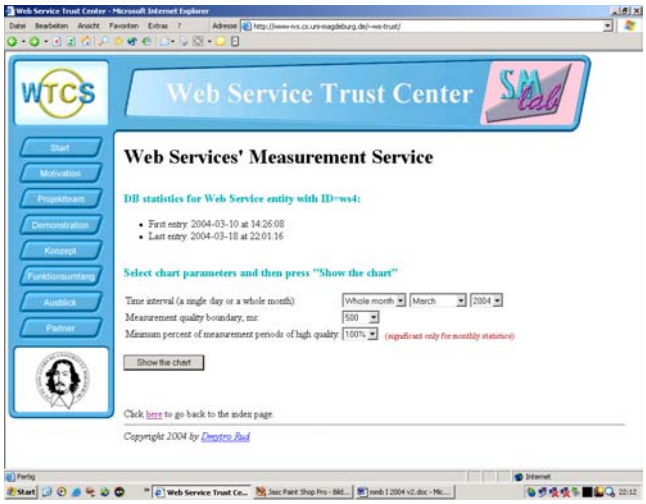

Figure 5: Configuring access to the Web service

In addition to the option of processing the measurement results in other programs such as Excel or SPSS via a data exchange format (currently the XML format shown in Appendix A), the measurement service provides a comprehensive view of the actual measurements made, in the form of its own graphical analyses.

The current version allows you not only to examine the measurements for an entire month (the relevant configuration dialog is shown in Figure 5) but also to display the measurements for a particular day. When generating the analyses, relevant threshold values can be defined. When selecting an entire month, the following data is output:

- Number of days in the selected month for which there is measurement data in the database;
- Number of days on which the required quality was achieved;
- Percentage of days on which the required quality was achieved;
- Total number of measurements carried out in the selected month;
- Number of failed measurements;
- Number of changes to the WSDL document detected in the selected month.

Figure 6 shows the measurement output for a complete day. Both the ping time and the actual call time (invocation time) of the Web service functionality are displayed. Users also receive the following information relating to the day (not shown in Figure 6):

- Number of measurements carried out on the selected day;
- Number of failed measurements on the selected day;
- Number of measurements for the day that were of the required quality;
- The relative proportion of these (%);
- Number of changes to the WSDL document detected on the selected day.

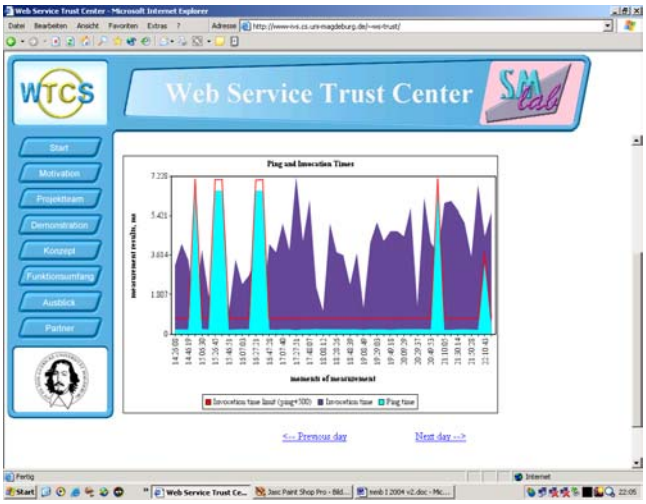

Figure 6: Results display for measurements carried out

5 Analysis of a specific Web service

The Web service "XigniteQuotes" was subject to an appropriate analysis with the aid of the measurement service. This Web service provides information on share prices and indices on the US stock market. A total of 17 methods are provided for querying this information. In an initial analysis, the method *GetQuickQuotes* was subjected to an initial test using the measurement service. After a delay of 20 minutes, this provided the relevant share price, with information on the previous price, the percentage change, and the new price being supplied. The measurement was configured using the following values:

R=2; IP=120; WP=1440; FT=4, OWC=true

In line with the configuration, 2 test samples were carried out for each measurement (R=2), with the measurement itself taking place every 120 minutes (IP=120), and a check every 1440 minutes to ascertain whether the WSDL file had changed. Parameter FT was used to define the permitted number of successive errors (in this case, 4) after which the Web service is classed as being unavailable. The parameter OWC=true specifies that the service is to behave optimistically in the case of a potential change to the WSDL file, i.e. measurements will continue to be taken. This service was monitored from July 19, 2004 until the end of 2004. With reference to the days on which the relevant measurements were carried out, it was possible to validate the series of measurements and identify potential faults in the measurement service itself. This led to a fault being identified in the measurement service in the months of August and September. For the remainder of the analysis, we shall concentrate on the month of October. An overview of the results obtained in October:

- average call time (1st measurement): 1072 ms
- average call time (2nd measurement): 547 ms
- average network time (ping time): 217 ms
- measurement errors identified: 4 (i.e. 1st and 2nd measurements greater than 3 seconds)
- network errors identified (ping time > 1 sec): 1
- Checks carried out: 369 – availability 99.08%.

Basically, the series of measurements carried out established that the time for the first call is greater than that for subsequent calls. This is due to the Web service being initialized, leading to the generation of object instances during the first call. This is also highlighted in Figures 7 and 8, with this feature also being evident when other Web services were measured (not shown here).

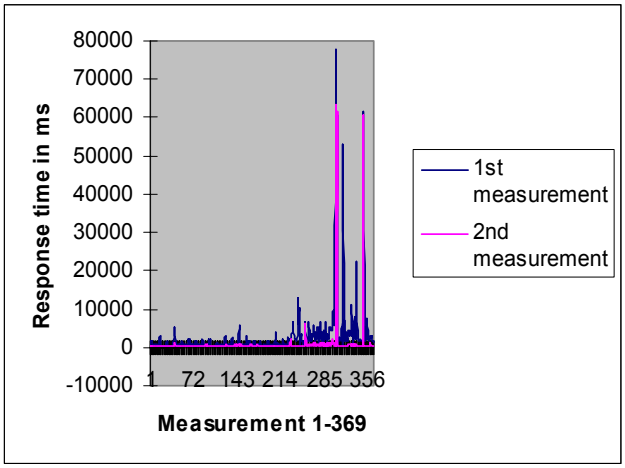

Figure 7: Response time behavior for 1st and 2nd measurement

Figure 7 shows a comparison between the 1st and 2nd measurements for the entire month of October.

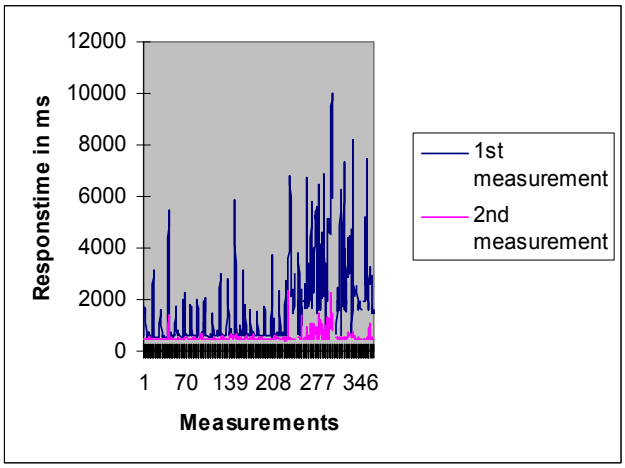

Figure 8: Adjusted measurements excluding response times > 10 secs

In order to accentuate the effect of the slower response times for the 1st measurement, we adjusted the measurement results for values greater than 10 seconds (see Figure 8).

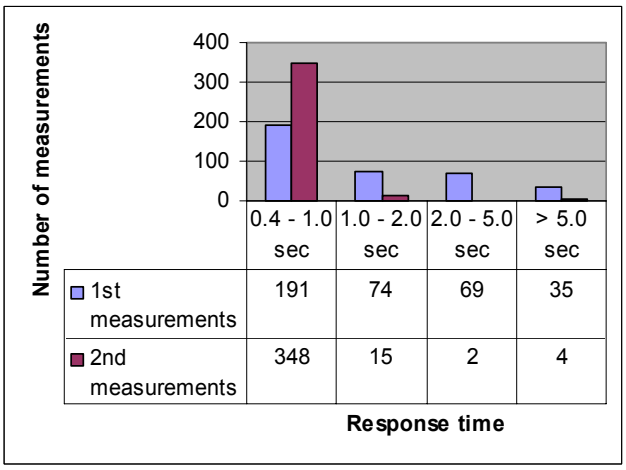

Figure 9: Comparison of 1st and 2nd measurements

Figure 9 shows the distribution of the results from the 1st and 2nd measurements. The difference between the 1st and 2nd measurements can be clearly seen here as well.

6 Summary and prospects

The Web services currently available on the Internet vary from simple functions (simple services) such as weather or authentication services to complete business transactions such as booking all the services required in a travel portal (combined services). The more attractive the Web service functions on offer, the greater the number of potential users and therefore the load on the hardware and software resources used by the service. In a commercial environment, this gives rise to costs that should be charged to the customer accordingly. The supplier must also ensure the qualitative properties of the Web service.

In this context, it makes sense to use an independent measurement service, thus supporting the establishment of a wide variety of SLA-supported settlement models. The software measurement laboratory is currently working on implementing an appropriate billing component that will provide configurable business models for marketing Web services. However, it is not possible to carry out access-related settlement with the existing Web service specifications. Either the Web service itself could provide the relevant access statistics, or an appropriate broker could log the accesses. A suitable initial approach can be found in the WSLA specification (see [4]).

We are also focusing on the prediction component. The aim is to infer the future qualitative behavior of the Web service from an existing empirical base of experience. In the context of the performance properties of the Web service, a simple forecasting model is currently being implemented based on the operational analysis. However, implementing this procedure for existing Web services will not be straightforward. An extension of the interface specification to include details of the efficiency of the Web service, or alternatively the provision of an explicit test access would permit further progress in this area. In addition, the measurement service is being embedded in an appropriate Web service trust center that registers Web services available on the Internet in a directory structure and provides appropriate valued-added services, some of which build on the functionality of the measurement service we have described here.

7 References

[1] Alonso, G.; Casati, F.; Kuno, H.; Machiraju, V.: Web Services – Concepts, Architectures and Applications, Springer Berlin Heidelberg, 2004

[2] Dumke, R.; Schäfer, U.; Wille, C.; Zbrog, F.: Agent-based Web technology evaluation for the performance engineering (only in German), in Proc. of PE2004

[3] ISO 14756: Measurement and rating of performance of computer-based software systems. ISO/IEC JTC1/SC7 Secretariat, CANADA, 1997

[4] Keller, A.; Ludwig, H.: The WSLA Framework: Specifying and Monitoring Service Level Agreements for web Services, IBM Research Report, May 2002

[5] Menascé, D.: Scaling the Web - QoS Issues in Web Services, IEEE Internet Computing, vol. 6, no. 6 pp. 72–75, NOVEMBER/DECEMBER 2002

[6] Menascé, D.; Almeida, V.: Capacity Planning for Web services, Prentice Hall, Upper Saddle River, NJ, 2002

[7] Menascé, D.; Ruan, H.; Gomaa, H.: A framewok for QoS-Aware Software Components, in Proc. of WOSP 2004

[8] Patel, C.; Supekar, K.; Lee, Y.: A QoS Oriented Framework for Adaptive Management of Web Service based Workflows, University of Missouri-Kansas City, 2003

[9] QoS for Web Services: Requirements and Possible Approaches, W3C Working Group Note 25 November 2003, URL: http://www.w3c.or.kr/kr-office/TR/2003/ws-qos/

[10] Sahai, A.; Machiraju, V.; Sayal, M.; Jin, L. J.; Casati, F.: Automated SLA Monitoring for Web Services, in Feridun, M.; Kropf, P. G.; Babin, G. (Eds.): Management Technologies for E-Commerce and E-Business Applications, LNCS 2506 Springer 2002

[11] Schmietendorf, A.; Dumke, R.: Empirical Analysis of available Web Services, Tagungsband zur IWSM 2003, Shaker-Verlag, 2003

[12] Shah, R.; Apte, N.: Performance and Load-Testing of Axis with Various Web Services Styles, Pearson Education - Prentice Hall PTR, Indianapolis, Indiana/USA, 2004 (http://www.phptr.com/articles/)

[13] Sneed, H. M.; Sneed, S. H.: Web-based System integration (only in German), Vieweg – Braunschweig/Wiesbaden, 2003

[14] Sriganesh, R. P.: Web Services Performance, Sun Microsystems, 2003 (www.sun.com/developers/evangcentral)

[15] Thielen, M.: Quality assurance of Web services – diploma thesis (only in German), University of Koblenz-Landau, 2004

[16] Tian, M.; Voigt, T.; Naumowicz, T.; Ritter, H.; Schiller, J.: Performance Impact of Web Services on Internet Servers, Freie Universität Berlin, Computer Systems & Telematics, 2003

[17] Yoon S.; Kim, D.; Han, S.: WS-QDL containing static, dynamic, and statistical factors of Web services quality, in Proc. of IEEE International Conference on Web Services, San Diego/CA, 2004

[18] Orfali, R.; Harkey, D.; Edwards, J.: The Essential Distributed Objects Survival Guide, Wiley & Sons, 1996

Appendix A – Example of an exported XML-file

```
<?xml version="1.0" encoding="utf-8" ?>
<wesementData                                    xmlns="http://www.cs.uni-
magdeburg.de/~rud/wesement/Export"
xmlns:xsi="http://www.w3.org/2001/XMLSchema-instance"
xsi:schemaLocation="http://www.cs.uni-magdeburg.de/~rud/wesement/Export
http://www.cs.uni-magdeburg.de/~rud/wesement/Export.xsd"
creationTime="2004-11-20T14:18:37" user="andreas" startDate="2004-11-20"
endDate="2004-11-21">
<entity owner="andreas" creation="1100953476361" id="ws8" state="OK"
wsdlUrl="http://wavendon.dsdata.co.uk/axis/services/CarRentalQuotes?wsdl
">
       <configuration              serviceName="CarRentalQuotesService"
       portName="CarRentalQuotes" operIndex="1" operName="getCountries"
       endpoint="http://wavendon.dsdata.co.uk/axis/services/CarRentalQu
       otes"    repeatings="1"    operPeriod="10"    wsdlPeriod="10080"
       maxFailures="0" optimisticWsdlChanges="true" />
           <batch date="2004-11-20" time="13:29:35" repeatings="1">
              <measurement number="0" ping="49" invoke="304" />
           </batch>
           <batch date="2004-11-20" time="13:31:12" repeatings="1">
              <measurement number="0" ping="53" invoke="249" />
           </batch>
           <batch date="2004-11-20" time="13:41:17" repeatings="1">
              <measurement number="0" ping="50" invoke="251" />
           </batch>
           <batch date="2004-11-20" time="13:51:23" repeatings="1">
              <measurement number="0" ping="53" invoke="253" />
           </batch>
           <batch date="2004-11-20" time="14:01:28" repeatings="1">
              <measurement number="0" ping="49" invoke="257" />
           </batch>
           <batch date="2004-11-20" time="14:11:34" repeatings="1">
              <measurement number="0" ping="49" invoke="250" />
              </batch>
</entity>
</wesementData>
```

Performance Distributions of Continuous Time Single Server Queueing Model with Batch Renewal Arrivals: $GI^G/M/1/N$ *

Wei Li, Rod Fretwell, Demetres Kouvatsos
Performance Modelling and Engineering Research Group
University of Bradford, Bradford, UK, BD7 1DP
email:{w.li1, r.j.fretwell, and d.d.kouvatsos@brad.ac.uk}

Abstract

It has been proven that the batch renewal process (BRP) is the least biased process given the infinite sets of measures of the traffic correlation, (i.e. indices of dispersion, covariance or correlation function) in the discrete time domain. The similar argument is expected for the continuous time BRP but not shown in here.

The correlation induced by BRP is analysed and a queueing model fed by BRP is studied. In this context, a continuous time $GI^G/M/1/N$ queueing model is analysed having a single server, general batch renewal arrival process, exponential service time and finite buffer size N. Closed form expressions for performance distribution, such as, queue length, blocking probability and waiting time distributions are derived. As a consequence, these analytic tools can be used to efficiently assess the adverse effect of traffic correlation induced by the BRP on the queue.

Keywords: batch renewal process (BRP),continuous time queueing model, performance distributions, correlation

1 Introduction

A persistent problem in the field of performance modelling and evaluation is to choose the most appropriate queueing model. Unfortunately, due to the need for analytical tractability most works assume a Poisson arrival process [9], which is not realistic as shown, for example in [12]. On the other hand, in actual networks, such as IP or ATM networks, it is most possible that packets arrive at the queue in batches rather than individually.

Recently, queueing models fed by batch arrival process have received significant attention [6-11]. Most of the research work falls in the discrete time domain, whilst batch arrival process could be also applied into continuous time domain. The latter removes the restriction that the packets, in discrete time domain, must arrive at the end of a time slot.

BRP is a general case of batch arrival process which involves both count and interval correlations. Note that indices of dispersion have long been known as powerful tools in the analysis of the second-order properties of point processes [13] [14] and computer traffic measurements [1-5].

Sriram and Whitt [1] analysed superposition of bursty correlated arrival processes in terms of indices of dispersion for intervals (IDI). Heffes and Lucantoni [2] modelled the superposition of bursty arrival processes approximated by a correlated Markov modulated Poisson process (MMPP) matching three features of indices of dispersion for counts (IDC) and mean arrival rate. Gusella [3] characterized the variability of measured packet arrival process with indices of dispersion and discussed the merits of these indices as well as the pitfalls of their indiscriminate use. Moreover he estimated the indices of dispersion for measured LAN traffic which

*This work is partially supported by the EU Network of Excellence (NoE) Euro-NGI.

was approximately modelled by 2-phase MMPP which matched on the three IDCs and the squared coefficient of variation (SCV) of the inter-arrival times.

Fowler and Leland [14] reported LAN traffic with unbounded IDC. However, it is expected that performance of a restricted buffer system with deterministic service would not be affected by the magnitude of IDC for long intervals. Andrade and Martinez-Pascua showed that the queue length distribution and other statistics are affected by IDC only up to a certain size of interval (determined by the buffer size) whilst the value of the IDC at infinity is of little importance.

Only a limited number of papers studying on finite-buffer queues with batch renewal process have appeared so far in the literature. In this context, the batch renewal process in a discrete time domain was introduced and applied to the analysis of queueing models by Fretwell and Kouvatsos [5-7], where the generating functions of IDI and IDC were expressed in terms of corresponding generating functions of batch inter-arrival time and batch size distributions. Moreover, Frey [15] analysed a finite-capacity vacation queue with batch arrivals but considered batch Poisson arrivals only. Niu [9] studied a vacation queue with setup and close-down times and batch Markovian arrival processes in discrete time domain. A queueing model with batch arrivals and batch-dedicated servers was analysed by Gullu [11], which nevertheless, has an infinite number of servers and buffer sizes. Finally, Takaki and Wu [10] studied queue fed by a semi-Markovian batch arrival process but with infinite waiting rooms.

The BRP is employed in the continuous time domain and the following analysis of a $GI^G/M/1/N$ queue with a general batch renewal arrival process GI^G, as defined in Section 2. Performance distributions of queue length, blocking probability and waiting time distributions are determined.

Section 2 introduces the continuous time batch renewal process and associated properties. Section 3 gives the transforms of IDI and IDC of continuous time batch renewal process. The performance distributions of a single server queue with batch renewal arrival process and finite-capcacity are presented in Section 4. Conclusions are drawn in Section 5.

2 Batch Renewal Processes

A batch renewal process as a traffic process allows simultaneous arrivals such that

- the number of arrivals in different batches are independent and identically distributed
- the intervals between batches are independent and identically distributed
- the batch sizes (number of arrivals in one batch) are independent of intervals between batches

In the continuous time domain, a batch renewal process has continuous inter-arrival times and discrete counts. In the discrete time domain a batch renewal process has been found to exhibit both interarrival correlation between individual arrivals and count correlation between successive epochs. In this paper the corresponding correlations are investigated in the context of a continuous time batch renewal process.

3 Correlation in Batch Renewal Process

Consider a continuous time batch renewal process in which

- the distribution of batch size is given by the probability mass function (pmf) $b(n)$, $n = 1, 2, \ldots$, with mean b, squared coefficient of variation (SCV) C_b^2 and probability generating function (pgf) $B(z) = \sum_{n=1}^{\infty} b(n) z^n$.
- the distribution of interval between batches is given by the probability density function (pdf) $a(t)$, $t > 0$, with mean a, SCV C_a^2 and Laplace transform $A(\theta) = \int_0^{\infty} a(t) e^{-\theta t} dt$.

Let $\nu(n,t)$ be the probability that exactly n customers arrive during the interval of length t, $n = 0, 1, \ldots$, $t > 0$. Then the transform function of $\nu(n,t)$ is defined as

$$\begin{aligned} N(z,\theta) &= \sum_{n=0}^{\infty} \int_{t=0}^{\infty} \nu(n,t) z^n e^{-\theta t} dt \\ &= \frac{1}{\theta} - \frac{1}{a \cdot \theta^2} \cdot \frac{(1 - A(\theta))(1 - B(z))}{1 - A(\theta)B(z)} \end{aligned} \tag{1}$$

The IDC, I_t, is defined to be the variance of the number of arrivals during an interval of length t divided by the mean number $E(N_t)$ of arrivals in t, namely

$$I_t = \frac{Var(N_t)}{E(N_t)} \tag{2}$$

Let $I(\theta)$ to be the generating function of I_t. From the well-known connection between the indices of dispersion and correlation functions (covariances), the transform of count correlation function $K(\theta)$ can be determined by (c.f.[16]):

$$K(\theta) = b\left(C_b^2 + \frac{1 + A(\theta)}{1 - A(\theta)} - \frac{2}{a} \cdot \frac{1}{\theta}\right) \tag{3}$$

Let $\tau(n,t)$ be the probability that there are n intervals between $n+1$ successive individual arrivals during interval of length t. Then the transform function of $\tau(n,t)$ is defined as

$$\begin{aligned} T(z,\theta) &= \sum_{n=0}^{\infty} \int_{t=0}^{\infty} \tau(n,t) z^n e^{-\theta t} dt \\ &= \frac{1}{1-z} - \frac{z}{b \cdot (1-z)^2} \cdot \frac{(1 - A(\theta))(1 - B(z))}{1 - A(\theta)B(z)} \end{aligned} \tag{4}$$

The IDI, J_n, is defined to be the n times SCV of intervals X between individual arrivals.

$$J_n = \frac{n \cdot Var(X)}{E(X)^2} \tag{5}$$

Defining $J(z)$ to be the generating function of J_n. The transform of interval correlation function $L(z)$ can be obtained by

$$L(z) = b\left(C_a^2 + \frac{1 + B(z)}{1 - B(z)} - \frac{1}{b} \cdot \frac{1+z}{1-z}\right) \tag{6}$$

Note that $K(\theta)$ is expressed in terms of batch interarrival time distribution and $L(z)$ in terms of batch size distribution.

From equations (3) and (6), $A(\theta)$ and $B(z)$ can be expressed in terms of $K(\theta)$ and $L(z)$, repectively, by:

$$1 - B(z) = \frac{2b}{L(z) - b(C_a^2 - 1) + \frac{1+z}{1-z}} \tag{7}$$

$$1 - A(\theta) = \frac{2b}{K(\theta) - b(C_b^2 - 1) + 2\lambda \cdot \frac{1}{\theta}} \tag{8}$$

It may be shown that equations (7) and (8) define $A(\theta)$ and $B(z)$ uniquely given $K(\theta)$ and $L(z)$ (c.f.[15]). It may be also shown that counting process $\nu(n,t)$ and timing process $\tau(n,t)$, taken together, define $A(\theta)$ and $B(z)$ uniquely.

4 Censored $GI^G/M/1/N$ Queue

This section specifies the $GI^G/M/1/N$ queue and derives the performance distributions.

4.1 Model Discription and Specification

Consider a $GI^G/M/1/N$ queue with a batch renewal arrival process where customers within an arriving batch are turned away and simply lost (i.e. censored arrivals) when the number of occupied buffers reaches capacity N. The service times are assumed to be exponentionally distributed and the first customer arriving to an empty system receives service immediately and departs after serivce completion (immediate service policy). In the following sections, $a(t)$ denotes the probability density function of inter-arrival time between batches, $b(n)$ the probability mass function of batch sizes and $N(0 < N < \infty)$ the buffer size of the queue.

4.2 Two Embedded Processes

Consider within a continuous time domain two processes embedded at points immediately before and after each batch arrivals. Each process may be described independently by a Markov chain but the processes are mutually dependent.

- For the first chain (chain 'A'), the state is the number of customers in the queue after allowing for any departure at that instant but discounting the new arrivals at that instant. Let $P_N^A(n)$ be the steady state probability that the state be $n = 0, 1, \cdots, N-1$ (where N is the capacity of the system)

- For the second chain (chain 'D'), the state is the number of customers in the queue after allowing for any departure at that instant but including the new arrivals. Let $P_N^D(n)$ be the steady state probability that state be $n = 1, 2, \cdots, N$

- Let $P_N(n)$ be the steady state probability that there are $n = 0, 1, \cdots, N$ customers in the system (including queueing and receiving service) at any time

To see the relation between the two Markov chains, first consider the state of each chain at an arrival instant. Chain 'D' may be in state $n = 1, 2, \cdots, N-1$ when chain 'A' is in state $k = 0, 1, \cdots, n-1$ and there are $n-k$ arrivals in the batch. Alternatively, chain 'D' may be in state N when chain 'A' is in state $k = 0, 1, \cdots, N-1$ and there are at least $N-k$ arrivals in the batch, therefore

$$P_N^D(n) = \begin{cases} \sum_{k=0}^{n-1} P_N^A(k) b(n-k) & \text{n=1,2,}\cdots\text{,N-1} \\ \sum_{k=0}^{N-1} P_N^A(k) \sum_{r=N-k}^{\infty} b(r) & \text{n=N} \end{cases} \tag{9}$$

Now consider the states of each chain at successive arrival instants. At the later instant, the chain 'A' may be in state $n = 1, 2, \cdots, N-1$ when the chain 'D' may be in state $k = n+1, \cdots, N$ at earlier arrival instant and there are $k-n$ departures in the interval between two arrivals of batches. Since the service times are exponentially distributed, the probability that $k-n$ customers depart during interval of length t is given by

$$\int_0^{\infty} e^{\mu t} \cdot \frac{(ut)^{k-n}}{(k-n)!} dt \tag{10}$$

The realtionship between P_N^A and P_N^D at two successive arrival instants

$$P_N^A(n) = \begin{cases} \sum_{k=0}^{N-n} P_N^D(n+k) \int_0^\infty e^{-\mu t} \cdot \frac{(\mu t)^k}{k!} \cdot a(t)dt & n = 1, 2, \cdots, N \\ \sum_{k=0}^{N} P_N^D(k) \int_0^\infty \int_0^t e^{-\mu s} \cdot \frac{(\mu s)^k}{k!} ds \cdot a(t)dt & n = 0 \end{cases} \tag{11}$$

4.3 Queue Length Distribution

If immediately after the arrival of a batch, there are $n+k = 1, 2, \cdots, N$ customers in the system and the interval between that and the next batch be the length of t, then

$$P_N(n) = \begin{cases} \sum_{k=0}^{N-n} P_N^D(n+k) \int_0^\infty \int_0^t e^{-\mu s} \cdot \frac{(\mu s)^k}{k!} \cdot \frac{1}{a} \cdot ds \cdot a(t)dt & n = 1, 2, \cdots, N \\ \sum_{k=1}^{N} P_N^D(k) \int_0^\infty \int_0^t e^{-\mu s} \cdot \frac{(\mu s)^k}{k!} \cdot \frac{1}{a} \cdot (t-s) \cdot ds \cdot a(t)dt & n = 0 \end{cases} \tag{12}$$

4.4 Blocking probability

If an arriving batch of size $N - k + r$ finds k customers in the finite buffer system, then only the first $N - k$ customers of the arriving batch enter the system and r customers will be blocked and lost.

The probability that the arriving batch finds k customers is $P_N^A(k)$, the probability that the batch be of size $N - k + r$ is $(N - k + r) \cdot \frac{1}{b} \cdot b(N - k + r)$ and the probability of a customer being in one of the r positions, given tha batch being of size $N - k + r$, is $\frac{r}{N-k+r}$. Therefore, the blocking probability Π_N^B is given by

$$\Pi_N^B = \sum_{k=0}^{N-1} P_N^A(k) \sum_{r=1}^{\infty} \frac{r}{b} b(N - k + r) \tag{13}$$

4.5 Waiting time distribution

The waiting time of a customer is given by the interval from the instant at which it arrives in the queue to that it is receiving service.

If the new arrival batch finds k customers in the system, then the waiting time be the service time of k customers plus the service time of $i - 1$ customers before the tagged customer given it is in the i^{th} position in the batch.

$$W_N(t) = \frac{\sum_{k=0}^{N-1} \sum_{r=i}^{\infty} \sum_{r=1}^{N-k} P_N^A(k) b(r) \int_0^\infty \frac{(\mu t)^{k+i-2} \cdot \mu}{(k+i-2)!} e^{-\mu t} dt}{b(1 - \Pi_N^B)} \tag{14}$$

5 Conclusions

A continuous time $GI^G/M/1/N$ queue with single server, general batch renewal arrivals process, exponentially distributed service time and finite capacity N is analysed. Closed form expressions for basic performance distributiions, such as queue length, waiting time and blocking probability distributions are derived. As a consequence, these analytic tools can be used to efficiently assess the adverse effect of traffic correlation induced by the BRP on the queue.

Numerical results on the effects of correlation on the behaviour of queueing system will be given in a sequel paper.

References

[1] Kotikalapudi Sriram, Ward Whitt, *Characterizing Superposition Arrival Porcesses in Packet Multiplexers for Voice and Data*, IEEE Journal on Selected Areas in Communication, Vol. SAC-4, No. 6, pp. 833-846, September 1986

[2] Harry Heffes, David M. Lucantoni, *A Markov Modulated Characterization of Packetized Voice and Data Traffic and Related Statistical Multiplexer Performance*, IEEE Journal on Selected Areas in Communication, Vol. SAC-4, No. 6, pp. 856-868, September 1986

[3] Riccardo Gusella, *Characterizing the Variability of Arrival Processes with Indexes of Dispersion*, IEEE Journal on Selected Areas in Communication,Vol. 9, No. 2, pp. 203-211, February 1991

[4] Leonard Kleinrock, *Queueing Systems Volume1: Theory*,A Wiley-Interscience Publication, John Wiley and Sons, Canada, 1975.

[5] Demetres Kouvatsos, Rod Fretwell, *Discrete Time Batch Renewal Processes with Application to ATM Performance*, Proceeding of the 10th UK Performance Engineering Workshop, Hilston, J.Etal(eds.). Edinburgh University Press, pp. 187-192, Sep.1994

[6] Demetres Kouvatsos, Rod Fretwell, *Closed Form Performance Distribution of a Discrete Time* $GI^G/D/1/N$ *Queue with Correlated Traffic*, In Data Communications and their Performance, Fdida S. and Onvural.(eds.), Chapman and Hall, pp. 141-163, 1995

[7] R.J.Fretwell, *An Investigation into traffic correlation in high speed communication networks by means of discrete time models*, Ph.D thesis, 2002

[8] Sebastia Galmes, Ramon Ruigjaner, *Correlation analysis of a discrete-time flexible arrival process*, Computer Networks, Vol. 41 (2002), pp. 795-814

[9] ZhiSheng Niu, Tao Shu, Yoshitaka Takahashi, *A vacation queue with setup and close-down times and batch Markovian arrival processes*, Performance Evaluation, Vol. 54 (2003), pp 225-248

[10] Hideaki Takagi, De-An Wu, *Multiserver queue with semi-Markovian batch arrivals*, Computer Communications, Vol. 27 (2004), pp 549-556

[11] Refik Gullu, *Analysis of an* $M/G/\infty$ *queue with batch arrivals and batch-dedicated servers*, Operations Research Letters, Vol. 32 (2004), pp 431-438

[12] Vern Paxson, Sally Floyd, *Wide-Area Traffic: The Failure of Poisson Modeling*, ATM/IEEE Transactions on Networking, 3 (3), pp. 226-244, June 1995

[13] D.D.Brillinger, *Comparative aspects of the study of ordinary time series and of point processes*, in Development in Statistics, P.R.Krishnaiah, Ed. New York: Academic, 1978, Vol.1, pp33-133

[14] D.R.Cox and P.A.W.Lewis, *The Statistical Analysis of Series of Events*. London: Chapman and Hull, 1966.

[15] A.Frey, Y.Takahashi, *An* $M^{[x]}/GI/1/N$ *queue with close-down and vacation time*, J.Appl.Math.Stochast.Anal.12 (1999) 63-83

[16] W.Li, R.Fretwell, D.D.Kouvatsos, *Continuous Time Batch Renewal Processes and the Application to Analysis of Queueing Models*, Research Report, May 2005

A New Backoff Algorithm for MAC Protocol in MANETs

Saher S. Manaseer **Mohamed Ould-Khaoua**

Department of Computing Science
University of Glasgow
Glasgow G12 8RZ
{Saher, Mohamed}@dcs.gla.ac.uk

Abstract: IEEE 802.11 Medium Access Control (MAC) uses The Binary Exponential Backoff (BEB). BEB uses a uniform random distribution to choose the backoff value that often leads to reducing the effect of window size increment. This paper introduces a modified logarithmic backoff algorithm that uses logarithmic increment instead of exponential extension of window size to eliminate the degrading effect of random number distribution. Results from simulation experiments reveal that the new algorithm achieves higher throughput when in a mobile ad hoc environment.

Keywords: IEEE 802.11, Ad Hoc networks, Medium access control, Backoff algorithm.

1. Introduction

Mobile Ad Hoc Networks (MANETs) are getting more and more attention. The reason for this is that unlike wired networks, MANETs are easily deployed, and need no infrastructure [1]. Such networks can be useful in disaster recovery where there is not enough time or resources to configure a wired network. Ad hoc networks are also used in military operations where the units are moving around the battlefield in a random way and a central unit cannot be used for synchronization [1].

In MANETs, a central station is not needed in order to control the different types of operations taking place allover the network. A node participating in an ad hoc network must have the ability to act as a client, a server, and a router [1]. Nodes should also have the ability to connect to the network and to automatically configure to start transmitting data over the network. This is the reason why ad hoc protocols in general are functioning in a distributed manner. The distributed Coordination Function (DCF) is used for synchronous, contention-based, distributed access to the channel [3]. MANETs use a shared medium to transfer data between its nodes.

The wireless medium used by MANETs has a number of problems related to it. Bandwidth sharing, signal fading, noise, interference, etc…. with such a shared medium, an efficient and effective medium access control (MAC) is essential to share the scarce bandwidth resource [12] [1].

As a part of an efficient medium access control protocol, a backoff algorithm is used to avoid collisions when more than one node try to access the channel. Only one of the nodes is granted access to the channel, while other contending nodes are suspended into a backoff state for some period (BO) [9]. Many backoff algorithms have been developed in the literature [4, 9]. One example is the Multiplicative Increase Linear Decrease (MILD) algorithm [4]. This algorithm improves the total throughput of the network, but the cost is that MILD needs a partial knowledge of the number of nodes over the network, which is a high cost knowledge.

In a normal LAN, the total number of nodes on the network is easily obtained. However, as nodes in MANETs are mobile, knowing the number of nodes may incur a high cost, since this knowledge needs to be updated. One approach to update and keep the knowledge coherent is by exchanging "hello" packets between neighboring nodes. The "hello" packets sending process is a broadcast over the network. The broadcast generates extra traffic load over the network, consumes a part of the network resources, causes a longer delay, more control processing, and even gives more work to the backoff algorithm itself. Other backoff algorithms have tried to find a fixed optimum backoff value to use. However, the distribution functioning was not complete [8].

In the IEEE 802.11 standard MAC protocol, the Binary Exponential Backoff (BEB) is used. This algorithm functions in the following way [2].

When a node over the network has a packet to send, it first senses the channel using a carrier sensing technique. If the channel is found to be idle and not being used by any other node, the node is granted access to start transmitting. Otherwise, the node waits for an inter-frame space and the backoff mechanism is invoked. A random backoff time will be chosen in the range [0,CW-1]. A uniform random distribution is used here, where CW is the current contention window size. The following equation is used to calculate the backoff time (BO):

Backoff time (BO) = (Rand () MOD CW) X aSlotTime (1)

The backoff procedure is preformed then, by putting the node on a waiting period of length BO. Using carrier sense mechanism, the activity of the medium is sensed at every time slot. If the medium is found to be idle then the backoff period is decremented by one time slot.

Backoff time (BO) new = (BO) old - aSlotTime (2)

If the medium is determined to be busy during backoff, then the backoff timer is suspended. This means that backoff period is counted in terms of the idle time slots. Whenever the medium is idle for longer than an inter-frame space, backoff is resumed. When backoff is finished with a BO value of zero, a transfer should take place. If the node succeeds to send a packet and receive an acknowledgment, the CW for this node is reset to the minimum, which is equal to 31 in the case of BEB. If the transfer fails, the node starts another backoff period. In the next backoff period, the contention window size is exponentially increased with a maximum of 1023 [5].

BEB has a number of disadvantages. One major disadvantage is the problem of fairness [7]. BEB tends to prefer last contention winner and new contending nodes to other nodes when allocating channel access. Backoff time is decided by choosing a random backoff value from a contention window (CW) that has a smaller size for new contending nodes and contention winners. This behavior causes what is known as "Channel capture effect" in the network [10]. Another problem of BEB is related stability. BEB has been designed to be stable for large number of nodes. Studies showed that it is not [9].

The rest of this paper is organised as follows. Section 2 describes the new modified logarithmic backoff algorithm. Section 3 describes simulation environment and discusses the results and there behavior compared to IEEE 802.11 BEB algorithm.

Finally, Section 4 concludes the paper.

2. The modified backoff algorithm

BEB algorithm uses the following equation to increase the contention window size

Backoff time (BO) = (Rand () MOD CW) X aSlotTime

The new algorithm used the Logarithm of the current backoff time as the increment factor to calculate the next backoff. The following formula is used:

$(BO)_{new} = (\log (BO)_{old}) \text{ X } (BO)_{old} \text{ X aSlotTime} \quad (3)$

This formula provides different outcome for the backoff times. The behavior of the two formulas can be seen in Figure1 and 2. The further we go with backoff; the closer will become the new values to the old values generated by the modified algorithm.

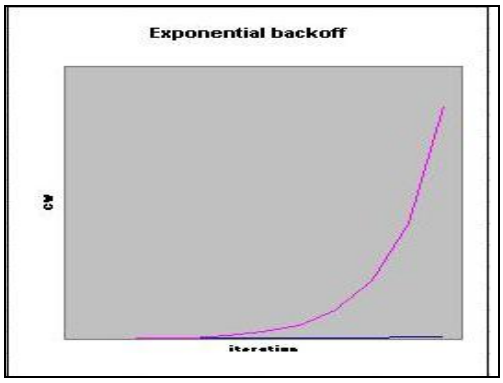

Fig. 1: CW increases in BEB.

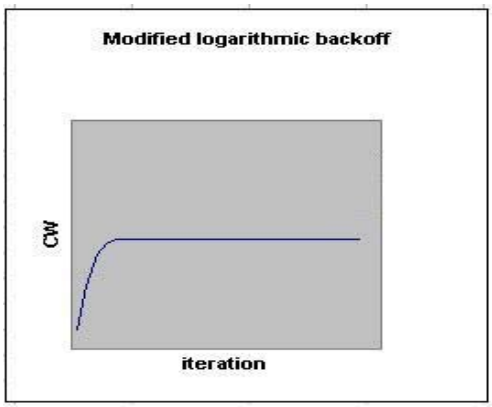

Fig. 2: CW increases in logarithmic algorithm

Figure 3 explains the modified algorithm.

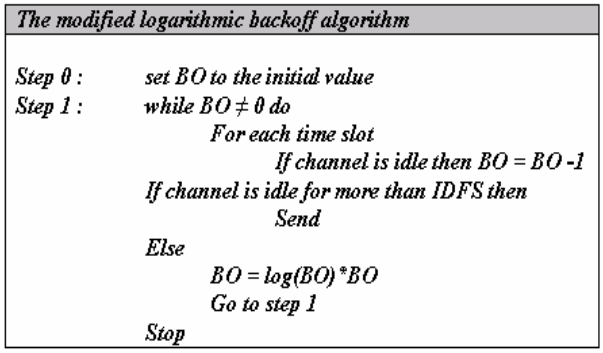

Figure 3 The modified backoff algorithm.

The main idea behind choosing such an equation for calculating backoff time is that instead of going on a back off period for X time slots, the node goes into two consecutive backoff periods say i_1 and i_2, where $i_1 + i_2 \approx X$ when the node is backing of for a consecutive number of times. This allows the node a chance to access the channel and transmit in a way like if backoff is stopped in the middle of the backoff period X.

Reducing the channel capture effect [7] is another perspective of the new algorithm. In BEB, when a node loses in contention for channel access, there is a good chance that the next backoff timer will be double as the current value, this assigns the node larger probability to lose in the next contention against new arrivals and contention winners [10]. When using the logarithmic algorithm, the difference between the backoff periods is smaller, and so the chance of losing is not increased by the logarithmic algorithm. The cost in of using the modified algorithm is one extra invocation of the backoff handler to restart the timer. The modified algorithm also has stopped using the uniform random distribution. Which, as shown in the results in Section 4, hides the effect of the increase behavior of the CW, the thing causing research results to be masked by a side factor.

3. Simulation Results and analysis

Simulation has been performed using nine topologies with different number of nodes in each topology. The traffic over the network has been generated as Constant Bit Rate (CBR) traffic, maximum speed is 10.0 m/s, and the pause time is 10 s. Queue length is 50 packets.

Figure 4 displays the result of running the modified algorithm against the standard IEEE 802.11 binary exponential backoff algorithm. The figure shows that the throughput is higher for the modified algorithm. A network with larger number of nodes has a better throughput than the case of small number of nodes. The reason of this is, for larger number of nodes, contention is much higher and so, it is more probable for a node to backoff for more consecutive periods, this leads a more significant effect of the behavior of logarithmic algorithm and backoff values start to be closer.

The BEB uses a uniform random number distribution generator. The random distribution used covers the effect of contention window increment behavior. The following graph in Figure 5, show a comparison of the same modified algorithm with another version of itself, where a random number distribution is used in the same way used by the BEB algorithm.

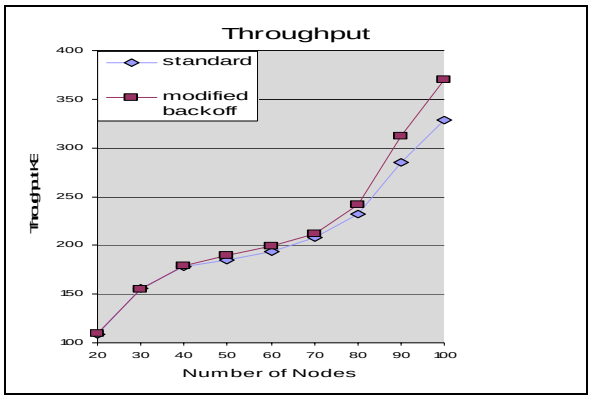

Fig. 4: Throughput of BEB vs. modified backoff algorithm.

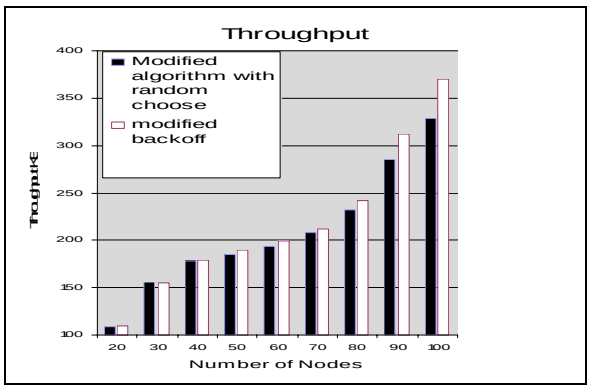

Fig. 5: Throughput of two versions of the modified algorithm.

The reason that the random number distribution is excluded in our algorithm is that a uniform distribution generates only 50% of the random values from the added size of the contention window.

5. Conclusions

The Binary Exponential Backoff (BEB) is used by the IEEE 802.11 Medium Access Control (MAC) protocol. BEB uses uniform random distribution to choose the backoff value. In this paper, we have introduced a modified logarithmic backoff algorithm, which uses logarithmic increments instead of exponential extension of window size to eliminate the effect of random number distribution. Results from simulations have demonstrated that the modified algorithm increased the total throughput of the mobile ad hoc networks especially when the system size is large.

References

[1] Z.Fang, et al., “Performance evaluation of a fair backoff algorithm for IEEE 802.11 DFWMAC.” International Symposium on Mobile Ad Hoc Networking & Computing

[2] S. Xu, And T. Saadawi, “Does the IEEE 802.11 MACprotocol work well in multihop wireless ad hoc networks?” *IEEE Communications Magazine*, pp 130 – 137, 2001.

[3] L.Bononi, et al., "Design and Performance Evaluation of a Distributed Contention Control (DCC) Mechanism for IEEE 802.11 Wireless Local Area Networks", Journal of Parallel and Distributed Computing (JPDC), Vol. 60, N.4, April 2000, pp. 407-430.

[4] K. Sakakibara, et al., "Backoff Algorithm with Release Stages for Slotted ALOHA Systems." ECTI Transactions On Electrical Eng., Electronics, And Communications vol.3, no.1 pp 59-70 ,2005.

[5] H. Zhai and Y. Fang,”Performance of Wireless LANs Based on IEEE 802.11 protocols.” 14th IEEE International Symposium on Personal, Indoor and Mobile Radio Communication Proceedings, pp 2586-2590, 2003.

[6] K. Fall and K. Varadhaa. editors. “NS notes and Documentation.” The V l N l Project UC Berkeley. LBL. USC/ISI. and Xeros PARC. 2002

[7] B. ENSAOU, et al.,” Fair Media Access in 802.11 based Wireless Ad-Hoc Networks.” In *IEEE/ACM MobiHOC* (Boston, MA., August 2000).

[8] L. Bao and J. J. Garcia-Luna-Aceces, “A New Approach to Channel Access Scheduling for Ad Hoc Networks,” in *ACM MOBICOM*, pp. 210–221, 2001.

[9] J. Goodman, et al., “Stability of Binary Exponential Backoff”, app. In the Proc. of the 17-th Annual ACM Symp. Theory of Comp., Providence, May 1985.

[10] J. Hastad , et al., “Analysis of Backoff Protocols for Multiple Access Channels”, Siam J. Computing vol. 25, No. 4, 8/1996, pp. 740-

[11] C. Sauer, E. MacNair, "Simulation of Computer Communication Systems", Prentice-Hall, INC., 1983.

[12] F. Cali', et al.., “IEEE 802.11 Wireless LAN: Capacity Analysis and Protocol Enhancement”, Proc. INFOCOM'98, San Francisco, CA, March 29 - April 2, 1998, pp. 142-149.

Analysis of the QBSS Load Element Parameters of 802.11e for a priori Estimation of Service Quality

Burak Simsek, Katinka Wolter *
Institut für Informatik, HU Berlin
Unter den Linden 6
10009 Berlin

Hakan Coskun †
ETS, TU Berlin
Franklinstr.28/29
10587 Berlin

Abstract

IEEE is preparing its new WLAN standard 802.11e in order to be able to cope with the emergent needs of real time traffic over wireless networks. Within this new standard there is an element called the QBSS (QoS enhanced) load element which should help in choosing the better access point among many. In this paper we show that this element cannot help making true decisions in many cases and address some of these cases. Additionally we suggest a small adjustment in the element which performs better than the current version.

1 Introduction

The tremendous success of the 802.11 technology is highly visible. The WLAN standard 802.11 has already proven to be one of the best marketing products for wireless services. Through Quality of Service (QoS) capabilities which are still in making, QoS demanding services such as Video on demand, Voice over IP (VoIP) and gaming can then be used in a wireless setting. A crucial feature which is required to enable flawless operation of the mentioned services is guaranteed traffic treatment, in the sense that the needed traffic characteristics are adhered by the wireless network infrastructure. The IEEE 802.11e task group envisages solving this problem in the near future with a new standard [1] [6].

For service providers hotspots are very attractive. Hotspots make it possible to have high connection rates on the move, while it should be noted that moving stations are not in the focus of the current WLAN standards [7, 8]. Hotspots are easily installed and very often several access points, sometimes belonging to different service providers, cover intersecting regions. A station has to choose from all reachable access points the one offering the best service quality.

The new standard IEEE 802.11e extends the existing 802.11 standard by adding QoS parameters. By this, 802.11e enables QoS enhanced access points

*{simsek, wolter}@informatik.hu-berlin.de
†coskun@cs.tu-berlin.de
[1] current draft version is 12.0

(QAP) to cope with real-time traffic that is delay-sensitive, jitter-sensitive, error-prone etc. such as voice and video streams (see [1] for a detailed overview). In consequence, the whole new 802.11 series is supposed to operate on access points and wireless stations with QoS enhancement (QAP and QSTAs) and without it (AP and STAs). The issue of QoS is addressed in the new standard IEEE 802.11e by introducing a new element called the QBSS (QoS enhanced basic service set) load element, which is part of the beacon frames generated by QoS enhanced access points (QAP) and contains information on the current traffic situation. It includes three parameters: station count, channel utilization and available admission capacity. The station count is the total number of stations currently associated with the access point. The channel utilization rate is the normalized value of the total channel utilization which gives the percentage of the time the channel is sensed to be busy using either the physical or virtual carrier sense mechanism of the access point. The available admission capacity gives the amount of time that can be used by explicit admission control. These three parameters can be used on one hand by a QoS enhanced access point to decide whether to accept an admission control request. On the other hand the QBSS load element parameters can also be used by a wireless station to decide which of the available access points to choose.

Research in the area of QoS in 802.11 networks concentrates mainly on the evaluation of the performance of the 802.11e drafts and related improvement proposals [3, 4, 5]. In this paper we assume that QoS handling is given and works as expected, the main question we strive to answer is: how should a QoS enhanced station (QSTA) decide which QoS enhanced access point to use, when multiple QAPs are present in its environment. Does the extension proposed in the standard 802.11e provide sufficient information to select the appropriate access point?

We evaluate the significance of the three parameters of the QBSS load element in a simulation study using the ns-2 network[2] simulator [2], where we determine the coefficient of correlation with some QoS metric. Different QoS metrics are used depending on the type of traffic (voice, video, etc) under consideration.

It turned out that none of the three QoS parameters of the QBSS load element shows a significant correlation with any of the QoS metrics for different types of traffic. We conclude that the parameters of the QBSS load element are neither sufficient nor suitable for describing the expected QoS. Instead we found the number of already present connections of the regarded type (if we look at video traffic that is the number of already connected video transmissions) correlates strongly with the respective QoS metric. Therefore we propose to enhance the QoS description of the QBSS load element by another field holding the number of existing connections.

The rest of the paper is structured as follows: After a summary of the current status of the 802.11e MAC protocol and its functioning in Section 2, we present different scenarios that were simulated with the ns-2 network simulator in Section 3. Section 4 discusses the simulation results in detail. Based on the gained results, we suggest an enhancement in the QBSS load element to achieve improvements in finding the best suited QAP depending on the required QoS in Section 5. Finally, Section 6 concludes this paper.

[2]Several implementations of 802.11e mechanisms are already available

2 The Basics of the IEEE 802.11e Standard

There are two main functional blocks defined in 802.11e. These are the channel access functions and the traffic specification (TSPEC) management. We will in this section describe the channel access function which is a key part of the simulation study. The main idea behind the development of the IEEE 802.11e QoS facility is the lack of sufficient QoS management over WLAN. To solve this problem, the IEEE 802.11e task group introduced an obligatory function for the MAC layer called hybrid coordination function (HCF) composed of a combination of two sub functions, EDCA (enhanced distributed channel access) for prioritized channel access (similar to DiffServ) and HCCA (HCF controlled channel access) for parameterized channel access (similar to IntServ). The HCF splits the time frame into a contention and a contention-free period assigning it to EDCA or HCCA respectively. Different applications having different QoS requirements are differentiated and handled correspondingly using one or both of these functions.

In the draft, there exists a new central control mechanism of HCF which is called the hybrid coordinator (HC). The hybrid coordinator, which is collocated at the QoS enhanced access points, is responsible for the management of the use of EDCA and HCCA in a cooperative manner. Basically the hybrid coordinator makes the decision about when and how to use EDCA and HCCA, it assigns transmission opportunities (TXOP) to the stations defining the time interval in which they are allowed to send their MPDUs (MAC Protocol Data Unit). TXOPs can be given by using one of these two functions with respect to the needs of the stations. The HC can start a contention free period during the contention period by sending a *CFPoll (contention free poll)*. A possible combination of contention periods and contention free periods is illustrated within the standard draft as given in Figure 1 where a CAP is the controlled access phase of the hybrid coordinator. As can be observed from this figure, there is no observable regularity of the occurrences of controlled access phases. After sending a beacon period, hybrid coordinator starts contention free period. Following the end of the contention free period, contention period is started. In the second beacon period one can see that additional contention free period is started in between two contention periods for a short period of time. A summary of both functions/periods and how HCF uses them is given in the following two subsections.

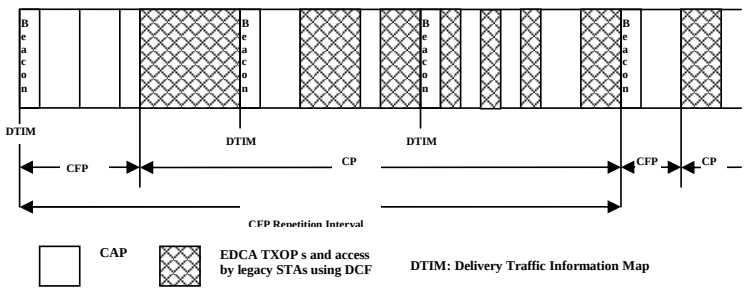

Figure 1: CAP/CFP/CP periods

In the following two subsections, we try to make it clear which functional-

ities of EDCA and HCCA affect their behavioural prediction. This will help understanding the correlation analysis of the third section.

2.1 Enhanced Distributed Channel Access (EDCA)

The enhanced distributed channel access function is defined to offer prioritized channel access. Traffic streams using this function are assigned user priorities at layers higher than the MAC layer. The assignment of user priorities is left to the service providers offering a high flexibility for network management. At the MAC layer, user priorities are grouped into 4 access categories. The access to the channel during the use of the EDCA function is also called a contention period because all access categories compete with each other to win the so called EDCA transmission opportunities. Stations receiving EDCA TXOPs are allowed to send their packets to the access point. Each access category has a backoff timer that is used for the contention process and is measured in *slotTimes*. There is a different maximum length of the transmission opportunity assigned to each access category. Different TXOPs makes sure that channel is not occupied with long frames of low priority packets. The maximum time length an access category can use for sending one frame is restricted with the TXOPs.

Consequently, there are four main parameters enabling the traffic differentiation by the use of EDCA. These are *CWmin[AC]* and *CWmax[AC] (minimum and maximum contention window lengths for each access category)*, *AIFS[AC] (arbitration inter frame space)* and *TXOPLimit[AC] (maximum duration an access category can use to send a frame)*. The values of these parameters are advertised at the beginning of each beacon period by the access point within the EDCA parameter set element. This element includes all EDCA related parameter values needed for the proper operation of the QoS facility during the contention period. Access points can tune the values of these parameters during run time with respect to channel load situation and networking policies. This point is open for further research and will be product specific on each access point.

The contention procedure is very well defined for EDCA, making simple reasoning possible such as if there is more traffic on the channel, there will be more collisions during contention. Additionally there will be more sources occupying the channel if there is more traffic. These two problems increase the loss and delay rates directly. Although some exceptions exist, which will be discussed in the third section, the loss, delay and jitter rates of traffic streams are mostly directly proportional to the load element parameters.

2.2 HCF Controlled Channel Access (HCCA)

In case a traffic stream has some constraints which cannot be dealt with the use of EDCA, the owner of this stream can tell the access point that this specific traffic stream needs to be polled in the schedule of HCCA. The hybrid coordination function uses HCCA in order to make sure that strict QoS requirements such as delay and loss rates of real time traffic streams are satisfied. During transmissions, the hybrid coordinator has a higher medium access priority compared to non access point stations by waiting only one *point coordination function inter frame space (PIFS)* period, which is smaller than *AIFS[AC]* (see above). Thus,

the hybrid coordinator can send its own packets and assigns HCCA TXOPs to other stations before any station using EDCA can have access to the channel after the channel has been sensed to be idle. All stations are informed about the beginning and the end of the use of HCCA. This allows the hybrid coordinator to have control over transmissions.

Any station wanting to use the HCCA for transmission sends a management frame to the QAP, which includes the traffic specification (TSPEC) of the current stream, thus giving details about its requirements. Traffic specifications include all necessary information to describe a type of traffic like nominal MAC protocol data unit (MSDU) size, mean data rate, suspension interval, delay, surplus bandwidth allowance and maximum service interval where the service interval (SI) is the time between successive transmission opportunities assigned to a traffic stream. Using this information, the hybrid coordinator should decide whether or not to accept the incoming traffic stream and what kind of scheduling mechanism to use in case of acceptance. This decision algorithm is an open issue in the standard and is one of the most challenging tasks to be realized.

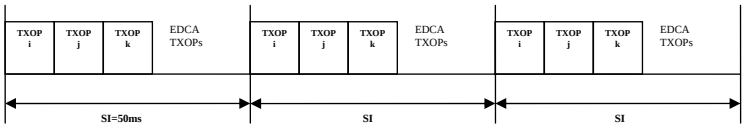

Figure 2: Schedule for three (i-k) QSTA streams

If the QSTAs send traffic specifications including their allowable maximum service intervals, then the draft recommends a scheduling method which has relatively a better organized structure, affecting the traffic treatment and the experienced QoS significantly Figure 2 shows the difference. Compared to Figure 1, where a regularity of the access phases does not exist, here on the contrary the transmission schedule shows an ordered behaviour. One can see that the distributed TXOPs are repeated at the beginning of each service interval so that stations have the chance to send their packets periodically. The recommended practice of the standard describes the choice of the service intervals as follows. First of all, the access point finds the smallest of the maximum service intervals. Afterwards, it selects a number which is smaller than the smallest maximum service interval and which is a sub multiple of the beacon interval. This means the service interval is determined by the incoming traffic and this information is only implicitly available to the stations. Additionally the amount of time reserved for contention free period, hence to the HCCA TXOPs, is left to the hybrid coordinator except that it must be smaller than the so called dot11CAPlimit (max percentage of time that can be reserved for controlled access phases). These two variables (service interval and the time reserved for contention free period) are the main factors determining the structure of the schedule. In the following section, we are going to concentrate on the effects of these two variables to the quality of information given by QBSS load elements and see that depending on these variables, the new protocol shows unpredictable behaviour which avoids that load element parameters give reliable information about the QoS one may expect from an access point.

3 Simulations

In order to show the information given by the QBSS load element, we run simulations with different traffic and parameter combinations. We concentrated on the effects of the percentage of time reserved for HCF controlled channel access and the service interval length chosen by the access point under mixed traffic load.

The aim of this paper is to find parameters that are indicative for QoS of each traffic type (like voice, or video traffic) in an environment exposed to mixed traffic as described below. For this purpose we measure the amount of useful information in the QBSS load element through its correlation with our QoS metric of interest. The considered QoS metric depends on which type of traffic from the traffic mixture is of interest. We expect that channel utilization and number of connected stations show positive correlation with all QoS metrics while the available admission capacity correlates negatively with all QoS metrics. Note that alternating sign of the correlation across the system parameters as well as a high variability indicates low reliable expressive power of the QBSS load element.

The results of the following subsections show that, the information captured by the QBSS load element is seemly inconsistent. Therefore we included an extra parameter in the correlation study that is the number of traffic streams of the different types of traffic. Traffic is divided up into different priority classes and some of the different types of traffic are associated with different priority classes, we therefore will discuss the priority classes rather than the traffic types. We show that this extra parameter is in many cases highly correlated with the QoS metric and therefore we propose to include the number of stations guaranteed the different priority levels as an additional parameter in the QBSS load element. Especially for voice and video traffic streams QoS evaluation can be substantially improved.

3.1 Simulation Environment

We consider as infrastructure a QoS enabled basic service set (QBSS) composed of a QoS enabled access point (QAP) and a number of stations (QSTAs) associated with the QAP. A slightly modified version of Qiang Ni's ns2 implementation of EDCF/HCF is used to perform simulation runs based on this infrastructure [9].

Although 802.11e defines many parameters, we focused on the service interval (SI) and the relative amount of time reserved for HCCA as system specific variables. Together with the considered traffic types, we input a total of three variables. We define 7 different traffic types similar to the work in [3, 5, 12] as follows.

1. Bidirectional constant bit rate (CBR) voice traffic using UDP with a packet size of 160 bytes and packet interval 20ms (8 Kbytes/s) corresponding to the VoIP codec G.711. (1st access category)
2. CBR video traffic using UDP with a packet size 1280 bytes and packet interval of 10ms (128 Kbytes/s). (2nd access category) (High quality Video)
3. 12 simulated VBR video traffic streams using UDP with minimum packet size of 28 and maximum packet size of 1024 bytes with an average packet interval

of 23ms corresponding to 30Kbytes/s. (2nd access category) (Average Quality Video)

4. Bidirectional interactive traffic using TCP with a packet size of 1100 bytes and exponentially distributed arrival rates having an average of 50ms on time, 30ms off time and sending rate of 60Kbits/s during on times corresponding to an average of 10Kbytes/s. This complies with the interactive traffic definition of 3GPP TS 22.105 and ITU G.1010. (3rd access category)
5. CBR Background traffic using UDP with a packet size of 1200 bytes and inter arrival time of 100ms corresponding to 12Kbytes/s. (4th access category)
6. VBR Background traffic using TCP with a packet size of 1200 bytes and exponentially distributed inter arrival times having an average of 1000ms off and 1000ms on times with a sending rate of 300Kbits/s corresponding to heavy load 160Kbytes/s traffic. (4th access category)
7. VBR Background traffic using TCP with a packet size of 1200 bytes and exponentially distributed inter arrival times having an average of 1000ms off and 200ms on times with a sending rate of 100Kbits/s corresponding to low load 11Kbytes/s traffic. (4th access category) (3GPP TS 22.105 Web Browsing-HTML definition.)

We investigate three different scenarios, where HCCA obtains 40%, 80% and 98% of the model time, respectively. We chose service intervals of length 4.5ms and 50ms as they were representative for the behaviour of most of the other combinations we tried. A simulation takes 30 seconds model time. Traffic streams enter to the simulation within the first 5 seconds with small intervals and the measurements of delay, jitter and loss rates are done over the last 10 seconds. The simulation results in general converge to steady state within the first 10 to 15 seconds. The traffic load in a simulation is composed of up to 7 bidirectional voice traffic streams (1st traffic type), 5 video traffic streams (2nd or/and 3rd traffic types), 10 bidirectional interactive traffic streams (4th traffic type) and 10 background traffic streams (5th and/or 6th and/or 7th traffic types).

4 Results

We ran simulations of an access point under the load as described in the previous section. The considered metrics are delay, jitter and loss rates of a certain traffic stream so that one can have an intuition about the possible QoS received by the users. For VoIP streams (1st traffic type), as opposed to the other traffic types, we evaluate the results on the basis of the mean opinion score (MOS) values defined in ITU-T Rec. G.107 which is the widely accepted metric of industrial organizations to measure the quality of VoIP applications [10, 11]. MOS rates calls on a scale of 1 to 5. The calculation of the MOS value is done firstly by calculating the so called rating factor R which is also defined in ITU-T Rec. G.107.

$$R = Ro - Is - Id - Ie - eff + A \tag{1}$$

$$MOS = 1 + 0.035R + R(R-60)(100-R)7 * 10^{-6} \tag{2}$$

where the factor Is represents impairments occuring simultaneously with the voice signal, Id represents delay impairments and Ie represents codec impairments. Additionally A is a compensation of impairments when there are some

advantages existing on the user side. Ro, Is and Id are also other impairment factors decreasing the total MOS value. [10]. For calculating the MOS values we used a tool in which a number of default values are preset.

If from the mixed traffic on the access point one is interested in the voice traffic, the obtained MOS values must be studied, while for video traffic delay, loss rate and jitter are directly used as QoS metrics. The following two subsections are devoted to our results for voice and video traffic respectively. We skip here results for interactive and background traffic.

4.1 Voice Traffic Results

The common QoS metric for voice traffic is the MOS value. To find out what system parameters are indicative for the obtained MOS value we correlate the MOS value of the voice streams in our mixed traffic with the three QBSS load element parameters station count, channel utilisation and available admission capacity. Additionally we correlate the MOS value with a fourth system parameter, the number of existing voice traffic streams (labelled 1st priority #). We simulated different scenarios with two variables, the service interval length and the percentage of time reserved for HCCA. We distinguish two cases of service interval length, 4.5ms and 50ms and three different percentages of time reserved for HCCA, 40%, 80% and 98%, as shown in the total of six different configurations in Table 1. This table summarizes the correlation between MOS values and the QBSS Load elements and between MOS values and the number of voice traffic streams.

Table 1: Correlations of voice traffic; SI and HCCA percentage versus QBSS load elements and voice traffic number

	40%HCCA		80%HCCA		98%HCCA	
Service Interval	4.5ms	50ms	4.5ms	50ms	4.5ms	50ms
Station Count	-0.11	-0.29	-0.27	-0.25	0	-0.19
Channel Util.	0.55	0.01	0.20	-0.01	0.28	0.05
Avail. Adm.C.	0.06	0.26	0.14	0.59	0.11	0.08
1st priority #	-0.86	-0.69	-0.90	-0.70	-0.79	-0.73

We observe that the number of stations indeed correlates negatively with the QoS metric, but correlation is for none of the system configurations more than roughly 30% which we consider low correlation. There is an intuitive explanation for this result. Some stations, like the ones producing small background traffic, put very little load on the system and hence have very little effect on QoS. Therefore one cannot estimate QoS based on the number of stations. It should be noted, however, that for the larger service interval the MOS value and the station count correlate slightly more since the hybrid controller can reserve transmission opportunities for each demanding stream and the remaining time used for EDCA determines the quality of the packets sent later on which is directly correlated with the number of stations.

For the short service interval, the number of connected stations correlates less with the MOS value and if 98% of the time is reserved for HCCA, lower priority streams only obtain TXOPs if there is no first priority stream requiring

admission. Similar to the above argument then the number of stations does not correlate with the MOS value of the first priority stream.

For the correlation between channel utilisation and MOS value we observe the reverse. For the long service intervals correlation is negligible. This is because voice traffic has the highest priority and does in many cases not get disturbed by lower priority traffic. When using the short service intervals, however, voice traffic competes with many background traffic streams and surprisingly correlation between channel utilisation and MOS value gets rather high (See Fig. 3(a)). This result is mainly due to the increasing number of internal collisions over the access point. As the number of stations increases, the number of internal collisions increases and channel utilization becomes less (See Fig. 3(b)). Therefore we get lower channel utilization rates for high loads where the MOS values are very low. For lower loads we get channel utilization up to a hundred percent where the MOS values are very high. As a result, there is high positive correlation with the channel utilization rate.

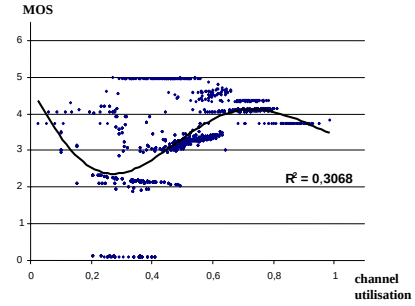

(a) MOS versus channel utilization (Note that most of the points are between 0.2 and 0.9 causing a positive correlation of 0.55)

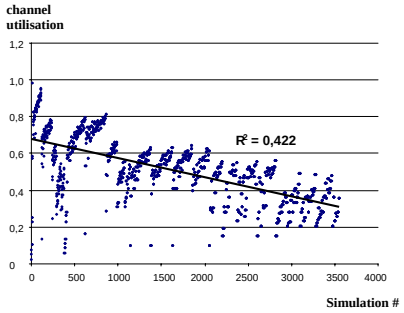

(b) channel utilization in the course of simulation runs (Note that the numbers of active streams of different types increase with the simulation number)

Figure 3: The relationship between Channel Utilization and MOS values during small service intervals

In case of longer service intervals, more available admission capacity means better MOS values for voice traffic. On the other hand if the service interval drops to 4.5ms, than there is no observable relationship between the available admission capacity and the MOS values. It is reasonable to have some positive correlation if the service interval is high. In such a case, if also the percentage of HCCA is enough, available admission capacity means that TXOPs could have been assigned for all the traffic on the access point, which indicates a positive correlation with MOS values. On the other hand, such a relationship does not exist if there is a small service interval. Available admission capacity reaches to minimum values just after one video and one voice traffic. At this point, depending on the percentage of HCCA being used, the results are mainly affected by the length of EDCA and not HCCA.

As illustrated in the last row in Table 1, we find that the number of connected 1st priority streams correlates much more (and negatively) with the MOS value than any of the QBSS load element parameters and hence seems to be a good indication for the expected QoS of voice streams.

4.2 Video Traffic

Because we do not have a metric like MOS defined for video traffic streams, we are going to give the correlations of the information elements with delay, jitter and loss rates of the video traffic streams. In fact, as given in Table 2, the results are very unstable for video traffic. If the traffic combination changes the results change also. Nevertheless the sign of the correlation is constant. The delay and the number of stations correlate positively, as expected.

Since voice traffic has higher priority than video traffic, the number of voice traffic streams increases the delay of video traffic directly. Additionally, video traffic streams affect each other more than all the other traffic streams, because video packets come more often and are larger. This causes a positive correlation between station count and delay. If the number of traffic streams associated with the access point increases, the schedule of the HC becomes more stable and therefore the jitter values decrease, which results in negative correlation. The correlation with the loss rate is more stable compared to others, which can be explained in a straightforward manner. On the other hand, channel utilization and available admission capacity shows nearly no correlation with delay, jitter or loss rates.

Table 2: Correlations of video traffic; SI and HCCA percentage versus QBSS load elements and video traffic number

	4.5 ms SI			50ms SI		
	Delay	Jitter	Loss	Delay	Jitter	Loss
	40% HCCA					
Station Count	-0.11	0.08	0.22	0.23	-0.23	0.22
Channel Util.	-0.21	0.05	-0.40	-0.05	-0.14	-0.06
Avail. Adm.C.	-0.23	0.59	0.68	-0.02	0.07	-0.02
2st priority #	0.69	-0.37	0.11	0.90	-0.71	0.89
	80% HCCA					
Station Count	-0.11	0.08	0.22	0.23	-0.23	0.22
Channel Util.	-0.21	0.05	-0.40	-0.05	-0.14	-0.06
Avail. Adm.C.	-0.23	0.59	0.68	-0.02	0.07	-0.02
2st priority #	0.69	-0.37	0.11	0.90	-0.71	0.89
	98% HCCA					
Station Count	0.12	0.01	0.15	0.26	-0.15	0.29
Channel Util.	-0.18	0.10	-0.18	-0.09	-0.07	0.23
Avail. Adm.C.	0	-0.02	0	0.13	0.04	-0.19
2st priority #	0.57	0.07	0.51	0.72	-0.81	0.83

The effect of the number of video traffic streams has mostly a high correlation with delay, jitter and loss rates of the video traffic. This is due to the fact that video traffic streams are relatively heavy loaded and constitute the main channel utilization. If the service interval is small, at most one video traffic can receive TXOP and the remaining use the contention period. Because the contention period is short and video packets come very often, the bandwidth reserved to the video traffic is not enough and the loss rate increases suddenly. The jitter rate drops because the video packets coming very often allow a self repeating schedule keeping delays nearly constant. But this does not have any importance if the service interval is low, because the loss rate increases very fast making it impossible to have more than two video traffic streams with an acceptable level of QoS.

If the service interval is large and the time reserved for contention free period is long, TXOPs given at the beginning of the service interval do not fully utilise the amount of time reserved for scheduling which results the start of contention period. Within the contention period, as the number of voice streams increases, the loss rate increases due to collisions and delay increases as well. On the other hand longer delays achieve saturation, decreasing the variation in delay.

5 Evaluation of Results and Enhancement Recommendation

The results of the Sections 4.1 and 4.2 show that the load element parameters channel utilization and available admission capacity are capable of giving meaningful information in some of the parameter combinations because they are moderately correlated with the metric of interest (MOS or delay, jitter and loss rates) in these cases. However this information is not reliable because it depends on many other variables and is not stable. The station count is in none of the cases a reliable source of information to estimate the expected QoS over an access point as there is no observed correlation bigger than -0.30. Such a low correlation cannot be regarded as a source of information in decision making. Even more so since there is another parameter, the number of streams belonging to the respective priority class, that correlates much stronger.

In fact the number of traffic streams in each priority should definitely give an idea about the expected QoS, because in most cases, the number of any kind of traffic that can be transmitted over an access point has a maximum value and this depends on the standard being used. For 802.11b the maximum number of voice calls using G.711 codec is about 5 which can further be optimized to 7 with more efficient algorithms [13]. For this reason we also compared the correlation between the number of traffic streams in each priority class and the QoS indicator values (MOS, delay, jitter and loss rates). The correlations between the number of traffic streams using the first priority and the QoS indicators can be found in Table 1 and the second priority can be found in Table 2. As it can be observed, the correlations reach up to -0.9 for some of the cases. Except for the correlation between jitter and the number of second priority traffic, the magnitude of the correlations is significantly higher than what we had for the load element parameters. Hence, it is worth having this additional information in the QBSS load element which does not bring a considerably extra load to the beacon frame. An extension of the current draft with the number of traffic using different priority levels can ease the choice procedure substantially.

6 Conclusion

In this paper, we presented the QBSS load element and its use in the context of 802.11e. Our simulation results showed that choosing a QAP based upon the fields of the received QBSS load element fields, does not always lead to an association with the best available access point.

In order to delineate the poorness of the QBSS load element information, we listed the results of the correlation between the QBSS load element parameters and QoS factors like delay, jitter and loss rate. We showed that, in most of

the cases the correlation is very low and unfortunately even the sign of the correlation can change if one uses a different set of parameters.

We observed that in all cases with decreasing HCCA percentage, the decision accuracy improved significantly supporting our claim that the HCCA brings extra irregularity and complexity to the new standard. We conclude that, depending on the internal configuration of the QAP, meaning the settings of the 802.11e relevant parameters, the provided network service cannot be bound barely on the load information.

Although we presented two of the most important parameters affecting the performance of 802.11e, incorporating more parameters into the decision process, for instance considering the number of traffic streams in different priorities, can improve the accuracy of the decision. We are going to analyse other parameters of the TSPEC like surplus bandwidth allowance and delay bound, which will be included in our next study.

References

[1] D. Chalmers, M. Sloman, A Survey Of Quality Of Service In Mobile Computing Environment. IEEE Communications Surveys, pages 1-10, Second Quarter 1999.

[2] NS software and documentation is available at the following site: http://www.isi.edu/nsnam/ns/

[3] P.Ansel et a.l., "An Efficient Scheduling Scheme for IEEE 802.11e", conference proceedings, WiOpt, Modeling and Optimization in Mobile, Ad Hoc and Wireless Networks, Cambridge, UK, March 2004.

[4] G. Boggia et a.l., "Feedback based bandwidth allocation with call admission control for providing delay guarantees in IEEE 802.11e networks", Computer Communications, Elsevier, 28(3):325-337, February 2005.

[5] Sunghyun Choi, "Protection and guarantee for voice and video traffic in IEEE 802.11e wireless LANs", IEEE Conference on Computer Communications, pp.0-0, Mar. 2004

[6] IEEE 802.11 WG, Draft Supplement to Part 11: Wireless Medium Access Control (MAC) and physical layer (PHY) specifications: Amendment 7: Medium Access Control (MAC) Enhancements for Quality of Service (QoS), IEEE Std 802.11e/D9.0, August 2004.

[7] Zhang Q. et a.l., Efficient mobility management for vertical handoff between WWAN and WLAN. IEEE Communications, 41 (11) (2003) 102–108.

[8] K. Murray, D. Pesch, "Intelligent Network Access and Inter-System Handover Control in Heterogeneous Wireless Access Networks for Smart Space Environments", conference proceedings, 1st IEEE International Symposium on Wireless Communication Systems, Mauritius, September 2004

[9] http://www-sop.inria.fr/planete/qni/fhcf/

[10] ITU-T Rec. G.107. The E-Model, a Computational Model for Use in Transmission Planning. International Telecommunication Union, CHGenf, 2002.

[11] ITU-T Rec. P.85. A Method for Subjective Performance Assessment of the Quality of Speech Voice Output Devices. International Telecommunication Union, CHGenf, 1994.

[12] Zhu, H. and Chlamtac, I, "An Analytical Model for IEEE 802.11e EDCF Differential Services", IEEE ICCCN, Dallas, October 2003.

[13] Coupechoux, M. et a.l.,"Voice over IEEE 802.11b Capacity", ITC Specialist Seminar on Performance Evaluation of Wireless and Mobile Systems, Antwerp, 2004.

Performance Evaluation of Processor Allocation Strategies in the 2-Dimensional Mesh Network

S. Bani-Mohammad[1], M. Ould-Khaoua[1] and I. Ababneh[2]

[1]Department of Computing Science
University of Glasgow
Glasgow G12 8RZ
UK
Email: {saad, Mohamed}@dcs.gla.ac.uk

[2]Department of Computing Science
Al al-Bayt University
Mafraq, Jordan
Email: ismail@alalbayt.aabu.edu.jo

Abstract

Contiguous allocation of parallel jobs usually suffers from the degrading effects of fragmentation as it requires that the allocated processors be contiguous and have the same topology as the network connecting these processors. In this paper, two non-contiguous processor allocation strategies, referred to as Paging and Greedy-Available respectively, are suggested for the 2D mesh network, and are compared using simulation against the well-known contiguous First Fit strategy. The results reveal that the proposed non-contiguous strategies exhibit superior performance properties despite the added contention that results from non-contiguity.

Keywords: Multicomputers, Fragmentation, Scheduling Effectiveness, Turnaround Time, External Message Interference, Dispersal Ratio, Performance Comparison, Simulation.

1. Introduction

In a multicomputer, processor allocation is responsible for selecting the set of processors on which parallel jobs are executed. Most strategies employed in a multicomputer are based on *contiguous* allocation, where the processors allocated to a parallel job are physically contiguous and have the same topology as the network connecting the processors [3, 9, 10, 12]. These strategies often result in high external processor fragmentation, as has been shown in [12]. External fragmentation occurs when there are free processors sufficient in number to satisfy the number requested by a parallel job, but they are not allocated to it because the free processors are not contiguous or they do not have the same topology as the network topology connecting these processors.

Several studies have attempted to reduce such fragmentation [2, 4, 10]. One solution suggested is non-contiguous allocation [2, 10]. In such a strategy, a job can

execute on multiple disjoint smaller sub-networks rather than always waiting until a single sub-network of the requested size is available. Although non-contiguous allocation increases message contention in the network, lifting the contiguity condition is expected to reduce processor fragmentation and increase processor utilization [10]. Folding has also been proposed for the 2D mesh [2, 4]. Folding permits applications to execute on fewer processors than they have requested, when necessary. This could improve the performance of contiguous and non-contiguous allocation, as demonstrated in [2, 4]. The problem with folding is that it requires that jobs be able to execute on a number of processors determined at load time.

Existing research studies [2, 4, 10] on both contiguous and non-contiguous allocation have been carried out in the context of the 2D mesh. The 2D mesh has been used as the underlying network in a number of practical and experimental parallel machines, such as iWARP [1] and Delta Touchstone [7]. In this study, we investigate the performance merits of non-contiguous allocation for reducing processor fragmentation on the 2D mesh and compare its performance to that of the contiguous allocation. To do so, two non-contiguous allocation strategies, notably Greedy-Available and Paging, are suggested. The Greedy-Available and Paging strategies combine the desirable features of both contiguous and non-contiguous allocation strategies. The Greedy-Available strategy only allocates jobs non-contiguously when external fragmentation occurs (i.e., when contiguous allocation fails to allocate an incoming job). In the Paging strategy, a request for a given number of processors is satisfied by the first free pages in a row major scan of the mesh, and some degree of contiguity is maintained through the nature of the row major scan. The performance of both strategies will be compared against the existing well known contiguous First Fit [12] under contention and contention-free communication models. The First Fit strategy allocates an incoming job to the first available sub-mesh that is found [12]. In this study, First Fit has been used to represent the contiguous class of strategies as it has been found to perform well [12]. In order to make comparison fair and realistic, we will consider the contention model to assess the effects of contention on the performance of non-contiguous allocation when comparing against the First fit strategy.

The rest of the paper is organised as follows. Section 2 contains a brief summary of allocation strategies previously proposed for 2D mesh. Section 3 contains the proposed non-contiguous allocation strategies. Section 4 compares the performance of the contiguous and non-contiguous allocation strategies. Section 5 concludes this study.

2. Related Work

Two Dimensional Buddy System (2*DBS*): The 2*DBS* allocation [8] applies to square mesh systems with power of two side lengths. Processors allocated to jobs also form square sub-meshes with power of two side lengths. If a job requests a sub-mesh of size $a \times b$ such that $a \leq b$, the 2DBS allocates a sub-mesh of size $s \times s$, where $s = 2^{\lceil log(max(a,b)) \rceil}$. This strategy suffers from high fragmentation. Also, it cannot be used for non-square meshes and does not have complete sub-mesh recognition ability.

Frame Sliding (*FS*): The frame sliding strategy [9] searches for an appropriate allocation using a set of sequenced non-overlapping processor frames that cover the whole target mesh. It is assumed that arriving jobs request processor subsets of rectangular shape. Processor frames of the same side lengths as the requested sub-mesh are searched from left to right and from bottom to top. Jumps to successive frames are by the job's width and height. The goal of searching is to find a suitable

frame for allocation; i.e., all its processors are free and it is big enough to accommodate the allocation request. This process ends either with finding a suitable allocation or when all frames are scanned and no appropriate frame is found. A problem with this strategy is that it cannot recognise all free frames because the jumps are by the job's width and height [10]. In this strategy, the search process starts with the lowest leftmost available node. If processors in the currently examined frame are not all available, the frame is slide over the plane of the mesh to the next candidate frame, with horizontal and vertical strides equivalent to, respectively, the width and the length of the requested sub-mesh. The frame first slides horizontally from left to right until it exceeds the boundary of the mesh. At that point, a vertical slide takes place. Further sliding again takes place horizontally from right to left, and so on. This strategy does not guarantee complete sub-mesh recognition, i.e., an available free sub-mesh can go undetected by the strategy [3].

First Fit (*FF*) *and Best Fit* (*BF*): The problem of missing an existing possible allocation explained above is solved using First Fit and Best Fit allocation strategies [12]. The free sub-meshes are scanned and First Fit allocates the first sub-mesh that is large enough to hold the job, whereas Best Fit allocates the smallest suitable sub-mesh. Bit arrays are used for scanning of available processors.

The above allocation strategies consider only contiguous regions for the execution of a job and are referred to as contiguous allocations. Distance of the communication path is expected to be minimized in contiguous allocations. Only messages generated by the same process are expected within a sub-mesh and therefore cause no interjob contention in the network. On the other hand, the restriction that jobs have to be allocated to contiguous processors reduces the chance of successfully allocating a job. It is possible for the mesh to fail to allocate a job while a sufficient number of processors are available [2], i.e., fragmentation are occurred in these strategies.

Hardware advances such as wormhole routing and faster switching techniques have made the communication latency less sensitive to the distance between the communicating nodes. This makes allocating a job to non-contiguous processors plausible. Allocation of jobs to non-contiguous nodes allows jobs to be executed without waiting if the number of available processors is sufficient [2]. In the next paragraphs, we present non-contiguous allocation strategies that have been proposed in previous studies [2, 10, 11].

Random: The random allocation is a straightforward strategy in which a request for a given number of processors is satisfied with a number of processors selected randomly [10]. Both internal and external fragmentations are eliminated since all jobs are assigned exactly the requested number of processors if available. Because no contiguity is enforced under this strategy, we would expect much communication interference amongst jobs.

Naive: In the naive algorithm [11], a request for a given number of processors is allocated to the first free nodes found in a row major scan.

Multiple Buddy System (*MBS*): The *MBS* is an extension of the 2D buddy strategy. The mesh is divided into non-overlapped square sub-meshes with side lengths equal to the powers of two upon initialization. The number of processors, p, requested by an incoming job is factorized into a base of four representation of $\sum_{i=0}^{\lfloor \log_4 p \rfloor} d_i \times \left(2^i \times 2^i\right)$, where $0 \le d_i \le 3$. The request is then allocated to the mesh according to the factorized number in which d_i number of $2^i \times 2^i$ blocks is required. If a required block is unavailable, *MBS* recursively searches for a bigger block and

repeatedly breaks it down into buddies until it produces blocks of the desired size. If that fails, the requested block is then broken into four requests for smaller blocks and the searching process repeats [10].

Adaptive Non-Contiguous Allocation (*ANCA*): In [2], *ANCA* always attempts to allocate a job contiguously. When contiguous allocation fails, it breaks a job request into equal-sized sub-frames. These sub-frames are then allocated to available locations if possible; otherwise, each of these sub-frames is broken into two equal-sized sub-frames, and then *ANCA* try to allocate these sub-frames to available locations and thus take advantage of non-contiguous allocation, and so on.

The random and naive strategies ignore the contiguity of processors allocated to a job, while may cause increases in the communication delay. *MBS* and *ANCA* strategies maintain some degree of contiguity between processors allocated to the job and alleviate communication overhead.

Our proposed strategy (Greedy-Available) maintains degree of contiguity between processors larger than that of the previous non-contiguous allocation strategies if the number of requested processors is available in the mesh so that the communication between processors in Greedy-Available is lower than that of previous non-contiguous allocation strategies. Moreover, it eliminates both internal and external fragmentation.

3. Proposed Allocation Strategies

The target system is a $W \times L$ 2D mesh, where W is the width of the square mesh and L its length. Every processor is denoted by a coordinate (x, y), where $1 \le x \le W$ and $1 \le y \le L$ [5]. Each processor is connected by bidirectional communication links to its neighbour processors, as depicted in Fig. 1. This figure shows an example of a 4×4 2D mesh, where allocated processors are shaded and free processors are white. If a job requests the allocation of sub-mesh of size 2×2 contiguous allocation fails because no 2×2 sub-mesh of free processors is available, however the four free processors can be allocated to the job if allocation is non-contiguous. In what follows we assume that a parallel job requests, when it arrives, the allocation of a 2D sub-mesh $S(a,b)$ of width $a \le W$ and length $b \le L$. The following definitions have been adopted from [5].

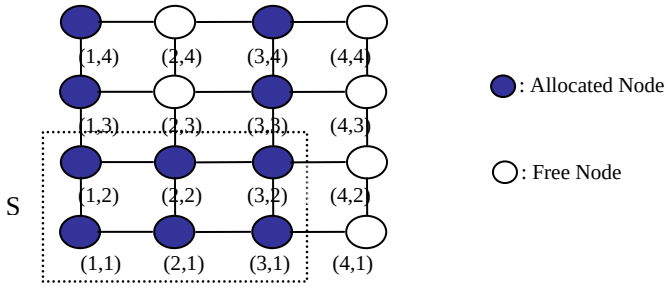

Fig. 1: An Example of a 4×4 2D

***Definition* 1**: *A sub-mesh* $S(w,l)$ *of width* w *and length* l, *where* $1 \le w \le W$ *and* $1 \le l \le L$ *is specified by the coordinates* (x,y) *and* (x',y'), *where* (x,y) is the lower left corner of S, (x',y') *is the upper right corner, and so* $w = x' - x + 1$ *and* $l = y' - y + 1$. *The lower left corner node is called the base node of the sub-mesh,*

whereas the upper right corner node is the end node. For example (1, 1, 3, 2) *represents the* 3×2 *sub-mesh* S *in Fig. 1. The base node of the sub-mesh is* (1, 1), *and its end node is* (3, 2).

***Definition* 2**: *The size of* $S(w,l)$ *is* $w \times l$.

***Definition* 3**: *An allocated sub-mesh is one whose processors are all allocated to a parallel job.*

***Definition* 4**: *A free sub-mesh is one whose processors are all unallocated.*

***Definition* 5**: *A suitable sub-mesh* $S(x,y)$ *is a free sub-mesh that satisfies the conditions:* $x \geq a$ *and* $y \geq b$ *assuming that the allocation of* $S(a,b)$ *is requested.*

In this study, it is assumed that parallel jobs are selected for allocation and execution using FCFS strategy. This strategy is chosen because it is fair and it is widely used in other studies [2, 3, 5, 10] and because this research deals with the allocation problem. In the next two sub-sections, we describe the two non-contiguous allocation strategies.

3.1 Greedy-Available Strategy

In the Greedy-Available strategy, when a parallel job is selected for allocation a sub-mesh suitable for the entire job is searched for. If such sub-mesh is found it is allocated to the job and allocation is done. Otherwise, the largest free sub-mesh that can fit inside $S(a,b)$ is allocated. Then, the largest free sub-mesh whose side lengths do not exceed the corresponding side lengths of the previous allocated sub-mesh is searched for and allocated if this does not result in allocating more processors than $a \times b$. This last step is repeated until $a \times b$ processors are allocated.

This allocation process is implemented by the algorithm bellow, illustrated in Fig. 2. Note that allocation always succeeds if the number of free processors $\geq a \times b$, and scanning for free sub-meshes uses the First Fit strategy. Moreover, it can be noticed that this strategy maintains some contiguity by allocating large sub-meshes.

***Procedure Greedy-Available_Submesh_Allocation* (*a, b*):**

Total_allocated = 0; Job_Size = a×b

Step 1. If (*number of free processors < Job_Size*) *return failure*

Step 2. If (*there is a free S* (*x, y*) *suitable for S*(*a, b*)) *allocate the first one* (*i.e., First Fit*) *and return success*

Step 3. aa=a and bb=b

Step 4. Subtract 1 from max(*aa, bb*) *if max > 1*

Step 5. If (*Total _allocated+ aa×bb > Job_Size*) *go to step 4*

Step 6. If (*there is a free S*(*aa, bb*)) *allocate it using First Fit,Total_allocated = Total_allocated + aa×bb*

Step 7. If (*Total_allocated = Job_Size*) *return success else go to step 5*

End.

Fig. 2: Outline of the Greedy-Available allocation algorithm

3.2 Paging Strategy

The entire 2D mesh is divided into pages that are sub-meshes with equal sides' length of 2^{size_index}, where $size\_index$ is a positive integer. A page is the allocation unit. The pages are indexed according to the row-major indexing scheme, as illustrated in Fig. 3. Busy arrays are used for scanning of available processors.

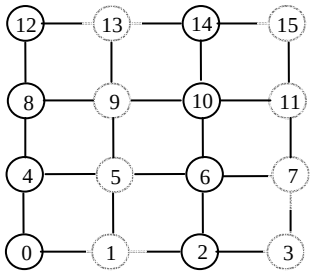

Fig. 3: Row-Major indexing

If the number of free pages is greater than or equal to the allocation request the pages are scanned starting with page zero until the needed number of free pages is allocated. A paging strategy is denoted as Paging($size\_index$). For example, Paging(2) means that the pages are 4×4 sub-mesh. The number of pages a job requests is computed using the equation:

$$Prequest = \lceil (a \times b) / Psize \rceil \quad (1)$$

where $Psize$ is the size of the pages, and a and b are again the side lengths of the requested sub-mesh. This allocation process is implemented by the Paging algorithm, illustrated in Fig. 4.

***Procedure Paging_Allocation* (*a, b*):**

Pside=2^{size_index}; *Psize*=*Pside*×*Pside*; *Mesh-Size* = $\lceil (W \times L)/Psize \rceil$;

Prequest = $\lceil (a \times b)/Psize \rceil$

Step 1. If (*number of free pages* < *Prequest*) *return failure else go to step 2*

Step 2. Allocate the first Prequest free pages to the job, and return success

End.

Fig. 4: Outline of the Paging allocation algorithm

The time taken by this algorithm to scan for and allocate free pages is in the worst case bounded from above by $W \times L$; that is, its time complexity is in $O(W \times L)$. Paging suffers from internal fragmentation when *size_index* > 0. The internal fragmentation of running jobs is computed using:

$$Internal\_Fragmentation = \sum_{jobs} \frac{Lost\_Processors}{Allocate\_Processors} \quad (2)$$

where $Lost\_Processors$ for a parallel job that requests $Program\_Size$ processors, but is allocated $Number\_of\_Allocated\_Pages$ is calculated using:

$$Lost\_Processors = Number\_of\_Allocated\_pages \times Psize - Program\_Size \quad (3)$$

To illustrate this, consider a paging strategy with $size\_index$ =1, and suppose a parallel job requests the allocation of a 3×3 sub-mesh. When allocation is carried out for the job it is allocated 3 pages (12 processors). Since only 9 processors are needed there is internal fragmentation of 3/12.

4. Performance Evaluation

Simulation has been used to evaluate the proposed allocation algorithms and compare them to First Fit for various mesh sizes and system loads. The main performance parameters used are the mean turnaround times of jobs and the mean scheduling effectiveness S_e. The scheduling effectiveness measures the ability of the allocation algorithms to avoid processor fragmentation [6]. At simulation time t the scheduling effectiveness is defined by the following equation:

$$S_e(t) = P_a(t) / \min(P, P_d(t)) \quad (4)$$

where P_a is the number of allocated processors, P the number of processors in the multicomputer, and P_d the total processor demand of the jobs in the multicomputer, running or waiting. For example, if $P = 100$, $P_d = 140$ and $P_a = 80$ the scheduling effectiveness is 0.8 and processor fragmentation is 0.2 (1.0 minus 0.8). However, if $P_d = 40$ and $P_a = 40$ the scheduling effectiveness is 1.0 and fragmentation is 0.0. The turnaround time is the time that a parallel job spends in the mesh, from arrival to departure. The mean scheduling effectiveness is taken over the entire simulation time, and the mean turnaround time is the average turnaround time taken for all completed jobs.

Every simulation run completes the execution of 500 parallel jobs. The runs are repeated enough times so that the mean performance values obtained have relative errors that do not exceed 5% under a confidence level of 95%. The side lengths of the sub-meshes requested by programs are uniformly distributed over the range from 1 to the mesh side length. Unless it is other specified the target mesh has equal sides of 32 processors.

As in previous studies [5, 6], we assume that programs arrive from a Poisson source at a rate of λ jobs per time unit. The rate is computed using the equation $\lambda = L \times P / (N \times T_e)$, where N is the mean number of processors requested by jobs, T_e their mean execution time, and L is the system load. The execution times are exponentially distributed with $T_e = 1$ time unit.

The performance of non-contiguous allocation depends on the contention that results from external message interference. The messages of two or more jobs may need to use the same communication link simultaneously. Therefore, this study uses two contention models. The first is the contention-free model, which ignores external message interference. The second is the contention model, where external message interference is modelled. The execution time of a job is not changed if the sub-mesh it is allocated is contiguous. However, if allocation is non-contiguous the execution time of the job is changed using the following formula, proposed by Chang and Mohapatra

[2].

$$New\_Execution\_Time = 1.60 \times Initial\_Execution\_Time \quad (5)$$

Figs. 5 and 6 show the mean scheduling effectiveness achieved by the non-contiguous allocation strategies and the contiguous allocation strategy First Fit under the two contention models. It can be noticed in the figures that Paging(0), Paging(1) and Greedy-Available are better than first fit for most system loads. Moreover, they are highly superior under medium to high loads. This is due to the fact that contiguous policies, represented by first fit, produce high external fragmentation under such loads. The scheduling effectiveness of first fit is high when the load is low because it is highly likely that a suitable contiguous sub-mesh is available for allocation to a job when it arrives to the mesh. The poor performance of Paging(2) and Paging(3) can be easily noticed. It is due to internal fragmentation caused by their large pages, respectively, (4×4 processors) and (8×8 processors) compared to the size of the mesh. It can also be noticed that the performance of Paging(0), Paging(1) and Greedy-Available strategies differs by little using contention-free model. Also, you can notice that Greedy-Available is better than Paging(0) and Paging(1) using contention model.

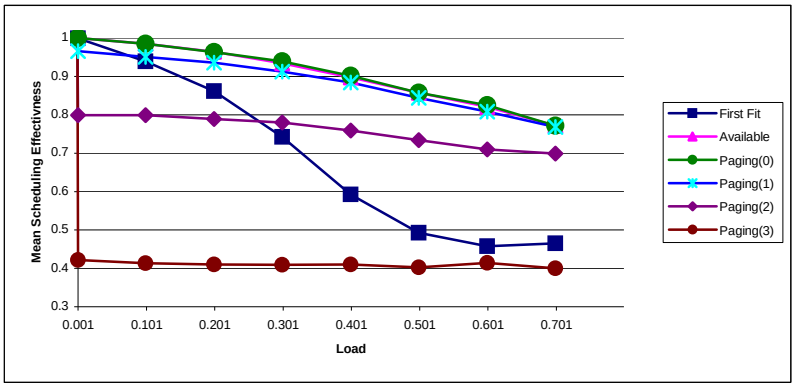

Fig. 5: Mean scheduling effectiveness for First Fit and the non-contiguous strategies using the contention-free model in a 32×32 mesh.

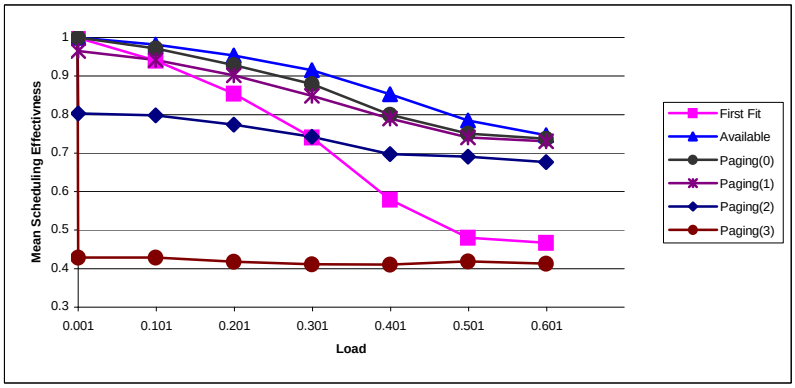

Fig. 6: Mean scheduling effectiveness for First Fit and the non-contiguous strategies using the contention model in a 32×32 mesh.

Figs. 7 and 8 show the mean turnaround times of First Fit and non-contiguous allocation strategies using both the contention-free and contention models. As can be seen in Fig. 7, Paging(0), Paging(1), Paging(2), and Greedy-Available perform much better than first fit using contention-free model. On the other hand, the performance of contiguous first fit strategy is superior to non-contiguous strategy Paging(3) for most system loads using both the contention-free and contention models, this is due to internal fragmentation caused by its large pages (8×8 processors). Moreover, the performance of Paging(0), Paging(1), and Greedy-Available is almost identical, and is better than Paging(2) is substantially better than Paging(3) using contention-free model. The poor performance of Paging(3) is due to its large pages size. This produces poor scheduling effectiveness as revealed in Figs. 5 and 6. It can also be noticed that, and as revealed in Fig. 8, Greedy-Available perform much better than first fit and Paging strategies for most system loads using contention model.

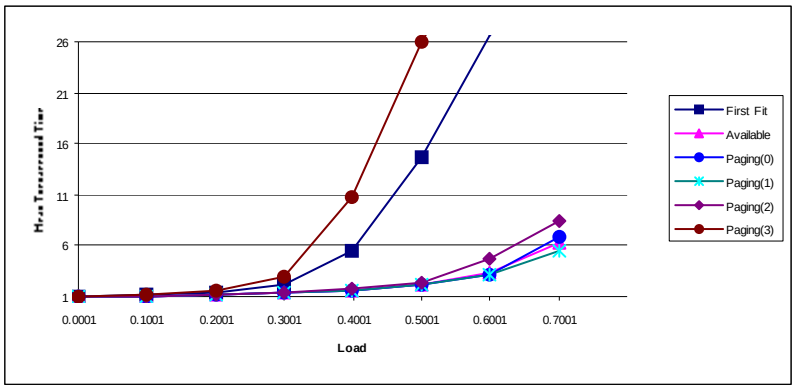

Fig. 7: Mean turnaround times for First Fit and the non-contiguous strategies using the contention-free model in a 32×32 mesh.

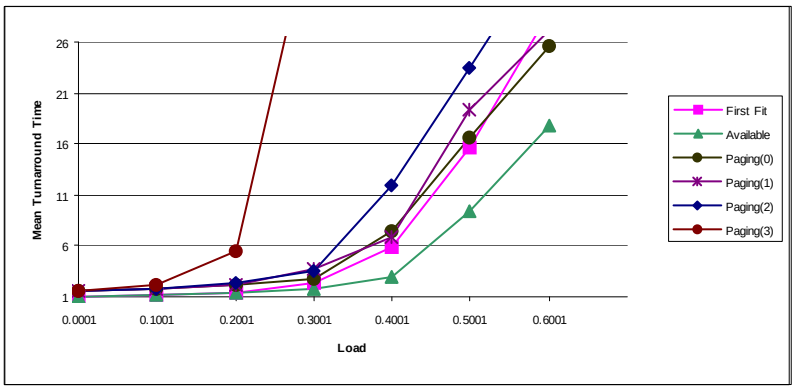

Fig. 8: Mean turnaround times for First Fit and the non-contiguous strategies using the contention model in a 32×32 mesh.

As expected, the advantage of non-contiguous allocation over contiguous allocation is lower when contention is modelled, however it remains substantial. We have also carried out simulation experiments for other mesh sizes, but this did not change the relative performance of the allocation strategies.

In addition to the scheduling effectiveness and turnaround times, we have measured two other performance parameters for the non-contiguous strategies. These

are the *mean dispersal ratio* and *mean distance* computed for all jobs. The dispersal ratio is a measure of the degree to which the sub-meshes allocated to a job are dispersed over the entire mesh. The higher the dispersal ratio the more likely it is that the job's messages will travel through nodes allocated to other jobs, potentially causing more contention in the interconnection network [10]. The dispersal ratio is defined as follows

$$Dispersal\ ratio = \sum_{jobs} \frac{(Xend - Xstart + 1) \times (Yend - Ystart + 1)}{(a \times b)} \tag{6}$$

where $(Xstart, Ystart)$ is the base of the smallest sub-mesh that includes all processors allocated to a job, and $(Xend, Yend)$ is its end. The values a and b are the side lengths of the parallel job's request.

The mean distance for a parallel job is defined as the sum of the distances amongst all pairs of processors allocated to it. The distance is defined as follows

$$Distance = \sum_{jobs} \frac{(abs(x - x_1)) + (abs(y - y_1))}{(a \times b)} \tag{7}$$

where (x, y, x_1, y_1) are the coordinates of the pairs of the processors allocated to a job. The values a and b are the side lengths of the parallel job's request. This distance is an indicator of contention; that is, the higher the distance the higher contention is likely to be.

Fig. 9 shows the mean dispersal ratio for the two non-contiguous strategies that yields the best performance (Greedy-Available and Paging(0)). The results reveal that Greedy-Available and Paging(0) have the same dispersal ratio for lighter loads (less than 0.3). However, the dispersal ratio of Greedy-Available is higher for high loads (greater than about 0.4).

Fig. 10 displays the mean distance calculated for all jobs in Paging(0) and Greedy-Available. As can be seen in the figure, the mean distance for Greedy-Available is less than that of Paging(0) for loads less than 0.6 approximately, while the mean distance for Greedy-Available is equivalent to that of Paging(0) for loads greater than 0.6 approximately. This suggests that it is expected that Paging(0) and Greedy-Available yield comparable performance across all loads. This conclusion is compatible with the values of the mean scheduling effectiveness and the mean turnaround times shown above. These results suggest that the mean distance is a better performance parameter than the dispersal ratio so that Greedy-Available is better than Paging(0).

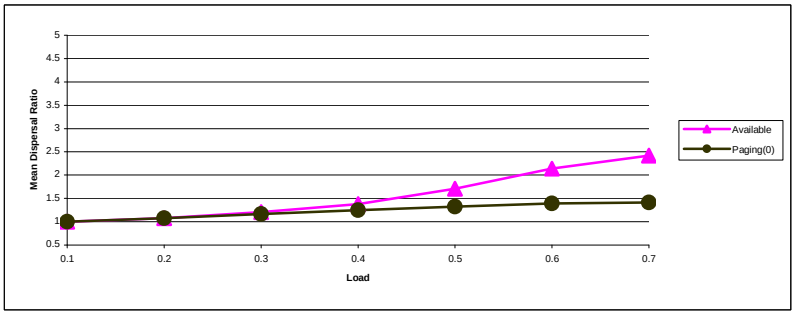

Fig. 9: Mean dispersal ratio for Paging(0) and Greedy-Available using the contention model in a 32×32 mesh.

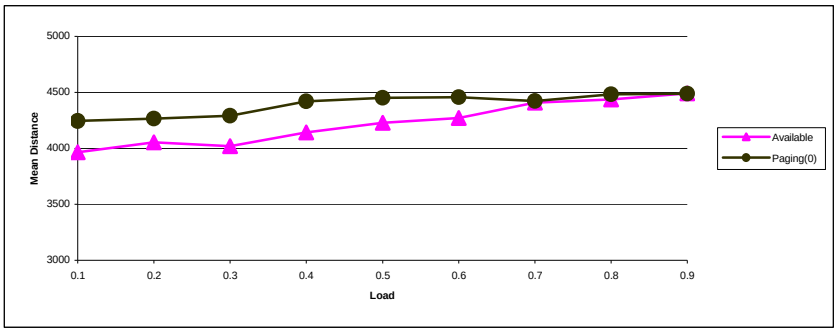

Fig. 10: Mean distance for Paging(0) and Greedy-Available using the contention model in a 32×32 mesh.

5. Conclusions

This study has investigated the performance merits of non-contiguous allocation in the 2D mesh. To this end, two non-contiguous allocation strategies, notably Greedy-Available and Paging, have been presented. The performance of both strategies has been compared against the existing contiguous First Fit under contention and contention-free communication models. The aim of using the contention model is to assess the effects of contention on the performance of non-contiguous allocation. Simulation results have revealed that non-contiguous allocation greatly improves performance despite the additional message contention inside the network that results from the interference among the messages of different jobs. Non-contiguous allocation produces superior utilization than its contiguous allocation counterpart. Results have also shown that when pages are small the proposed strategies exhibit good performance levels. However, when the pages are large the performance of Paging degrades because of internal fragmentation. An advantage of paging over Greedy-Available is that it can easily be implemented efficiently. Its execution time complexity is $O(W \times L)$.

As a continuation of this research in the future, it would be interesting to evaluate the performance of the contiguous and non-contiguous allocation strategies with different scheduling approaches. It would be also interesting to assess of the existing allocation strategies on a practical multicomputer.

References

[1] C. Peterson, J. Sutton, P. Wiley, iWARP: a 100-MPOS VLIW microprocessor for multicomputers, *IEEE Micro*, vol. 11, no. 13, 1991.

[2] C.-Y. Chang, P. Mohapatra, Performance improvement of allocation schemes for mesh-connected computers, *Journal of Parallel and Distributed Computing*, vol. 52, no. PC981459, pp. 40-68, 1998.

[3] G.-M. Chiu, S.-K. Chen, An efficient submesh allocation scheme for two-dimensional meshes with little overhead, *IEEE Transactions on Parallel & Distributed Systems*, vol. 11, no. 5, pp. 471-486, 1999.

[4] I. Ababneh, F. Fraij, Folding contiguous and non-contiguous space sharing policies for parallel computers, *Mu'tah Lil-Buhuth wad-Dirasat, Natural and Applied Sciences Series*, vol. 16, no. 3, pp. 9-34, 2001.

[5] I. Ababneh, S. Bani Mohammad, Noncontiguous Processor Allocation for

Three-Dimensional Mesh Multicomputers, *AMSE Advances in Modelling & Analysis*, vol. 8, no. 2, pp. 51-63, 2003.

[6] I. Ismail, J. Davis, Program-based static allocation policies for highly parallel computers, *Proc. IPCCC* 95, *IEEE Computer Society Press*, pp. 61-68, 1995.

[7] Intel Corporation, A Touchstone DELTA system description, 1991.

[8] K. Li, K.-H. Cheng, A Two-Dimensional Buddy System for Dynamic Resource Allocation in a Partitionable Mesh Connected System, *Journal of Parallel and Distributed Computing*, vol. 12, no. 1, pp. 79-83, 1991.

[9] P.-J. Chuang, N.-F. Tzeng, Allocating precise submeshes in mesh connected systems, *IEEE Transactions on Parallel and Distributed Systems*, vol. 5, no. 2, pp. 211-217, 1994.

[10] V. Lo, K. Windisch, W. Liu, B. Nitzberg, Non-contiguous processor allocation algorithms for mesh-connected multicomputers, *IEEE Transactions on Parallel and Distributed Systems*, vol. 8, no. 7, pp. 712-726, 1997.

[11] V. Lo, K. Windisch, W. Liu, B. Nitzberg, Non-contiguous processor allocation algorithms for distributed memory multicomputers, *Proceedings of Supercomputing* 94, pp. 227-236, 1994.

[12] Y. Zhu, Efficient processor allocation strategies for mesh-connected parallel computers, *Journal of Parallel and Distributed Computing*, vol. 16, no. 4, pp. 328-337, 1992.

Fault Detection Mechanisms for Autonomic Distributed Applications.

E.Grishikashvili Pereira[1], R. Pereira[2], A. Taleb-Bendiab[2]

Abstract

Autonomic computing includes a range of desirable properties, which are best achieved through middleware support. One of these properties is self-healing, the ability that systems may have to reconfigure themselves following the failure of some component. Recently, we have witnessed the development of models to provide middleware-based support for self-healing, service oriented distributed systems. The On-Demand Assembly and Delivery (OSAD) proposed previously by the authors consists of a number of components associated with fault-detection and fault-recovery. In this paper, we consider the performance impact of a number of fault-detection mechanisms, including pre-emptive detection and on-use detection.

1. Introduction

There is a growing body of knowledge associated with techniques related to self-healing [1] [2] [3] [4] . Although to a certain extent self-healing is not yet well defined in terms of scope and architectural models, it has received increased attention lately. A short definition of a self-healing system is a system that is capable of performing a reconfiguration step in order to recover from a permanent fault. The following requirements are likely to be relevant to most self-healing systems [5]: adaptability, dynamicity, awareness, autonomy, robustness, distributability, mobility and traceability. In addition, it is also essential that self-healing systems have strong monitoring abilities.

Self-healing properties are particularly useful in dynamic systems, particularly distributed, service oriented systems, where new services may be added and removed from the network, leading to the need for applications to reconfigure themselves [6] [7]. Ideally, such reconfiguration steps would be carried out without user intervention. Distributed service oriented systems provide application developers with the ability to build applications using services provided by other systems across available in a network. Such arrangement requires some form of organisation, normally involving a look up service, which contains information about all services that are available in the network. Applications wishing to use a networked service would carry out a search on the look up service and select, based on some criteria, the service that best matches its requirements. A well-known system based on distributed services is JINI, which provides some support for distributed service-oriented systems [8] [9].

[1] Department of Computing and IS Edge Hill Uni. College, St. Helen's Road, Ormskirk, L39 4QP, pereirae@edgehill.ac.uk

[2] School of Computing and Mathematical Sciences Liverpool John Moores University, Byrom Street, Liverpool, L3 3AF, UK, R.Pereira@livjm.ac.uk

This paper is organised as follows. Section 2 describes some relevant related work; section 3 provides an overview of the OSAD model architecture; section 4 describes fault detection mechanisms; section 5 describes the experiment and presents the results of the simulation; section 6 discusses the evaluation of the experiment and section 7 presents our conclusions.

2. Related Work

In order to perform self-healing systems should have the ability to modify their own behaviour in response to changes in their environment, such as resource variability, changing user needs, mobility and system faults. The lifecycle of self-healing systems consists of five major elements [10]:

1. Runtime monitoring of a given target, be it the system itself or its system parts or others;
2. Exception Event detection, including: an event arising from a deviation from a given model, normal system states and/or behaviour;
3. Diagnosis, including: identification of events and the right course of action;
4. Generating a plan of change such as architectural transformation during a software reconfiguration process;
5. Validation and enactment of a given change plan.

The monitoring and problem detection was described as one of the essential features of autonomic/self-healing systems in the report: "The Vision of Autonomic Computing" published by IBM [1]. Since then a number of architectural models for Self-Healing systems, based on monitoring, problem detection and repair have been developed. The use of architectural models as the centrepiece of model-based adaptation has been explored by Garlan et al. [11], where the architectural models are used for the runtime system's monitoring and reasoning; for instance, to understand what the running system is doing in high level terms, detect when architectural constraints are violated, and reason about repair actions at the architectural level.

The idea of distributed object system monitoring and supervision of a self-healing process is shared and extended in Reilly and colleagues work [12], in which an architecture and associated middleware services were developed to support dynamic instrumentation to detect abnormal systems' states (events) and trigger and control a self-healing process thereby ensuring safety.

Gross and colleagues from Columbia University [13] also agree that it is essential for self-healing systems to have strong system monitoring abilities. Their work "An Active Event Model for Systems Monitoring" is based on an intelligent event model called ActiveEvent. ActiveEvents build on conventional event concepts by augmenting raw and structural data with semantic information, thereby allowing recipients to be able to dynamically understand the content of new kinds of events. Two submodels of ActiveEvents are proposed: SmartEvents, which are lightweight XML structured events containing references to their syntactic and semantic models, and GaugeEvents, which are heavier but more flexible mobile agents. By classifying the events as lightweight and sophisticated it becomes easer to deal with system monitoring.

3. The OSAD model

The On-demand Service Assembly and Delivery (OSAD) model [14] provides an abstract view of the relationship of the distributed components and services. The objective of the OSAD model is to organize the following issues in a uniform framework:

- On-demand service delivery and invocation regardless of the location of the service;
- The automatic assembly of the application in ad-hoc manner based on the user's requirements;
- The ability to self-heal at runtime in terms of replacing a failed component of an application (hot swapping).

One of the tasks of the model is to find distributed components offering specific functionalities/services. After the component is found the following task is to make use of this functionality. To describe these events we use the term 'on-demand service delivery'. The OSAD model can be described as combination of different building blocks - component services. Figure1 shows the generic model including all core components of OSAD model.

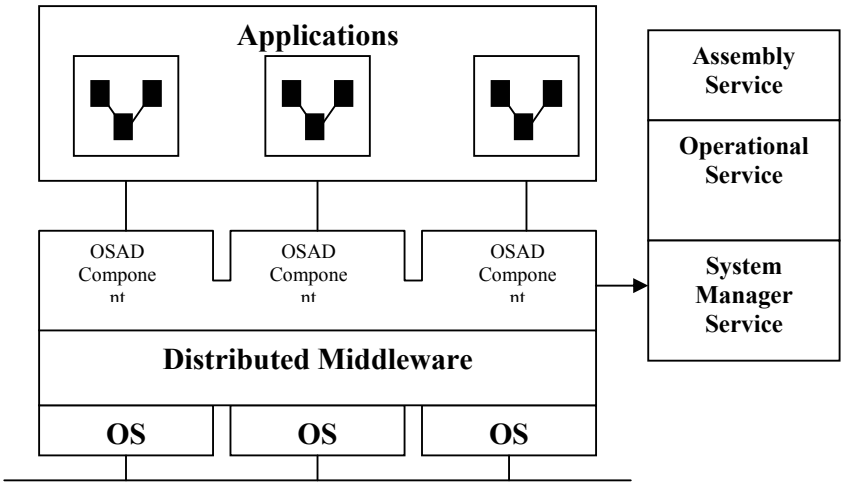

Figure 1: Core components of the OSAD model

One of the tasks of the model is to find distributed components offering specific functionality, that we call offering the service. After the component is found the next task is to make use of this functionality. Finding and assembling components is the role of the Assembly Service:

Assembly Service – this is the core service of the framework and it combines a number of functionalities of the model. Therefore the Assembly service is a combination of different sub-services and modules. It contains:

- *A Task Definition service*;
- *Registration and Discovery Service*;
- *Service Invocation Service*.

Control and monitoring are needed to identify failure, and alert the system to find an alternative replacement for the failed service as the control mechanism should be implemented with self-healing behaviour, in order to improve the newly formed application performance. The lifecycle of self-healing behaviour of OSAD model is shown in figure 2. The control and monitoring are encapsulated into the System

Manager, which is another core component of the OSAD model. The system manager is responsible for recovering the application from failure. Following failure detection, it notifies the assembly service that a replacement service should be found and selected amongst possible alternatives.

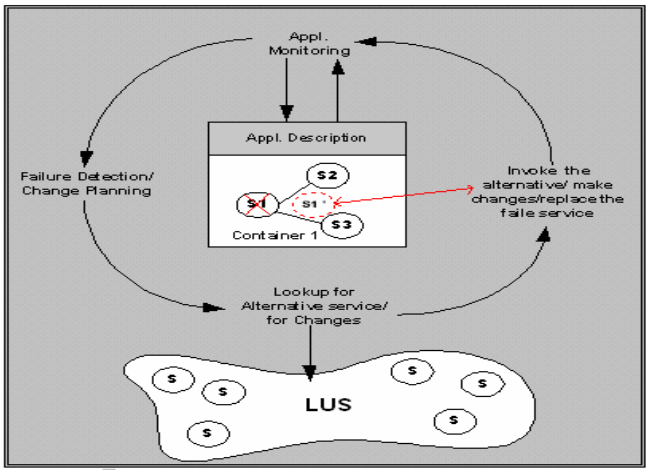

Figure 2: The lifecycle of self-healing behaviour in OSAD

4. Fault Detection Mechanisms

Failure detection can be implemented in different ways, which can have considerable impact on the performance of the system. Two mechanisms that we put forward for consideration are: Pre-emptive detection and on-use detection. With pre-emptive detection, the service manager checks, on a regular basis, that each of the services associated with the application is alive. If a service fails to respond to the service manager, it is assumed that the service has failed and the recovery process is started and the service manager then notifies the assembly service. With the on-use detection, the service manager monitors locally the service requests and, if a request times-out, it is assumed that the service has failed and the recovery process is started and the service manager then notifies the assembly service.

The performance considerations in this study relates to how these two mechanisms impact on service replacement waiting time and on network traffic. The notion of service replacement waiting time is important: It is the amount of time the application is prevented from using the service, because the service is found to have failed and is being replaced. The main advantage of the pre-emptive detection is that, as the service manager periodically polls the services, services may be found to be faulty prior to the moment when the application would wish to use them, therefore they can be replaced with zero replacement waiting time. The figure below shows the replacement waiting time for the on-use replacement mechanism, against the total number of services in used by the application:

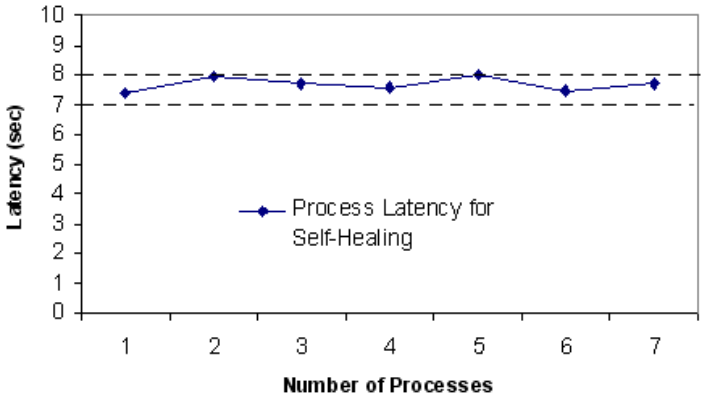

Figure 3: Service replacement latency as a function of the number of processes

On the other hand, the pre-emptive mechanism, although reducing the replacement waiting time, generates more network traffic, which may lead to congestion if there are large numbers of applications and services being used by these applications.

Qualitatively, the relative merits of pre-emptive detection and on-use detection are quite clear: With pre-emptive detection, services are monitored regularly, potentially enabling the application to detect a failure prior to the moment when the service would be invoked: Therefore, replacement of that service can be carried out before the service is required for use, so no delay is incurred. However, on closer inspection, the design of such a mechanism is difficult to optimise: If the monitoring frequency is too high, then the system may generate high overheads and network traffic. If the frequency is too low compared to the component failure rate, then it may not be effective, by not detecting faults in time to replace components prior to use. On the other hand, the on-use detection is a simple model that does not attempt to reduce component replacement delay: It assumes that the component is alive and working, and invokes the service when it is required. If the service is down, then the failure is detected, and the recovery process is initiated, and the full service replacement waiting time is incurred.

Even though it is easy to argue the merits of the pre-emptive detection mechanism, quantifying the benefits is not straightforward. In addition to the added complexity of the system, which increases when there are many services in a network and many applications using them, and also the fact that services may be scattered across internetworks, there is the problem of modelling components failure behaviour and service use behaviour.

According to some well-known models available in the literature, component failure frequency follow the bathtub behaviour [15] [16]:

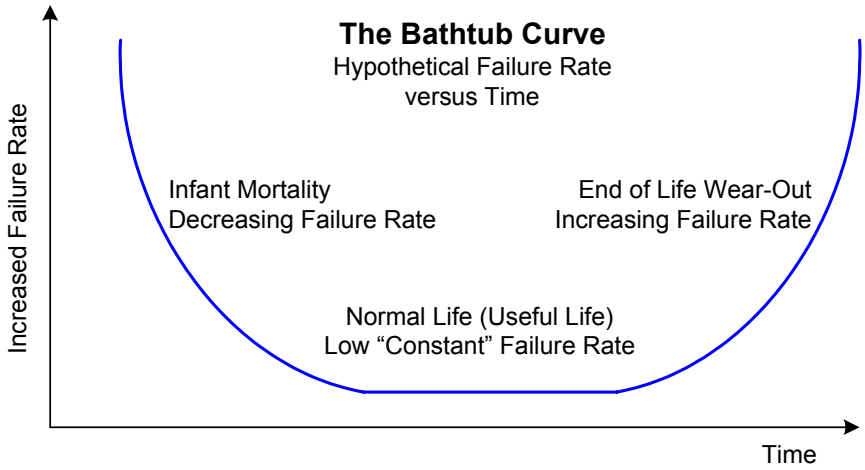

Figure 4: The failure rate of a component over its lifecycle

This is the failure rate through the life cycle of a component. In normal conditions, we would be considering components with a fixed failure rate, which is often referred to by its inverse, the Mean Time Between Failures (MTBF). It is at this stage that we would consider the components of a service-based application to be operating. Failure can be caused by a variety of events: Machine crash, software error, network disconnection, device hardware failure, etc.

At the constant failure rate stage, inter failure intervals may be modelled according to different distributions. The use of the negative exponential distribution has been proposed in the literature [16] [17] and we have used it in our model for simplicity. We anticipate the use of other distributions in the future in order to obtain more robust results, particularly as there are a number of distinct possible causes of failure.

5. The Experiment

The experiment consists of simulation of a distributed, service-based application, where services fail according to some failure rate (different rates for different services), and following the negative exponential distribution. We make the following assumptions:

- When a service fail, if pre-emptive detection is used, the service is replaced by another service providing similar functionality, according to the self-healing behaviour provided in the OSAD model. Overheads are incurred for replacing the service as illustrated in Fig. 3. Once a service that failed has been replaced, the replacement service is subject to failure at the same rate.
- If on-use detection is used, we assume that the service remains down after it fails, until an attempt is made to invoke it: As the failure has not been detected by the application until an attempt at using the service takes place, the service is then unavailable.

In order to understand the type of scenario in which each of the above strategies are suitable, we selected, for simulation, two scenarios:

The first scenario is the scenario where an application consists of a large number of services, all of which have a fairly high failure rate. This could, for instance, represent a network of sensors and similar small devices, interconnected through a combination of unreliable wireless links and fixed networks.

The second scenario represents a more stable environment where services are more reliable, having lower failure rate and being connected through a more reliable fixed network infra structure.

In addition to that, for both scenarios, we assume the application invokes the services on a regular basis, for instance to monitor temperature, take a pressure reading or similar action.

5.1 First Scenario

For this simulation, the following setting was adopted:

Number of Services: 15

Distribution of Interfailure Interval: Negative exponential, with mean values $MTBF_{i,}$:

$MTBF_1$: 5 Mins,
$MTBF_{i+1} = MTBF_i + 5$ Mins

The simulation was allowed to run for 15 hours.
Service invocation frequency: 1 invocation of each service, every 5 Mins.

For the pre-emptive detection scheme, the service manager monitors each service also on a regular basis: 2 monitoring periods were chosen: 1 minute and 2.5 minutes.

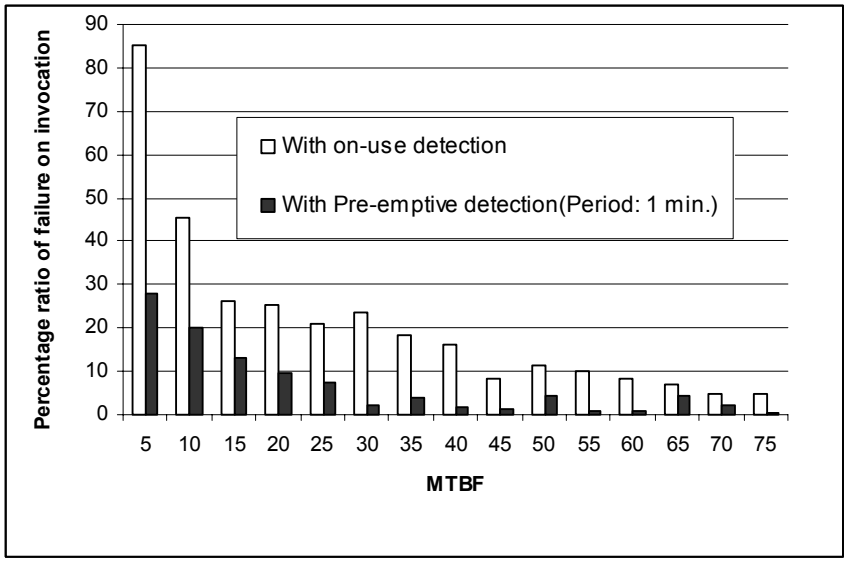

Figure 5: The ratio, in percentages, of failed service invocation to total number of service invocation, as a function of the MTBF, for a system with pre-emptive failure detection (monitoring period = 1 minute) and on-use failure detection.

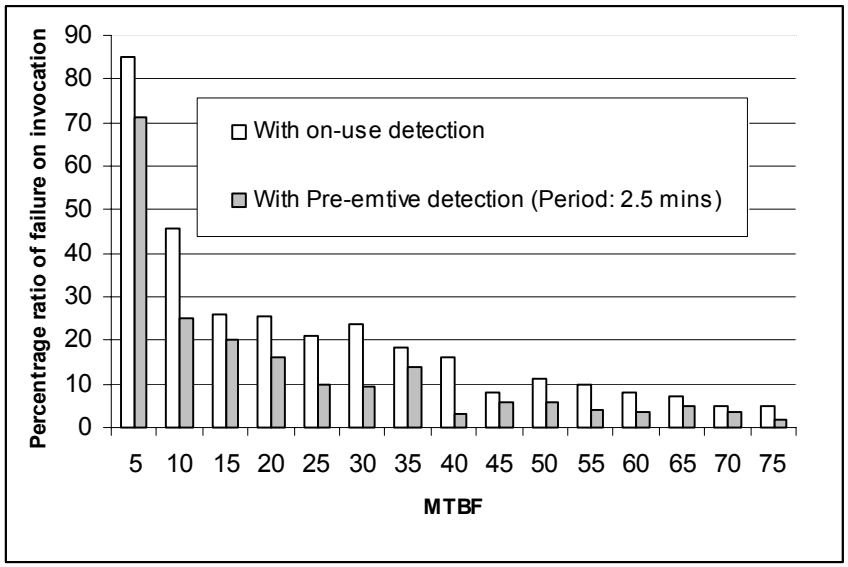

Figure 6: The ratio, in percentages, of failed service invocation to total number of service invocation, as a function of the MTBF, for a system with pre-emptive failure detection (monitoring period = 2.5 minutes) and on-use failure detection.

The results indicate the percentage ratio of the number of times the service was down when invoked, to the total number of service invocation, with both schemes. As would be expected, for a given invocation rate, the larger the MTBF, the lower the percentage of invocations that fail. However, it is the frequency of failure monitoring, relative to the invocation frequency, which determines the percentage of failed services that are detected successfully. From figures 5 and 6, we see the obvious fact that, for a fixed invocation rate, the higher the failure rate, the higher the percentage of failed invocations. The white bars in both graphs show the same values. The black bar in figure 5 shows the percentage of failures not detected, when pre-emptive detection was used, with a period of 1 min. The grey bar in figure 6 show the percentage of failures not detected, when pre-emptive detection was used, with a period of 2.5 minutes.

5.2 Second Scenario

For this simulation, the following setting was adopted:

Number of Services: 1

Distribution of Interfailure Interval: Negative exponential, with mean values $MTBF_{1,}$:

MTBF1: 300 Mins.

The application was allowed to run for 50 hours of simulated time.
Service invocation frequency: every 5 Mins.

As in the first scenario, the pre-emptive fault detection scheme periods use were: 1 minute and 2.5 minutes.

With on use detection, the percentage of failed invocations were 1.5 %. With pre-emptive detection, with period 1 min., the percentage was 0.68% and with 2.5 minute period it was 1.2%.

This reinforces the conclusions from the first scenario: With very low failure rate, compared to the service invocation rate, it is very unlikely that a service will fail in the first place, so improvement in failure detection is relatively small by using pre-emptive detection

6. Evaluation of the experiment

The experiment made a number of assumptions, due to the lack of available data:

Inter-failure intervals distributions were assumed to be negative exponential. This may not be a very accurate model when there are many possible, independent causes of failure.

Service invocations were assumed to take place at regular intervals. This may be justifiable in some cases, such as monitoring physical values such as temperature and pressure, but is less justifiable in other types of systems.

However, it provides an approximated overall understanding of the issue of failure monitoring, and some guidance as to the range of usability of the different schemes proposed.

7. Conclusion

This paper presents a performance discussion of the relative merits of two mechanisms for fault detection in our middleware for self-healing applications. The pre-emptive and on-use mechanisms are introduced and a discussion of their relative merits presented. It is shown that the pre-emptive mechanism reduces waiting time at the expense of higher network traffic. Future work will include the use of different failure interval distributions, and a random pattern for service invocation.

References

1. J. O. Kephart, D.M.C., *The Vision of Autonomic Computing*. 2003, IBM Tomas J. Watson Research Center.
2. IBM, *Introduction to Autonomic Computing*. 2001, IBM Corporation, Software Group: Somers, NY.
3. Koopman, P. *Elements of the Self-Healing System Problem Space*. in *ICSE WADS03*. 2003. Portland.
4. P. Oriezy, M.M.G., R. N. Taylor, G. Johnson, N. Medvidovic, A. Quilici, D. Rosenblum, and A. Wolf, *An Architecture-Based Approach to Self-Adaptive Software.* IEEE Intellingent Systems, 1999.
5. M. Mikic-Rakic, N.M., N. Medvidovic. *Architectural Style Requirements for Self-Healing Systems*. in *Wass'02*. 2002. Charleston, South Carolina, USA.
6. E. Grishikashvili, N.B., A. Taleb-Bendiab. *Service-Oriented Approach for Distributed application Assembly and Management*. in *The 4th Annual Postgraduate Symposium on the Convergence, Telecommunication, Networking and Broadcasting. PgNet*. 2003. Liverpool, UK: LJMU.
7. Bieber, G., *Openwings - Closing the Personal Digital Divide*. 2001, Motorola.
8. Microsystems. *Jini Network Technology*. Sun Microsystems. 2000. http://wwws.sun.com/software/jini
9. Newmarch, J. *Guide to Jini technology*. J. Newmarch. 1999. 13 October 2004. http://jan.netcomp.monash.edu.au/java/jini/tutorial/Jini.xml
10. Badr, N. *An Investigation into Autonomic Middleware Control Services to Support Distributed Self-Adaptive Software*. Academic. Department, Liverpool John Moores University. 2003. Liverpool
11. D. Garlan, B.S. *Model-Based Adaptation for Self-Healing Systems*. in *WOSS'02*. 2002. Charleston, South Carolina, USA.
12. D. Reilly, A.T.-B., A. Laws, N. Badr. *An Instrumentation and Control-Based Approach for Distributed Application Management and Adaptation*. in *Woss'02*. 2002. Charleston, South Carolina, USA.
13. Gross, P.N. *An Active Events Model for Systems Monitoring*. in *Complex and Dynamic System Architecture*. 2001. Brisbane, Australia.
14. Pereira, E.G. *IMPROMPTU: Software Framework for Self-Healing Middleware Services*. Academic. Department, Liverpool John Moores University. 2005. Liverpool

15. Wilkins, D.J. *The Bathtub Curve and Product Failure Behavior*. Reliability Hot Wire. 2002. 11/01/2005. http://www.weibull.com/hotwire/issue21/hottopics21.htm
16. SemiconFareast. *Life Distribution*. Semicon Fareast. 2004. http://www.semiconfareast.com/lifedist.htm
17. Chang, Y.K., S., *Computing System Failure Frequencies and Reliability Impotance Measures Using OBDD*. IEEE Transactions on Computers, 2004. Vol. 53.